University of Bath

PHD

LMTO studies of transition metals: Non-collinear magnetism and axial pressures

Crockford, Derek John

Award date:
1990

Awarding institution:
University of Bath

Link to publication

Alternative formats
If you require this document in an alternative format, please contact:
openaccess@bath.ac.uk

Copyright of this thesis rests with the author. Access is subject to the above licence, if given. If no licence is specified above, original content in this thesis is licensed under the terms of the Creative Commons Attribution-NonCommercial 4.0 International (CC BY-NC-ND 4.0) Licence (https://creativecommons.org/licenses/by-nc-nd/4.0/). Any third-party copyright material present remains the property of its respective owner(s) and is licensed under its existing terms.

Take down policy
If you consider content within Bath's Research Portal to be in breach of UK law, please contact: openaccess@bath.ac.uk with the details. Your claim will be investigated and, where appropriate, the item will be removed from public view as soon as possible.

Download date: 05. May. 2023

LMTO STUDIES OF TRANSITION METALS:

NON-COLLINEAR MAGNETISM AND AXIAL PRESSURES

submitted by Derek John Crockford

for the degree of Ph.D.

of the University of Bath

1990

COPYRIGHT

Attention is drawn to the fact that copyright of this thesis rests with its author. This copy of the thesis has been supplied on condition that anyone who consults it is understood to recognise that its copyright rests with its author and that no quotation from the thesis and no information derived from it may be published without the prior written consent of the author.

This thesis may be made available for consultation within the University Library and may be photocopied or lent to other libraries for the purposes of consultation.

UMI Number: U601452

All rights reserved

INFORMATION TO ALL USERS
The quality of this reproduction is dependent upon the quality of the copy submitted.

In the unlikely event that the author did not send a complete manuscript
and there are missing pages, these will be noted. Also, if material had to be removed,
a note will indicate the deletion.

UMI U601452
Published by ProQuest LLC 2013. Copyright in the Dissertation held by the Author.
Microform Edition © ProQuest LLC.
All rights reserved. This work is protected against
unauthorized copying under Title 17, United States Code.

ProQuest LLC
789 East Eisenhower Parkway
P.O. Box 1346
Ann Arbor, MI 48106-1346

Abstract.

In this thesis the LMTO-ASA method is applied to the calculation of some electronic properties of transition metals. After an introduction to the LMTO method, the ASA, and density functional theory, a formalism is derived for the treatment of the non-collinear antiferromagnets in FCC manganese and iron, which are shown to pose particular difficulties in representation. The band structures are calculated and it is found that the results for manganese can be interpreted reasonably well within a localised electron picture. The axial pressure is then presented as a means of estimating the tendency of a material to distort so as to alter its $\frac{c}{a}$ ratio and a scheme is described whereby it may be calculated in the LMTO-ASA method. The electrostatic contribution to the axial pressure is shown, given certain assumptions, to be of only second order importance provided that calculations are for HCP or FCT materials at ideal close-packing. The axial pressures are then evaluated for both the above non-collinear magnets and for a number of HCP transition metals. The results are used to estimate the equilibrium $\frac{c}{a}$ ratios using classical elasticity theory and experimental values for the elastic constants. For comparison, the same calculations are also done using data drawn from curves of the ASA total energy. The results obtained from from the total energies are found to be in good accord with experiment but those obtained from the axial pressure for the HCP elements are not. Following this, conclusions are drawn as to the usefulness of the charge density from an ASA calculation in the investigation of non-isotropic properties.

Acknowledgements.

The author wishes to thank David Bird for his support through all the ups and downs of this work, and Martin Long for sharing some of his ideas and enthusiasm. The author is indebted to the SERC for financial support. Thanks are also due to Ole Andersen and his group, in particular Ove Jepsen, for their hospitality and their time, and David Bullett for arranging my stay with them. The program used in this work was derived from the code written by Ove Jepsen. Last but not least I would like to thank my parents for always letting me do my own thing (no matter how crazy it seemed to them!), and especially Sarah, without whom this thesis might have been finished a whole lot quicker (but probably wouldn't have been finished at all).

To my parents.

CONTENTS.

INTRODUCTION.

This thesis is devoted to the investigation of non-collinear magnetism and non-isotropic distortion in transition metals using bandstructure techniques. These are both areas in which relatively little bandstructure work has been done. In the case of non-collinear magnetism the impediment has been the complications of representing a system with non-trivial spin dependence. In the case of non-isotropic distortion the problem resides in the use of the atomic sphere approximation (ASA), which is essential to the modern, *fast* bandstructure methods. The ASA is in essence a spherical approximation, and its success in the prediction of non-spherical properties has not been overwhelming.

The bandstructure method used in this investigation is the LMTO method of Andersen (1975), the calculations being done within the ASA. The LMTO method is, up to a certain order, equivalent to the older KKR method (Ham & Segall, 1961; Heine, 1980) but has the advantage that its chief equation takes the form of an eigenvalue problem. The program used here is derived from the code written by Ove Jepsen of the Max Planck Institute in Stuttgart. The LMTO method had gone through a number of different phases, with emphasis in different places, and consequently the literature contains many divergent notations. The description of the method given here in chapter one is oriented towards the "tranformation theory", and the notation is consistent with the most recent papers (see §1.1). The usefulness of the tranformation theory is that it defines an equivalence class of basis sets, from which may be chosen a basis with the most desirable features. The tranformation theory is not directly used in the investigations pursued here, but being the most recent it is probably the most

sensible approach to the LMTO method as a whole.

A bandstructure method, being founded on a single electron equation, must make some attempt to include many-electron effects if it is to produce reasonable results. The usual way of doing this is to introduce an additional element in the single electron potential called an exchange-correlation potential. There are a number of different recipes for producing this but the most popular in current usage is the local density approximation (LDA) to the density functional theory of Hohenberg, Kohn & Sham. In this thesis we shall take a particular interest in magnetic systems. As a result, the exchange-correlation will be calculated according to the *spin* density functional theory of von Barth & Hedin (1972) rather than the original formulation. This approach, together with the work of Hohenberg, Kohn & Sham, will be briefly reviewed in chapter two.

Chapter three brings us to one of the main themes of this thesis, the investigation of non-collinear magnetism. To the author's knowledge, the only bandstructure work that has been done in this area has been performed by Kübler, Höck, Sticht & Williams (1988) using the LASW method and by Cade (1981a) using LMTO. The systems of interest here will be the frustrated antiferromagnets that are believed to exist in the γ (FCC) phases of manganese and iron. These systems pose peculiar problems of representation, which are not posed by the materials studied by the above group. The system studied by Cade is included in the set to be examined here, but the methods used were not systematic and the results obtained were not complete.

The existence of the non-collinear magnetism in γ Mn and Fe is related to the frustrated nature of antiferromagnetism on a FCC lattice, as can be shown

using a localised spin model. The representation for a spin density wave on an FCC lattice is developed and is found to lead to a particular algebraic problem for which a solution is given. Results of bandstructure calculations for three classes of spin arrangement are presented for both Mn and Fe. In addition, using the techniques of chapter 4, estimates are made for the distortions in $\frac{c}{a}$ ratio that are associated with these materials. The localised electron picture is found to be of use as an interpretational tool, both with respect to the distortions and in the more general results.

There have been few attempts to investigate non-isotropic distortions by muffin tin techniques. To the author's knowledge the only work in this area is by Cade (1981b) and by Christensen (1984), both of whom employed LMTO-ASA. As mentioned previously, this lack of interest is probably due to the necessity of making a spherical approximation (the ASA) in the self-consistent field calculations, which casts some doubt on the usefulness of the results for this purpose. In particular, the work of Christensen (1984) brings out the importance of the electrostatic part of the energy, and the difficulty involved in getting this quantity right. Nevertheless, Christensen was able to obtain reasonable results for elastic constants in palladium and gold, and Cade correctly predicted the sign of the $\frac{c}{a}$ distortion for the simple antiferromagnet in γ Mn.

The purpose of chapter four is to further investigate the usefulness of ASA results in the calculation of non-spherical properties. The work concentrates on the simplest possible non-spherical distortion, the axial distortion, and looks at the $\frac{c}{a}$ ratios of both the magnetic materials of chapter three and the HCP transition metals of the first two rows. The problem is approached in two ways.

The more sophisticated approach is to calculate an axial pressure using a generalisation of the virial expression, the axial pressure being defined by analogy with the isotropic or bulk pressure. The second simpler approach is to consider the curve of ASA total energy against $\frac{c}{a}$. Both of these approaches are fraught with hazards but it is shown that, with proper regard for their limitations, they can each give rise to interesting results.

CHAPTER ONE: AN INTRODUCTION TO LMTO-ASA.

1.1) The self-consistent field.

In order to determine the behaviour of the electrons in a crystal we have to solve the Schrödinger equation to arrive at a state function. This constitutes a many-body problem which cannot be solved exactly. We start off therefore by adopting the one-electron approximation, with each electron being regarding as an independent body moving in some average field v_{eff} due to the atomic nuclei and the other electrons. This leads to the Schrödinger equation,

$$\left[-\frac{1}{2}\nabla^2 + v_{\text{eff}}(\mathbf{r})\right]\Psi_j(\mathbf{r}) = E_j\Psi_j(\mathbf{r}). \tag{1.1}$$

where Ψ_j is the wavefunction corresponding to the one-electron energy E_j. The effective one-electron potential v_{eff} is the sum of three parts: the ionic term, the Hartree term and the exchange-correlation term. The ionic term consists of the field due to the fixed atomic nuclei. The Hartree term is the mean field due to all the electrons. Explicitly, the ionic and Hartree terms are given by (Ashcroft & Mermin, 1976):

$$V_{\text{ionic}} = -\sum_{\text{sites,i}} \frac{Z_{\text{i}}}{|\mathbf{r} - \mathbf{R}_{\text{i}}|} \tag{1.2}$$

$$V_{\text{Hartree}}(\mathbf{r}) = -\int \frac{d\mathbf{r}'\rho(\mathbf{r}')}{|\mathbf{r} - \mathbf{r}'|}. \tag{1.3}$$

The exchange-correlation term is an attempt to take into account the fact that we cannot really regard the electrons as independent and comes from density functional theory (see chapter 2). For the moment it is only necessary to know that it can be chosen to be a functional of the electron density $\rho(\mathbf{r})$.

An approximation that is frequently used in electronic structure calculations is the frozen-core approximation (Harrison, 1970). Given that the electrons in

complete shells have little or no interaction with the electrons of the neighbouring atoms it is not necessary to include them in the electronic calculations. Their presence is taken into account by redefining the ionic term to include their mean electrostatic field. As these inert or "core" electrons are not considered when calculating the wave function their contribution is "frozen" throughout the calculation. The Hartree term must also be redefined in this scheme, as the mean electrostatic field of the non-core or "valence" electrons.

Given that we do not know a priori the exact form of v_{eff} our input potential must be some sort of guess (based on the atomic potential, say). Having solved (1.1) for this v_{eff} we can construct a charge density $\rho(\mathbf{r})$ for our crystal by populating the one-electron states according to the Pauli principle and using,

$$\rho(\mathbf{r}) = \sum_{\text{occupied } j} |\Psi_j(\mathbf{r})|^2 . \tag{1.4}$$

We use this to construct a new Hartree potential according to (1.3) and a new exchange-correlation potential. Adding these components along with the unchanged ionic potential gives a new one-electron potential v_{eff}. We iterate this procedure in the hope that v_{eff} will converge to self-consistency. This approach is called the self-consistent field approach, and is used in most of the methods for calculating the band structures of solids. The main differences between these methods lies in the way in which (1.1) is solved.

In this chapter we shall develop the LMTO method, starting from its parent the KKR method, and trying to keep the algebra and notation to a minimum. The contents of this chapter are based on a number of standard references: Andersen, 1975; Andersen & Jepsen, 1984; Skriver, 1984; Andersen, Jepsen & Glötzel, 1985; Andersen, Pawlowska & Jepsen, 1986; Andersen, Jepsen & Sob,

1987. The units used here and in chapter 2 are atomic units: $\frac{\hbar^2}{m} = \frac{e^2}{4\pi\epsilon_0} = 1$ and the unit of energy is the Hartree, 1 Hartree = 2 Rydbergs. For consistency with the literature and with the LMTO code chapter 4 is given in atomic Rydberg units: $\frac{\hbar^2}{2m} = \frac{1}{2}\frac{e^2}{4\pi\epsilon_0} = 1$.

1.2) The muffin tin potential.

Consider what the potential might look like in a typical solid. In the region deep inside an atom we know that the atomic forces must dominate over the interactions with neighbouring atoms. It is therefore reasonable to assume that the potential is spherically symmetric. In the interstitial region between the atoms we might expect the potential to be weakly varying compared to that in the atoms. We formalise these ideas in the definition of a muffin tin potential, which is a model for a system of atoms in which the potential is assumed to be spherically symmetric within spheres centred at the atomic sites and constant in the interstitial region. The spheres are chosen so that they touch without overlap but beyond that there are no conditions on their sizes. The constant potential between the spheres is called the muffin tin zero, V_{mtz}.

There are several methods of calculating band structures which rely on the use of a muffin tin potential. However, we shall concern ourselves only with the LMTO method and the older KKR method from which it was derived. In both cases the first stage in the process is the choice of an appropriate basis set. The members of the basis set are called, logically enough, muffin tin orbitals. In the case of the KKR method the muffin tin orbitals are energy dependent. However, in the LMTO method the orbitals are energy independent and this leads to a final equation that is linear in energy (§1.7). It is for this reason that the method

has acquired the title "linear muffin tin orbital", or LMTO for short, and it is sometimes described as being the linearised form of the KKR method.

Both of these methods are normally used inside a self-consistency loop, as described in the last section. In each case the new potential which emerges from an iteration is not of muffin tin form and has to be "flattened out" before entry to the next band structure calculation. The standard method of producing a muffin tin potential is based on the procedure employed by Mattheis in his paper on the band structure of solid argon (Mattheis, 1964). Mattheis considered the material to be an array of equal sized, touching muffin tin spheres with each sphere containing an atom of argon. First the value of V_{mtz} was chosen. Mattheis decided this by adding together the potentials due to all the atoms and taking a spatial average in the region between the muffin tin spheres. To obtain the potential in a sphere at $\mathbf{R}$ the potentials from all sites $\mathbf{R}' \neq \mathbf{R}$ were expanded about $\mathbf{R}$ (Löwdin, 1956) and the $l = 0$ components were added to the potential due to the atom already there. The potential due to each atom was taken to be that of a Hartree-Fock calculation for an isolated argon atom. After the first iteration of a self-consistency loop the new muffin tin potential would of course be calculated from the output of the previous iteration rather than from atomic Hartree-Fock data. Moreover, for a solid with more than one atomic species the choice of the sphere sizes might not be quite as obvious as for argon. However, the method of calculation is essentially that of Mattheis.

The muffin tin methods have been successful for calculations on materials that have good close-packed structures, where the properties of interest do not depend on the detailed shape of the potential (e.g. Fermi surfaces and bulk

pressures of transition metals, see Mackintosh & Andersen, 1980). The thing about close-packed structures is that they have small intestitial regions with small charge densities and hence a potential which really is almost flat. For open structures or for properties that are sensitive to the form of the potential the conventional muffin tin potential is not well suited. The problem with open structures is that they tend to have very directional bonding: a potential which is flat in the interstital region is therefore not appropriate. This problem has been overcome to some extent by the introduction of "empty spheres" at all vacant high-symmetry sites in the crystal. By this means accurate band structures have been produced for materials such as diamond, silicon and germanium (Glötzel, Segall & Andersen, 1980). The empty spheres method takes partial account of the inhomogeneity of the electron density in the interstitial region, but at the expense of having to use a larger basis set with "unphysical" empty sphere orbitals. The problem with potential sensitive properties (e.g. phonon frequencies) seems inherent in the muffin tin potential itself, and progress here has only been made by abandoning the assumption that the interstitial potential is flat (Brey, Weyrich & Christensen, 1988; Weyrich, 1988; Methfessel, 1988).

In order to solve (1.1) for a muffin tin potential we first have to choose a basis set $\{\chi_{\mathbf{R}L}\}$, where $\chi_{\mathbf{R}L}$ is centred at site $\mathbf{R}$ and has labels $L = \{l, m\}$. Although the orbitals used in the KKR and LMTO methods are different the process of construction is similar. In both cases the first step is the specification of what the orbitals are to be in the interstitial region. The form of an orbital in the spheres is then determined by demanding that the orbital be smooth in all space. The orbital $\chi_{\mathbf{R}L}$ is constructed from the corresponding (i.e. labels

$\mathbf{R}, l, m$) atomic wave function together with a function chosen to make it join smoothly to the interstitial function at the boundary. In a sphere at $\mathbf{R}' \neq \mathbf{R}$ the same orbital is defined by an expansion about $\mathbf{R}'$ of suitable functions, the coeffiecients being those of the multipole expansion of the interstitial function at $\mathbf{R}$. This choice of coefficients ensures that the orbital is smooth at the sphere boundary.

Once a basis has been fixed the next step is to determine those linear combinations of orbitals that correspond to solutions of (1.1). It is here that one finds the biggest difference between the KKR and LMTO methods. The KKR method is based on the idea that in a given sphere the effects of the surrounding atoms must cancel the function added to the resident atomic function to ensure smoothness. In this way we obtain solutions which are linear combinations of original atomic functions. The idea that the solutions should be atomic-like in the spheres is certainly consistent with the philosophy behind the muffin tin potential. The "tail cancellation" condition gives rise directly to the KKR equations (Skriver, 1984; Andersen, Jepsen & Sob, 1986). Unfortunately, these equations are non-linear and difficult to solve. In the LMTO method the variational principle is applied to a linear combination of LMTO orbitals to obtain an equation which is linear in energy and much easier to solve. Moreover the LMTO solutions can be made to agree with the KKR to third order in a Taylor expansion of the energy (§1.7).

There is one further complication with the basis functions, which arises because there is a certain amount of freedom in the choice of the interstitial functions. As the overall form of the muffin tin orbitals is determined by the

interstitial functions (through the smoothness conditions) one is able to vary the properties of the basis by varying the choice of interstitial function. This freedom can be put to good use in the LMTO method.

1.3) The interstitial function.

The essential problem in the construction of a muffin tin basis set is that the piecewise nature of the muffin tin potential means that the orbitals must be built up piecewise as well. In this section we derive a set of functions which is complete in the interstitial region, acting as though the atomic spheres aren't there at all (although each interstitial function is still centred at some atomic site **R**). In the next section we shall decide that the atomic spheres really are there after all, and we shall accordingly reduce the scope of the functions derived here to the interstitial region only. In the spheres their place shall be taken by more appropriate functions, subject to the constraint that whatever we choose must match smoothly at the sphere boundaries.

In order to simplify our manipulations we shall frequently adopt a combined bra-ket and matrix notation, with superscripts denoting the scope of any bra or ket. From here on a superscript ∞ will indicate a function valid in all space, an i will indicate a function which is zero outside the interstitial region and the lack of a superscript will mean a function which is zero outside its associated sphere. The arbitrary function $N^{\infty}_{\mathbf{R}}$ can therefore be written in ket form as:

$$|N_{\mathbf{R}}\rangle^{\infty} = |N_{\mathbf{R}}\rangle + |N_{\mathbf{R}}\rangle^{i} + \sum_{\mathbf{R}' \neq \mathbf{R}} |N_{\mathbf{R}',\mathbf{R}}\rangle. \qquad (1.5)$$

Here the first term on the right hand side is the part of $N^{\infty}_{\mathbf{R}}$ in its "home" sphere at **R**, the second term is the part in the interstitial region and the third term is

the sum of the components $N_{\mathbf{R}',\mathbf{R}}$ in the "away" spheres at $\mathbf{R}' \neq \mathbf{R}$. In order to bring in the matrices we shall define that the ket $|N\rangle$ is a row vector with elements $N_{\mathbf{R}}$ and that the bra $\langle N|$ is a column vector with elements $N^*_{\mathbf{R}}$. The juxtaposition of two objects will denote a summation over sites $\mathbf{R}'$, along with any other common indices that the objects may have. The multiplication of a vector $\mathbf{N}$ by a matrix M can therefore be given either by $M\langle N|$ or by $|N\rangle M$.

Returning to the derivation of the interstitial functions we now solve (1.1) about each site $\mathbf{R}$ in turn with potential V_{mtz} in all space. Introducing κ^2 to represent the "kinetic energy" $E - V_{mtz}$ of the solution Φ we have to solve:

$$\left[-\frac{1}{2}\nabla^2 + \kappa^2\right] \Phi_{\mathbf{R}lm\kappa}(\mathbf{r}) = 0. \tag{1.6}$$

Separating variables we find that $\Phi_{\mathbf{R}lm\kappa}$ must be a product of a spherical harmonic $Y_{\mathbf{R}lm}$ and a solution $\phi_{\mathbf{R}l\kappa}$ of the radial Helmholtz equation:

$$\left[-\frac{d^2}{dr^2} + \frac{l(l+1)}{r^2} - \kappa^2\right] r\phi_{\mathbf{R}l\kappa}(r) = 0. \tag{1.7}$$

Equation (1.7) has two independent solutions, the spherical Bessel and Neumann functions, $j_{\mathbf{R}l}(\kappa r)$ and $k_{\mathbf{R}l}(\kappa r)$ respectively (Bransden & Joachain, 1983). The function $j_{\mathbf{R}l}$ is analytic in any finite region but diverges at infinity while $k_{\mathbf{R}l}$ has a single pole at its origin $\mathbf{R}$. Dropping for convenience the subscript κ and putting $L = lm$ the two solutions of (1.6) may be written:

$$\begin{aligned} J^0_{\mathbf{R}L} &= j_{\mathbf{R}l}(\kappa r) Y_{\mathbf{R}L}(\theta, \phi) \\ \text{and } K^0_{\mathbf{R}L} &= k_{\mathbf{R}l}(\kappa r) Y_{\mathbf{R}L}(\theta, \phi) \end{aligned} \tag{1.8}$$

Being solutions of the self-adjoint equation (1.6) we know that the set of functions given by (1.8) is complete. As the functions $J^0_{\mathbf{R}L}$ are not analytic in the interstitial region we define our basic interstitial function to be $K^0_{\mathbf{R}L}$.

A property of $K^0_{\mathbf{R}L}$ that we shall use extensively is that it may be expanded about any other centre $\mathbf{R}'$ in terms of the set $J^0_{\mathbf{R}'L'}$. In fact, this is not surprising as $K^0_{\mathbf{R}L}$ is analytic in any sphere at $\mathbf{R}' \neq \mathbf{R}$ and $J^0_{\mathbf{R}'L'}$ is analytic in any finite region. The expansion is valid in a sphere about $\mathbf{R}'$ of radius $|\mathbf{R} - \mathbf{R}'|$ so it is certainly valid in a muffin tin sphere. It is given by,

$$K^0_{\mathbf{R}L} = -\sum_{L'} \frac{J^0_{\mathbf{R}'L'}}{2(2l'+1)} S^0_{\mathbf{R}'L',\mathbf{R}L}.$$

The Hermitian matrix $S^0_{\mathbf{R}'L',\mathbf{R}L}$ is called the structure matrix (Andersen, Jepsen & Glötzel, 1985), the minus sign being purely conventional. It is usual to absorb the denominator into the definition of the $J^0_{\mathbf{R}'L'}$ so that we get,

$$K^0_{\mathbf{R}L} = -\sum_{L'} J^0_{\mathbf{R}'L'} S^0_{\mathbf{R}'L',\mathbf{R}L}. \tag{1.9}$$

Using the bra-ket notation the interstitial functions can be written as:

$$|K^0_{\mathbf{R}L}\rangle^\infty = |K^0_{\mathbf{R}L}\rangle + |K^0_{\mathbf{R}L}\rangle^i - \sum_{\mathbf{R}'L'} |J^0_{\mathbf{R}'L'}\rangle S^0_{\mathbf{R}'L',\mathbf{R}L}.$$

In matrix notation this is,

$$|K^0\rangle^\infty = |K^0\rangle + |K^0\rangle^i - |J^0\rangle S^0. \tag{1.10}$$

This equation is really just (1.5) with $N_{\mathbf{R}}$ replaced by $K^0_{\mathbf{R}L}$ and the "away" components given explicitly using the expansion (1.9). It should be noted that the matrix S^0 has elements identically zero for $\mathbf{R}' = \mathbf{R}$ so that the diagonal components of the "away" part cannot affect the "home" part.

There is one disadvantage in defining the interstitial functions in terms of $K^0_{\mathbf{R}L}$, and this is that the $K^0_{\mathbf{R}L}$ are long-ranged functions and force the corresponding muffin tin orbitals $\chi^0_{\mathbf{R}L}$ to be long-ranged also. In order to interpret

results in terms of atomic orbitals and for computational reasons it is better to adopt a basis which is relatively short-ranged. The function $K^0_{\mathbf{R}L}$ can be reduced in range if the pole at $\mathbf{R}$ is "screened" by the addition of extra poles at all other sites $\mathbf{R}' \neq \mathbf{R}$ (Andersen & Jepsen, 1984; Andersen, Jepsen & Glötzel, 1985). This can be achieved by introducing the new functions $J^\alpha_{\mathbf{R}L}$ and $K^\alpha_{\mathbf{R}L}$ given by:

$$|J^\alpha_{\mathbf{R}L}\rangle = |J^0_{\mathbf{R}L}\rangle - |K^0_{\mathbf{R}L}\rangle \alpha_{\mathbf{R}L} \tag{1.11}$$

$$\text{and } |K^\alpha_{\mathbf{R}L}\rangle^\infty = |K^0_{\mathbf{R}L}\rangle + |K^\alpha_{\mathbf{R}L}\rangle^{\mathbf{i}} - \sum_{\mathbf{R}'L'} |J^\alpha_{\mathbf{R}'L'}\rangle S^\alpha_{\mathbf{R}'L',\mathbf{R}L}. \tag{1.12}$$

Here $\alpha_{\mathbf{R}L}$ controls the "strength" of the added poles and the superscript α serves to distinguish the new functions from the conventional unscreened functions $J^0_{\mathbf{R}L}$ and $K^0_{\mathbf{R}L}$ (the label α will always denote an arbitrary screening with no special properties).

The difference between (1.12) and (1.10) consists of the introduction of the poles through (1.11) and the replacement of $|K^0\rangle^{\mathbf{i}}$ and S^0 by $|K^\alpha\rangle^{\mathbf{i}}$ and S^α respectively. We can determine these last two objects by demanding that the new set of functions given by (1.12) be related to the old set (1.10) by an invertible linear transformation. This is necessary in order to ensure that the new set is complete. Substituting from (1.11) into (1.12) we obtain,

$$\begin{aligned} |K^\alpha_{\mathbf{R}L}\rangle^\infty &= |K^0_{\mathbf{R}L}\rangle + |K^\alpha_{\mathbf{R}L}\rangle^{\mathbf{i}} - \sum_{\mathbf{R}'L'} (|J^0_{\mathbf{R}'L'}\rangle S^\alpha_{\mathbf{R}'L',\mathbf{R}L} - |K^0_{\mathbf{R}'L'}\rangle \alpha_{\mathbf{R}'L'} S^\alpha_{\mathbf{R}'L',\mathbf{R}L}) \\ &= \sum_{\mathbf{R}'L'} |K^0_{\mathbf{R}'L'}\rangle (\delta_{\mathbf{R}'L',\mathbf{R}L} + \alpha_{\mathbf{R}'L'} S^\alpha_{\mathbf{R}'L',\mathbf{R}L}) \\ &\qquad + |K^\alpha_{\mathbf{R}L}\rangle^{\mathbf{i}} - \sum_{\mathbf{R}'L'} |J^0_{\mathbf{R}'L'}\rangle S^\alpha_{\mathbf{R}'L',\mathbf{R}L}. \end{aligned}$$

Defining the matrix α to be diagonal in $\mathbf{R}'L', \mathbf{R}L$ with elements $\alpha_{\mathbf{R}L}$ we can

write this in matrix notation as,

$$|K^\alpha\rangle = |K^0\rangle(1+\alpha S^\alpha) + |K^\alpha\rangle^i - |J^0\rangle S^\alpha. \tag{1.13}$$

Multiplying (1.10) by $(1+\alpha S^\alpha)$ we get,

$$|K^0\rangle^\infty(1+\alpha S^\alpha) = |K^0\rangle(1+\alpha S^\alpha) + |K^0\rangle^i(1+\alpha S^\alpha) - |J^0\rangle S^0(1+\alpha S^\alpha).$$

Comparing this with (1.13) it is seen that consistency can be achieved by defining,

$$|K^\alpha\rangle^\infty = |K^0\rangle^\infty(1+\alpha S^\alpha) \tag{1.14}$$

$$\text{with} \quad S^\alpha = S^0(1+\alpha S^\alpha). \tag{1.15}$$

What has been done here is to find a linear transformation which is equivalent to screening the pole at any site by the addition of poles at surrounding sites. The only restriction on this transformation (i.e. on the matrix α) is that the matrix $(1+\alpha S^\alpha)$ is invertible. In fact, putting $\alpha_{\mathbf{R}L} = \alpha_l$ independent of $\mathbf{R}$ and m it is possible to find a choice of α which minimizes the range of K^α and this gives the so-called "tight-binding" basis (Andersen & Jepsen, 1984). Another choice of α_l yields the "nearly orthogonal" basis, which will be important in §1.7 and will be denoted by γ.

1.4) Muffin tin orbitals and the K.K.R. method.

It is clear that (1.12) as it stands is not a good basis function because $K^0_{\mathbf{R}L}$ and $J^\alpha_{\mathbf{R}L}$ are not solutions of (1.1) in the sphere, and $K^0_{\mathbf{R}L}$ has a pole at $\mathbf{r} = \mathbf{R}$. To arrive at the muffin tin orbital $|\chi^\alpha_{\mathbf{R}L}\rangle^\infty$ we take (1.12) and substitute $|K^0_{\mathbf{R}L}\rangle$ and $|J^\alpha_{\mathbf{R}L}\rangle$ by more suitable functions (to be defined shortly):

$$|\chi^\alpha_{\mathbf{R}L}\rangle^\infty = |\psi^\alpha_{\mathbf{R}L}\rangle + |K^\alpha_{\mathbf{R}L}\rangle^i - \sum_{\mathbf{R}'L'} |\tilde{J}^\alpha_{\mathbf{R}'L'}\rangle S^\alpha_{\mathbf{R}'L',\mathbf{R}L}. \tag{1.16}$$

As the potential in a sphere is spherically symmetric (1.1) can be solved by separation of variables. We define the solutions of (1.1) in the sphere at $\mathbf{R}$ with unit normalisation to be $\psi^{\gamma}_{\mathbf{R}L}$. Here the superscript γ indicates that the choice of unit normalisation implies a particular choice of the screening matrix α, as will be seen shortly. The general $\psi^{\alpha}_{\mathbf{R}L}$ will be defined by,

$$\psi^{\alpha}_{\mathbf{R}L} = N^{\alpha}_{\mathbf{R}L}\psi^{\gamma}_{\mathbf{R}L} + P^{\alpha}_{\mathbf{R}L}\tilde{J}^{\alpha}_{\mathbf{R}L},$$

and the $N^{\alpha}_{\mathbf{R}L}$ and $P^{\alpha}_{\mathbf{R}L}$ will be determined by the condition that $|\chi^{\alpha}_{\mathbf{R}L}\rangle^{\infty}$ is sufficiently smooth in all space. Hence to go any further we now have to consider the smoothness conditions.

We take as the smoothness criterion for $|\chi^{\alpha}_{\mathbf{R}L}\rangle^{\infty}$ the requirement that it be continuous and differentiable in all space. The problem of matching $\psi^{\alpha}_{\mathbf{R}L}$ smoothly to $K^{0}_{\mathbf{R}L}$ (the α dependence of $\psi^{\alpha}_{\mathbf{R}L}$ arises through its dependence on $\tilde{J}^{\alpha}_{\mathbf{R}L}$) is clearly one of matching their dependences on r at $r = s_{\mathbf{R}}$, where $s_{\mathbf{R}}$ is the sphere radius at $\mathbf{R}$. Bearing this in mind we derive a general expression for matching a function $f(r)$ up to the first derivative to a linear combination $\zeta a(r) + \eta b(r)$ at a point $r = s$. We require,

$$f(s) = \zeta a(s) + \eta b(s)$$

$$\text{and} \quad f'(s) = \zeta a'(s) + \eta b'(s).$$

Solving for ζ and η yields,

$$\zeta = \frac{f(s)b'(s) - f'(s)b(s)}{a(s)b'(s) - a'(s)b(s)}$$

$$\text{and} \quad \eta = -\frac{f(s)a'(s) - f'(s)a(s)}{a(s)b'(s) - a'(s)b(s)},$$

and defining the Wronskian of m(r) and n(r) at $r = s$ to be,

$$W(m,n) = m(s)n'(s) - m'(s)n(s), \tag{1.17}$$

the above result can then be written more concisely as,

$$\zeta a(r) + \eta b(r) = \frac{a(r)W(f,b) - b(r)W(f,a)}{W(a,b)}. \tag{1.18}$$

From (1.18) it is clear that this form of matching may be achieved for any pair $a(r), b(r)$ for which $W(a,b) \neq 0$.

Having obtained the matching formulae (1.17) and (1.18) and defining $\psi^{\alpha}_{\mathbf{R}L}$ as,

$$\psi^{\alpha}_{\mathbf{R}L} = N^{\alpha}_{\mathbf{R}L}\psi^{\gamma}_{\mathbf{R}L} + P^{\alpha}_{\mathbf{R}L}\tilde{J}^{\alpha}_{\mathbf{R}L}, \tag{1.19}$$

the forms of $N^{\alpha}_{\mathbf{R}L}$ and $P^{\alpha}_{\mathbf{R}L}$ are determined to be (Andersen, Pawlowska & Jepsen, 1986),

$$N^{\alpha}_{\mathbf{R}L} = \frac{W(K^{0}_{\mathbf{R}L}, \tilde{J}^{\alpha}_{\mathbf{R}L})}{W(\psi^{\gamma}_{\mathbf{R}L}, \tilde{J}^{\alpha}_{\mathbf{R}L})} \tag{1.20}$$

$$\text{and} \quad P^{\alpha}_{\mathbf{R}L} = -\frac{W(K^{0}_{\mathbf{R}L}, \psi^{\gamma}_{\mathbf{R}L})}{W(\psi^{\gamma}_{\mathbf{R}L}, \tilde{J}^{\alpha}_{\mathbf{R}L})}. \tag{1.21}$$

The function $N^{\alpha}_{\mathbf{R}L}$ is sometimes referred to as the "normalisation" and $P^{\alpha}_{\mathbf{R}L}$ as the "potential function". If $N^{\alpha}_{\mathbf{R}L}$ is not far from unity and $P^{\alpha}_{\mathbf{R}L}$ is small it can be seen that (1.19) is simply $\psi^{\gamma}_{\mathbf{R}L}$ "perturbed" so as to make it match to $K^{0}_{\mathbf{R}L}$. In addition, equation (1.19) indicates that for unit normalisation the general function $\psi^{\alpha}_{\mathbf{R}L}$ must correspond to $N^{\alpha}_{\mathbf{R}L} = 1$ and $P^{\alpha}_{\mathbf{R}L} = 0$, so putting conditions on the matrix α through (1.20) and (1.21). If α satisfies these conditions then we have by definition the γ basis of the previous section. The function $\tilde{J}^{\alpha}_{\mathbf{R}L}$ is defined to be analytic in the sphere and to match to $J^{\alpha}_{\mathbf{R}L}$ at $r = s_{\mathbf{R}}$, but is arbitrary otherwise. The smoothness of $|\chi^{\alpha}_{\mathbf{R}L}\rangle^{\infty}$ at the spheres at $\mathbf{R}' \neq \mathbf{R}$ then follows immediately from (1.12). Summing up, for a given α we first determine $K^{\alpha}_{\mathbf{R}L}$ and then everything else about the basis is fixed, apart from the exact form of $\tilde{J}^{\alpha}_{\mathbf{R}L}$.

write this in matrix notation as,

$$|K^\alpha\rangle = |K^0\rangle(1+\alpha S^\alpha) + |K^\alpha\rangle^{\mathbf{i}} - |J^0\rangle S^\alpha. \tag{1.13}$$

Multiplying (1.10) by $(1+\alpha S^\alpha)$ we get,

$$|K^0\rangle^\infty(1+\alpha S^\alpha) = |K^0\rangle(1+\alpha S^\alpha) + |K^0\rangle^{\mathbf{i}}(1+\alpha S^\alpha) - |J^0\rangle S^0(1+\alpha S^\alpha).$$

Comparing this with (1.13) it is seen that consistency can be achieved by defining,

$$|K^\alpha\rangle^\infty = |K^0\rangle^\infty(1+\alpha S^\alpha) \tag{1.14}$$

$$\text{with} \quad S^\alpha = S^0(1+\alpha S^\alpha). \tag{1.15}$$

What has been done here is to find a linear transformation which is equivalent to screening the pole at any site by the addition of poles at surrounding sites. The only restriction on this transformation (i.e. on the matrix α) is that the matrix $(1+\alpha S^\alpha)$ is invertible. In fact, putting $\alpha_{\mathbf{R}L} = \alpha_l$ independent of $\mathbf{R}$ and m it is possible to find a choice of α which minimizes the range of K^α and this gives the so-called "tight-binding" basis (Andersen & Jepsen, 1984). Another choice of α_l yields the "nearly orthogonal" basis, which will be important in §1.7 and will be denoted by γ.

1.4) Muffin tin orbitals and the K.K.R. method.

It is clear that (1.12) as it stands is not a good basis function because $K^0_{\mathbf{R}L}$ and $J^\alpha_{\mathbf{R}L}$ are not solutions of (1.1) in the sphere, and $K^0_{\mathbf{R}L}$ has a pole at $\mathbf{r}=\mathbf{R}$. To arrive at the muffin tin orbital $|\chi^\alpha_{\mathbf{R}L}\rangle^\infty$ we take (1.12) and substitute $|K^0_{\mathbf{R}L}\rangle$ and $|J^\alpha_{\mathbf{R}L}\rangle$ by more suitable functions (to be defined shortly):

$$|\chi^\alpha_{\mathbf{R}L}\rangle^\infty = |\psi^\alpha_{\mathbf{R}L}\rangle + |K^\alpha_{\mathbf{R}L}\rangle^{\mathbf{i}} - \sum_{\mathbf{R}'L'} |\tilde{J}^\alpha_{\mathbf{R}'L'}\rangle S^\alpha_{\mathbf{R}'L',\mathbf{R}L}. \tag{1.16}$$

As the potential in a sphere is spherically symmetric (1.1) can be solved by separation of variables. We define the solutions of (1.1) in the sphere at **R** with unit normalisation to be $\psi^{\gamma}_{\mathbf{R}L}$. Here the superscript γ indicates that the choice of unit normalisation implies a particular choice of the screening matrix α, as will be seen shortly. The general $\psi^{\alpha}_{\mathbf{R}L}$ will be defined by,

$$\psi^{\alpha}_{\mathbf{R}L} = N^{\alpha}_{\mathbf{R}L}\psi^{\gamma}_{\mathbf{R}L} + P^{\alpha}_{\mathbf{R}L}\tilde{J}^{\alpha}_{\mathbf{R}L},$$

and the $N^{\alpha}_{\mathbf{R}L}$ and $P^{\alpha}_{\mathbf{R}L}$ will be determined by the condition that $|\chi^{\alpha}_{\mathbf{R}L}\rangle^{\infty}$ is sufficiently smooth in all space. Hence to go any further we now have to consider the smoothness conditions.

We take as the smoothness criterion for $|\chi^{\alpha}_{\mathbf{R}L}\rangle^{\infty}$ the requirement that it be continuous and differentiable in all space. The problem of matching $\psi^{\alpha}_{\mathbf{R}L}$ smoothly to $K^{0}_{\mathbf{R}L}$ (the α dependence of $\psi^{\alpha}_{\mathbf{R}L}$ arises through its dependence on $\tilde{J}^{\alpha}_{\mathbf{R}L}$) is clearly one of matching their dependences on r at $r = s_{\mathbf{R}}$, where $s_{\mathbf{R}}$ is the sphere radius at **R**. Bearing this in mind we derive a general expression for matching a function $f(r)$ up to the first derivative to a linear combination $\zeta a(r) + \eta b(r)$ at a point $r = s$. We require,

$$f(s) = \zeta a(s) + \eta b(s)$$

$$\text{and} \quad f'(s) = \zeta a'(s) + \eta b'(s).$$

Solving for ζ and η yields,

$$\zeta = \frac{f(s)b'(s) - f'(s)b(s)}{a(s)b'(s) - a'(s)b(s)}$$

$$\text{and} \quad \eta = -\frac{f(s)a'(s) - f'(s)a(s)}{a(s)b'(s) - a'(s)b(s)},$$

and defining the Wronskian of m(r) and n(r) at $r = s$ to be,

$$W(m,n) = m(s)n'(s) - m'(s)n(s), \tag{1.17}$$

the above result can then be written more concisely as,

$$\zeta a(r) + \eta b(r) = \frac{a(r)W(f,b) - b(r)W(f,a)}{W(a,b)}. \tag{1.18}$$

From (1.18) it is clear that this form of matching may be achieved for any pair $a(r), b(r)$ for which $W(a,b) \neq 0$.

Having obtained the matching formulae (1.17) and (1.18) and defining $\psi^{\alpha}_{\mathbf{R}L}$ as,

$$\psi^{\alpha}_{\mathbf{R}L} = N^{\alpha}_{\mathbf{R}L}\psi^{\gamma}_{\mathbf{R}L} + P^{\alpha}_{\mathbf{R}L}\tilde{J}^{\alpha}_{\mathbf{R}L}, \tag{1.19}$$

the forms of $N^{\alpha}_{\mathbf{R}L}$ and $P^{\alpha}_{\mathbf{R}L}$ are determined to be (Andersen, Pawlowska & Jepsen, 1986),

$$N^{\alpha}_{\mathbf{R}L} = \frac{W(K^{0}_{\mathbf{R}L}, \tilde{J}^{\alpha}_{\mathbf{R}L})}{W(\psi^{\gamma}_{\mathbf{R}L}, \tilde{J}^{\alpha}_{\mathbf{R}L})} \tag{1.20}$$

$$\text{and } P^{\alpha}_{\mathbf{R}L} = -\frac{W(K^{0}_{\mathbf{R}L}, \psi^{\gamma}_{\mathbf{R}L})}{W(\psi^{\gamma}_{\mathbf{R}L}, \tilde{J}^{\alpha}_{\mathbf{R}L})}. \tag{1.21}$$

The function $N^{\alpha}_{\mathbf{R}L}$ is sometimes referred to as the "normalisation" and $P^{\alpha}_{\mathbf{R}L}$ as the "potential function". If $N^{\alpha}_{\mathbf{R}L}$ is not far from unity and $P^{\alpha}_{\mathbf{R}L}$ is small it can be seen that (1.19) is simply $\psi^{\gamma}_{\mathbf{R}L}$ "perturbed" so as to make it match to $K^{0}_{\mathbf{R}L}$. In addition, equation (1.19) indicates that for unit normalisation the general function $\psi^{\alpha}_{\mathbf{R}L}$ must correspond to $N^{\alpha}_{\mathbf{R}L} = 1$ and $P^{\alpha}_{\mathbf{R}L} = 0$, so putting conditions on the matrix $\boldsymbol{\alpha}$ through (1.20) and (1.21). If α satisfies these conditions then we have by definition the γ basis of the previous section. The function $\tilde{J}^{\alpha}_{\mathbf{R}L}$ is defined to be analytic in the sphere and to match to $J^{\alpha}_{\mathbf{R}L}$ at $r = s_{\mathbf{R}}$, but is arbitrary otherwise. The smoothness of $|\chi^{\alpha}_{\mathbf{R}L}\rangle^{\infty}$ at the spheres at $\mathbf{R}' \neq \mathbf{R}$ then follows immediately from (1.12). Summing up, for a given α we first determine $K^{\alpha}_{\mathbf{R}L}$ and then everything else about the basis is fixed, apart from the exact form of $\tilde{J}^{\alpha}_{\mathbf{R}L}$.

Looking back we see that each of the sets of functions $\{|K^{\alpha}_{\mathbf{R}L}\rangle^{i}\}$ and $\{|\psi^{\gamma}_{\mathbf{R}L}\rangle\}$ spans the solutions of the Schrödinger equation for a part of space and that together they cover all of space. The problem in solving the Schrödinger equation in all space is therefore that of finding those linear combinations of $\{|K^{\alpha}_{\mathbf{R}L}\rangle^{i}\}$ and $\{|\psi^{\gamma}_{\mathbf{R}L}\rangle\}$ which are smooth at all sphere boundaries. With $N^{\alpha}_{\mathbf{R}L}$ and $P^{\alpha}_{\mathbf{R}L}$ represented by the diagonal matrices N and P (c.f. $\alpha_{\mathbf{R}L}$ and the diagonal matrix α) we can use (1.16) and (1.19) to write $|\chi^{\alpha}_{\mathbf{R}L}\rangle^{\infty}$ as,

$$\begin{aligned} |\chi^{\alpha}\rangle^{\infty} &= |\psi^{\alpha}\rangle - |\tilde{J}^{\alpha}\rangle S^{\alpha} + |K^{\alpha}\rangle^{i} \\ &= |\psi^{\gamma}\rangle N^{\alpha} + |\tilde{J}^{\alpha}\rangle P^{\alpha} - |\tilde{J}^{\alpha}\rangle S^{\alpha} + |K^{\alpha}\rangle^{i}. \end{aligned} \tag{1.22}$$

Following Andersen, Jepsen & Sob (1987) we take the linear combination of (1.22) given by $(N^{\alpha})^{-1}\mathbf{u}^{\alpha}$, where $\mathbf{u}^{\alpha}$ is a column vector with components $u^{\alpha}_{\mathbf{R}L}$, to obtain,

$$|\chi^{\alpha}\rangle^{\infty}(N^{\alpha})^{-1}\mathbf{u}^{\alpha} = |\psi^{\gamma}\rangle\mathbf{u}^{\alpha} + |\tilde{J}^{\alpha}\rangle(P^{\alpha} - S^{\alpha})(N^{\alpha})^{-1}\mathbf{u}^{\alpha} + |K^{\alpha}\rangle^{i}(N^{\alpha})^{-1}\mathbf{u}^{\alpha}.$$

The vectors $\mathbf{u}^{\alpha}$ for which the $|\tilde{J}^{\alpha}\rangle$s drop out leaving smooth linear combinations of $\{|K^{\alpha}_{\mathbf{R}L}\rangle^{i}\}$ and $\{|\psi^{\gamma}_{\mathbf{R}L}\rangle\}$ only are therefore given by (Andersen, Jepsen & Sob, 1987),

$$[P^{\alpha}(E) - S^{\alpha}(E)][N^{\alpha}(E)]^{-1}\mathbf{u}^{\alpha} = 0. \tag{1.23}$$

The condition that the $|\tilde{J}^{\alpha}\rangle$s drop out is called the "tail cancellation" condition and equation (1.23) is the matrix form of the KKR equations (for an alternative derivation see Ham & Segall, 1980; Heine, 1980). It should be noted that the energy dependence of S^{α} arises because the function $K^{\alpha}_{\mathbf{R}L}$ is energy dependent owing to the suppressed index $\kappa^2 = E - V_{mtz}$ (see (1.6)). It is also apparent now why $\psi^{\alpha}_{\mathbf{R}L}$ was defined (in (1.19)) to involve $\tilde{J}^{\alpha}_{\mathbf{R}L}$ and hence to be dependent on α: it is only by having both $|\tilde{J}^{\alpha}\rangle P^{\alpha}$ and the tails $|\tilde{J}^{\alpha}\rangle S^{\alpha}$ in terms of the same

function that we can obtain a condition for them to cancel, i.e. equation (1.23). The exact form taken by $\tilde{J}^{\alpha}_{\mathbf{R}L}$ is clearly not important here as all that matters is that it satisfies the same boundary as $J^{\alpha}_{\mathbf{R}L}$ at the sphere.

It turns out that the strict KKR method is only valid when performed in the $\alpha = 0$ basis (Andersen, Pawlowska & Jepsen, 1986). By definition $|\chi^0\rangle$ is made up from solutions of the Schrödinger equation in both the sphere and interstitial regions, and so to span the same Hilbert space the general basis $|\chi^{\alpha}\rangle$ must be related to $|\chi^0\rangle$ by an invertible linear transformation, valid in *all space*. However, the function $|\tilde{J}^{\alpha}_{\mathbf{R}L}\rangle$ is defined without reference to transformation properties so we cannot show that the atomic parts transform in the same way as the interstitial parts. It will be indicated in §1.6 how if we adopt the approximation scheme of the next section and expand the energy dependence of (1.23) in a Taylor series to second order then the different KKR sets do become equivalent. Moreover the equations obtained turn out to be exactly those of the LMTO method.

1.5) The atomic sphere approximation.

A major problem with the KKR method as presented so far is that the KKR equation (1.23) is non-linear in energy and is difficult to handle computationally. To solve it we have to find each root E_j separately and then solve the resulting systems one by one to obtain the vectors $\mathbf{u}_j$. When this is done, to obtain the potential for the next self-consistency loop it is necessary to perform the integral (1.3). The integration in the spheres is relatively easy but that in the interstitial region, with its more complicated geometry, is not. A simplifying assumption which is often employed in order to overcome these problems is the

atomic sphere approximation or ASA.

The ASA consists of two separate approximations. The first one is to put κ^2 in (1.6) equal to zero. This means that we set $V_{mtz} \equiv E$ and that the $K^{\alpha}_{\mathbf{R}L}$ are no longer true solutions of the Schrödinger equation in the interstitial region. However, since they are now independent of E the structure constants become independent of E also. Moreover, with $\kappa^2 \equiv 0$ equation (1.6) reduces to the Laplace equation and the functions $k_{\mathbf{R}L}$ and $j_{\mathbf{R}L}$ of (1.8) become:

$$\begin{aligned} k_{\mathbf{R}l} &= \left(\frac{r}{w}\right)^{-l-1} \\ j_{\mathbf{R}l} &= \frac{1}{2(2l+1)}\left(\frac{r}{w}\right)^{l}. \end{aligned} \tag{1.24}$$

Here the unit of distance is no longer set by κ and has been chosen to be the average sphere radius w. From (1.24) it can be seen that the functions $k_{\mathbf{R}L}$ and $j_{\mathbf{R}L}$ are now independent of the scale of the structure and this renders the structure constants independent of scale. Structure constants calculated for $\kappa = 0$ are called canonical structure constants (Skriver, 1984).

The second approximation of the ASA consists of performing the calculations over Wigner-Seitz spheres. A Wigner-Seitz sphere is a sphere whose radius $S_{\mathbf{ws}}$ is such that the sphere volume is equal to the volume of the associated atom's Wigner-Seitz cell. The potential in a Wigner-Seitz sphere is usually calculated in the same way as the the muffin tin potential, the only difference is that the sphere is bigger. When we perform the integral (1.3) over the Wigner-Seitz sphere we are therefore including an "interstitial region" of volume equal to that bounded by the Wigner-Seitz cell and the inscribed muffin tin sphere. The hope is that the ASA integrals will include the contribution that would have been made by the more difficult integral over the interstitial region.

The above definition of a Wigner-Seitz sphere can lead to ambiguity if we are dealing with a lattice with a basis, or are using empty spheres. In practice the sphere sizes tend to be chosen by looking at the size of an atom in a similar chemical environment, subject to the constraint imposed by the unit cell volume. The volumes of any empty spheres are then chosen to fill up the remaining space in the unit cell once the volumes of the real atoms are decided.

There are a number of objections to the ASA. First of all, there are bound to be errors due to the requirement $\kappa^2 = 0$. Secondly, the integral over a muffin tin sphere with a spherical potential and the region between this and the Wigner-Seitz cell, with potential V_{mtz}, has been replaced by an integral over a larger Wigner-Seitz sphere with spherical potential only, and this must make a difference. The first of these objections can be argued around by stating that the states of interest (the valence states) will lie close to Fermi level and this is usually sufficiently near to V_{mtz} that κ^2 is close to zero anyway. However, the second objection is harder to resolve, and is even stronger in the case of an open solid, where there is a larger interstital region anyway (although this can be reduced by using empty spheres). Probably the best defence to these objections lies in the fact that in the LMTO method it is possible to calculate the difference between the ASA integrals and the muffin tin ones and to include them in the calculation as a perturbation (the "combined correction term": Andersen, 1975; Skriver, 1984). The difference, at least for good close-packed materials, is found to be of third order importance.

In practice there is another inaccuracy in the KKR method which is not a product of the ASA. It is due to the l-summation in (1.23) being taken only to

$l = 2$ or $l = 3$ in order to keep the matrix size manageable. This truncation is reasonable for the parts of the basis inside the spheres, as we would not expect unoccupied, atomic-like orbitals of high l-value to have much effect on the ground state. However, there is no corresponding argument for the interstitial functions and by imposing the truncation on them as well we may end up with a solution that is poorly converged in the interstitial region. Again, the difference can be calculated by including the different summation limits in the calculation of the combined correction term, and in most cases is sufficiently small that it can be ignored.

1.6) Linear muffin tin orbitals.

It was shown in §1.4 how the solution of the muffin tin problem by the KKR method leads to an equation that is computationally difficult to solve. To obtain a solution we have to find the roots of,

$$\det\left[P^{\alpha}(E) - S^{\alpha}(E)\right] = 0, \tag{1.25}$$

and then solve (1.23) separately for each one in turn. The problem can be considerably simplified by adopting the ASA. First of all, the ASA eliminates the energy dependence of the structure constants. Secondly it can be shown that, within the ASA, the potential function may be expanded about energy E_ν as (Andersen, Pawlowska & Jepsen, 1986),

$$[P^{\alpha}(E)]^{-1} = \frac{\Delta^{\gamma}}{E - C^{\gamma}} + \gamma - \alpha + O(E - E_\nu)^3, \tag{1.26}$$

where C and Δ are *potential parameters* defined by (Andersen, Jepsen & Glötzel, 1985),

$$C = E_\nu - \frac{W(K^0, \psi_\nu^\gamma)}{W(K^0, \dot{\psi}_\nu^\gamma)}, \tag{1.27}$$

$$\text{and } \Delta = \frac{W(J^\gamma, \psi_\nu^\gamma)}{W(K^0, \dot{\psi}_\nu^\gamma)}. \tag{1.28}$$

Here $\psi_\nu^\gamma = \psi^\gamma(E_\nu)$, $\dot{\psi}_\nu^\gamma = \left[\frac{\partial}{\partial E}\psi^\gamma(E)\right]_{E_\nu}$, and γ is the representation for which $N = 1$ and $P = 0$, α a general representation. We shall re-encounter the potential parameters in §1.7. For the moment what is significant is that (1.26) implies a linear dependence of $P^\alpha(E)$ on energy, provided $\alpha = \gamma$. This leads to a linearised form of the KKR equations given by (Andersen, Jepsen & Glötzel, 1985),

$$\left[C + \Delta^{\frac{1}{2}} S^\gamma \Delta^{\frac{1}{2}}\right] \mathbf{u} = E\mathbf{u}, \tag{1.29}$$

which agrees with (1.23) (in the ASA) to order $(E - E_\nu)^2$, where E_ν is the fixed energy of (1.26). Equation (1.29) has the form of an eigenvalue problem with "Hamiltonian" given by the term in square brackets, and there exist efficient numerical routines for solving this problem. It should be noted that (1.29) is also relevant in a general representation α, but in this case the agreement with (1.23) is only to first order.

In §1.4 we defined a set of energy dependent orbitals (1.22) and showed how they could be used to build a solution of the Schrödinger equation for a muffin tin potential, hence also demonstrating their completeness. What has been done in this section is to indicate that, within the assumptions of the ASA, equation (1.23) may be linearised to obtain (1.29). This is not the only way to proceed: it is also possible to do the linearisation step first and then apply the Schrödinger equation in the guise of the variational principle. In this context the linearisation step consists of the derivation of a set of *energy independent* muffin tin orbitals. The variational principle, when applied to such a set, gives rise to an eigenvalue problem that is linear in energy (see next section). In

fact, taken to order $(E - E_\nu)^2$ the equation we obtain is exactly (1.29). It is this approach, linearisation first then Schrödinger equation, that constitutes the LMTO method.

Looking at (1.22) it can be seen that, within the ASA (so $\tilde{J}^\alpha$ is not a function of E), the energy dependence of a muffin tin orbital comes from,

$$\psi^\gamma(E)N^\alpha(E) + \tilde{J}^\alpha P^\alpha(E).$$

The derivative of this with respect to energy (denoted by overdot) is,

$$\dot{\psi}^\gamma(E)N^\alpha(E) + \psi^\gamma(E)\dot{N}^\alpha(E) + \tilde{J}^\alpha \dot{P}^\alpha(E).$$

If we demand that the orbital, evaluated at $E = E_\nu$, have energy derivative zero then the form of $\tilde{J}^\alpha$ is fixed,

$$\tilde{J}^\alpha = -\frac{N^\alpha_\nu}{\dot{P}^\alpha_\nu}(\dot{\psi}^\gamma_\nu + \psi^\gamma_\nu o^\alpha), \tag{1.30}$$

where the subscript ν indicates an expression evaluated at $E = E_\nu$ and

$$o^\alpha \equiv \frac{\dot{N}^\alpha_\nu}{N^\alpha_\nu}. \tag{1.31}$$

Substituting the new $\tilde{J}^\alpha$ into $\chi^\alpha(E_\nu)$, (1.22) gives,

$$\begin{aligned}|\chi^\alpha_{\nu\mathbf{R}L}\rangle^\infty =& |\psi^\gamma_{\nu\mathbf{R}L}\rangle\, N^\alpha_{\nu\mathbf{R}L} - \left(|\dot{\psi}^\gamma_{\nu\mathbf{R}L}\rangle + |\psi^\gamma_{\nu\mathbf{R}L}\rangle o^\alpha_{\mathbf{R}L}\right) N^\alpha_{\nu\mathbf{R}L}(\dot{P}^\alpha_{\nu\mathbf{R}L})^{-1} P^\alpha_{\nu\mathbf{R}L} \\ &+ \sum_{\mathbf{R}'L'} \left(|\dot{\psi}^\gamma_{\nu\mathbf{R}'L'}\rangle + |\psi^\gamma_{\nu\mathbf{R}'L'}\rangle o^\alpha_{\mathbf{R}'L'}\right) N^\alpha_{\nu\mathbf{R}'L'}(\dot{P}^\alpha_{\nu\mathbf{R}'L'})^{-1} S^\alpha_{\mathbf{R}'L'\mathbf{R}L} \\ &+ |K^\alpha_{\mathbf{R}L}\rangle^i.\end{aligned}$$

It is conventional to define the "energy independent" or linear muffin tin orbital to match to $|K^\alpha\rangle^i(N^\alpha)^{-1}$ rather than $|K^\alpha\rangle^i$. Hence, in matrix notation,

$$|\chi^\alpha_\nu\rangle^\infty = |\psi^\gamma_\nu\rangle(1 + o^\alpha h^\alpha) + |\dot{\psi}^\gamma_\nu\rangle h^\alpha + |K^\alpha\rangle^i (N^\alpha_\nu)^{-1}, \tag{1.32}$$

where h^α is given by,

$$h^\alpha_{\mathbf{R}'L'\mathbf{R}L} = -(\dot{P}^\alpha_{\nu\mathbf{R}'L'})^{-\frac{1}{2}}(P^\alpha_{\nu\mathbf{R}'L'}\delta_{\mathbf{R}'L'\mathbf{R}L} - S^\alpha_{\mathbf{R}'L'\mathbf{R}L})(\dot{P}^\alpha_{\nu\mathbf{R}'L'})^{-\frac{1}{2}}, \qquad (1.33)$$

the division by $\dot{P}^\alpha_{\nu\mathbf{R}'L'}$ being written symmetrically.

There is one point which we have omitted to check so far, which is that the explicit form (1.30) for $\tilde{J}^\alpha$ agrees with the definition of $\tilde{J}^\alpha$ given in §1.4. The analytic property of the new $\tilde{J}^\alpha$ is clear but there is still the matter of matching to J^α at the sphere. Using (1.18) and the result $W(\dot{\psi}^\gamma(E), \psi^\gamma(E)) = 1$ (Andersen, Pawlowska & Jepsen, 1986) we find that the linear combination of $\dot{\psi}^\gamma_\nu$ and ψ^γ_ν that matches to J^α is given by,

$$W(J^\alpha, \psi^\gamma_\nu)\dot{\psi}^\gamma_\nu(\mathbf{r}) - W(J^\alpha, \dot{\psi}^\gamma_\nu)\psi^\gamma_\nu(\mathbf{r}).$$

Taking the first coefficient of (1.30) and using the result $(N^\alpha)^2 = W(K^0, J^\alpha)\dot{P}^\alpha$ (Andersen, Pawlowska & Jepsen, 1986) together with (1.20) we obtain,

$$\begin{aligned} -\frac{N^\alpha_\nu}{\dot{P}^\alpha_\nu} = -\frac{W(K^0, J^\alpha)}{N^\alpha_\nu} &= -W(K^0, J^\alpha)\frac{W(\psi^\gamma_\nu, J^\alpha)}{W(K^0, J^\alpha)} \\ &= -W(J^\alpha, \psi^\gamma_\nu). \end{aligned}$$

Similarly, taking the second coefficient and using (1.21) we have,

$$\begin{aligned} -\frac{N^\alpha_\nu}{\dot{P}^\alpha_\nu}o^\alpha = -\frac{\dot{N}^\alpha_\nu}{\dot{P}^\alpha_\nu} &= \frac{W(K^0, J^\alpha)W(\dot{\psi}^\gamma_\nu, J^\alpha)}{W(\psi^\gamma_\nu, J^\alpha)^2}\frac{W(K^0, J^\alpha)}{(N^\alpha_\nu)^2} \\ &= W(\dot{\psi}^\gamma_\nu, J^\alpha) \\ &= -W(J^\alpha, \dot{\psi}^\gamma_\nu). \end{aligned}$$

Hence the coefficients given by (1.30) turn out to be exactly those required for $\tilde{J}^\alpha$ to match to J^α at the sphere.

It has been established that the linear muffin tin orbital (LMTO) may be defined as,

$$|\chi^\alpha_\nu\rangle^\infty = |\psi^\gamma_\nu\rangle(1 + o^\alpha h^\alpha) + |\dot{\psi}^\gamma_\nu\rangle h^\alpha + |K^\alpha\rangle^i(N^\alpha_\nu)^{-1}. \qquad (1.34)$$

and that this is consistent with everything that has gone before. In the ASA, of course, the interstitial function is not needed, as the interstitial region does not exist. It is usual (Andersen, Pawlowska & Jepsen, 1986) to define a function $|\psi_\nu^\alpha\rangle$ as,

$$|\psi_\nu^\alpha\rangle = \left[|\dot{\psi}_\nu^\gamma\rangle + |\psi_\nu^\gamma\rangle o^\alpha\right]. \tag{1.35}$$

Making use of (1.35) the LMTO may be written alternatively as,

$$|\chi_\nu^\alpha\rangle^\infty = |\psi_\nu^\gamma\rangle + |\psi_\nu^\alpha\rangle h^\alpha + |K^\alpha\rangle^{\mathrm{i}}(N_\nu^\alpha)^{-1}. \tag{1.36}$$

In summary, what has been done in this section is to use the ASA to eliminate the energy dependence of the muffin tin orbital (1.22), to first order. To do this we define $\tilde{J}^\alpha$ according to (1.30) and this leads, with the appropriate definitions of o^α (1.31) and h^α (1.33), to (1.34). The orbital given by (1.34) matches to $|K^\alpha\rangle(N_\nu^\alpha)^{-1}$ at the sphere boundaries, and being defined only for the ASA the interstitial part is not relevant. Adopting the definition (1.35) for $|\psi_\nu^\alpha\rangle$ the orbital can finally be expressed in the form (1.36). In the next section we shall apply the variational principle to a linear combination of these orbitals and so obtain the LMTO eigenvalue problem.

1.7) The LMTO eigenvalue problem.

In this section we shall apply the Rayleigh-Ritz variational principle (Bransden & Joachain, 1983) to the trial function Ψ given by,

$$|\Psi\rangle = |\chi_\nu^\alpha\rangle \mathbf{u}^\alpha, \tag{1.37}$$

where the implicit summation is over $i = (\mathbf{R}, L)$, and $\mathbf{R}$ covers the set of lattice

points. Placing (1.37) in the energy functional $E[\Psi]$ we get,

$$E[\Psi] = \frac{\langle\Psi|\hat{H}|\Psi\rangle}{\langle\Psi|\Psi\rangle} = \frac{\sum_{i'i} u^*_{i'} u_i H^\alpha_{i'i}}{\sum_{i'i} u^*_{i'} u_i O^\alpha_{i'i}}.$$

Here $H^\alpha_{i'i}$ and $O^\alpha_{i'i}$ are the Hamiltonian and overlap matrices in the basis χ^α_ν, i.e.

$$H_{i'i} = \langle\chi_{i'}|\hat{H}|\chi_i\rangle \tag{1.38}$$

$$\text{and} \quad O_{i'i} = \langle\chi_{i'}|\chi_i\rangle. \tag{1.39}$$

The above equation can be rewritten as,

$$E[\Psi]\sum_{i'i} u^*_{i'} u_i O^\alpha_{i'i} = \sum_{i'i} u^*_{i'} u_i H^\alpha_{i'i},$$

and the requirement that $E[\Psi]$ is stationary,

$$\frac{\partial E}{\partial u^*_{i'}} = 0, \quad \forall i',$$

then leads to the equations,

$$E[\Psi]\sum_{i} u_i O^\alpha_{i'i} = \sum_{i} u_i H^\alpha_{i'i},$$

or in matrix form,

$$(H^\alpha - EO^\alpha)\,\mathbf{u}^\alpha = \mathbf{0}. \tag{1.40}$$

This equation is the LMTO eigenvalue problem (Andersen, Jepsen & Glötzel, 1985). It is now evident why the energy independence of the basis is required in order to achieve a problem that is linear in energy: if χ^α_ν were a function of E then H^α and O^α would have to be as well. The use of the ASA is essential if this is to be avoided.

In order to handle the matrices H^α and O^α we need a few new definitions and results. As $\psi^\gamma(E)$ is a solution of Schrödinger's equation in the sphere we have,

$$(\hat{H} - E)|\psi^\gamma(E)\rangle = 0.$$

Differentiating this with respect to E gives,

$$(\hat{H} - E)|\dot{\psi}^\gamma(E)\rangle = |\psi^\gamma(E)\rangle$$

$$\Rightarrow \qquad \hat{H}|\dot{\psi}_\nu^\gamma\rangle = |\psi_\nu^\gamma\rangle + E_\nu|\dot{\psi}_\nu^\gamma\rangle. \tag{1.41}$$

The unit normalisation of $\psi^\gamma(E)$ can be written as,

$$\langle\psi^\gamma(E)|\psi^\gamma(E)\rangle = 1$$

and differentiating this with respect to E we get,

$$\langle\psi^\gamma(E)|\dot{\psi}^\gamma(E)\rangle = 0.$$

Hence,

$$\langle\psi_\nu^\gamma|\psi_\nu^\gamma\rangle = 1 \tag{1.42}$$

$$\text{and} \quad \langle\psi_\nu^\gamma|\dot{\psi}_\nu^\gamma\rangle = 0. \tag{1.43}$$

We define a new "potential parameter" p by,

$$p = \langle\dot{\psi}_\nu^\gamma|\dot{\psi}_\nu^\gamma\rangle. \tag{1.44}$$

Finally, substituting from (1.34) into (1.38) and (1.39),

$$\begin{aligned} H^\alpha &= (1 + o^\alpha h^\alpha)^\dagger\langle\psi_\nu^\gamma|\hat{H}|\psi_\nu^\gamma\rangle(1 + o^\alpha h^\alpha) + (h^\alpha)^\dagger\langle\dot{\psi}_\nu^\gamma|\hat{H}|\dot{\psi}_\nu^\gamma\rangle h^\alpha \\ &\quad + (1 + o^\alpha h^\alpha)^\dagger\langle\psi_\nu^\gamma|\hat{H}|\dot{\psi}_\nu^\gamma\rangle h^\alpha + (h^\alpha)^\dagger\langle\dot{\psi}_\nu^\gamma|\hat{H}|\psi_\nu^\gamma\rangle(1 + o^\alpha h^\alpha) \\ &= (1 + o^\alpha h^\alpha)^\dagger E_\nu(1 + o^\alpha h^\alpha) + (h^\alpha)^\dagger E_\nu p h^\alpha + (1 + o^\alpha h^\alpha)^\dagger h^\alpha \end{aligned} \tag{1.45}$$

and

$$O^\alpha = (1 + o^\alpha h^\alpha)^\dagger(1 + o^\alpha h^\alpha) + (h^\alpha)^\dagger p h^\alpha. \tag{1.46}$$

There are no terms involving interstitial functions here because we are working in the ASA.

It is at this point useful to consider the transformation properties of the linear muffin tin orbital (LMTO). The easiest way to do this is to look again at (1.34),

$$|\chi_\nu^\alpha\rangle^\infty = |\psi_\nu^\gamma\rangle(1 + o^\alpha h^\alpha) + |\dot{\psi}_\nu^\gamma\rangle h^\alpha + |K^\alpha\rangle^i (N_\nu^\alpha)^{-1},$$

and to note that it is the screening parameter α that determines the coefficients of ψ_ν^γ and $\dot{\psi}_\nu^\gamma$ through the matching conditions. We shall assume that h^α is an invertible function of α for the range of α of interest to us, so the two are in one-to-one correspondence. Considering two different basis sets with screening matrices α and β, in the ASA, we have,

$$|\chi_\nu^\alpha\rangle^\infty = |\psi_\nu^\gamma\rangle(1 + o^\alpha h^\alpha) + |\dot{\psi}_\nu^\gamma\rangle h^\alpha$$

$$\text{and } |\chi_\nu^\beta\rangle^\infty = |\psi_\nu^\gamma\rangle(1 + o^\beta h^\beta) + |\dot{\psi}_\nu^\gamma\rangle h^\beta,$$

which can be rewritten as,

$$|\chi_\nu^\alpha\rangle^\infty (1 + o^\alpha h^\alpha)^{-1} = |\psi_\nu^\gamma\rangle + |\dot{\psi}_\nu^\gamma\rangle h^\alpha (1 + o^\alpha h^\alpha)^{-1}$$

$$\text{and } |\chi_\nu^\beta\rangle^\infty (1 + o^\beta h^\beta)^{-1} = |\psi_\nu^\gamma\rangle + |\dot{\psi}_\nu^\gamma\rangle h^\beta (1 + o^\beta h^\beta)^{-1}.$$

Now each left hand side is just an invertible linear combination of $|\chi_\nu^\alpha\rangle^\infty$ or $|\chi_\nu^\beta\rangle^\infty$ and so must correspond to some choice of screening matrix, ι and κ say. However, the coefficient of $|\dot{\psi}_\nu^\gamma\rangle$ is the same in both cases, so the ι and κ must be the same. Hence the transformation between bases with different screening constants is given by,

$$|\chi_\nu^\alpha\rangle^\infty (1 + o^\alpha h^\alpha)^{-1} = |\chi_\nu^\beta\rangle^\infty (1 + o^\beta h^\beta)^{-1} \tag{1.47}$$

and we also have,

$$h^\alpha (1 + o^\alpha h^\alpha)^{-1} = h^\beta (1 + o^\beta h^\beta)^{-1}. \tag{1.48}$$

The fact that there exists an invertible linear transformation between LMTO basis sets means that they are all equally good for the solution of (1.40), which was not the case for the energy dependent orbitals and the KKR equations (1.23) (Andersen, Pawlowska & Jepsen (1986)). This means that we are free to choose α so as to achieve a basis set with properties we want.

Looking again at (1.45) and (1.46) it is clear that these expressions may be simplified by a change of basis, in fact by exactly that change of basis used above on the α and β representations. The resulting basis corresponds to the γ basis of §1.4, as the coefficient of $|\psi_\nu^\gamma\rangle$ is unity (c.f. (1.16) and (1.19) with $N^\alpha = N^\gamma \equiv 1$). Evaluating (1.45) and (1.46) in this basis gives,

$$H^\gamma = E_\nu + h^\gamma + (h^\gamma)^\dagger E_\nu p h^\gamma \tag{1.49}$$

$$\text{and} \quad O^\gamma = 1 + (h^\gamma)^\dagger p h^\gamma. \tag{1.50}$$

From (1.50) we see that the orbitals χ_ν^γ are orthogonal to second order in h^γ. However, the γ basis has also a more important property which may be seen by expanding the P_ν terms from (1.33) using (1.21). We have (Andersen, Pawlowska & Jepsen, 1986),

$$\begin{aligned} P_\nu^\gamma = \frac{W(K^0,\psi_\nu^\gamma)}{W(J^\gamma,\psi_\nu^\gamma)} &= \frac{W(K^0,\psi_\nu^\gamma)}{W(K^0,\dot\psi_\nu^\gamma)}\frac{W(K^0,\dot\psi_\nu^\gamma)}{W(J^\gamma,\psi_\nu^\gamma)} \\ &= (E_\nu - C)\Delta^{-1}, \end{aligned} \tag{1.51}$$

where the second line follows from (1.27) and (1.28), and further,

$$\dot P_\nu^\gamma = \frac{W(J^\gamma,\psi_\nu^\gamma)W(K^0,\dot\psi_\nu^\gamma) - W(K^0,\psi_\nu^\gamma)W(J^\gamma,\dot\psi_\nu^\gamma)}{W(J^\gamma,\psi_\nu^\gamma)^2}.$$

Now $N_\nu^\gamma \equiv 1$ and so differentiating (1.20),

$$\begin{aligned} \dot N_\nu^\gamma = -\frac{W(K^0,J^\gamma)W(\dot\psi_\nu^\gamma,J^\gamma)}{W(\psi_\nu^\gamma,J^\gamma)^2} &= 0 \\ \Rightarrow \qquad W(\dot\psi_\nu^\gamma,J^\gamma) &= 0, \end{aligned}$$

where we have used the result $W(K^0, J^\gamma) = \frac{w}{2}$ (Andersen, Jepsen & Glötzel, 1985), where w is the average sphere radius. Hence,

$$\dot{P}_\nu^\gamma = \frac{W(K^0, \dot{\psi}_\nu^\gamma)}{W(J^\gamma, \psi_\nu^\gamma)}$$
$$\Rightarrow (\dot{P}^\gamma)^{-\frac{1}{2}} = \Delta^{\frac{1}{2}}. \tag{1.52}$$

Substituting (1.51) and (1.52) into (1.33) gives,

$$h^\gamma = -\Delta^{\frac{1}{2}} \left[\Delta^{-\frac{1}{2}}(E_\nu - C^\gamma)\Delta^{-\frac{1}{2}} - S^\gamma\right] \Delta^{\frac{1}{2}}$$
$$= -E_\nu + C^\gamma + \Delta^{\frac{1}{2}} S^\gamma \Delta^{\frac{1}{2}}. \tag{1.53}$$

Comparing with (1.29) it is clear that putting $H^\gamma = E_\nu + h^\gamma$ and $O^\gamma = 1$ we obtain an eigenvalue problem that agrees with the KKR-ASA method to order $(E - E_\nu)^2$. This means that h^γ is related to $(E - E_\nu)$ by a unitary transformation and the LMTO (1.34) may thus be regarded as the linear term in a Taylor expansion of $\chi^\gamma(E)$. It follows that the energies obtained by exact solution of (1.40) are therefore correct to *third order* in $(E - E_\nu)$ for any basis α. In all but the most recent programs, however, the equation that is solved uses the second order Hamiltonian $E_\nu + h^\gamma$, together with $O^\gamma = 1$: third order energies are then achieved using perturbation theory. The property (1.53) of the γ basis provides the benchmark for the accuracy of LMTO-ASA.

The γ-basis is not the only special basis that can be produced. By choosing the screening matrix α so as to obtain the maximum localisation of χ_ν^α one obtains the so-called "tight binding" basis β (Andersen & Jepsen, 1984). The chief advantage of this basis is that, owing to the rapid decay of χ_ν^β, the structure constants may be evaluated in real space. This avoids the time consuming Ewald summation that is necessary to evaluate them in k-space. In addition the

tight binding structure constants turn out to be virtually independent of the crystal symmetry, depending only on the scale of the structure. This enables calculations on amorphous materials to be done and it also allows for interpretation in terms of chemical bonding: the Hamiltonian can be broken down into "tranferable parameters" which depend only on atomic species, bond length and the L, L' quantum numbers. The program used for this thesis calculated the unscreened structure constants S^0 in k-space then transformed to the γ basis in the construction of the Hamiltonian. It therefore solved (1.53) as its eigenvalue problem. More modern implementations of LMTO-ASA tend to use the β-basis.

1.8) The Bloch representation.

When we are dealing with a crystalline material we know that we have a unit cell which is repeated infinitely many times. In this case, rather than considering the effects of each site individually on every other site, we can take a Bloch sum of orbitals over all sites and consider what the effect of the Bloch sum is on the single representative site for all values of $\mathbf{k}$.

If the unit cell contains more than one atom, and if the atoms are either different or are not related by a Bravais lattice vector, then we have a lattice with a basis. In this case we have to retain real space labels in order to distinguish the basis sites $\mathbf{r}$. A Bloch sum can only be produced for orbitals sited on a Bravais lattice. As a result, when we are evaluating the effects of the other atoms on a particular atom at site $\mathbf{r_0}$ we have to partition the other atoms into sets at equivalent basis positions $\mathbf{r}$. We then consider separately the effects of each Bloch sum, labelled by $\mathbf{r}$.

Taking $\mathbf{R}, \mathbf{R}'$ to be lattice vectors the LMTO (1.36) centred at point $\mathbf{r}$ is

given by,

$$|\chi^{\alpha}_{\mathbf{r}L}\rangle = |\psi^{\gamma}_{\mathbf{r}L}\rangle + \sum_{\mathbf{r}'\mathbf{R}L'} |\psi^{\alpha}_{(\mathbf{r}'+\mathbf{R})L'}\rangle h^{\alpha}_{(\mathbf{r}'+\mathbf{R})L',\mathbf{r}L}, \tag{1.54}$$

where from (1.35) we have,

$$|\psi^{\alpha}_{(\mathbf{r}'+\mathbf{R})L'}\rangle = |\dot{\psi}^{\gamma}_{(\mathbf{r}'+\mathbf{R})L'}\rangle + |\psi^{\gamma}_{(\mathbf{r}'+\mathbf{R})L''}\rangle o^{\alpha}_{(\mathbf{r}'+\mathbf{R})L'}, \tag{1.55}$$

and $\mathbf{r}'$ runs over all basis vectors in the unit cell. The Bloch sum $|\chi^{\alpha\mathbf{k}}_{\mathbf{r}L}\rangle$ of orbitals $|\chi^{\alpha}_{(\mathbf{r}+\mathbf{R})L}\rangle$ is given by,

$$\begin{aligned} |\chi^{\alpha\mathbf{k}}_{\mathbf{r}L}\rangle &= \sum_{\mathbf{R}'} |\chi^{\alpha}_{(\mathbf{r}+\mathbf{R}')L}\rangle e^{i\mathbf{k}.\mathbf{R}'} \qquad (1.56)\\ &= \sum_{\mathbf{R}'} |\psi^{\gamma}_{(\mathbf{r}+\mathbf{R}')L}\rangle e^{i\mathbf{k}.\mathbf{R}'} + \sum_{\mathbf{R}'} \sum_{\mathbf{r}'\mathbf{R}L'} |\psi^{\alpha}_{(\mathbf{r}'+\mathbf{R})L'}\rangle h^{\alpha}_{(\mathbf{r}'+\mathbf{R})L',(\mathbf{r}+\mathbf{R}')L} e^{i\mathbf{k}.\mathbf{R}'}. \end{aligned}$$

To find what this is in the sphere at $\mathbf{r}_0$ we note that the first term must give zero unless $\mathbf{r} = \mathbf{r}_0$ and $\mathbf{R}' = \mathbf{0}$, and the second must give zero unless $\mathbf{r}' = \mathbf{r}_0$ and $\mathbf{R} = \mathbf{0}$. Hence,

$$|\chi^{\alpha\mathbf{k}}_{\mathbf{r}L}\rangle_{\mathbf{r}_0} = |\psi^{\gamma}_{\mathbf{r}_0 L}\rangle \delta_{\mathbf{r}_0,\mathbf{r}} + \sum_{\mathbf{R}'L'} |\psi^{\alpha}_{\mathbf{r}_0 L'}\rangle h^{\alpha}_{\mathbf{r}_0 L',(\mathbf{r}+\mathbf{R}')L} e^{i\mathbf{k}.\mathbf{R}'}. \tag{1.57}$$

From (1.33) we have,

$$\begin{aligned} h^{\alpha}_{\mathbf{r}_0 L',(\mathbf{r}+\mathbf{R}')L} &= -(\dot{P}^{\alpha}_{\mathbf{r}_0 L'})^{-\frac{1}{2}} (P^{\alpha}_{\mathbf{r}_0 L'})(\dot{P}^{\alpha}_{\mathbf{r}_0 L'})^{-\frac{1}{2}} \delta_{\mathbf{r}_0,\mathbf{r}} \delta_{\mathbf{R}',\mathbf{0}} \delta_{L'L}\\ &\quad + (\dot{P}^{\alpha}_{\mathbf{r}_0 L'})^{-\frac{1}{2}} S^{\alpha}_{\mathbf{r}_0 L',(\mathbf{r}+\mathbf{R}')L} (\dot{P}^{\alpha}_{\mathbf{r}_0 L'})^{-\frac{1}{2}}, \qquad (1.58) \end{aligned}$$

and hence,

$$\begin{aligned} |\chi^{\alpha\mathbf{k}}_{\mathbf{r}L}\rangle_{\mathbf{r}_0} &= |\psi^{\gamma}_{\mathbf{r}_0 L}\rangle \delta_{\mathbf{r}_0,\mathbf{r}} - |\psi^{\alpha}_{\mathbf{r}_0 L}\rangle (P^{\alpha}_{\mathbf{r}_0 L})(\dot{P}^{\alpha}_{\mathbf{r}_0 L})^{-1} \delta_{\mathbf{r}_0,\mathbf{r}} \qquad (1.59)\\ &\quad + \sum_{L'} |\psi^{\alpha}_{\mathbf{r}_0 L'}\rangle (\dot{P}^{\alpha}_{\mathbf{r}_0 L'})^{-\frac{1}{2}} \sum_{\mathbf{R}'} S^{\alpha}_{\mathbf{r}_0 L',(\mathbf{r}+\mathbf{R}')L} e^{i\mathbf{k}.\mathbf{R}'} (\dot{P}^{\alpha}_{\mathbf{r}_0 L'})^{-\frac{1}{2}}. \end{aligned}$$

It is natural to define $S^{\alpha\mathbf{k}}_{\mathbf{r}_0 L',\mathbf{r}L}$ by (Andersen, Jepsen & Glötzel, 1985),

$$S^{\alpha\mathbf{k}}_{\mathbf{r}_0 L',\mathbf{r}L} = \sum_{\mathbf{R}'} S^{\alpha}_{\mathbf{r}_0 L',(\mathbf{r}+\mathbf{R}')L} e^{i\mathbf{k}.\mathbf{R}'}, \tag{1.60}$$

and $h^{\alpha\mathbf{k}}_{\mathbf{r}_0L',\mathbf{r}L}$ by (1.58) with $S^{\alpha\mathbf{k}}$ substituted for S^{α}. We then obtain,

$$|\chi^{\alpha\mathbf{k}}_{\mathbf{r}L}\rangle_{\mathbf{r}_0} = |\psi^{\gamma}_{\mathbf{r}_0L}\rangle\delta_{\mathbf{r}_0\mathbf{r}} + \sum_{L'} |\psi^{\alpha}_{\mathbf{r}_0L'}\rangle h^{\alpha\mathbf{k}}_{\mathbf{r}_0L',\mathbf{r}L}. \tag{1.61}$$

The significance of this lies in the similarity between (1.61) and (1.36). What this means is that the matrix elements (1.38) and (1.39) will have exactly same form in the Bloch representation as in real space so that the results of §1.7 (and in particular (1.53)) will be equally valid, with $S^{\alpha\mathbf{k}}$ substituted for S^{α}. The fact that (1.61) is a one centre expansion (i.e. concerns the sphere at $\mathbf{r}_0$ only) whereas (1.36) is multicentre is not significant, as a linear combination of (1.61) over $\mathbf{r}$ and L can always be broken down in terms of multicentre expansions.

1.9) The calculation of physical quantities.

There are a number of quantities that are usually demanded from a band-structure technique and these include the bandstructure itself, the density of states, the charge density, total energy, and perhaps also, the pressure. The bandstructure is straightforward to obtain: all that is necessary is to choose a path around the irreducible wedge of the Brillouin zone (indicated by the point group symmetry of the real space lattice), find E for a set of points along this path, and plot the curves. The pressure is a quantity that indicates a system's response to distortion and is dealt with fully in chapter 4. In this section we shall consider the calculation of the density of states, the charge density and the total energy, and for clarity we shall not include the summations over spin. In addition, the sum over basis points for a lattice with a basis will be implicit in all expressions.

The density of states, particularly when expressed in terms of its projections onto angular momentum, $n_l(E)$, provides a useful means of looking at electronic

behaviour, and it is also used in the calculation of the charge density. The standard method employed to calculate it in LMTO programs is the tetrahedron method (Jepsen & Andersen, 1971 ; Lehmann & Taut, 1972). This method is based on the formula,

$$n_{ll}(E) = \frac{1}{8\pi^3} \int_{E(\mathbf{k})=E} \frac{dS}{|\nabla_{\mathbf{k}} E|} A_l(\mathbf{k}), \tag{1.62}$$

where,

$$A_l(\mathbf{k}) = \sum_m |u_{lm}|^2, \tag{1.63}$$

are called the angular momentun weights and $\mathbf{u}$ is the eigenvector at $E(\mathbf{k}) = E$. It also uses the fact that, knowing the values of $E(\mathbf{k})$ and $A_l(\mathbf{k})$ for a set of k-points forming the vertices of a tetrahedron, it is possible to derive linear interpolation expressions for these quantities within the tetrahedron. What is done therefore is to choose the set of k-points for which E is to be calculated so as to divide up the irreducible wedge into a set of tetrahedra. To obtain good results these tetrahedra must be as regular as possible. The contributions from each of the tetrahedra are then just added up. Of course, one has to index the k-points and keep track of which tetrahedra each one is associated with, and there are other complications relating to how the energies and A_l can be ordered at the vertices of a tetrahedron, but the problem is essentially one of book-keeping.

In ASA calculations it is only the spherically averaged charge density that is usually calculated as this is all that is needed for an ASA self-consistency loop. We define the spherical density per spin, $n(r)$, by (Andersen, Jepsen & Glötzel, 1985),

$$4\pi n(r) = \sum_l \int^{E_f} \phi_l(E,r)^2 n_{ll}(E) dE. \tag{1.64}$$

Here $\phi_l(E,r)$ is the radial component of the partial wave $\psi_l(E,\mathbf{r})$ in the sphere. It is evident that with unit normalisation of the spherical harmonics the integral of $|\psi_l(E,\mathbf{r})|^2$ over the sphere will come to the right hand side of (1.64), and the factor of 4π arises because $n(r)$ is defined as a density over the sphere. Expanding $\phi_l(E,r)$ as a Taylor series in $(E-E_\nu)$ and defining the energy moments $m_l^{(q)}$ by,

$$m_l^{(q)} = \int^{E_f} (E-E_\nu)^q n_{ll}(E)dE, \tag{1.65}$$

we can rewrite (1.64) as,

$$4\pi n(r) = \sum_l \left[m_l^{(0)}\phi_\nu(r)^2 + 2m_l^{(1)}\phi_\nu(r)\dot{\phi}_\nu(r) + m_l^{(2)}(\dot{\phi}_\nu(r)^2 + \phi_\nu(r)\ddot{\phi}_\nu(r)) \right] + O(E-E_\nu)^3. \tag{1.66}$$

It can be recognised from (1.65) that $m_l^{(0)}$ is in fact the l-projection of the number of states function. Thus the second two terms in (1.66) must be responsible only for the redistribution of charge, and cannot contribute overall charge to the sphere. In practice (1.66) is generally taken to third order.

The total energy expression used in most LMTO programs is essentially the second line of (2.13), with the non-spherical density replaced by the spherically averaged version, $n(r)\,4\pi r^2$. Specifically, we have (Andersen, Jepsen & Glötzel, 1985; Andersen, Jepsen & Sob, 1987),

$$E_{\rm tot} = \int V(r)n(r)4\pi r^2 dr + \frac{1}{2}\int\int \frac{n(r)n(r')4\pi r'^2}{|\mathbf{r}-\mathbf{r}'|} dr'\, 4\pi r^2 dr + T_s[n] + E_{xc}[n], \tag{1.67}$$

where (c.f. 2.12),

$$T_s[n] = \int^{E_f} EN(E)dE - \int v_{\rm eff}(r)n(r)4\pi r^2 dr. \tag{1.68}$$

The potential $v_{\text{eff}}(r)$ is the effective one electron potential calculated from the spherical density, while $V(r)$ (the external potential) is just the electrostatic field from the nucleus and is given by,

$$V(r) = -\frac{Z}{r}, \tag{1.69}$$

where Z is the atomic number. It is clear that (1.67) can be rearranged to give,

$$E_{\text{tot}} = T + U, \tag{1.70}$$

where

$$U = \int n(r) \left[\epsilon_{\text{xc}}[n(r)] - \frac{Z}{r} + \frac{1}{2} \int \frac{n(r') 4\pi r'^2 dr'}{|\mathbf{r} - \mathbf{r}'|} \right] 4\pi r^2 dr. \tag{1.71}$$

In practice, in a lattice containing inequivalent atoms, the atomic spheres may not be electrically neutral and we should add an intersphere term to the sum over basis sites implicit in (1.71). This term is,

$$\frac{1}{2} \sum_{\mathbf{R} \neq \mathbf{R}'} \frac{z_{\mathbf{R}} z_{\mathbf{R}'}}{|\mathbf{R} - \mathbf{R}'|}, \tag{1.72}$$

where $z_{\mathbf{R}}$ is the charge on the sphere centred at **R**. In addition, where the frozen core approximation is being used, $n(r)$ will be a sum of a static core term $n_c(r)$ and a valence term $n_v(r)$ given by (1.66) (Gunnarsson, Harris & Jones, 1977).

CHAPTER TWO: DENSITY FUNCTIONAL THEORY.

2.1) Introduction.

In this chapter we shall adopt the idea of working with the electron density as the basic variable, only to then drop this approach and go back to the usual wave function formalism. However, in so doing we shall introduce quantities which in principle at least can take care of exchange and correlation exactly, and which in practice can be approximated with some feel for the scope and validity of the approximation. This theory will enable us to deal in a systematic way with exchange and correlation, but without going beyond the one-electron framework.

2.2) Basic formalism.

The basis of density functional theory lies in two theorems found in a much cited paper (Hohenberg & Kohn, 1964). The system being dealt with consists of N enclosed electrons moving in an external potential $V(\mathbf{r})$. The Hamiltonian for the system is given by,

$$\begin{aligned}\hat{H} &= \hat{T} + \hat{U} + \hat{V} \\ &= \sum_{i=1}^{N}\left(-\frac{1}{2}\nabla_i^2\right) + \frac{1}{2}\sum_{i\neq j}\frac{1}{|\mathbf{r_i}-\mathbf{r_j}|} + \sum_{i=1}^{N} V(\mathbf{r_i}) \qquad (2.1)\end{aligned}$$

Here $\hat{T}$ is the kinetic energy operator, $\hat{U}$ the Coulomb repulsion between electrons, and the units employed are atomic ones. In the first theorem it is shown that, for a non-degenerate ground state Ψ with corresponding electron density $n(\mathbf{r})$, the external potential is a unique functional of $n(\mathbf{r})$, up to an additive constant. Now with $V(\mathbf{r})$ specified the Hamiltonian of the system is specified and hence the ground state Ψ. So a given charge density $n(\mathbf{r})$ determines a unique

ground state. The significance of this is that we know that we can legitimately use $n(\mathbf{r})$ as the basic variable in the determination of the ground state: there are no other variables which we need consider.

The second theorem in the Hohenberg-Kohn paper goes on to indicate how we might go about determining the ground state. We know from conventional quantum mechanics that the energy, as a functional of the ground state wave function Ψ and subject to the conservation of electron number, is minimal at the ground state. Now as all ground state properties are functionals of $n(\mathbf{r})$ we can write the energy functional as,

$$E[n] = \int V(\mathbf{r})n(\mathbf{r})d\mathbf{r} + F[n], \tag{2.2}$$

where F[n] is the sum of the kinetic and interaction energies. The second theorem states that, written in the form (2.2) and subject to the same conservation condition, the energy is minimal at the ground state density. Hence we may use the variational principle as a tool in determining the ground state density.

Knowing that we can use the variational principle to find $n(\mathbf{r})$ we can immediately write down the equation:

$$\delta\left\{\int V(\mathbf{r})n(\mathbf{r})d\mathbf{r} + F[n] - \mu\int n(\mathbf{r})d\mathbf{r}\right\} = 0.$$

$$\Rightarrow V(\mathbf{r}) + \frac{\delta F[n]}{\delta n(\mathbf{r})} - \mu = 0. \tag{2.3}$$

Here μ is a Lagrange multiplier whose value is chosen so as to obtain,

$$\int n(\mathbf{r})d\mathbf{r} = N. \tag{2.4}$$

This is all very well but for practical purposes we still don't know what the functional $F[n]$ is and in fact, since $F[n]$ contains all the unknown many-body

effects, we have little hope of ever determining it exactly. It is this problem that is considered in a second classic paper (Kohn & Sham, 1965). What Kohn and Sham do first is to split off from $F[n]$ what can be considered as the "easy bits" by writing:

$$F[n] = \frac{1}{2}\int\int \frac{n(\mathbf{r})n(\mathbf{r}')}{|\mathbf{r}-\mathbf{r}'|}d\mathbf{r}\,d\mathbf{r}' + T_s[n] + E_{xc}[n]. \tag{2.5}$$

Here the first term is just the Hartree term written in terms of the electron density, the second is the kinetic energy of a gas of non-interacting electrons with density $n(\mathbf{r})$, and the third is the correction which makes the $F[n]$ the same as that in (2.2). This term must contain all the unknown exchange and correlation effects and we rely on it being small compared with the others. To handle $E_{xc}[n]$ the "local density approximation" (LDA) is introduced. This consists of writing,

$$E_{xc}[n] = \int n(\mathbf{r})\varepsilon_{xc}[n(\mathbf{r})]d\mathbf{r}, \tag{2.6}$$

where ε_{xc} is the exchange-correlation energy density (i.e. energy per electron) of a uniform electron gas of density $n(\mathbf{r})$. This is something that can be calculated (von Barth & Hedin, 1972; Hedin & Lundquist, 1971). The variational equation (2.3) now becomes,

$$V(\mathbf{r}) + \int \frac{n(\mathbf{r}')}{|\mathbf{r}-\mathbf{r}'|}d\mathbf{r}' + \frac{\delta T_s[n]}{\delta n(\mathbf{r})} + v_{xc}[n] - \mu = 0, \tag{2.7}$$

where,

$$v_{xc}[n] = \frac{d\{n\varepsilon_{xc}[n]\}}{dn}, \tag{2.8}$$

the so-called exchange-correlation potential. We thus have an equation in which all the input is known apart from $T_s[n]$. However, we know very well what T_s is as a single-particle operator so what Kohn and Sham do next is to reformulate

(2.7) in the good, old Schrödinger representation. They do this by noticing that (2.7) also represents the problem of finding the ground state of a system of N independent electrons subject to an effective potential $v_{\rm eff}$ given by,

$$v_{\rm eff}(\mathbf{r}) = v(\mathbf{r}) + \int \frac{n(\mathbf{r}')}{|\mathbf{r}-\mathbf{r}'|} d\mathbf{r}' + v_{xc}(\mathbf{r}). \tag{2.9}$$

This can be seen by simply putting $V(\mathbf{r}) = v_{\rm eff}(\mathbf{r})$ in (2.3), regarding $v_{\rm eff}(\mathbf{r})$ as independent of $n(\mathbf{r})$, and $F[n] = T_s[n]$ in (2.5). In terms of single-particle wave functions this is equivalent to solving:

$$\left[-\frac{1}{2}\nabla^2 + v_{\rm eff}(\mathbf{r})\right]\psi_i = \epsilon_i \psi_i, \tag{2.10}$$

with,

$$n(\mathbf{r}) = \sum_{i=1}^{N} |\psi_i(\mathbf{r})|^2. \tag{2.11}$$

The ϵ_i are Lagrange multipliers which ensure that the ψ_i are normalised to unity so that the integral of $n(\mathbf{r})$ really does add up to N. Once (2.10) is solved we can calculate a new $v_{\rm eff}(\mathbf{r})$ using (2.11) and (2.9), so it is clear that what we have arrived at is a self-consistency problem.

To obtain an expression for the ground state energy E in terms of the output of our self-consistency calculations we now use (2.10) and (2.11) together with the unit normalisation of the ψ_i to get:

$$\begin{aligned} [(-\nabla^2) + v_{\rm eff}(\mathbf{r})]\psi_i(\mathbf{r}) &= \epsilon_i \psi_i(\mathbf{r}) \\ \Rightarrow \int \psi_i^*(\mathbf{r})(-\nabla^2)\psi_i(\mathbf{r})d\mathbf{r} + \int \psi_i^*(\mathbf{r}) v_{\rm eff}(\mathbf{r})\psi_i(\mathbf{r})d\mathbf{r} &= \epsilon_i \\ \Rightarrow T_s[n] + \int v_{\rm eff}(\mathbf{r}) n(\mathbf{r}) d\mathbf{r} &= \sum_{i=1}^{N} \epsilon_i. \end{aligned} \tag{2.12}$$

Now the energy E is given by,

$$
\begin{aligned}
E &= \int V(\mathbf{r})n(\mathbf{r})d\mathbf{r} + F[n] \\
&= \int V(\mathbf{r})n(\mathbf{r})d\mathbf{r} + \frac{1}{2}\int\int \frac{n(\mathbf{r})n(\mathbf{r}')}{|\mathbf{r}-\mathbf{r}'|}d\mathbf{r}d\mathbf{r}' + T_s[n] + E_{xc}[n] \\
&= \int v_{\text{eff}}(\mathbf{r})n(\mathbf{r})d\mathbf{r} - \frac{1}{2}\int\int \frac{n(\mathbf{r})n(\mathbf{r}')}{|\mathbf{r}-\mathbf{r}'|}d\mathbf{r}d\mathbf{r}' \\
&\qquad - \int v_{xc}(\mathbf{r})n(\mathbf{r})d\mathbf{r} + T_s[n] + E_{xc}[n], \quad (2.13)
\end{aligned}
$$

where we have used (2.9) to introduce $v_{\text{eff}}(\mathbf{r})$. Substituting from (2.12) into (2.13) we end up with:

$$
E = \sum_{i=1}^{N} \epsilon_i - \frac{1}{2}\int\int \frac{n(\mathbf{r})n(\mathbf{r}')}{|\mathbf{r}-\mathbf{r}'|}d\mathbf{r}d\mathbf{r}' - \int v_{xc}(\mathbf{r})n(\mathbf{r})d\mathbf{r} + E_{xc}[n]. \qquad (2.14)
$$

The second and third terms in (2.14) are called double-counting terms. They arise whenever an interacting system is dealt with using an effective single particle Hamiltonian because in such schemes the interaction energy between any pair of particles is included twice in $v_{\text{eff}}(\mathbf{r})$.

2.3) Further discussion.

An obvious question to ask about the scheme presented so far is, "to what extent is the LDA a good approximation to $E_{xc}[n]$?" In the final analysis the justification for the LDA is practical: it generally works well and the cases for which it doesn't are well known. The cases for which it doesn't work are in highly-localised systems, just outside metal surfaces and where van der Waals' interactions are important. The reason for the failure in the case of highly localised systems is evident: in such systems the many-body effects will be strong and the one-electron equation will be dominated by v_{xc}, so any approximation to it will not work. In fact the whole one-electron formalism is then inappropriate.

In the latter two cases the failure is blamed on non-local effects, which clearly cannot be handled using a local approximation. However, there is still a very large number of systems for which the LDA is successful. Why does it work so well?

Probably the best known explanation for the success of the LDA employs the so-called exchange-correlation hole (see e.g. Kohn & Vashishta, 1983). This consists of a region of electron depletion which surrounds every electron due to exchange and correlation effects. It turns out that if one works out the energy due to the Coulomb attraction of the electrons and exchange-correlation holes it comes to none other than the exchange-correlation energy $E_{xc}[n]$. It was shown by Gunnarson & Lundquist (1976) that the expression for $E_{xc}[n]$ depends on the amount of charge in the exchange-correlation hole, and is relatively insensitive to its shape. So the degree of homogeneity of an electron gas is usually a small factor in determining $E_{xc}[n]$.

Density functional theory is based on the variational principle as applied to the ground state. Therefore the eigenvalues ϵ_i of the one electron equation only have significance in as far as their sum is related to the ground state energy: with a single exception, they are not related to excitation energies. A consequence of this is that the band structure obtained is useful for the investigation of ground state properties but not for properties that depend on excitations. A well-known shortcoming of density functional theory is its failure in predicting the band gap of insulators: the difference between the first unoccupied level and the last occupied one is typically only 50% of the experimental band gap. The reason for the failure is that the band gap is the difference between the

lowest excited state and the highest occupied one, and the former is *not* given by the first unoccupied ϵ_i. The one exception mentioned applies to the highest occupied ϵ_i, which is related to the ionisation energy of the material.

There are also a number of formal problems which deserve a mention. First of all the proofs of the two Hohenberg-Kohn theorems depend on the ground state being non-degenerate and assume the existence of a potential corresponding to every possible charge density. Secondly the Kohn-Sham results assume that any charge density can be realised by a non-interacting system and is expressible in the form (2.11). These assumptions, although to some extent circumvented by more modern (and less accessible!) formulations of the theory (see e.g. Levy, 1982), can all in principle lead to problems. In practice the working hypothesis is that for any reasonably smooth $n(\mathbf{r})$ this sort of thing will not cause any trouble.

2.4) Systems with spin.

The theory so far has not contained any spin labels and therefore applies only to systems that are spin degenerate. The extension of the theory to non-degenerate systems is straighforward but in order to allow for the fact that the spin polarisation may point in different, non-collinear directions in different regions the basic variable is now the ***density matrix*** in spin space. This may be defined as,

$$n_{\alpha\beta}(\mathbf{r}) = \sum_{E_i<E_f} \psi_\alpha^{(i)}(\mathbf{r})\psi_\beta^{(i)}(\mathbf{r}), \tag{2.15}$$

where $\alpha, \beta \in \{-\frac{1}{2}, \frac{1}{2}\}$ are the spin labels for an electron and $\psi_\alpha^{(i)}$, $\psi_\beta^{(i)}$ are the spin components of the i th single particle wave functions. Clearly, in a collinear system where all states must be either parallel or antiparallel to a common spin

axis the density matrix will be diagonal. The spin dependent, external potential must also be represented by a matrix, which we shall call $W_{\alpha\beta}(\mathbf{r})$.

The two Hohenburg-Kohn theorems are readily extended to the spin polarised density matrix, with the normalisation condition (2.11) now given by,

$$\sum_{\alpha} \int d\mathbf{r}\, n_{\alpha\alpha}(\mathbf{r}) = N. \tag{2.16}$$

The Kohn-Sham theory also goes through, but with a number of modifications. The local density approximation now consists of writing (c.f. 2.6),

$$E_{\mathrm{xc}}[n_{\alpha\beta}] = \int d\mathbf{r}\, \left(n^{+}(\mathbf{r}) + n^{-}(\mathbf{r})\right) \epsilon_{\mathrm{xc}}\left[n^{+}(\mathbf{r}), n^{-}(\mathbf{r})\right], \tag{2.17}$$

where $n^{+}(\mathbf{r})$, $n^{-}(\mathbf{r})$ are the spin up and spin down densities relative to the *local* spin axis in the volume element at $\mathbf{r}$. The relation between $n_{\alpha\beta}$ and $n^{\pm}$ is given by the rotation in spin space that maps the spin dependence relative to (what has been chosen as) the reference axis to that relative to the local axis (§3.7). The function $\epsilon_{\mathrm{xc}}\left[n^{+}, n^{-}\right]$ is again estimated from a uniform spin polarised electron gas. The definition of $v_{\mathrm{xc}}[n_{\alpha\beta}]$ is analogous to (2.8),

$$v_{\mathrm{xc}}[n_{\alpha\beta}] = \frac{dE_{\mathrm{xc}}[n_{\alpha\beta}]}{d_{\alpha\beta}(\mathbf{r})}. \tag{2.18}$$

The single particle equations are given by,

$$\sum_{\beta}\left[\delta_{\alpha\beta}(-\frac{1}{2}\nabla^2) + w^{\mathrm{eff}}_{\alpha\beta}(\mathbf{r})\right]\psi^{(i)}_{\beta}(\mathbf{r}) = \epsilon_i \psi^{(i)}_{\alpha}(\mathbf{r}), \tag{2.19}$$

$$\text{where} \quad w^{\mathrm{eff}}_{\alpha\beta}(\mathbf{r}) = W_{\alpha\beta}(\mathbf{r}) + \delta_{\alpha\beta}\sum_{\gamma}\int \frac{n_{\gamma\gamma}(\mathbf{r}')}{|\mathbf{r}-\mathbf{r}'|} + v^{\alpha\beta}_{\mathrm{xc}}(\mathbf{r}), \tag{2.20}$$

(c.f. 2.10 and 2.9) and γ is a dummy variable. Here the $\delta_{\alpha\beta}$s occur because the kinetic energy and Coulomb repulsion of the electrons are both independent of spin. In the collinear spin case, where the off-diagonal elements of $n_{\alpha\beta}$ are

zero, the off-diagonal elements of $w_{\alpha\beta}$ must also be zero and equations (2.19) uncouple to give an independent equation for each spin direction.

The above extension of the Hohenburg-Kohn-Sham theory was first proposed by von Barth & Hedin (1972) who also provided parameterised forms of ϵ_{xc} and v_{xc} for the spin polarised electron gas. The theory has been extensively used in band structure calculations on collinear magnetic systems (§3.2) and has recently (Kübler, Höck, Sticht & Williams, 1987) been applied to non-collinear systems using the linear augmented spherical wave method. Here the calculations were made tractable by adopting the ASA and assuming that there exists a local spin direction for *each atomic sphere*, rather than for each of an impossibly large number of small volume elements. The theory will be further applied, within LMTO-ASA, in the next chapter.

CHAPTER 3: NON-COLLINEAR MAGNETISM IN Mn & Fe.

3.1) Introduction.

In this chapter we shall look at the magnetic structures which are thought to exist in the γ (FCC) phases of manganese and iron. We shall pick out three particularly symmetric structures from those possible, two of which will involve non-collinear spin directions. The existence of these structures as possible ground states will be shown to be linked to the frustrated nature of an antiferromagnet on an FCC lattice. For the first time, a standard LMTO-ASA program will be modified to handle non-collinear configurations. This will be used to investigate the relative stabilities of the three structures, and their tendency to distort tetragonally. It will be found that, at least for manganese, the results can be interpreted reasonably well using a localised spin model.

In §3.2 a brief introduction is given to magnetism in solids and in §3.3 the plausibility of the non-collinear spin structures will be demonstrated using the classical limit of the Heisenberg model. Sections 3.4 and 3.5 are devoted to the experimental and theoretical work that has already been done, while §3.6 gives an overview of the problems involved in dealing with non-collinear systems, and with Mn and Fe in particular. In §3.7 we consider the description of the potential in a non-collinear system and in §3.8 we look at the crystal structure dependence. Section 3.9 is devoted to the problem of representing non-collinear structures on an FCC lattice and an algebraic solution is presented. This form of representation is a new result and its implementation in a standard LMTO code is discussed in §3.10. In §3.11 the band structures and associated information are presented and a partial interpretation is given using the theory of localised

orbitals. Finally, with the techniques of the next chapter in mind, in §3.12 we look at the tetragonal distortions that are observed in these systems. These will be explained in terms of the tendency of the system to unfrustrate, and theoretical predictions will be made based on the LMTO calculations. These predictions will be shown to be in surprisingly good agreement with experiment.

3.2) Background to magnetism.

The magnetic behaviour of electrons in isolated atoms can generally be predicted using Hund's rules (Ashcroft & Mermin, 1976). In a solid, however, the situation is more complicated because there is another important factor at work: delocalisation. In terms of tight binding language this is the energy saving that can be gained when there is an overlap between the orbitals of two electrons. The total energy saving in a given structure is therefore a balance between those possible through exchange and through delocalisation. If exchange is bigger we retain the atomic picture of what's going on, perturbed by bandstructure effects. This is to a large extent what happens for f-electrons in rare earth metals (Elliott, 1972). In transition elements the d-electrons tend to delocalise more strongly. In this case an observed moment cannot necessarily be ascribed to an inherent atomic one and it may be more profitable to approach the problem through the magnetic ordering.

The existence of ferromagnets can be justified on energy grounds, and the result obtained is the "Stoner criterion" for a ferromagnet (White, 1983; Pettifor, 1977). To convert a paramagnetic solid into a ferromagnet we have to flip the spins of some of the electrons. To obtain a moment m we have to place $\frac{1}{2}m$ of the spin down electrons, say, into spin up states. Suppose that m is

sufficiently small that the density of states at the Fermi level, $n = n(E_f)$, can be considered the same before and after the spin flip. There must then be a penalty in bandstructure energy of $\frac{1}{4}\frac{m^2}{n}$ (figure 3.1). This is so because each flipped electron must gain $\frac{1}{2}\frac{m}{n}$ in bandstructure energy and there are $\frac{1}{2}m$ electrons flipped. Energy is got back through exchange: electrons of the same spin are kept apart by Pauli exclusion and contribute less to the Coulomb energy. In the Hubbard model (Callaway, 1974; Jones & March, 1973) the saving due to the magnetism can be written as $\frac{1}{4}Im^2$, where I is the Stoner (or Hubbard) parameter. The total change in energy due to the spin flip is therefore,

$$\frac{1}{4}\frac{m^2}{n}(1 - In).$$

The Stoner criterion for instability to ferromagnetic ordering is hence,

$$In > 1 \qquad (3.1).$$

In materials with more complicated magnetic structures the energy justification of the magnetic ordering is not so straightforward. In principle, the most stable configuration can always be predicted from a calculation of the susceptibility, $\chi(\mathbf{q})$, to spin density waves of wave vector $\mathbf{q}$ (Young, 1975). Here, $\chi(\mathbf{0})$ corresponds to ferromagnetism while $\chi(\mathbf{q})$, $\mathbf{q} \neq 0$, correspond to the possible AF orderings. However, for $\mathbf{q} \neq \mathbf{0}$ the calculation of $\chi(\mathbf{q})$ in a realistic model is difficult, and calculations are often done using simplified models. In particular, Heine & Samson (1983) have shown theoretically that for a single tight-binding band the function $\chi(\mathbf{0}) - \chi(\mathbf{q})$ has two zeroes in the band as a function of the chemical potential. This means that the more favourable magnetic state must follow either of the sequences F-AF-F or AF-F-AF as the chemical potential

Figure 3.1: band splitting in Stoner theory.

(from Pettifor, 1977)

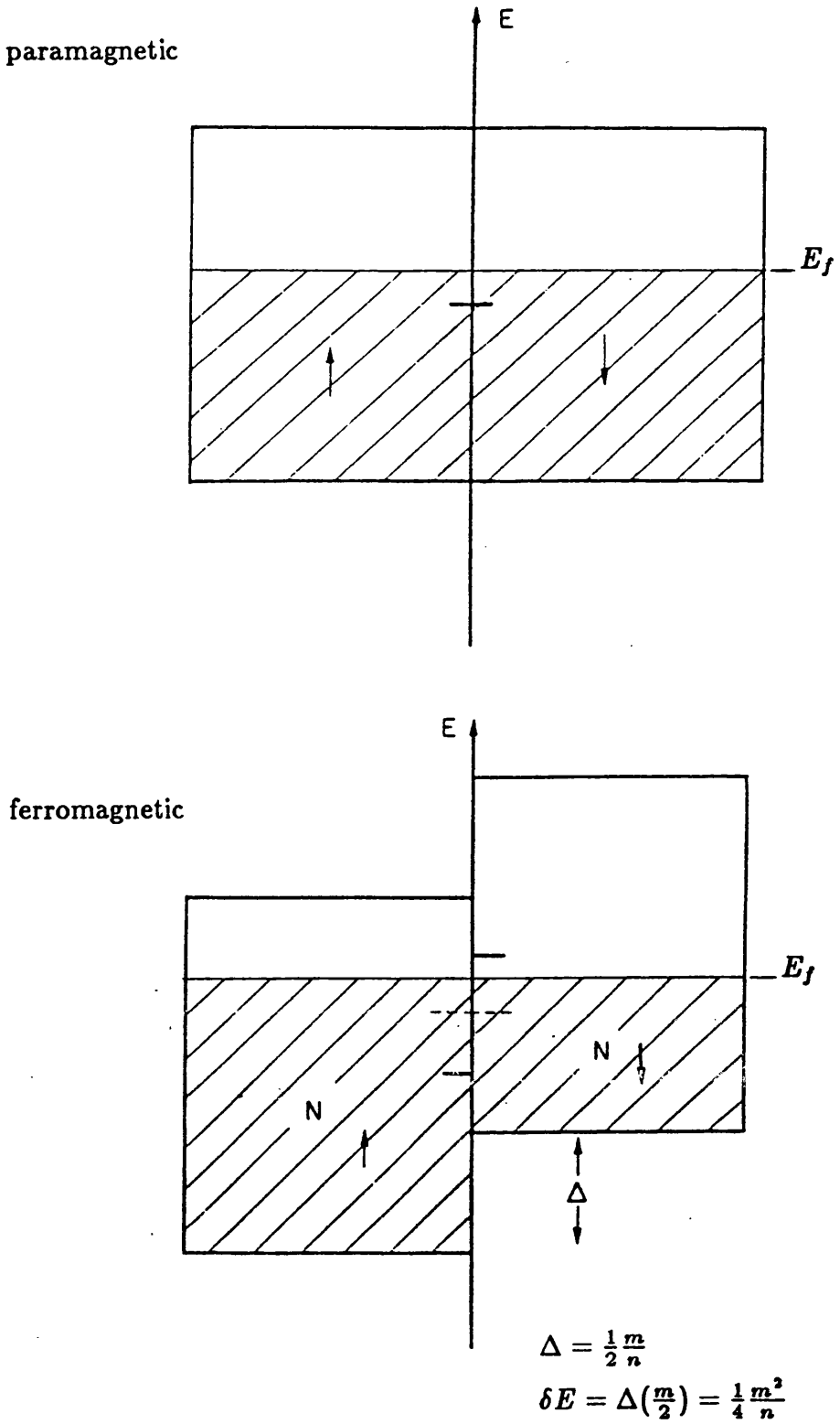

passes through the band. Using a Hubbard model Long & Yeung (1986) have shown that the probable sequence is F-AF-F and they also showed that, in a certain integral sense, antiferromagnetism is just as likely in general as ferromagnetism.

So far we have considered when a system may be susceptible to F or AF ordering but the electronic processes responsible for the ordering (and hence for the form of $\chi(\mathbf{q})$) have not been touched upon. There are a number of forms of "exchange" mechanism postulated, each most relevant for particular types of system. The RKKY interaction (Ziman, 1972) is based on the idea that a relatively localised electron can cause long-range oscillations in the spin polarisation of less localised "conduction" electrons. This can give rise to either F or AF ordering, depending on factors such as the degree of localisation of the localised electrons involved, and the density of the conduction electrons. It is a generally accepted mechanism for the antiferromagnetism of many metallic rare-earth systems. A mechanism relevant to fairly localised *d*-states in transition metals and driven by delocalisation is kinetic exchange (Mattis, 1981). This can be understood by noting that hopping always occurs between states of the same spin and that the Pauli principle precludes hopping between states that are both full. Hopping energy can therefore be gained by neighbouring atoms having opposite spin polarisation (figure 3.2). A similar process occurs in insulating compounds of transition metals and is called superexchange (Anderson, 1959). Here the driving force is again delocalisation, but the interaction occurs via an intermediate paramagnetic ion (e.g. O^{2-}). The situation is depicted in figure 3.3.

Figure 3.2: moment ordering by kinetic exchange.

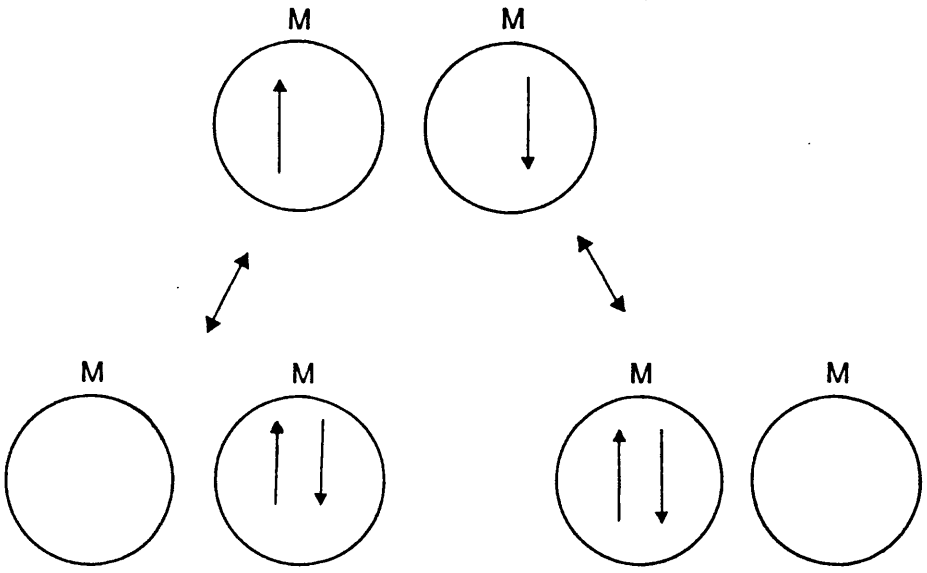

M = metal atom

Figure 3.3: moment ordering by superexchange.

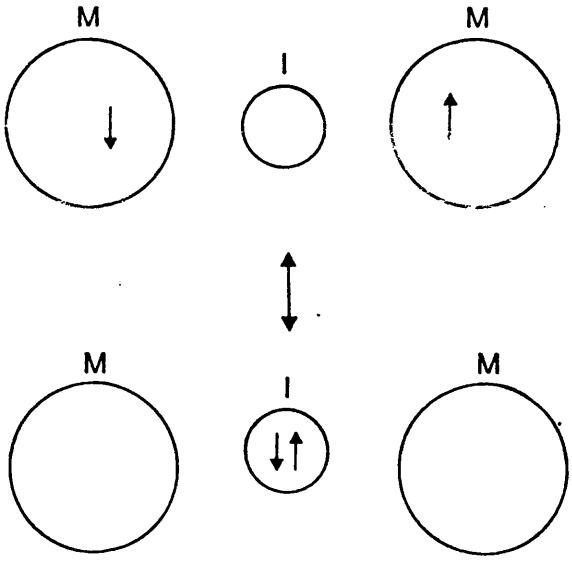

M = metal atom
I = paramagnetic ion

In addition to the above, there is also an AF mechanism that is specific to itinerant electrons and which is probably responsible for the antiferromagntism of chromium (Lomer, 1962). It is based on the fact that when a spin density wave occurs it must give rise to a corresponding oscillation in the (spin dependent) potential. The effect of this is to split the energies of Bloch waves that differ by the wave vector $\mathbf{q}$ of the oscillation, opening gaps in the bandstructure. This behaviour can be predicted using nearly free electron theory (Ashcroft & Mermin, 1976). If the Fermi surface happens to lie significantly in these gaps then energy is saved and the spin density wave is stabilised. The way to identify this mechanism in a real material is to look for large areas of electron and hole Fermi surface that can be mapped on to one another by a vector $\mathbf{q}$, a situation known as "nesting". This is precisely what is found for chromium, and it has also been postulated as a mechanism for the magnetism of γ-Mn (Arrott, 1966) and γ-Fe (Endoh & Ishikawa, 1971).

Magnetism is easiest to describe in the limits where it is caused by either well localised or well delocalised electrons. The models appropriate to these limits are the Heisenberg model and the band model respectively. The Heisenberg Hamiltonian (Jones & March, 1973) is given by,

$$\hat{H} = \sum_{\mathbf{i,j}} J_{\mathbf{ij}}\, \hat{\mathbf{S}}_{\mathbf{i}}.\hat{\mathbf{S}}_{j}, \tag{3.2}$$

where $\hat{\mathbf{S}}_{\mathbf{i}}$ is the spin operator for the electron at the i-th site, and $J_{\mathbf{ij}}$ is the Heisenberg exchange parameter. Clearly, if $J_{\mathbf{ij}}$ is negative then ferromagnetic ordering is favourable between electrons i and j, while if it is positive then antiferromagnetism is favoured. For well delocalised electrons the effective single electron Schrödinger equation (1.1) may be a suitable starting point for calcu-

lations. Band theory, performed within the spin density functional formalism (§2.4), has been applied to both F (e.g. Poulsen, Kollar & Andersen, 1976) and AF (e.g. Cade, 1980) systems. It has been particularly successful for transition metals and tends to fall down only with systems involving very localised electrons, and in Mott insulators. The advantage of the localised picture is that it lends itself readily to real space interpretation, and hence to simple physical pictures.

3.3) Frustrated magnetic systems.

In a ferromagnet it is energetically favourable for nearest neighbours to be aligned with parallel spins and it is clear that such an arrangement can be produced in any sort of lattice. With antiferromagnetism, however, this is not the case and the crystal lattices can be divided up according to whether the magnetism would be unfrustrated or frustrated. In an unfrustrated system the spins can be chosen so as to give each site a set of nearest neighbours with the opposite spin whereas in a frustrated system it cannot. The simplest example of a frustrated lattice is the two dimensional triangular lattice. This can be seen to be frustrated simply by drawing a triangle and marking an up-spin on one vertex and a down-spin on another: the third spin cannot then be chosen to be opposite to both of those already marked. More relevant here is the FCC lattice (Long, 1989). This lattice is frustrated because it can be built up from a layering of 2-d triangular lattices (Ashcroft & Mermin, 1976). It is interesting to compare the FCC with the BCC structure shown in figure 3.4, which is unfrustrated. It can be seen that the BCC structure is layered simultaneously in all three lattice directions, so that the neareat neighbours of a given atom can always be chosen

to be of the opposite spin. If we try to layer the FCC structure in this this way we find that it can only be done in one direction (figure 3.5).

The previous argument for the FCC lattice has assumed that all spins are either parallel or antiparallel to a common axis. However, given that this collinear arrangement gives no atom a completely favourable spin environment it is reasonable to consider the possible non-collinear structures. In fact, these arise quite naturally in frustrated systems, as can be shown by applying the Heisenberg model (3.2), in its classical limit, to the FCC lattice. The classical limit is the one in which $|\mathbf{S}_i| \to \infty$, and the spin operators $\mathbf{S}_i$ can be replaced by functions. Setting the parameter J independent of site the Heisenberg Hamiltonian can be written as,

$$H = J \sum_{<ij>} \mathbf{S}_i.\mathbf{S}_j, \tag{3.3}$$

where i runs over the set of sites, and j represents the nearest neighbours of site i for each site in turn. Given that we are interested in structures in which all spins are of the same magnitude we must impose the following condition on the spins,

$$\mathbf{S}_i.\mathbf{S}_i = S^2. \tag{3.4}$$

The Fourier transform of $\mathbf{S}_i$ is given by,

$$\begin{aligned} \mathbf{S}_i &= \sum_{\boldsymbol{k}} e^{i\mathbf{k}.\mathbf{R}_i} \mathbf{S}_{\mathbf{k}} \\ \text{and } \mathbf{S}_{\mathbf{k}} &= \frac{1}{N} \sum_i e^{-i\mathbf{k}.\mathbf{R}_i} \mathbf{S}_i, \end{aligned} \tag{3.5}$$

where N is the number of sites, and the Hamiltonian can be rewritten as,

$$\begin{aligned} H &= J \sum_{<ij>} \sum_{\mathbf{kk'}} e^{i\mathbf{k}.\mathbf{R}_i} e^{i\mathbf{k'}.\mathbf{R}_j} \mathbf{S}_{\mathbf{k}}.\mathbf{S}_{\mathbf{k'}} \\ &= J \sum_{<ij>} \sum_{\mathbf{kk'}} e^{i(\mathbf{k}+\mathbf{k'}).\mathbf{R}_i} e^{i\mathbf{k'}.(\mathbf{R}_j - \mathbf{R}_i)} \mathbf{S}_{\mathbf{k}}.\mathbf{S}_{\mathbf{k'}} \end{aligned}$$

Figure 3.4: the BCC antiferromagnet.

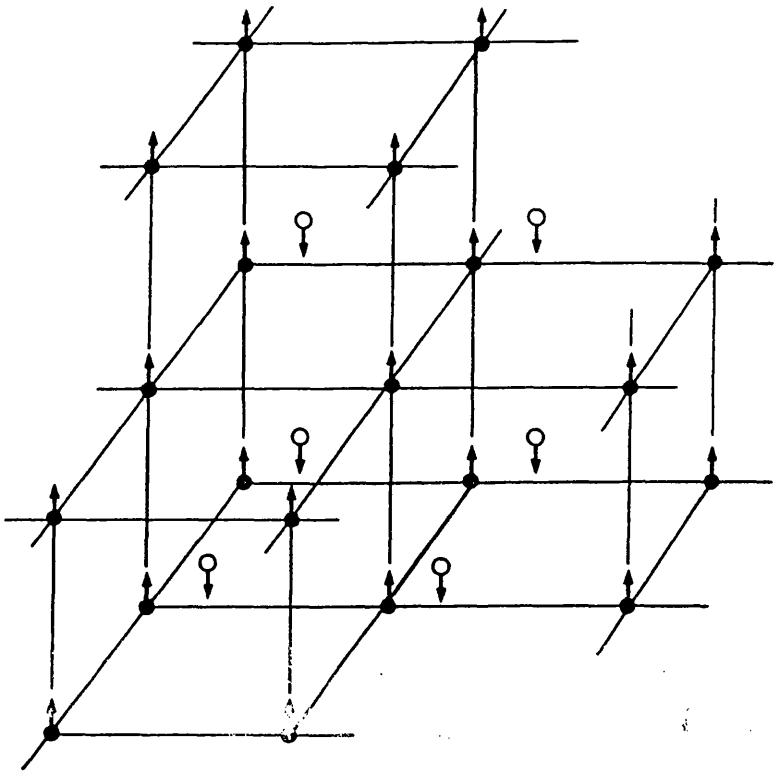

Figure 3.5: a frustrated FCC antiferromagnet (SSDW).

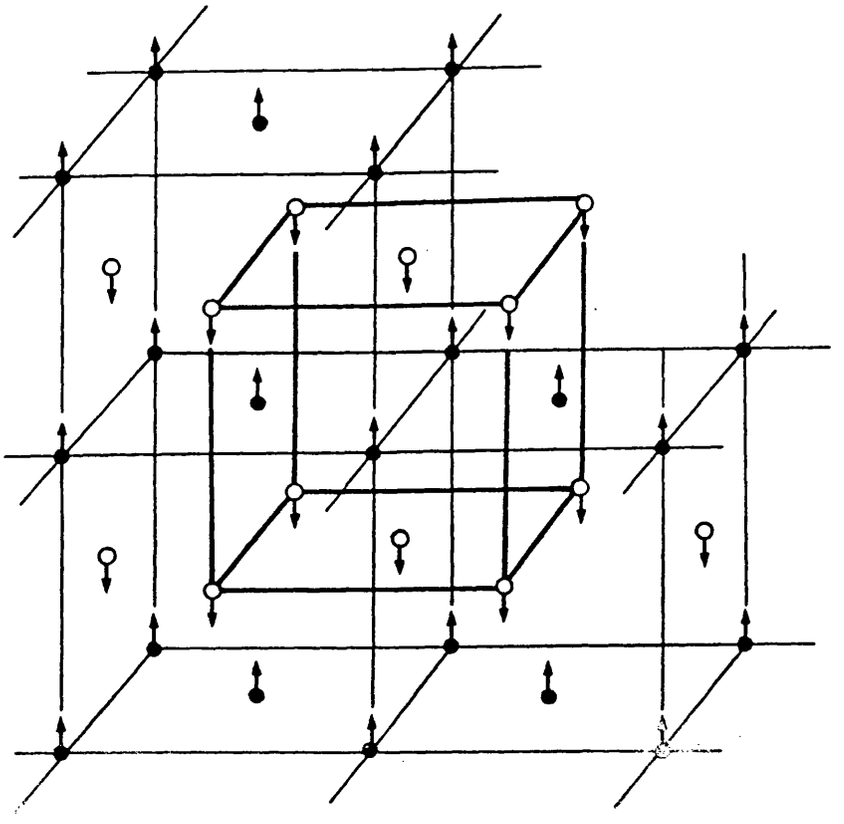

$$
\begin{aligned}
&= J \sum_{\mathbf{k}\mathbf{k}'} \sum_{i} e^{i(\mathbf{k}+\mathbf{k}').\mathbf{R}_i} \sum_{<0j>} e^{i\mathbf{k}'.\mathbf{R}_j} \mathbf{S}_{\mathbf{k}}.\mathbf{S}_{\mathbf{k}'} \\
&= NJ \sum_{\mathbf{k}} \gamma_{\mathbf{k}} \mathbf{S}_{\mathbf{k}}.\mathbf{S}_{-\mathbf{k}} \\
&= NJ \sum_{\mathbf{k}} \gamma_{\mathbf{k}} |\mathbf{S}_{\mathbf{k}}|^2. \qquad (3.6)
\end{aligned}
$$

Here the fourth line arises because the sum over i gives $\delta_{\mathbf{k}+\mathbf{k}',\mathbf{0}}$ and the last line because $\mathbf{S}_{-\mathbf{k}} = \mathbf{S}_{\mathbf{k}}^*$, which follows from (3.5). We define the structure factor $\gamma_{\mathbf{k}}$ by,

$$
\gamma_{\mathbf{k}} = \sum_{<0j>} e^{i\mathbf{k}.\mathbf{R}_j}. \qquad (3.7)
$$

In order to find the reciprocal space form of the constraint (3.4) we define the function $f(\mathbf{R}_i) = \mathbf{S}_i.\mathbf{S}_i$. The Fourier transform of f is then,

$$
\begin{aligned}
f(\mathbf{q}) &= \frac{1}{N} \sum_{i} e^{-i\mathbf{q}.\mathbf{R}_i} f(\mathbf{R}_i) \\
&= \frac{1}{N} \sum_{i} e^{-i\mathbf{q}.\mathbf{R}_i} \sum_{\mathbf{k}\mathbf{k}'} e^{i(\mathbf{k}+\mathbf{k}').\mathbf{R}_i} \mathbf{S}_{\mathbf{k}}.\mathbf{S}_{\mathbf{k}'} \\
&= \frac{1}{N} \sum_{\mathbf{k}\mathbf{k}'} \sum_{i} e^{i(\mathbf{k}-\mathbf{q}+\mathbf{k}').\mathbf{R}_i} \mathbf{S}_{\mathbf{k}}.\mathbf{S}_{\mathbf{k}'} \\
&= \sum_{\mathbf{k}\mathbf{k}'} \delta_{\mathbf{k}',\mathbf{q}-\mathbf{k}} \mathbf{S}_{\mathbf{k}}.\mathbf{S}_{\mathbf{k}'} \\
&= \sum_{\mathbf{k}} \mathbf{S}_{\mathbf{k}}.\mathbf{S}_{\mathbf{q}-\mathbf{k}},
\end{aligned}
$$

and from (3.4) we must also have,

$$
f(\mathbf{q}) = \frac{S^2}{N} \sum_{i} e^{-i\mathbf{q}.\mathbf{R}_i} = S^2 \delta_{\mathbf{q},\mathbf{0}}.
$$

Hence,

$$
\sum_{\mathbf{k}} |\mathbf{S}_{\mathbf{k}}|^2 = S^2 \qquad (3.8)
$$

$$
\text{and} \quad \sum_{\mathbf{k}} \mathbf{S}_{\mathbf{k}}.\mathbf{S}_{\mathbf{q}-\mathbf{k}} = 0, \quad \mathbf{q} \neq \mathbf{0}. \qquad (3.9)
$$

Having defined the problem in reciprocal space we now have to consider how to minimise (3.6) subject to (3.8) and (3.9). Given that $\gamma_{\mathbf{k}}$ is a fixed function

of $\mathbf{k}$ whereas $\mathbf{S_k}$ is not, one approach to this is to find that $\mathbf{k}$, $\mathbf{k}'$ say, which minimises $\gamma_{\mathbf{k}}$ and to set $|\mathbf{S_{k'}}| = S$, ignoring for the moment (3.9). For an FCC structure it is not difficult to show that,

$$\gamma_{\mathbf{k}} = 4\left(\cos\frac{k_x a}{2}\cos\frac{k_y a}{2} + \cos\frac{k_y a}{2}\cos\frac{k_z a}{2} + \cos\frac{k_z a}{2}\cos\frac{k_x a}{2}\right), \qquad (3.10)$$

where $\mathbf{k} = (k_x, k_y, k_z)$ and a is the lattice constant. To minimise this is not trivial and the general solution is given by Long (1989). The solution set is large and the value of $\gamma_{\mathbf{k}}$ associated with it is -4. It should be noted that this is well short of the value -12 which would be achieved in the FCC ferromagnet (which of course is unfrustrated). To demonstrate the inclusion of non-collinear spin structures in this set we need only consider the following subset $\Omega = \{\mathbf{k}_1, \mathbf{k}_2, \mathbf{k}_3\} = \{\frac{2\pi}{a}(1,0,0), \frac{2\pi}{a}(0,1,0), \frac{2\pi}{a}(0,0,1)\}$. Defining $\mathbf{S_k} = \mathbf{0}$ for $\mathbf{k} \notin \Omega$ equation (3.8) now yields,

$$|\mathbf{S_{k_1}}|^2 + |\mathbf{S_{k_2}}|^2 + |\mathbf{S_{k_3}}|^2 = S^2. \qquad (3.11)$$

Remembering (3.9) it is now clear that we need only consider satisfying this for those $\mathbf{q}$ for which $\mathbf{q} - \mathbf{k} \in \Omega$, as for other $\mathbf{q}$ we have $\mathbf{S_{q-k}} \equiv \mathbf{0}$, from above. There are three vectors $\mathbf{q}$ which, up to a reciprocal lattice vector, satisfy this requirement. They are: $\frac{2\pi}{a}(0,1,1)$, $\frac{2\pi}{a}(1,0,1)$, and $\frac{2\pi}{a}(1,1,0)$. Substituting the first of these into (3.9) we get,

$$\mathbf{S_{100}}.\mathbf{S_{\bar{1}11}} + \mathbf{S_{010}}.\mathbf{S_{001}} + \mathbf{S_{001}}.\mathbf{S_{010}} = 0$$

$$\Rightarrow \mathbf{S_{010}}.\mathbf{S_{001}} = 0.$$

The second line follows because $\mathbf{S_{\bar{1}11}}$ is a reciprocal lattice vector and is hence equivalent to $\mathbf{S_{000}}$. Similarly, for the other two $\mathbf{q}$ we obtain,

$$\mathbf{q} = \frac{2\pi}{a}(1,0,1) \Rightarrow \mathbf{S_{100}}.\mathbf{S_{001}} = 0,$$

$$\text{and } \mathbf{q} = \frac{2\pi}{a}(1,1,0) \Rightarrow \mathbf{S_{100}}.\mathbf{S_{010}} = 0.$$

An obvious (simultaneous) solution to these conditions is for the three non-zero $\mathbf{S_k}$ to be mutually perpendicular. Using (3.5) to transform back to real space we then get,

$$\mathbf{S}_i = \mathbf{S}_{\mathbf{k}_1} \cos \mathbf{k}_1.\mathbf{R}_i + \mathbf{S}_{\mathbf{k}_2} \cos \mathbf{k}_2.\mathbf{R}_i + \mathbf{S}_{\mathbf{k}_3} \cos \mathbf{k}_3.\mathbf{R}_i. \tag{3.12}$$

Here the replacement of the exponential by the cosine can be made owing to the inversion symmetry of the FCC lattice.

It can be seen that (3.12), together with the normalisation condition (3.11) and the fact that the $\mathbf{S_k}$s are orthogonal, defines a family of non-collinear structures with spins of equal magnitude on all sites. The directions of the $\mathbf{S_k}$s relative to the lattice are completely arbitrary, as there is nothing in the Heisenberg model to couple the spins to the lattice. Within the range of structures expressible by (3.12) we shall single out three in particular, on which we shall concentrate in the rest of this chapter. Putting $\mathbf{S}_{\mathbf{k}_1} = S\hat{\mathbf{n}}_1$, where $\hat{\mathbf{n}}_1$ is an arbitrary unit vector, and the other $\mathbf{S_k}$ equal to zero we obtain,

$$\mathbf{S}_i = S\hat{\mathbf{n}}_1 \cos \frac{2\pi}{a}(100).\mathbf{R}_i. \tag{3.13}$$

This clearly defines the layered antiferromagnet of figure 3.5 (or 3.6). As the spin density wave acts in one direction only (as there is only one non zero $\mathbf{k}$) we shall refer to this structure as the single spin density wave (SSDW). Putting $S_{\mathbf{k}_1} = \frac{S}{\sqrt{2}}\hat{\mathbf{n}}_1$, $S_{\mathbf{k}_2} = \frac{S}{\sqrt{2}}\hat{\mathbf{n}}_2$ and $\mathbf{S}_{\mathbf{k}_3} = \mathbf{0}$, where $\hat{\mathbf{n}}_1$ and $\hat{\mathbf{n}}_2$ are perpendicular, we obtain,

$$\mathbf{S}_i = \frac{S}{\sqrt{2}}\left(\hat{\mathbf{n}}_1 \cos \frac{2\pi}{a}(100).\mathbf{R}_i + \hat{\mathbf{n}}_2 \cos \frac{2\pi}{a}(010).\mathbf{R}_i\right). \tag{3.14}$$

This is a structure in which two spin density waves occur in the xy plane and we shall refer to it as the double spin density wave (DSDW), which for a particular

Figure 3.6: the SSDW in a cubic octant.

(from Long & Yeung, 1986)

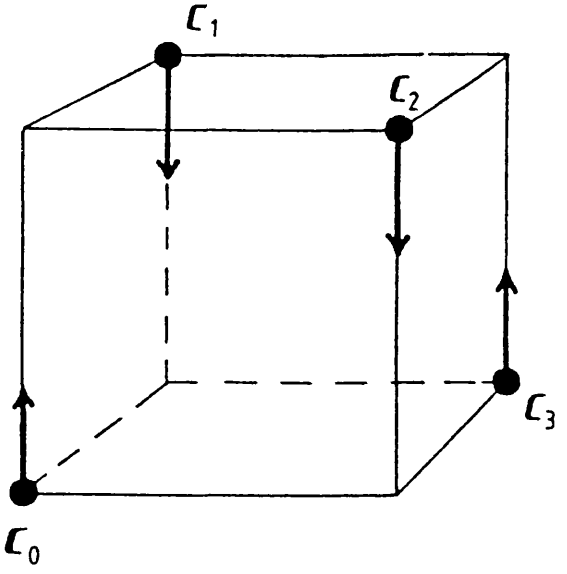

Figure 3.7: the DSDW in a cubic octant.

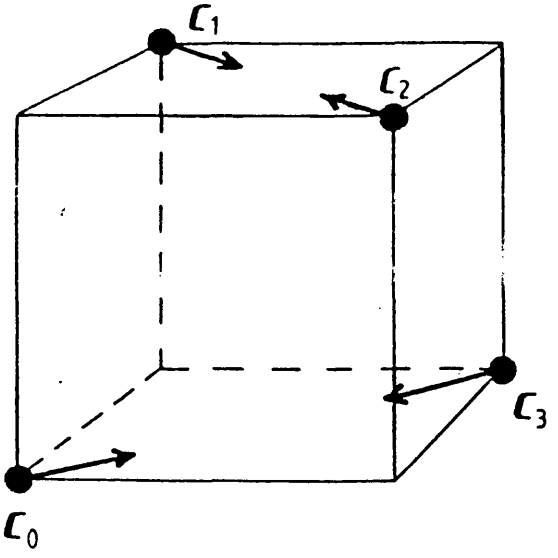

Figure 3.8: the TSDW in a cubic octant.

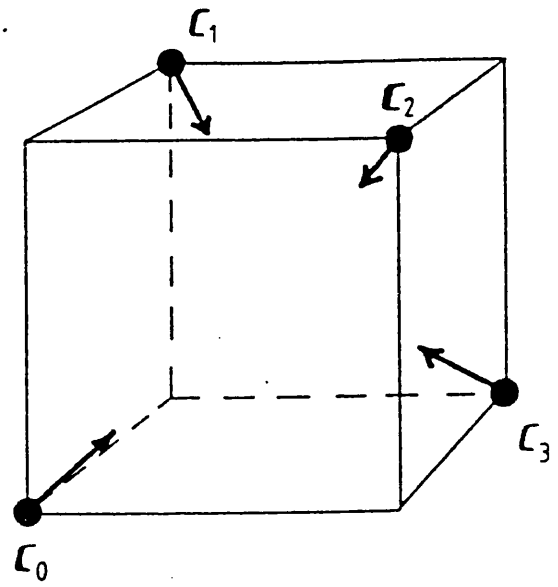

Figure 3.9: phase diagram due to Honda, Tanji & Nakagawa, (1976).

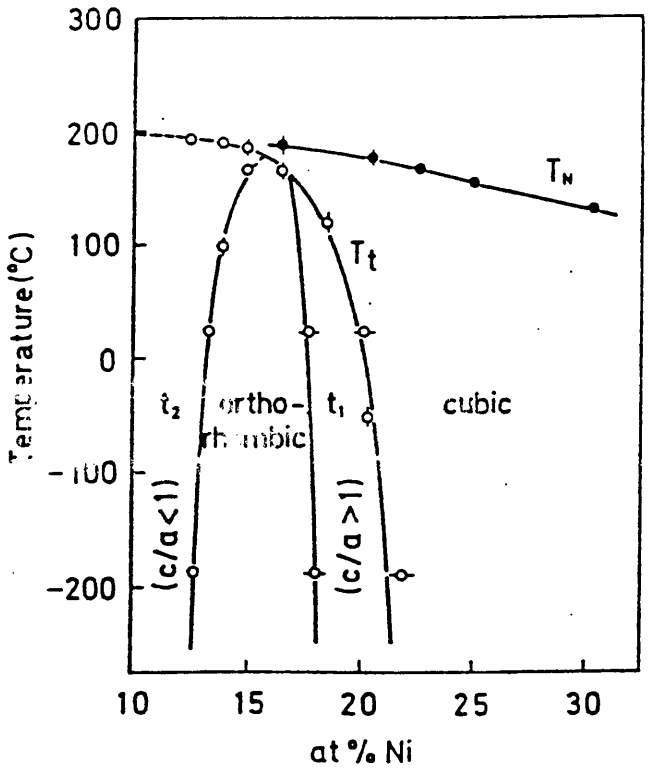

Magnetic and crystallographic phase diagram of the γ Mn–Ni alloy system. Both t_1 and t_2 are tetragonal; T_N is the Néel point and T_t is the distortion temperature.

choice of $\hat{\mathbf{n}}_1$, $\hat{\mathbf{n}}_2$ is shown in figure 3.7. The third structure we shall consider is obtained by putting $\mathbf{S}_{\mathbf{k}_1} = \frac{S}{\sqrt{3}}\hat{\mathbf{n}}_1$, $\mathbf{S}_{\mathbf{k}_2} = \frac{S}{\sqrt{3}}\hat{\mathbf{n}}_2$ and $\mathbf{S}_{\mathbf{k}_3} = \frac{S}{\sqrt{3}}\hat{\mathbf{n}}_3$, with the unit vectors $\hat{\mathbf{n}}$ mutually perpendicular,

$$\mathbf{S}_i = \frac{S}{\sqrt{3}}\left(\hat{\mathbf{n}}_1 \cos\frac{2\pi}{a}(100).\mathbf{R}_i + \hat{\mathbf{n}}_2 \cos\frac{2\pi}{a}(010).\mathbf{R}_i + \hat{\mathbf{n}}_3 \cos\frac{2\pi}{a}(001).\mathbf{R}_i\right). \tag{3.15}$$

Having a spin density wave in all three directions this will be referred to as the triple spin density wave (TSDW) and is illustrated in figure 3.8. Continuing the terminology of Long & Yeung (1986) any structure with more than one SDW will be called a multiple spin density wave (MSDW).

It has to be stressed that the degeneracy of these structures is a consequence of the classical spin model used. When quantum effects are included we would expect this degeneracy to be broken (Long, 1989). It is a quantum approach to the problem, within the framework of density functional theory, that will be pursued in this chapter. It is also interesting to note how the existence of non-collinear structures in the solution of the classical problem comes about: these solutions are a direct consequence of the form of $\gamma_{\mathbf{k}}$, which is clearly determined by the (frustrated) topology of the lattice. As explained in the next section, it is possible for these structures to unfrustrate by distorting tetragonally and such a distortion should also break the spin degeneracy of the classical model.

3.4) Experimental results.

In the real world there are a number of materials in which non-collinear magnetic structures may be relevant. These include materials with highly localised electrons, such as UO_2 (Giannozzi & Erdos, 1987), as well as more itinerant materials involving Mn and Fe. In this work we shall concentrate on the Mn and Fe systems. The main probe used to investigate magnetic structures is neutron diffraction: the neutron, having a spin of one half, undergoes scattering due to the spin density of the electrons as well as the usual nuclear scattering. Pure γ (FCC) manganese is only stable between 1095°C and 1133°C (Pearson, 1958) and at these temperatures there is no magnetic ordering. However when alloyed with copper an FCC material is produced which is stable at room temperature. With sufficiently high manganese content and at relatively low temperatures an antiferromagnetic structure is formed (e.g. with 85% manganese the Néel temperature is 380K). The existence of the antiferromagnetism was deduced from neutron diffraction data and the moment of pure γ-Mn was estimated to be $2.4\mu_B$ (Meneghetti & Sidhu, 1957; Bacon, Dunmur, Smith & Street, 1957). It is difficult to make direct determinations of an SDW structure type with neutrons, for reasons to be described shortly, but the structure proposed for this material was the SSDW. Pure γ-manganese was eventually produced by electrolysis and was found to be sufficiently stable for neutron diffraction measurements to be made (Smith & Vance, 1969). These were consistent with an SSDW structure with an estimated magnetic moment per atom of $2\mu_B$. X-ray diffraction results on this material yielded a $\frac{c}{a}$ ratio of 0.94, which agrees with estimates made by extrapolating from alloy data (Cowlam, Bacon & Gillott, 1977).

Alloys of manganese with other materials show similar behaviour to Mn-Cu. In particular, X-ray diffraction and elastic measurements made on Mn-Ni alloys (Honda, Tanji & Nakagawa, 1976) have produced a complete phase diagram, which is reproduced in figure 3.9. The significant point about this is that below the Néel temperature it is possible to have materials which are orthorhombic, tetragonal with $\frac{c}{a} < 1$ or > 1, or which retain their cubic symmetry. I was suggested by Uchishiba (1971) that in the Mn-Ni structure corresponding to $\frac{c}{a} > 1$ the spins are actually in planes perpendicular to the c-axis, in fact, one of the DSDW structures of (3.14). It is not difficult to see why the SSDW is likely where $\frac{c}{a} < 1$ and a structure with spins perpendicular to the c-axis where $\frac{c}{a} > 1$. In both cases, thinking in terms of the Heisenberg model, we can imagine the distortion bringing the favourable antiparallel spins closer together and moving the unfavourable parallel spins further apart.

Pure γ-iron, like γ-manganese, is not stable at low temperature. In addition, it is difficult to make stable FCC alloys of iron without the use of large proportions of other elements, which increases diffuse scattering and makes extrapolation to the pure material difficult. Early work was done on stainless steel, which contains large amounts of nickel and chromium. The first neutron diffraction measurements on anything like pure γ-iron (Abrahams, Guttman & Kasper, 1962) were done using a precipitate of the material in copper, which was found to be relatively stable. The measurements yielded an antiferromagnetic structure with a moment per atom of $0.72\mu_B$. This was assumed to be a SSDW, despite the fact that no tetragonal distortion was observed. The TSDW was first suggested by Kouvel and Kasper (1962) as a possible structure for

the (cubic) Fe-Mn-Ni alloys. However, Kouvel and Kasper also suggested that the same diffraction pattern could be obtained from a SDW structure with any angle θ between the c-axis and the spin axis, provided that the structure were contained in randomly oriented domains. In addition they pointed out that in the classical Heisenberg model all such SDW structures are degenerate, independent of θ, as shown in the last section. Further experimental evidence on this subject has recently been obtained by Long, Lowde & Sakata (1987). In a domain model the common spin direction in any domain could be fixed only by spin-orbit coupling forces, which are relatively weak. The application of an experimentally achievable stress can be predicted to cause a reorientation of spins through magnetoelastic coupling, and an associated phase transition. Neutron diffraction measurements were made on a cubic Mn-Ni-C alloy under tensile stress and no such phase transition was observed. This experiment therefore weighs against the domain theory in favour of the existence of the TSDW.

Considerable work on γ-iron alloys has been done by Endoh & Ishikawa (1971) who were able, by the addition of a small quantities of other elements, to study the properties of Fe-Mn alloys over the full composition range. They found that at above 40% iron the material was cubic, and so could be another example of the TSDW. A similarity was found in the temperature dependences of the resistivity and magnetic susceptibility in the cubic regime to those of chromium. This, together with theoretical work by Asano & Yamashita (1971), led them to suggest that the antiferromagnetism of the cubic phase may be Fermi surface driven, perhaps providing another example of the Lomer (1962) mechanism for chromium.

In addition to this work on bulk materials, there has recently been a large amount of thin film work involving this sort of system. Of particular interest here is the work of Chambers, Wagener & Weaver (1987) and Macedo & Keune (1988), who studied layered structures of FCC Fe on Cu.

3.5) Theoretical studies of SDW systems.

The early work on the band structures of the systems we are interested in was done by Asano & Yamashita (1971), who used the KKR method, non self-consistently, to obtain the band structures of γ-Mn in both the paramagnetic and SSDW states. By varying the strength of a (Slater) exchange parameter they could arrive at the accepted value for the magnetic moment, but they did not observe the nesting in the paramagnetic bands that would have suggested the Lomer (1962) argument as a mechanism for the antiferromagnetic order. Using these bands as input to an interpolation scheme they were able to produce Fermi surfaces and densities of states as a function of N (the total number of valence electrons) and found that the SSDW structure would be susceptible to Lomer-type spin density waves at $N = 7.4$. This suggested that a TSDW might be formed in MnFe alloy of $\sim$ 50%, which correlated well with the experimental results of Endoh & Ishikawa (1971), who found that the γ-MnFe alloy was cubic at above 40% Fe.

There was a revival of theoretical interest in magnetic systems in the early 80's, following the development of the linearised band structure methods. The first self-consistent band structure of the SSDW in γ-Mn was produced by Cade (1980), using the spin density functional (von Barth & Hedin, 1972) and LMTO-ASA. This was done by running the bandstructure part of the LMTO program

for the up spin only, then using the AF symmetry to deduce the down spin potential parameters and moments before entering the atomic part of the program. The results obtained were in good agreement with the work of Asano & Yamashita (1971) but the moment on the atoms was somewhat lower ($1.9\mu_B$). In particular Cade commented on the nesting of the bands in the $\Gamma - X$ direction, that is, in the real x or y direction. As this occurred close to the Fermi level it suggested a possible instability with respect to the TSDW. This instability was confirmed by Cade & Yeung (1980), using the results of the above calculation in a linear response theory. The band structure of the TSDW was then produced, non self-consistently (Cade, 1981a). This showed the opening of an antiferromagnetic gap in the $\Gamma - X$ direction, which was comparable in size to that produced by the adoption of the SSDW in the first place. So the calculation suggested that the magnitude of the energy saving possible from the TSDW was similar to that of the SSDW. Again using LMTO, Cade (1981b) calculated the axial pressure of the SSDW (§3.12). As explained in Chapter 4, the axial pressure is a measure of the tendency of a structure to distort tetragonally along a given axis, and is calculated in an analogous way to the bulk pressure (Pettifor, 1976). Its applicability within the ASA is not clear, but nevertheless Cade obained a result which suggested that the structure ought to have an equilibrium $\frac{c}{a}$ ratio of less than unity, as observed experimentally.

The first density functional calculations on the SSDW in γ-Fe were done by Kübler (1981) using the augmented spherical wave method (Williams, Kübler & Gelatt, 1979). These yielded a magnetic moment of $0.55\mu_B$, but the total energy produced was found to be *less than* that of a similar calculation on

ferromagnetic α-Fe. As possible reasons for the discrepancy, the ASA was cited as the most likely candidate, with the use of the LDA as a second possibility. In addition, the change in total energy caused by a small tetragonal distortion was found to be negligible. A systematic treatment of systems with non-collinear magnetism did not appear until the paper by Kübler, Höck, Sticht & Williams (1988). Again the framework was the spin density functional formalism, and the band structures were done by the augmented spherical wave method. To handle these systems the authors noted two essential points. Firstly, within the ASA the spin axis direction can be chosen independently for each sphere in the unit cell. The Hamiltonian is then non-diagonal in spin space as well as in the l, m and sublattice indices. Secondly, the directions of the sphere axes after any bandstructure calculation can be extracted from the matrix that diagonalises the spin dependence of the Hamiltonian. In this way results were obtained for a number of non-collinear systems. In particular they looked at MSDWs in (ordered) $\gamma - Mn_2Fe_2$ and found that the total energy was minimised in the DSDW structure with alternate planes of manganese and iron.

Other models of MSDW systems have also been investigated. The stabilities of the SSDW and TSDW have been compared by Jo (1983) using an impurity model in which a magnetic cell is embedded in a paramagnetic host, and were found to depend on band filling and width. Using a mean field approximation to the Hubbard model, Long & Yeung (1986) were able to reproduce the sort of behaviour with band filling exhibited in the experimental phase diagram of MnNi (Honda, Tangi & Nakagawa, 1976). The lifting of the degeneracy of the classical limit of the Heisenberg model by quantum fluctuations has also been explored

(Long, 1988). It was found that this mechanism favours the SSDW in the pure material but the TSDW when impurities are introduced. In addition it was found that in the Cu_3Au structure (Megaw, 1973) the degeneracy is lifted even in the classical limit, the TSDW being preferred. This is interesting when considered in the context of the experimental results of Yamaoka (1974) on MnIr alloys. Yamaoka found that the Cu_3Au type alloy had a Néel temperature that was 200K higher than that of the corresponding "random" alloy, indicating that the antiferromagnetism is considerably more stable in this structure. However, when considered in an itinerant (Hubbard) model Long found that the introduction of paramagnetic impurities actually favours the SSDW.

On the thin film side, multilayer studies of FCC Fe on Cu have been made by Fu & Freeman (1987), using LAPW, and by Fernando & Cooper (1988), using LMTO. In both cases it was found that the Fe behaved *ferromagnetically* when in a surface layer but was antiferromagnetic in interior layers.

3.6) Band structure calculations and MSDWs.

Implicit in the spin density functional formalism is the choice of a common axis to which all spins in the problem are referred. For a ferromagnet or a collinear antiferromagnet (SSDW) all the spins are either parallel or antiparallel to some axis. The operators used to build the Hamiltonian can therefore be chosen to be diagonal in spin space and the theory yields a pair of single particle equations, one for each spin direction. However, for MSDW systems the problem is more complicated as there is no natural choice of spin axis. To solve the problem exactly it would be necessary to have a local spin axis for each volume element considered. As pointed out in the last section, the adoption of the ASA

allows the local spin axes to be defined at the scale of the atomic spheres and renders the problem tractable.

It is characteristic of LMTO-ASA calculations that there is a separation of the potential and crystal structure dependence of the problem through the potential parameters and structure constants respectively. As the structure constants embody the spatial relations in the crystal it is convenient to define them to be independent of spin: the spin dependence then resides solely in the potential parameters. By analogy with standard LMTO we shall define the potential parameters as a direct product of the real space (l, m, and atomic species dependent) matrices and Pauli matrices. The difference here is that in order to represent the non-collinear structures we shall require the full set of Pauli matrices, unlike in the collinear case, where we need only the diagonal ones. As a result, the Hamiltonian for a MSDW will be non-diagonal in spin space and cannot be separated to yield a pair of independent equations (see §2.4).

We shall represent the FCC structure of γ-Mn and γ-Fe as a simple cubic lattice with a four point basis labelled as in figure 3.6. This is particularly convenient for the general SDW, which can be regarded as four cubic sublattices, each containing atoms with parallel spin directions. Moreover, in the pure materials all atomic species are identical and occupy equivalent positions in the crystal. Hence for each atom the spin-diagonalised potential parameters must be the same, independent of sublattice. With respect to a common axis the potential parameters can differ only by a unitary transformation in spin space. For a given atom this will correspond to the rotation necessary to make the local

axis coincide with the common axis, which is a function of sublattice only. One can therefore determine the potential parameters with respect to the common axis by calculating those for an atom on just one sublattice, and then deducing the overall form using the known symmetry of the spin directions in sublattice space. In spin/sublattice space the potential parameters and structure constants are 8×8 matrices (i.e. two choices for spin and four for sublattice), although the spin component of the structure constants is of course the identity.

The description of the problem up to this point corresponds precisely with that given by Kübler, Höck, Sticht & Williams (1988): all that has to be done is substitute the LMTO potential parameters and structure constants for the relevant augmented spherical wave quantities. However, a problem arises when one looks at SDWs in pure Mn or Fe, as in this case the representation gives rise to a degeneracy in every band for every k-point. The reason for this is that it includes matrices which commute with the Hamiltonian but not with each other (Long, private communication). It can be shown (Schiff, 1968) that such a set of operators must have degenerate eigenfunctions. The situation is peculiar to the pure FCC materials and does not occur in the γ-Mn_2Fe_2 systems considered by the above group. Theoretically, the degeneracy of the representation is not in the spirit of the Hohenburg-Kohn theorem, which requires a non-degenerate ground state. In practice, the degeneracy is split by numerical errors and what happens then is not determined. It should be noted that even if this problem did not exist it would still be desirable to reduce the order of the Hamiltonian matrix on grounds of computational speed and memory usage. The SDW structures were found to be extremely slow to converge.

The simplest manifestation of the above degeneracy occurs in the SSDW, where there is a clear symmetry between the sublattice and the spin directions (i.e. swapping the up and down ferromagnetic layers (figure 3.5) and reversing all spin directions). In this case the degeneracy can easily be got rid of by considering only up spins, say, in the bandstructure part of a calculation. However, in the MSDWs the Hamiltonian is not diagonal and the problem cannot be overcome so easily. In the language of group theory we have to find an irreducible representation with the same algebra as the degenerate one.

The purpose of the next few sections is to develop a non-degenerate representation of the LMTO-ASA Hamiltonian for the SDWs in γ-Mn and γ-Fe and so obtain their band structures. To do this we have to identify the algebra satisfied by the 8×8 matrices that are used to represent the potential parameters and structure constants in spin/sublattice space. We then look for a set of 4×4 matrices that satisfy the same algebra and use these to replace the 8×8 matrices in our calculations.

3.7) Representation of the potential parameters.

In the last section we decided to treat the FCC structure as a simple cubic lattice with a four point basis. In a SDW system there are then four sublattices, each with a characteristic spin direction. In this section we shall first consider what the potential parameters should look like for one sublattice, relative to a common spin axis which we shall choose to be the z-axis. We shall then deduce the overall form of the potential parameters in spin/sublattice space from the symmetry imposed on the spin directions by the MSDW structure. It will be found that the potential parameters can be expressed in terms of a

set of operators that give, respectively, the sum of the charge over the atoms of the unit cell, and the spin wave components associated with the x, y and z directions.

Consider an atom on arbitrary sublattice 0 with total spin in the direction of the unit vector $\hat{\mathbf{d}}$. Defining the reference axis for spin in the atomic sphere to be in direction $\hat{\mathbf{d}}$ the potential parameter P takes the form of a diagonal matrix in spin space,

$$P = \begin{pmatrix} P\uparrow & 0 \\ 0 & P\downarrow \end{pmatrix}. \tag{3.16}$$

Here $P\uparrow$ and $P\downarrow$ are the values yielded for P by the spin-up and spin-down charge densities respectively in the atomic sphere. Given that $\hat{\mathbf{d}}$ is expressed with respect to a set of global axes we need to know what P becomes when referred to the global spin reference (z) rather than the local (atomic sphere) axis. We shall call this object P'. If the rotation from the global axes to the local is described by Euler angles $(\alpha, \beta, 0)$ then that from the local to the global is described by Euler angles $(0, -\beta, -\alpha)$ (Edmonds, 1960). We identify P' to be the mapping of P under the transformation that rotates the local axes to the global.

We next have to identify how P transforms under rotations. As P is expressible as a 2×2 matrix in spin space we can treat P as a second order tensor transforming according to the $j = \frac{1}{2}$ representation of $\mathcal{R}^3$. We therefore have,

$$P'_{m'm} = \sum_{n'n} D_{m'n'} P_{n'n} D^{\dagger}_{nm}, \tag{3.17}$$

where the transformation matrix D is given by (Edmonds, 1960),

$$D_{mn} = \mathrm{e}^{im\gamma} \begin{pmatrix} \cos\frac{\beta}{2} & \sin\frac{\beta}{2} \\ -\sin\frac{\beta}{2} & \cos\frac{\beta}{2} \end{pmatrix} \mathrm{e}^{in\alpha}.$$

Now if $\hat{\mathbf{d}}$ is given in spherical polars by $(1, \theta, \phi)$ then the corresponding Euler angles are $(\phi, \theta, 0)$ (Edmonds, 1960) and the transformation we want is described by $(0, -\theta, -\phi)$. Hence we have,

$$\begin{aligned} D &= \begin{pmatrix} e^{-i\frac{\phi}{2}} \cos\frac{\theta}{2} & -e^{-i\frac{\phi}{2}} \sin\frac{\theta}{2} \\ e^{i\frac{\phi}{2}} \sin\frac{\theta}{2} & e^{i\frac{\phi}{2}} \cos\frac{\theta}{2} \end{pmatrix} \\ D^{\dagger} &= \begin{pmatrix} e^{i\frac{\phi}{2}} \cos\frac{\theta}{2} & e^{-i\frac{\phi}{2}} \sin\frac{\theta}{2} \\ -e^{i\frac{\phi}{2}} \sin\frac{\theta}{2} & e^{-i\frac{\phi}{2}} \cos\frac{\theta}{2} \end{pmatrix}, \end{aligned} \tag{3.18}$$

and P' is given by,

$$\begin{aligned} P' &= DPD^{\dagger} \\ &= \begin{pmatrix} P\uparrow \cos^2\frac{\theta}{2} + P\downarrow \sin^2\frac{\theta}{2} & \frac{1}{2}(P\uparrow - P\downarrow)e^{-i\phi}\sin\theta \\ \frac{1}{2}(P\uparrow - P\downarrow)e^{i\phi}\sin\theta & P\uparrow \sin^2\frac{\theta}{2} + P\downarrow \cos^2\frac{\theta}{2} \end{pmatrix} \\ &= \frac{1}{2}(P\uparrow + P\downarrow)\begin{pmatrix} 1 & 0 \\ 0 & 1 \end{pmatrix} + \frac{1}{2}(P\uparrow - P\downarrow)\begin{pmatrix} \cos\theta & e^{-i\phi}\sin\theta \\ e^{i\phi}\sin\theta & -\cos\theta \end{pmatrix} \\ &= \frac{1}{2}(P\uparrow + P\downarrow)\sigma_0 + \frac{1}{2}(P\uparrow - P\downarrow)(\sigma_z \cos\theta + \sigma_x \sin\theta\cos\phi + \sigma_y \sin\theta \sin\phi) \\ &= n\sigma_0 + m\hat{\mathbf{d}}.\boldsymbol{\sigma}, \end{aligned} \tag{3.19}$$

where $n = \frac{1}{2}(P\uparrow + P\downarrow)$, $m = \frac{1}{2}(P\uparrow - P\downarrow)$, $\sigma_0 = \begin{pmatrix} 1 & 0 \\ 0 & 1 \end{pmatrix}$, $\boldsymbol{\sigma} = (\sigma_x, \sigma_y, \sigma_z)$, and the σ_is are Pauli matrices. The coefficients n and m are clearly related to the total charge and magnetic moment respectively.

Equation (3.19) gives P' for an atom on the arbitrary sublattice 0. To find P' for an atom on any other sublattice all we have to do is to substitute the appropriate $\hat{\mathbf{d}}$ in (3.19). Now in a SDW the vector $\hat{\mathbf{d}}$ is constrained by certain symmetries. Labelling the four basis points according to figure 3.6 it is not difficult to see that for the SSDW the matrix P' takes the following form in

sublattice space,

$$P' = \begin{pmatrix} n + m\sigma_3 & & & \\ & n - m\sigma_3 & & \\ & & n - m\sigma_3 & \\ & & & n + m\sigma_3 \end{pmatrix}.$$

Similarly, from figures 3.7 and 3.8 we see that for the DSDW and TSDW the forms are respectively:

$$P' = \begin{pmatrix} n + \frac{m}{\sqrt{2}}(\sigma_1 + \sigma_2) & & & \\ & n + \frac{m}{\sqrt{2}}(\sigma_1 - \sigma_2) & & \\ & & n + \frac{m}{\sqrt{2}}(-\sigma_1 + \sigma_2) & \\ & & & n + \frac{m}{\sqrt{2}}(-\sigma_1 - \sigma_2) \end{pmatrix},$$

$$\text{and} \quad P' = \begin{pmatrix} n + \frac{m}{\sqrt{3}}(\sigma_1 + \sigma_2 + \sigma_3) & & & \\ & n + \frac{m}{\sqrt{3}}(\sigma_1 - \sigma_2 - \sigma_3) & & \\ & & n + \frac{m}{\sqrt{3}}(-\sigma_1 + \sigma_2 - \sigma_3) & \\ & & & n + \frac{m}{\sqrt{3}}(-\sigma_1 - \sigma_2 + \sigma_3) \end{pmatrix}.$$

Looking carefully at these three matrices it can be seen that P' can always be written in terms of the matrices:

$$\begin{aligned} \beta_0 &= \begin{pmatrix} 1 & 0 & 0 & 0 \\ 0 & 1 & 0 & 0 \\ 0 & 0 & 1 & 0 \\ 0 & 0 & 0 & 1 \end{pmatrix} \sigma_0, \quad \beta_1 = \begin{pmatrix} 1 & 0 & 0 & 0 \\ 0 & 1 & 0 & 0 \\ 0 & 0 & -1 & 0 \\ 0 & 0 & 0 & -1 \end{pmatrix} \sigma_1, \\ \beta_2 &= \begin{pmatrix} 1 & 0 & 0 & 0 \\ 0 & -1 & 0 & 0 \\ 0 & 0 & 1 & 0 \\ 0 & 0 & 0 & -1 \end{pmatrix} \sigma_2, \quad \beta_3 = \begin{pmatrix} 1 & 0 & 0 & 0 \\ 0 & -1 & 0 & 0 \\ 0 & 0 & -1 & 0 \\ 0 & 0 & 0 & 1 \end{pmatrix} \sigma_3. \end{aligned} \tag{3.20}$$

This is in fact true for any of the SDW structures describable by (3.12). Defining γ_i, $i = 0, 1, 2, 3$ to be the above 4×4 matrices this result can be written more

concisely as,

$$\beta_i = \gamma_i \sigma_i, \quad i = 0, 1, 2, 3, \tag{3.21}$$

where the juxtaposition represents a direct product. The P' for a general SDW can therefore be written as,

$$P' = n\beta_0 + m\hat{\mathbf{d}}.\beta, \tag{3.22}$$

where $\beta = (\beta_1, \beta_2, \beta_3)$.

The β matrices given by (3.22) are in fact the operators for the total charge/spin wave components over the unit cell, as can be seen by looking at their effects on the total spinor wavefunction Ψ (expressed with respect to the global axes):

$$\Psi = (\psi_0\uparrow \quad \psi_0\downarrow \quad \psi_1\uparrow \quad \psi_1\downarrow \quad \psi_2\uparrow \quad \psi_2\downarrow \quad \psi_3\uparrow \quad \psi_3\downarrow).$$

For example,

$$\langle\Psi|\beta_0|\Psi\rangle = \sum_{i=0}^{3} |\psi_i\uparrow|^2 + |\psi_i\downarrow|^2 = 4Q,$$

$$\begin{aligned}\text{and } \langle\Psi|\beta_3|\Psi\rangle &= |\psi_0\uparrow|^2 - |\psi_0\downarrow|^2 - (|\psi_1\uparrow|^2 - |\psi_1\downarrow|^2 + |\psi_2\uparrow|^2 - |\psi_2\downarrow|^2) \\ &\quad + |\psi_3\uparrow|^2 - |\psi_3\downarrow|^2 \\ &= S_z - (-S_z - S_z) + S_z \quad \text{(see figures 3.6-3.8)} \\ &= 4S_z,\end{aligned}$$

where Q is the charge in a single sphere and S_z is the magnitude of the spin in the global "z" direction, i.e. $|Q\uparrow| - |Q\downarrow|$. Hence, the expectation of β_0 gives the total electron number in the cell. The expectations of β_1, β_2 and β_3 give the respective spin wave magnitudes in the global x, y and z directions. To obtain the spin magnitude in a sphere (i.e. the value of the spin with respect to

the local direction $\hat{\mathbf{d}}$) we simply find the length of the vector $\frac{1}{4}(\langle\beta_1\rangle, \langle\beta_2\rangle, \langle\beta_3\rangle)$. The direction is fixed by the vector $\hat{\mathbf{d}}$ and the sublattice label. The β matrices tell us all we can know about the spin state (within the ASA) of the SDW and are hence a complete set of observables in spin space.

We now have an 8×8 representation of the potential parameters P' which includes both the spin and sublattice dependence (they are diagonal in l and m, so we can ignore this dependence here). The idea of expressing the potential parameters as a direct product is unfamiliar in LMTO theory but this is so because in the usual problems the spin representation is trivial and the Hamiltonian divides immediately into a pair of irreducible blocks which are treated separately. In fact, for the MSDWs the Hamiltonian is again reducible to (equivalent) blocks but this time the reduction involves both spin and sublattice variables and is not trivial.

3.8) The form of the structure constants in sublattice space.

In order to form the LMTO Hamiltonian we require a representation of the structure constants and potential parameters. The potential parameters were considered in the last section, and as the structure constants are independent of spin they can be represented by the direct product with σ_0 (the identity in spin space). However, the 8×8 Hamiltonian (in spin/sublattice space) so formed is degenerate in every band, for every **k**-point, and the state to which the LMTO program converges is not fixed by the Hohenberg-Kohn theory (Long, private communication). To overcome this problem we have to reduce the 8×8 representation to an equivalent 4×4, and this requires a knowledge of the form taken by the structure constants in sublattice space. In addition, it will be

necessary to redefine the structure constants so as to eliminate any sublattice dependent phase factors.

We take as our starting point the definition of the structure constants (1.60), ignoring everything but the basis dependence,

$$\begin{aligned} S^{\mathbf{k}}_{\mathbf{r_0},\mathbf{r}} &= \sum_{\mathbf{R}'} e^{i\mathbf{k}.\mathbf{R}'} S_{\mathbf{r_0},\mathbf{r}+\mathbf{R}'} \\ &= e^{i\mathbf{k}.(\mathbf{r_0}-\mathbf{r})} \sum_{\mathbf{R}'} e^{i\mathbf{k}.(\mathbf{R}'+\mathbf{r}-\mathbf{r_0})} S_{\mathbf{0},\mathbf{R}'+\mathbf{r}-\mathbf{r_0}} \end{aligned} \tag{3.23}$$

In the second line we simply removed a phase factor and used the identity,

$$S_{\mathbf{r_0},\mathbf{r}+\mathbf{R}'} = S_{\mathbf{0},\mathbf{R}'+\mathbf{r}-\mathbf{r_0}},$$

(Andersen, 1975).

The FCC structure in manganese or iron can be regarded as a simple cubic lattice with a four point basis $\{\mathbf{c}_p,\ p = 0,1,2,3\}$. Defining the basis vectors according to figure 3.6 we have,

$$\begin{aligned} \mathbf{c_0} &= (0,0,0) \\ \mathbf{c_1} &= \frac{a}{2}(0,1,1) \\ \mathbf{c_2} &= \frac{a}{2}(1,0,1) \\ \mathbf{c_3} &= \frac{a}{2}(1,1,0), \end{aligned} \tag{3.24}$$

where a is the lattice constant of the cubic lattice. It is these $\mathbf{c}$ vectors that must replace the arbitrary $\mathbf{r}, \mathbf{r_0}$ of (3.23). It is easy to see that to determine the form of the structure constants we have to know $\mathbf{c}_p - \mathbf{c}_{p'}$ for all possible p,p'. Now we know that the difference between any two FCC lattice vectors is another FCC lattice vector, so there must exist a relation,

$$\mathbf{c}_{p'} - \mathbf{c}_p = \mathbf{R}_{pp'} + \sum_{\zeta=0}^{3} \alpha^{\zeta}_{pp'} \mathbf{c}_\zeta. \tag{3.25}$$

where α^ζ has only a single non-zero element, unity, in any row or column. The simple cubic vector $\mathbf{R}_{pp'}$ takes account of the fact that on taking the difference we may end up in a different (cubic) unit cell to the one we start in, but the form of $\mathbf{R}_{pp'}$ is not relevant here. The determination of the α matrices is not difficult owing to the small number of non-trivial combinations (six) of the $\mathbf{c}$s. For example,

$$\begin{aligned}\mathbf{c}_1 - \mathbf{c}_2 = \frac{a}{2}(\bar{1},1,0) &= \frac{a}{2}(1,1,0) - \frac{a}{2}(2,0,0) \\ &\equiv \frac{a}{2}(1,1,0) \\ &= \mathbf{c}_3,\end{aligned}$$

so α^n_{21} is one for $n = 3$ but zero otherwise. In this way we obtain,

$$\begin{aligned}\alpha_0 &= \begin{pmatrix}1&0&0&0\\0&1&0&0\\0&0&1&0\\0&0&0&1\end{pmatrix}, \quad \alpha_1 = \begin{pmatrix}0&1&0&0\\1&0&0&0\\0&0&0&1\\0&0&1&0\end{pmatrix}, \\ \alpha_2 &= \begin{pmatrix}0&0&1&0\\0&0&0&1\\1&0&0&0\\0&1&0&0\end{pmatrix}, \quad \alpha_3 = \begin{pmatrix}0&0&0&1\\0&0&1&0\\0&1&0&0\\1&0&0&0\end{pmatrix}.\end{aligned} \tag{3.26}$$

Going back to the structure constants, (3.25) can now be substituted into (3.23) to give,

$$\begin{aligned}S^{\mathbf{k}}_{pp'} &= e^{i\mathbf{k}.(\mathbf{c}_p - \mathbf{c}_{p'})} \sum_{\mathbf{R}'} e^{i\mathbf{k}.(\mathbf{R}' + \mathbf{c}_{p'} - \mathbf{c}_p)} S_{\mathbf{0},\mathbf{R}'+\mathbf{c}_{p'}-\mathbf{c}_p} \\ &= e^{i\mathbf{k}.(\mathbf{c}_p - \mathbf{c}_{p'})} \sum_{\mathbf{R}} e^{i\mathbf{k}.\left[\mathbf{R} + \sum_\eta \alpha^\eta_{pp'}\mathbf{c}_\eta\right]} S_{\left[\mathbf{0},\mathbf{R}+\sum_\zeta \alpha^\zeta_{pp'}\mathbf{c}_\zeta\right]} \\ &= e^{i\mathbf{k}.(\mathbf{c}_p - \mathbf{c}_{p'})} \left[\prod_{\eta=0}^{3} e^{i\mathbf{k}.\alpha^\eta_{pp'}\mathbf{c}_\eta}\right] \sum_{\mathbf{R}} e^{i\mathbf{k}.\mathbf{R}} S_{\left[\mathbf{0},\mathbf{R}+\sum_\zeta \alpha^\zeta_{pp'}\mathbf{c}_\zeta\right]},\end{aligned} \tag{3.27}$$

where we have put $\mathbf{R} = \mathbf{R}' + \mathbf{R}_{pp'}$, and η is another dummy variable. It is clear from (3.26) that for any p, p' there is only one value of ζ for which $\alpha^\zeta_{pp'}$ is non-zero, and thus only one value of $e^{i\mathbf{k}.\alpha^\eta_{pp'}\mathbf{c}_\eta}$ which is not equal to one. Hence,

$$S^{\mathbf{k}}_{pp'} = e^{i\mathbf{k}.(\mathbf{c}_p - \mathbf{c}_{p'})} \sum_\zeta \alpha^\zeta_{pp'} \sum_{\mathbf{R}} e^{i\mathbf{k}.(\mathbf{R}+\mathbf{c}_\zeta)} S_{\mathbf{0},\mathbf{R}+\mathbf{c}_\zeta}. \tag{3.28}$$

Equation (3.28) shows that, up to a phase factor, the sublattice dependence of the structure constants can be written down entirely in terms of the four α matrices. In fact, we can simply drop this phase factor altogether and define our structure constants by,

$$(S^{\mathbf{k}}_{pp'})' = \sum_{\zeta} \alpha^{\zeta}_{pp'} \sum_{\mathbf{R}} e^{i\mathbf{k}.(\mathbf{R}+\mathbf{c}_\zeta)} S_{\mathbf{0},\mathbf{R}+\mathbf{c}_\zeta}. \tag{3.29}$$

To see why consider what has to be done to get from (3.28) to (3.29). It is not difficult to show that,

$$S = PS'P^{-1}, \tag{3.30}$$

where P is given by,

$$P = \begin{pmatrix} e^{i\mathbf{k}.\mathbf{c}_0} & 0 & 0 & 0 \\ 0 & e^{i\mathbf{k}.\mathbf{c}_1} & 0 & 0 \\ 0 & 0 & e^{i\mathbf{k}.\mathbf{c}_2} & 0 \\ 0 & 0 & 0 & e^{i\mathbf{k}.\mathbf{c}_3} \end{pmatrix}. \tag{3.31}$$

For example, for a lattice with a two point basis we have,

$$\begin{pmatrix} 0 & S_{12}e^{i\mathbf{k}.(\mathbf{c}_1-\mathbf{c}_2)} \\ S_{21}e^{i\mathbf{k}.(\mathbf{c}_2-\mathbf{c}_1)} & 0 \end{pmatrix}$$
$$= \begin{pmatrix} e^{i\mathbf{k}.\mathbf{c}_1} & 0 \\ 0 & e^{i\mathbf{k}.\mathbf{c}_2} \end{pmatrix} \begin{pmatrix} 0 & S_{12} \\ S_{21} & 0 \end{pmatrix} \begin{pmatrix} e^{-i\mathbf{k}.\mathbf{c}_1} & 0 \\ 0 & e^{-i\mathbf{k}.\mathbf{c}_2} \end{pmatrix}.$$

Now in the standard LMTO-ASA code the full LMTO problem is not solved but rather the second order problem of (1.53), with third order effects included afterwards as a perturbation. Using (1.15) to write (1.53) in terms of the unscreened structure constants we obtain,

$$[C + \Delta^{\frac{1}{2}} S(1-\gamma S)^{-1}\Delta^{\frac{1}{2}}]\mathbf{u} = E\mathbf{u}$$

$$[C + \Delta^{\frac{1}{2}} PS'P^{-1}(1-\gamma PS'P^{-1})^{-1}\Delta^{\frac{1}{2}}]\mathbf{u} = E\mathbf{u}, \tag{3.32}$$

where the second line follows from (3.30). Moreover,

$$PS'P^{-1}(1-\gamma PS'P^{-1})^{-1} = PS'P^{-1}[P(1-\gamma S')P^{-1}]^{-1}$$
$$= PS'P^{-1}P(1-\gamma S')^{-1}P^{-1}$$
$$= PS'(1-\gamma S')^{-1}P^{-1}.$$

Further, from the definition (1.27), (1.28) and (1.11) we know that C, Δ and γ are diagonal in sublattice space (but not, for an MSDW, in spin space). The phase factor P is diagonal in sublattice space and is represented by the identity in spin space, so P must commute with all the potential parameters. Hence (3.32) can be rewritten,

$$[C + P\Delta^{\frac{1}{2}} S'(1 - \gamma S')^{-1} \Delta^{\frac{1}{2}} P^{-1}]\mathbf{u} = E\mathbf{u}$$

$$\Rightarrow [P^{-1}CP + P^{-1}P\Delta^{\frac{1}{2}} S'(1 - \gamma S')^{-1} \Delta^{\frac{1}{2}} P^{-1}P]P^{-1}\mathbf{u} = EP^{-1}\mathbf{u}$$

$$[C + \Delta^{\frac{1}{2}} S'(1 - \gamma S')^{-1} \Delta^{\frac{1}{2}}]\mathbf{u}' = E\mathbf{u}', \qquad (3.33)$$

where $\mathbf{u}' = P^{-1}\mathbf{u}$. So by solving the eigenvalue problem with constants defined by (3.29) rather than (3.28) we obtain eigenvectors that differ by a phase factor. The presence of this phase factor cannot affect the expectation of any physical observable and so cannot affect our results.

3.9) Reduction of the Hamiltonian.

We now have matrices for both the potential parameters (3.22) and the structure constants (3.29) for a SDW in a FCC structure. The potential parameters are 8×8 in a combined spin/sublattice space while the structure constants, being given by the identity in spin space, can be regarded as 8×8 or 4×4. In previous sections it was established that we shall require a 4×4 representation, rather than an 8×8. This means finding a set of 4×4 matrices, $\{\beta'\}$ say, which is in some sense equivalent to the set $\{\beta\}$ of (3.22). The sense in which these matrices must be equivalent is one of algebra: the matrices β' must obey the same rules when multiplied amongst themselves, and also the same commutation relations with the αs, as do the original βs.

Thinking first about the multiplication of the β matrices it is not difficult to show that:

$$\beta_l \beta_m = \delta_{lm} + \mathrm{i}\,\varepsilon_{lmn}\beta_n, \quad l,m,n \in \{1,2,3\}. \tag{3.34}$$

For example,

$$\begin{aligned}
\beta_2\beta_3 &= \begin{pmatrix} 1 & 0 & 0 & 0 \\ 0 & -1 & 0 & 0 \\ 0 & 0 & 1 & 0 \\ 0 & 0 & 0 & -1 \end{pmatrix} \begin{pmatrix} 1 & 0 & 0 & 0 \\ 0 & -1 & 0 & 0 \\ 0 & 0 & -1 & 0 \\ 0 & 0 & 0 & 1 \end{pmatrix} \begin{pmatrix} 0 & -\mathrm{i} \\ \mathrm{i} & 0 \end{pmatrix} \begin{pmatrix} 1 & 0 \\ 0 & -1 \end{pmatrix} \\
&= \mathrm{i} \begin{pmatrix} 1 & 0 & 0 & 0 \\ 0 & 1 & 0 & 0 \\ 0 & 0 & -1 & 0 \\ 0 & 0 & 0 & -1 \end{pmatrix} \begin{pmatrix} 0 & 1 \\ 1 & 0 \end{pmatrix} \\
&= \mathrm{i}\gamma_1\sigma_1 \\
&= \mathrm{i}\beta_1,
\end{aligned}$$

where use has been made of the definition (3.20) of β and γ. The exact multiplication rules obeyed by the α matrices are not important here: all that matters is that the product of two α matrices is another α matrix (which is easily proved from 3.26), and that there are no complications involving sublattice dependent phase factors. The remaining elements of the algebra defined by the (8×8) α and β matrices are the commutation relations, which can be shown by direct multiplication to be,

$$\beta_\nu \alpha_\mu = (\gamma^\nu)_{\mu\mu}\alpha_\mu\beta_\nu, \tag{3.35}$$

where $(\gamma^\nu)_{\mu\mu}$ is the entry $\mu\mu$ in the matrix γ_ν of (3.22). For example,

$$\begin{aligned}
\beta_2\alpha_3 &= \begin{pmatrix} 1 & 0 & 0 & 0 \\ 0 & -1 & 0 & 0 \\ 0 & 0 & 1 & 0 \\ 0 & 0 & 0 & -1 \end{pmatrix} \begin{pmatrix} 0 & 0 & 0 & 1 \\ 0 & 0 & 1 & 0 \\ 0 & 1 & 0 & 0 \\ 1 & 0 & 0 & 0 \end{pmatrix} \begin{pmatrix} 0 & -\mathrm{i} \\ \mathrm{i} & 0 \end{pmatrix} \begin{pmatrix} 1 & 0 \\ 0 & 1 \end{pmatrix} \\
&= \begin{pmatrix} 0 & 0 & 0 & 1 \\ 0 & 0 & -1 & 0 \\ 0 & 1 & 0 & 0 \\ -1 & 0 & 0 & 0 \end{pmatrix} \begin{pmatrix} 0 & -\mathrm{i} \\ \mathrm{i} & 0 \end{pmatrix} \\
&= (-1) \begin{pmatrix} 0 & 0 & 0 & 1 \\ 0 & 0 & 1 & 0 \\ 0 & 1 & 0 & 0 \\ 1 & 0 & 0 & 0 \end{pmatrix} \begin{pmatrix} 1 & 0 & 0 & 0 \\ 0 & -1 & 0 & 0 \\ 0 & 0 & 1 & 0 \\ 0 & 0 & 0 & -1 \end{pmatrix} \begin{pmatrix} 1 & 0 \\ 0 & 1 \end{pmatrix} \begin{pmatrix} 0 & -\mathrm{i} \\ \mathrm{i} & 0 \end{pmatrix} \\
&= (\gamma^2)_{33}\alpha_3\beta_2.
\end{aligned}$$

The importance of the commutation relation is that it enables us to express any linear combination of products of powers of the αs and βs as a linear combination of products $\alpha_i\beta_j$. All one has to do is to use (3.35) to reorder the terms in any product of powers to get all the αs on the left, say, and all the βs on the right. The previous rules for the simplification of products involving αs or βs only can then be invoked.

Knowing the algebraic rules (3.34),(3.35) that the αs and βs satisfy we now look for a set of 4×4 matrices β' which can replace the βs. It can be verified that the following is a suitable set:

$$\begin{aligned}
\beta'_0 &= \begin{pmatrix} 1 & 0 & 0 & 0 \\ 0 & 1 & 0 & 0 \\ 0 & 0 & 1 & 0 \\ 0 & 0 & 0 & 1 \end{pmatrix}, \quad \beta'_1 = \begin{pmatrix} 0 & 1 & 0 & 0 \\ 1 & 0 & 0 & 0 \\ 0 & 0 & 0 & -1 \\ 0 & 0 & -1 & 0 \end{pmatrix}, \\
\beta'_2 &= \begin{pmatrix} 0 & -\mathrm{i} & 0 & 0 \\ \mathrm{i} & 0 & 0 & 0 \\ 0 & 0 & 0 & -\mathrm{i} \\ 0 & 0 & \mathrm{i} & 0 \end{pmatrix}, \quad \beta'_3 = \begin{pmatrix} 1 & 0 & 0 & 0 \\ 0 & -1 & 0 & 0 \\ 0 & 0 & -1 & 0 \\ 0 & 0 & 0 & 1 \end{pmatrix}.
\end{aligned} \tag{3.36}$$

For instance, repeating the previous examples,

$$\beta'_2\beta'_3 = \begin{pmatrix} 0 & -\mathrm{i} & 0 & 0 \\ \mathrm{i} & 0 & 0 & 0 \\ 0 & 0 & 0 & -\mathrm{i} \\ 0 & 0 & \mathrm{i} & 0 \end{pmatrix} \begin{pmatrix} 1 & 0 & 0 & 0 \\ 0 & -1 & 0 & 0 \\ 0 & 0 & -1 & 0 \\ 0 & 0 & 0 & 1 \end{pmatrix}$$
$$= \begin{pmatrix} 0 & \mathrm{i} & 0 & 0 \\ \mathrm{i} & 0 & 0 & 0 \\ 0 & 0 & 0 & -\mathrm{i} \\ 0 & 0 & -\mathrm{i} & 0 \end{pmatrix}$$
$$= \mathrm{i}\beta'_1,$$

and,

$$\beta'_2\alpha_3 = \begin{pmatrix} 0 & -\mathrm{i} & 0 & 0 \\ \mathrm{i} & 0 & 0 & 0 \\ 0 & 0 & 0 & -\mathrm{i} \\ 0 & 0 & \mathrm{i} & 0 \end{pmatrix} \begin{pmatrix} 0 & 0 & 0 & 1 \\ 0 & 0 & 1 & 0 \\ 0 & 1 & 0 & 0 \\ 1 & 0 & 0 & 0 \end{pmatrix}$$
$$= \begin{pmatrix} 0 & 0 & -\mathrm{i} & 0 \\ 0 & 0 & 0 & \mathrm{i} \\ -\mathrm{i} & 0 & 0 & 0 \\ 0 & \mathrm{i} & 0 & 0 \end{pmatrix}$$
$$= (-1) \begin{pmatrix} 0 & 0 & 0 & 1 \\ 0 & 0 & 1 & 0 \\ 0 & 1 & 0 & 0 \\ 1 & 0 & 0 & 0 \end{pmatrix} \begin{pmatrix} 0 & -\mathrm{i} & 0 & 0 \\ \mathrm{i} & 0 & 0 & 0 \\ 0 & 0 & 0 & -\mathrm{i} \\ 0 & 0 & \mathrm{i} & 0 \end{pmatrix}$$
$$= (\gamma^2)_{33}\alpha_3\beta'_2.$$

The form of the matrices (3.36) can be obtained by good guesswork or by tedious algebra, starting from (3.34) and (3.35). The matrices are not uniquely determined by these equations and the set given here was obtained by requiring β'_3 to be diagonal. In the simpler case of the SSDW, with the spin axis in the z direction, the real space symmetry of the spins is then evident (the elements of β'_3 correspond to spin up moments on sublattices 0 and 3, and down on 1 and 2, see figures 3.5 and 3.6). The α matrices, being represented by the identity in spin space, may be considered to be 4×4 already.

Once the reduced Hamiltonian has been diagonalised there is one further task to perform, which is to extract the spin information from the eigenfunctions. To do this it must be recognised that in the new representation the matrices β'

are the operators for the charge and spin wave components, summed over the unit cell (see §3.7). This is so because the β's are equivalent to the old matrices β. So to get the charge or spin component on atom 0 we find the expectation of the appropriate β' in the (4 atom) solution state Ψ, and divide by two rather than four (as the representation is 4×4 rather than 8×8). The total spin magnitude on any atom is given by the magnitude of $\frac{1}{2}(\langle\Psi|\beta_1|\Psi\rangle, \langle\Psi|\beta_2|\Psi\rangle, \langle\Psi|\beta_3|\Psi\rangle)$.

3.10) Implementation.

A standard LMTO-ASA program was adapted to use the representation described in §3.9. This involved the multiplication of the standard structure constants by the phase factor necessary to obtain (3.29), and the inclusion of new code for constructing the Hamiltonian from the potential parameters defined by (3.22), given the standard (diagonal) potential parameters as input. In addition, at the other side of the diagonalisation the angular momentum weights were constructed according to,

$$A_l^{\zeta}(\mathbf{k}) = \sum_m \mathbf{u}_{lm}^{\dagger}(\mathbf{k})\beta^{\zeta}\mathbf{u}_{lm}(\mathbf{k}), \tag{3.37}$$

rather than the standard formula (1.63). Here the index $\zeta \in (0, 1, 2, 3)$, and the corresponding weights, when integrated over the Brillouin zone, give respectively the total charge and the (x, y, z) spin wave components for the unit cell (see §3.7 and §3.9). It should be emphasised that $\mathbf{u}_{lm}(\mathbf{k})$ is a vector in spin/sublattice space, so each term in (3.37) is a contraction of two vectors with matrix β^{ζ}. It should also be noted that the spin components produced this way must be appropriate to the SDW being considered. For example, for a DSDW the integral of (3.37) must yield equal values for $\zeta = 1$ and $\zeta = 2$, and zero for $\zeta = 3$. This gives a good test of the validity of an implementation. In addition, the point

group symmetries of the three SDWs are not the same: the SSDW and DSDW are tetragonal whereas the TSDW is cubic. In practice calculations were done using the primitive orthorhombic Brillouin zone. The use of this zone was found necessary to preserve the symmetry for the case of the DSDW (which failed the above test when the tetragonal zone was used). Looking at (3.37) and noting that $\zeta = 1, 2, 3$ correspond to labels x, y and z, it cannot be assumed that A_l^ζ ($\zeta = 1, 2$) is invariant under reflection in $x = y$. This problem is not encountered for the SSDW (which has only a z-component anyway) or for the TSDW, but the orthorhombic zone was used in all cases for sake of comparison.

The atomic charge part of the LMTO code was unchanged as at this stage in the self-consistency cycle the representation is always the local (diagonal) one for the atomic sphere: the fact that an MSDW might be dealt with is contained entirely in the band structure part of the program.

3.11) Results and interpretation.

Self-consistent calculations were performed on γ-Mn with $S_{ws} = 2.73$AU and on γ-Fe with $S_{ws} = 2.555$AU. The Mn radius was chosen for consistency with Cade's (1980) work while the Fe radius was that which gave zero pressure in the paramagnetic material. The pressure of paramagnetic Mn at 2.73AU is strongly negative (-0.3Mbar) and at a radius that yields zero pressure the system does not go magnetic, so the manganese calculations could not be done at equilibrium volume. The Brillouin zone integrations were performed using the tetrahedron method (§1.9) in an irreducible wedge of the primitive orthorhombic zone, with 64 k-points in the wedge. The convergence of the SDW states was particularly slow, the results presented being the product of at least three hundred bandstructure iterations for each case.

The results obtained for the magnetisation, total energy and pressure of the three SDW systems are given below:

Table 3.1: Mn	SSDW	DSDW	TSDW
magnetisation/atom/μ_B	1.903	1.866	1.827
total energy/Ryd.	-126.1257	-126.1258	-126.1248
pressure/Mbar	-0.2803	-0.2840	-0.2839

Table 3.2: Fe	SSDW	DSDW	TSDW
magnetisation/atom/μ_B	0.711	0.748	0.732
total energy/Ryd.	-178.2363	-178.2380	-178.2372
pressure/Mbar	0.0141	0.0152	0.0146

Experimentally the moment obtained for the SSDW structure in Mn has been been determined as either $2\mu_B$ (Smith & Vance, 1969) or $2.4\mu_B$ (Bacon, Dunmur,

Smith & Street, 1957). The moment of what was believed (see §3.4) to be the the SSDW in Fe was given as $0.72\mu_B$ (Abrahams, Guttman & Kasper, 1962). These values are pretty much in line with the results given here, although that for the SSDW in Mn is perhaps a bit low. The SSDW result for Fe is considerably bigger than the value of $0.55\mu_B$ obtained previously using the augmented spherical wave method (Williams, Kübler & Gelatt, 1979). The experimental phase diagram of figure 3.8 suggests that pure Mn has the SSDW structure, while the work of Endoh & Ishikawa (1971) suggests that pure Fe should be cubic (i.e. TSDW). The differences between the total energies obtained by calculation are probably too small to be significant. For the SSDW and DSDW in Mn the axial pressure is quite large, indicating that for $\frac{c}{a} = 1$ the structures are a long way from equilibrium. In §3.12 an estimate will be made for the equilibrium total energies of these structures, based on the axial pressure. It is interesting to note that in Mn the bulk pressures of the SSDW and DSDW are considerably lower than that of the TSDW. This suggests that the SSDW and DSDW are more stable than the TSDW.

The bandstructures for the paramagnetic materials and the SDWs are given in figures 3.10 to 3.17. The Brillouin zone used is the small cubic one corresponding to a cubic real space lattice with a four point basis (figure 3.6). This zone is the most appropriate for the TSDW, which is cubic, but not for the SSDW or DSDW. For these the real space cell should really be tetragonal with a two point basis (Asano & Yamashita, 1971) giving a smaller real space cell than for the TSDW. The Brillouin zone should therefore be larger than that for the TSDW and the bands will fold back into the smaller zone. Similarly, the paramagnetic

materials should be FCC with only a single basis point, giving an even smaller real space cell and greater folding back of the bands. The symmetry labels used here are those of Bradley & Cracknell (1972) and the path (figure 3.10) is that used by Kübler, Höck, Sticht & Williams (1988) in their work on γ-Mn_2Fe_2. The band structures for the SSDW and TSDW in Mn were also plotted for the zones and paths used by Cade (1980,1981a) and were in good agreement. In all band structures the Fermi level is shifted to zero.

Looking first at the paramagnetic bandstructures (figures 3.10 & 3.14) we see that the features for Mn and Fe are very similar. The main difference between the plots is that in Fe, relative to the common features, the Fermi level is about 0.1 Ryd. higher than in Mn. This is only to be expected, as Fe has one more electron than Mn. Comparing the magnetic structures with the paramagnetic (figures 3.10–3.17) it can be seen that the chief effect of the magnetism is to split bands that were degenerate in the paramagnetic case. For example, looking at the Γ-point for the SSDW in Mn (figure 3.11) it can be seen that the parabolic bands between -0.2 and -0.3 Ryd. have been split, a band has been forced up from the concave/convex pair that meet just above -0.1 Ryd., and the pair above that (marked with $\updownarrow$) have been split apart altogether. In addition, looking around -0.3 Ryd. and 0.2 Ryd., between R and Γ, it is clear that bands that were at least triply degenerate in the paramagnetic material have been split and run almost parallel. Comparing the two materials it can be seen that it is the magnitudes of the magnetic splitting that really distinguish them. We can estimate the magnitude of the splittings in the SSDWs from the split band marked $\updownarrow$ in figures 3.11 and 3.15, and we obtain 0.04 Ryd. for Mn and 0.006

Figure 3.10: Band structure for paramagnetic Mn.

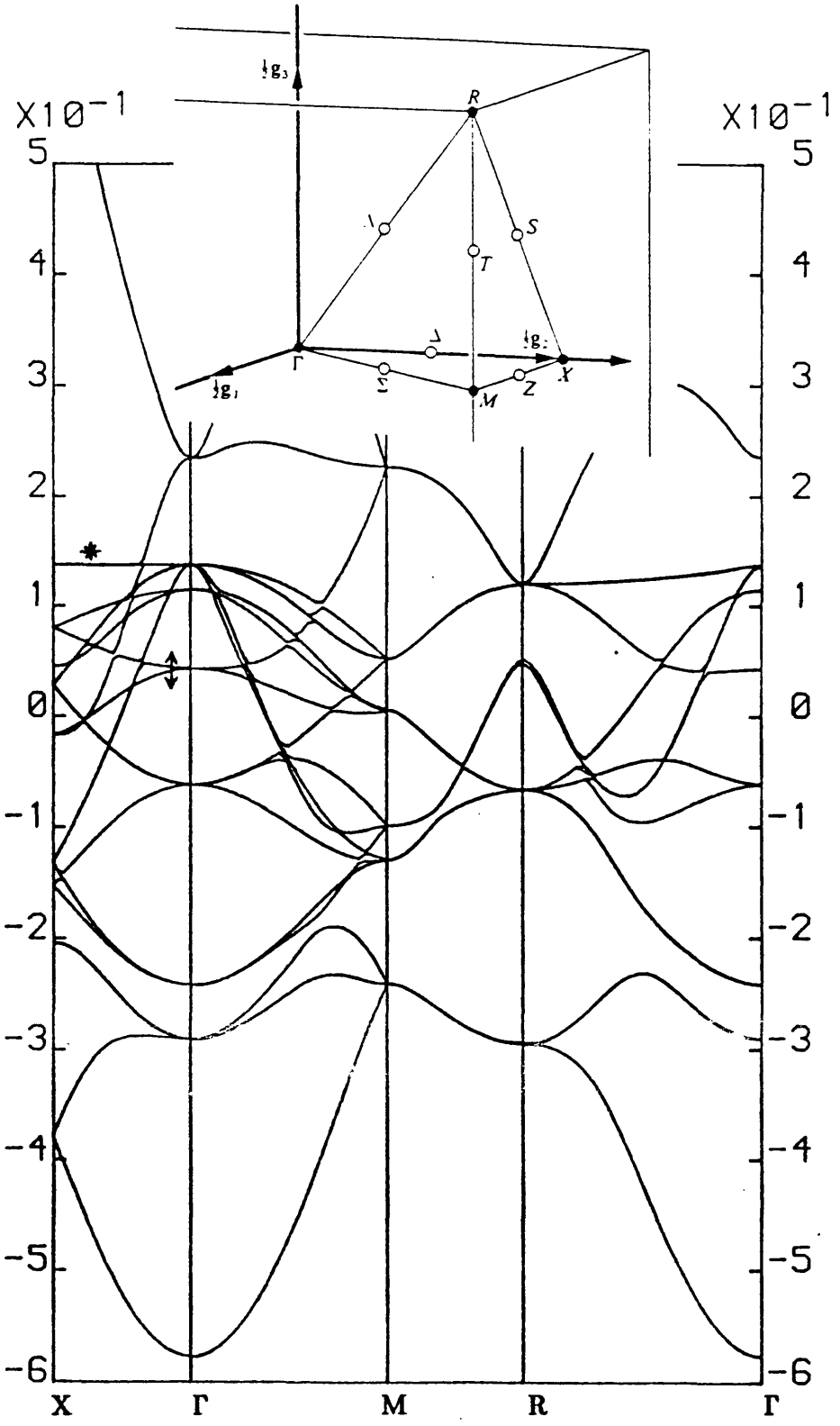

Figure 3.11: Band structure for SSDW in Mn.

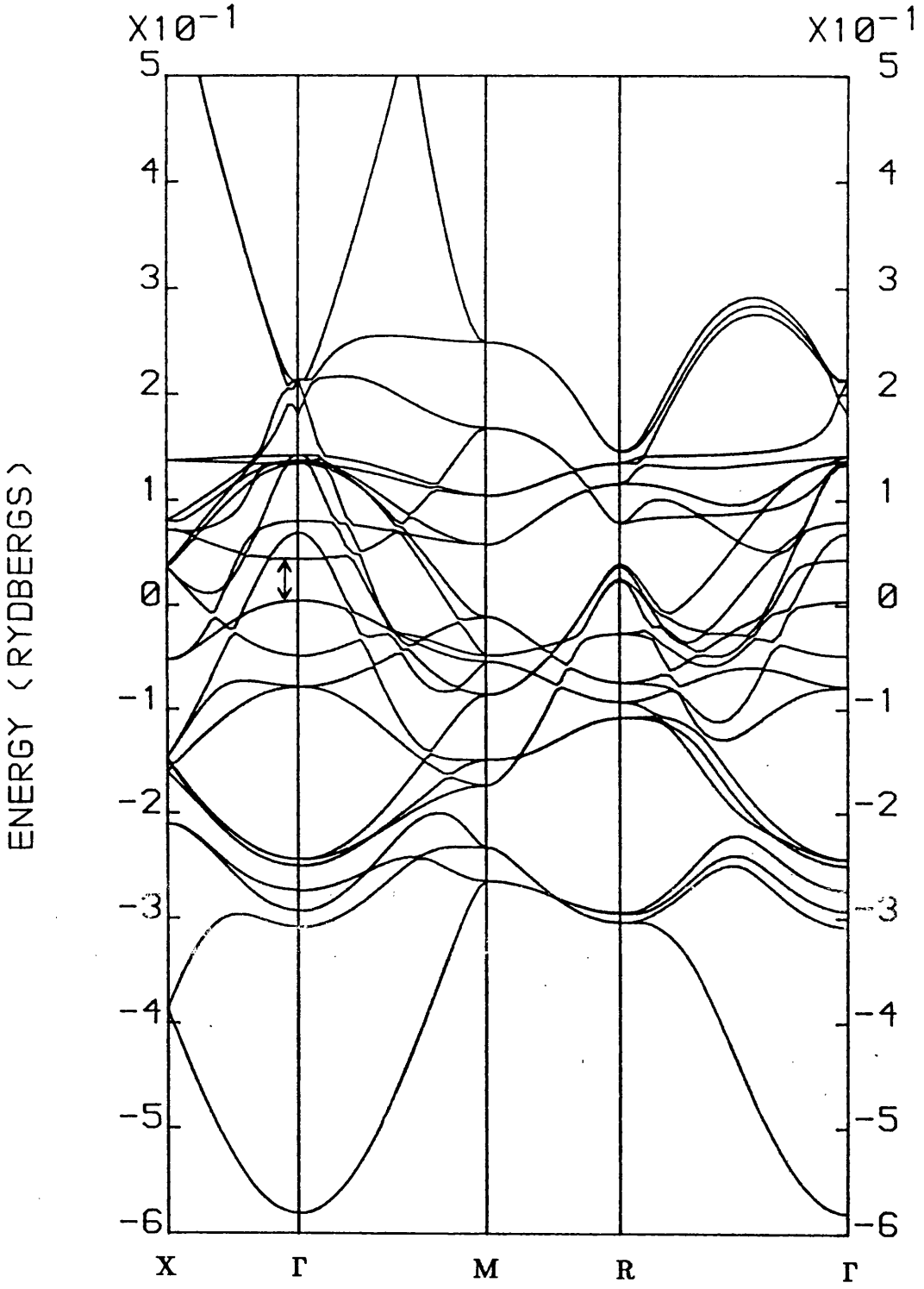

Figure 3.12: Band structure for DSDW in Mn.

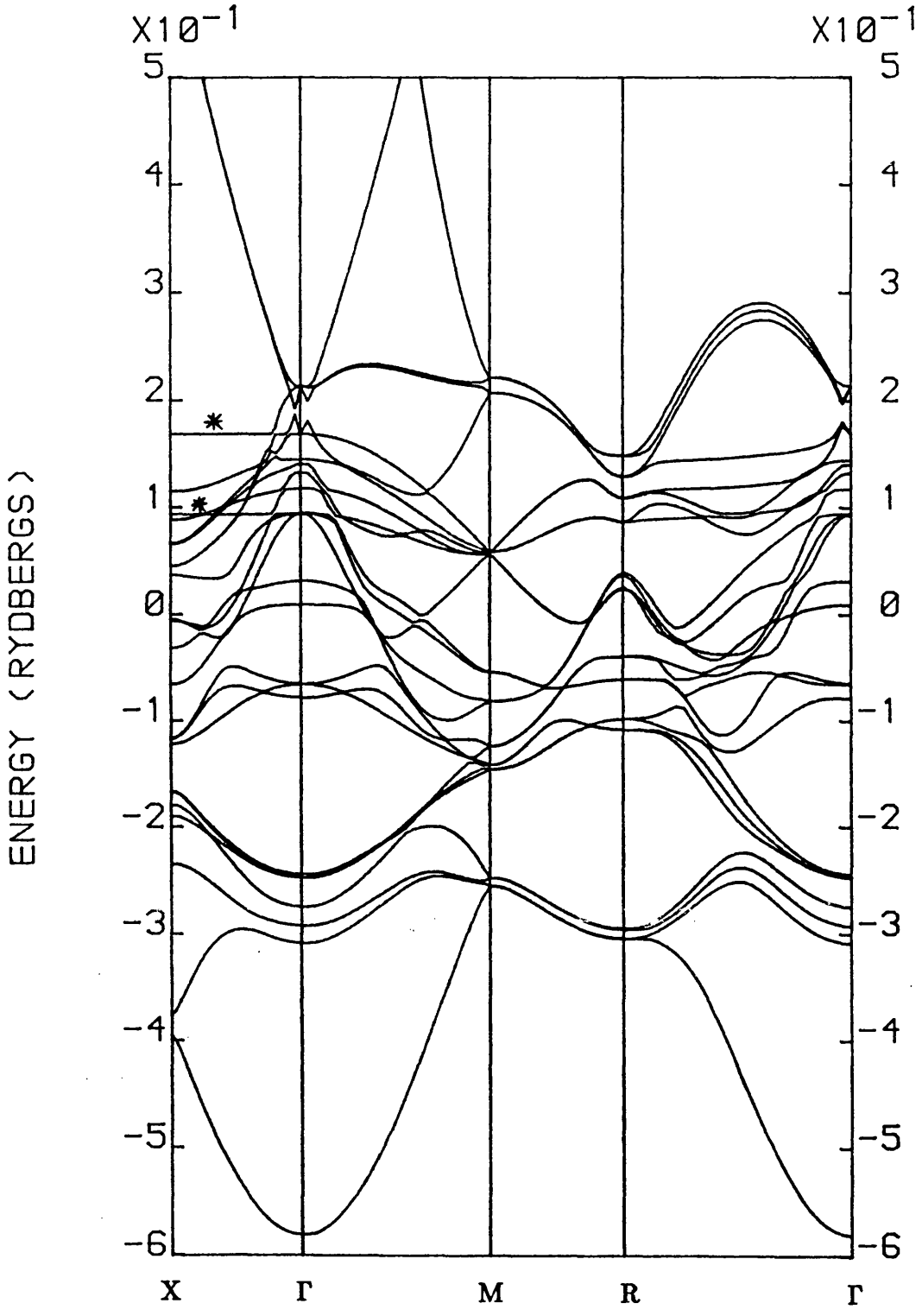

Figure 3.13: Band structure for TSDW in Mn.

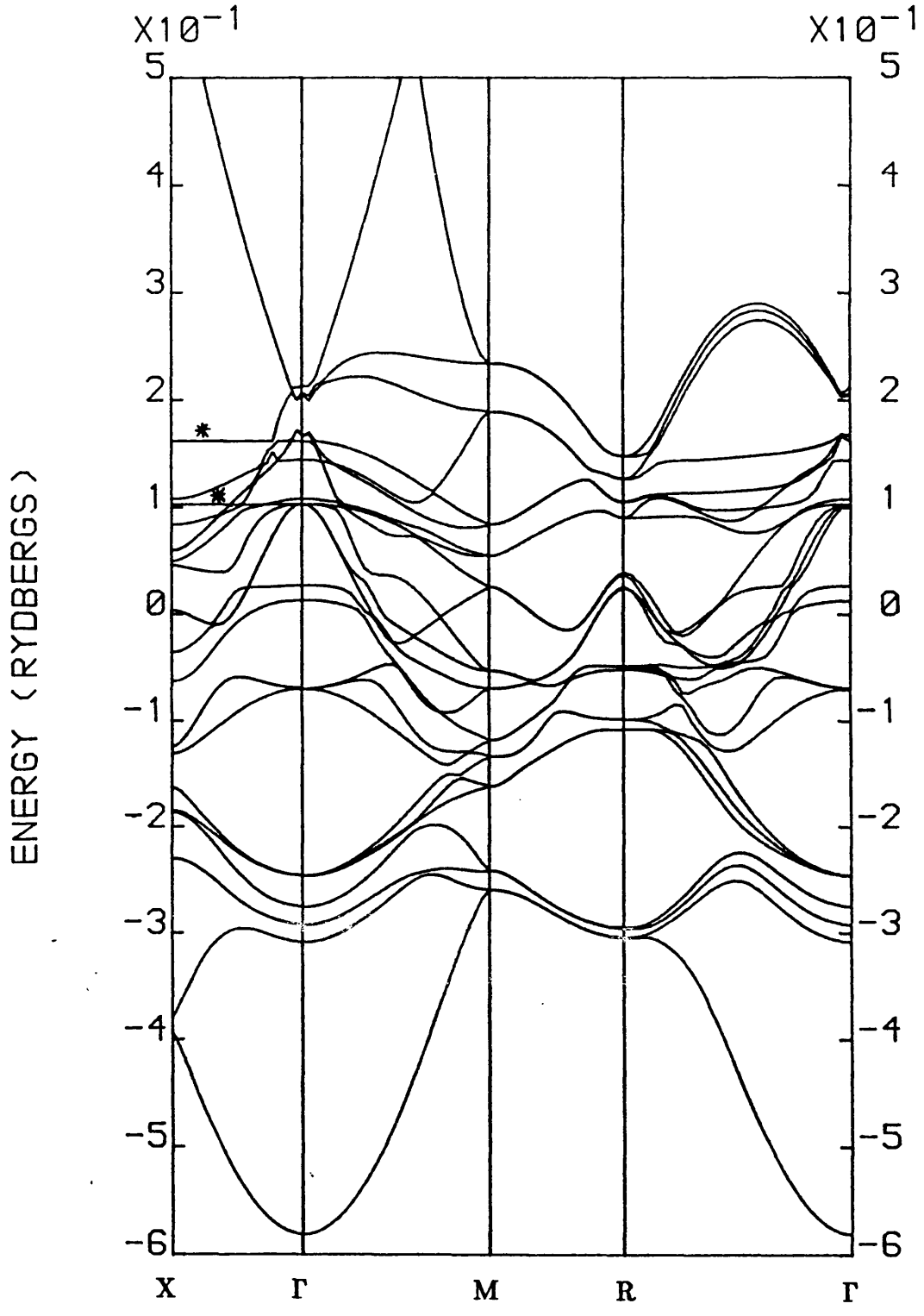

Figure 3.14: Band structure for paramagnetic Fe.

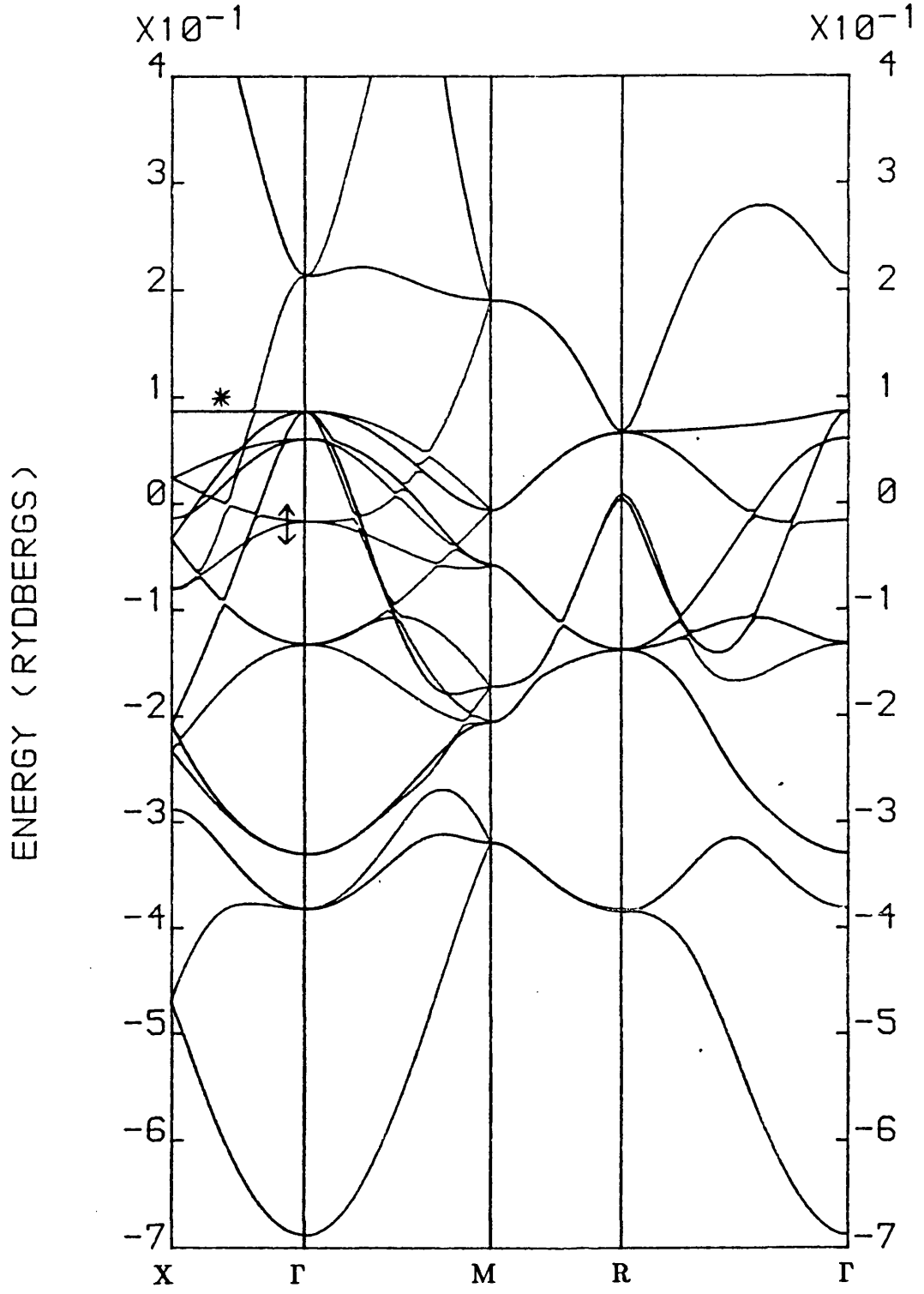

Figure 3.15: Band structure for SSDW in Fe.

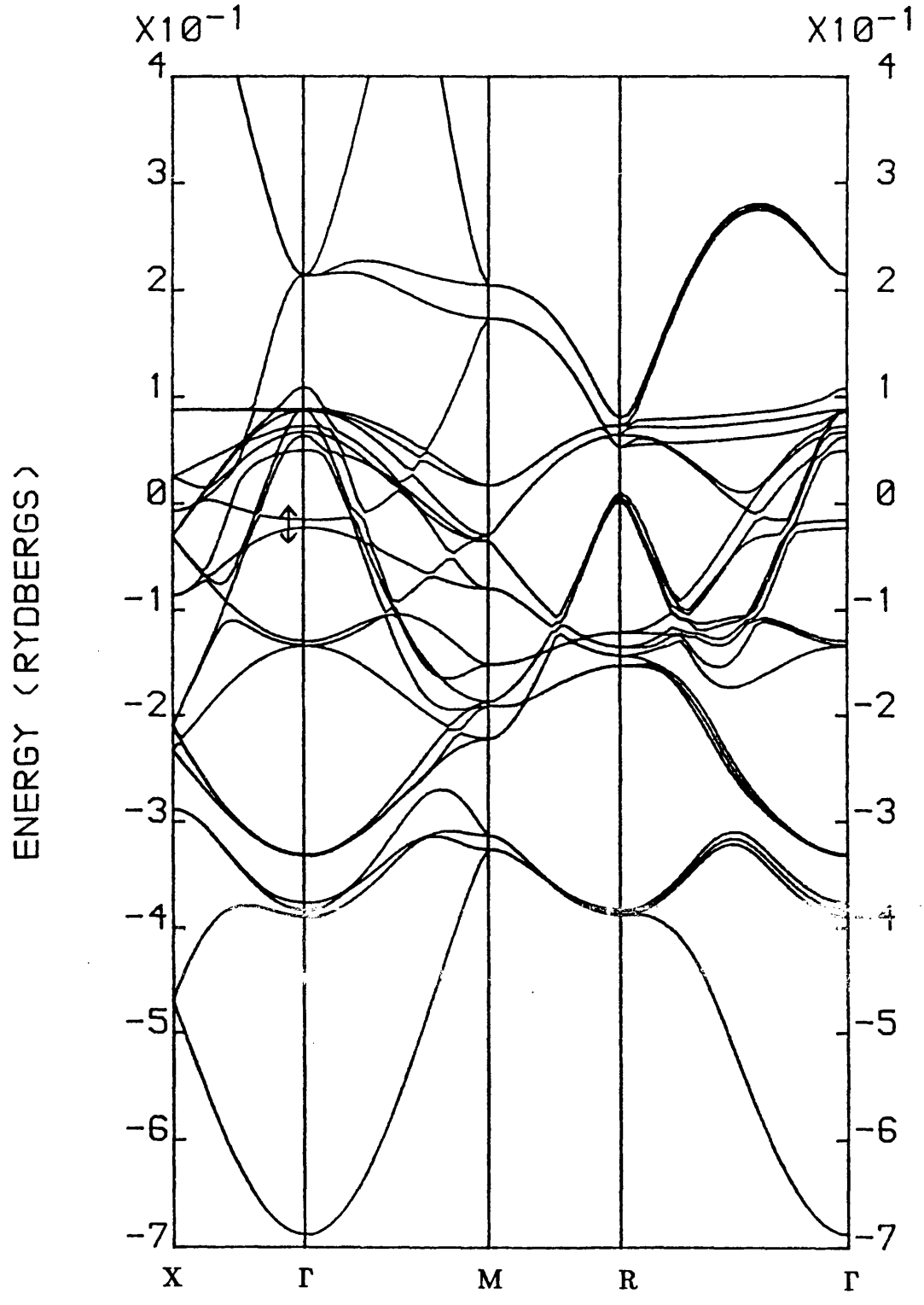

Figure 3.16: Band structure for DSDW in Fe.

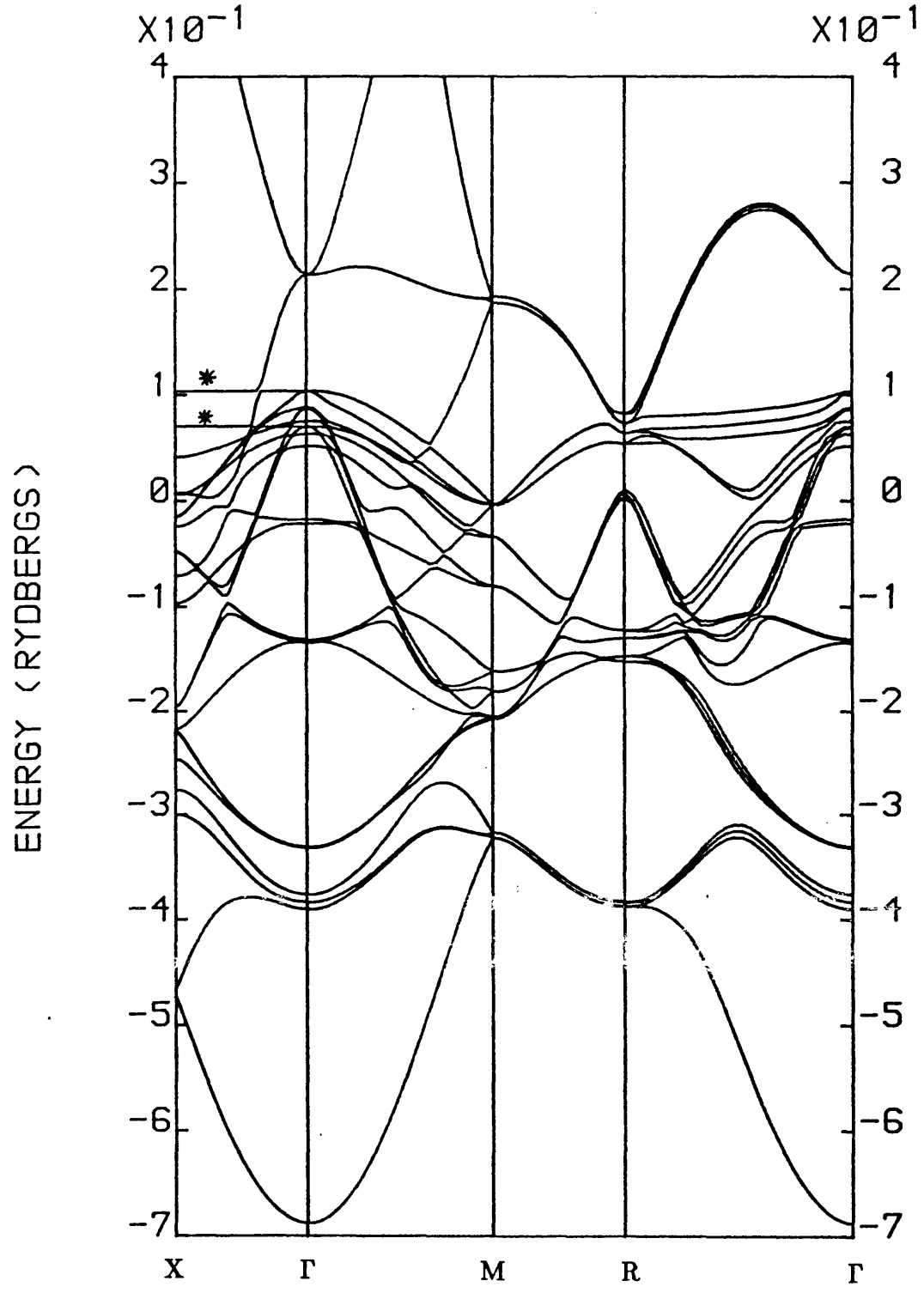

Figure 3.17: Band structure for TSDW in Fe.

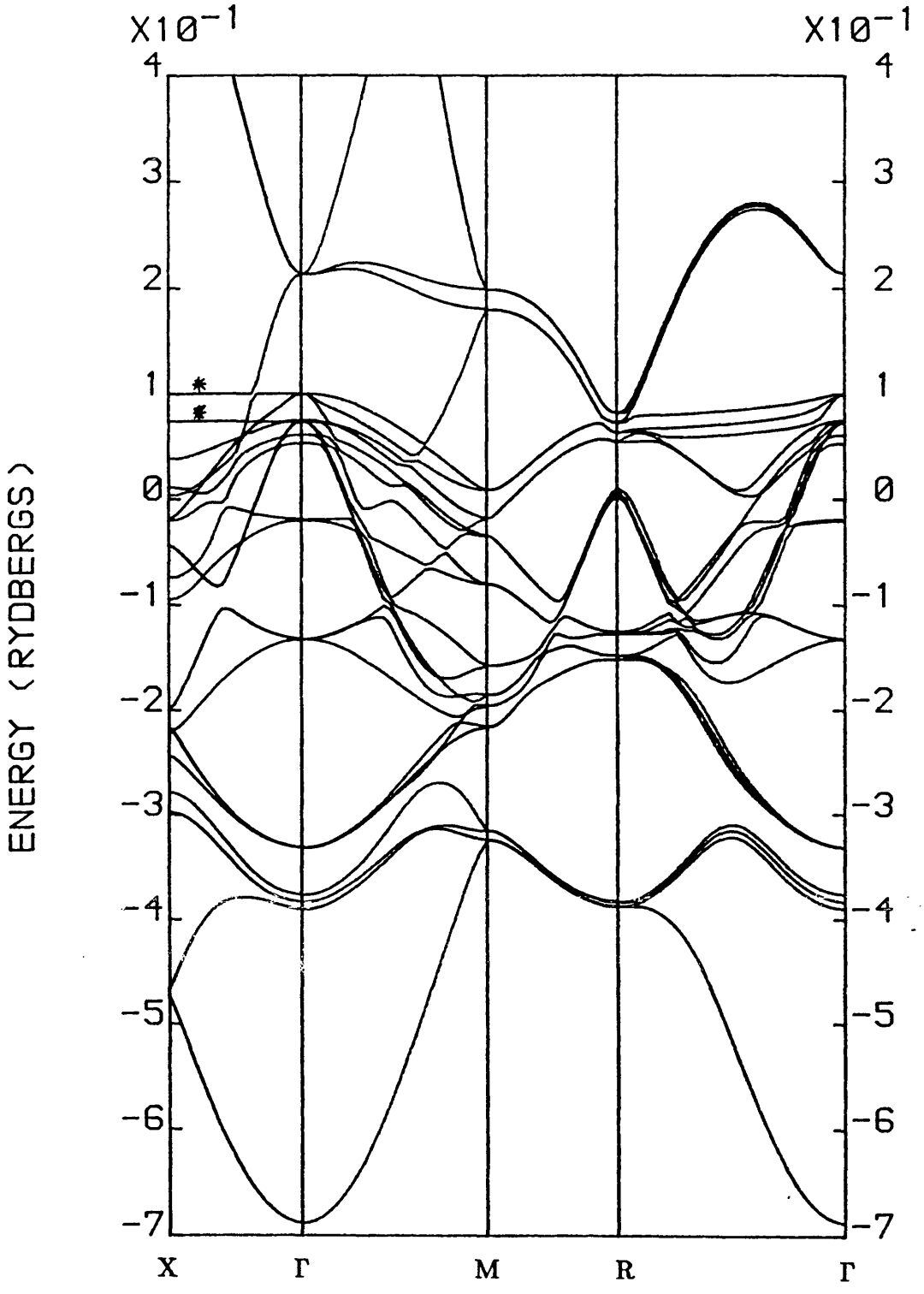

Ryd. for Fe. Looking at the band that is very flat between X and Γ (marked * in the figures) it can be seen to be split by 0.075 and 0.06 Ryd. in the DSDW and TSDW in Mn respectively (figures 3.12 and 3.13), and by 0.003 and 0.0025 Ryd. in Fe (figures 3.16 and 3.17). It is difficult to interpret these numbers directly but what they do show is that the splitting in Mn is generally an order of magnitude bigger than in Fe. It can also be seen that the dense d-electron parts of the Fe bandstructures are about 0.1 Ryd. wider in energy than those of Mn, suggesting that the d-electrons in Fe are more itinerant than in Mn.

The densities of states for the SDW materials, projected onto total angular momentum l and spin, are given in figures 3.18 to 3.23. Again, the Fermi level is set to zero. It is evident that the s and p densities of states are very small and do not seem to change on going between SDW structures. However, even with the d densities of states the different SDWs can be distinguished only by the relative magnitudes of the small spikes within an overall peak area. The graphs of the d-magnetisation density (majority density of states minus minority) are given in figures 3.24 and 3.25 and show that in both Mn and Fe there is a strong magnetic splitting with the Fermi level more or less between the up and down spin bands. Looking at the integral of the above quantity (figures 3.26 and 3.27) it can be seen that, apart from small shoulders in the Fe curves at -0.2 and -0.05 Ryd., the magnetism is built up pretty evenly throughout the band, showing that there are no really narrow bands involved. The position of the Fermi level is slightly more favourable to the moment in Mn than in Fe: in Fe it occurs just after the peak in magnetisation.

More interesting than the behaviour of the total d-electron density is thatof

Figure 3.18: Projected DOS for the SSDW in Mn.
(scale = 0.59 states/Ryd./atom/cm)

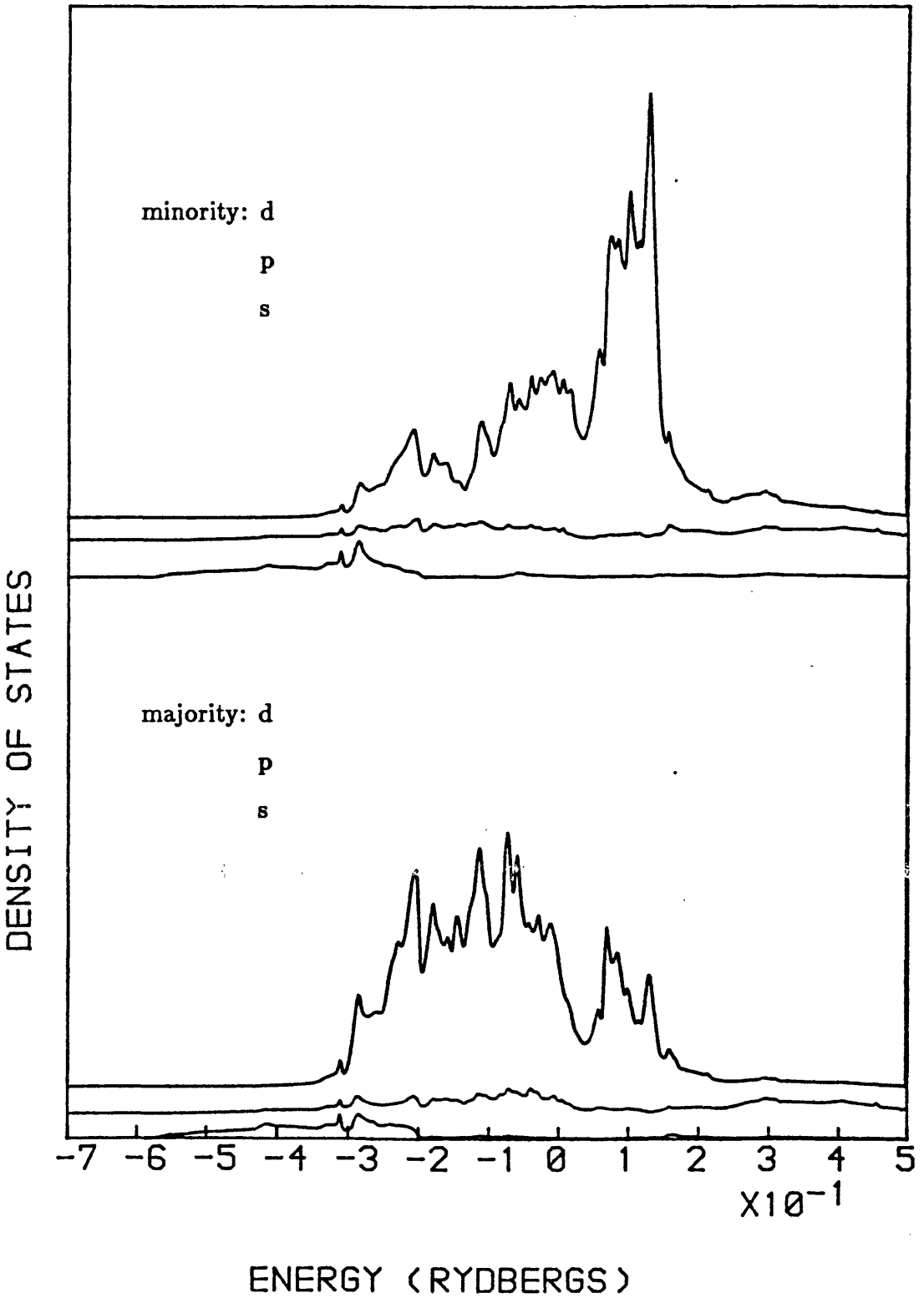

Figure 3.19: Projected DOS for the DSDW in Mn.
(scale = 0.59 states/Ryd./atom/cm)

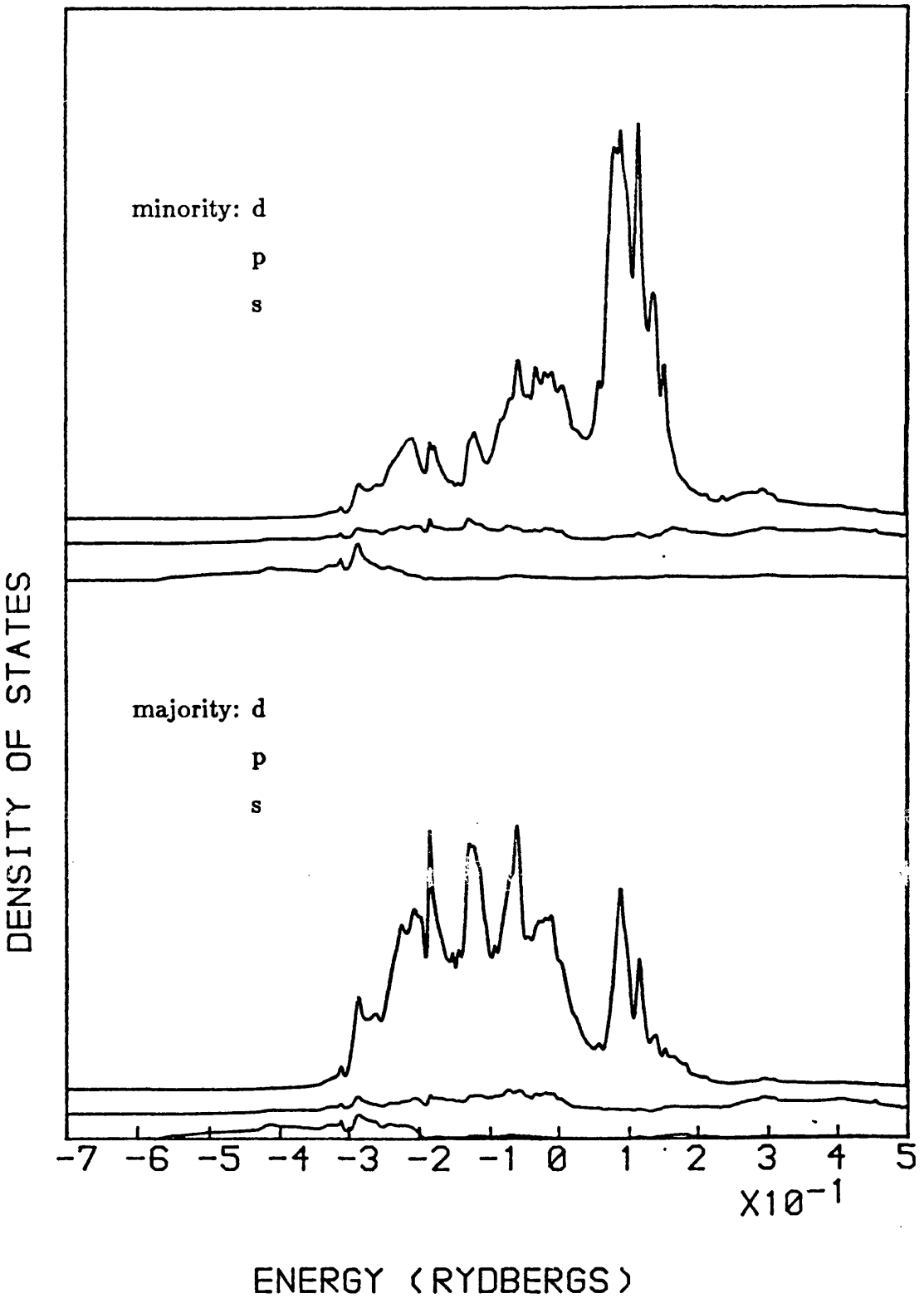

Figure 3.20: Projected DOS for the TSDW in Mn.
(scale = 0.59 states/Ryd./atom/cm)

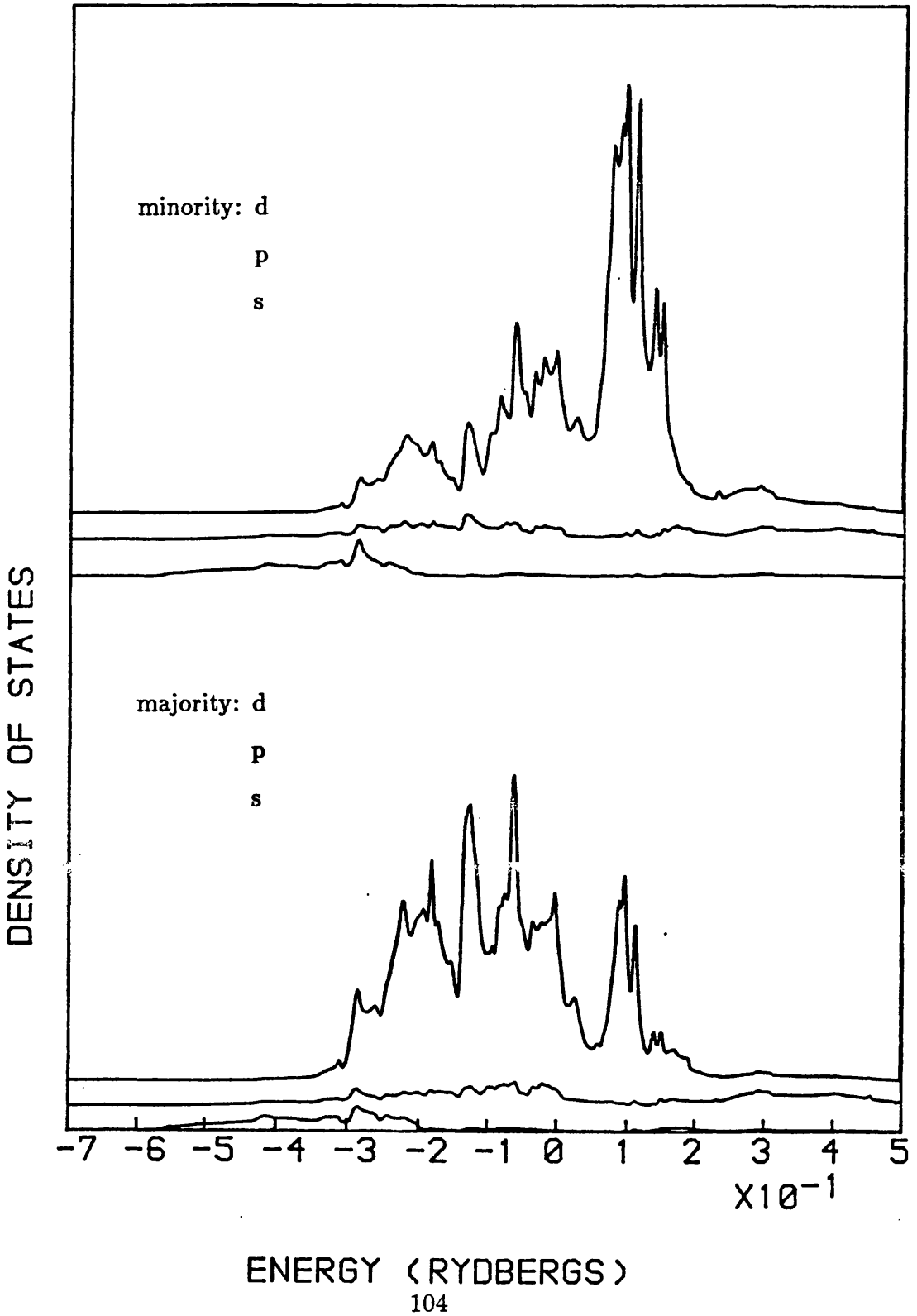

Figure 3.21: Projected DOS for the SSDW in Fe.
(scale = 0.40 states/Ryd./atom/cm)

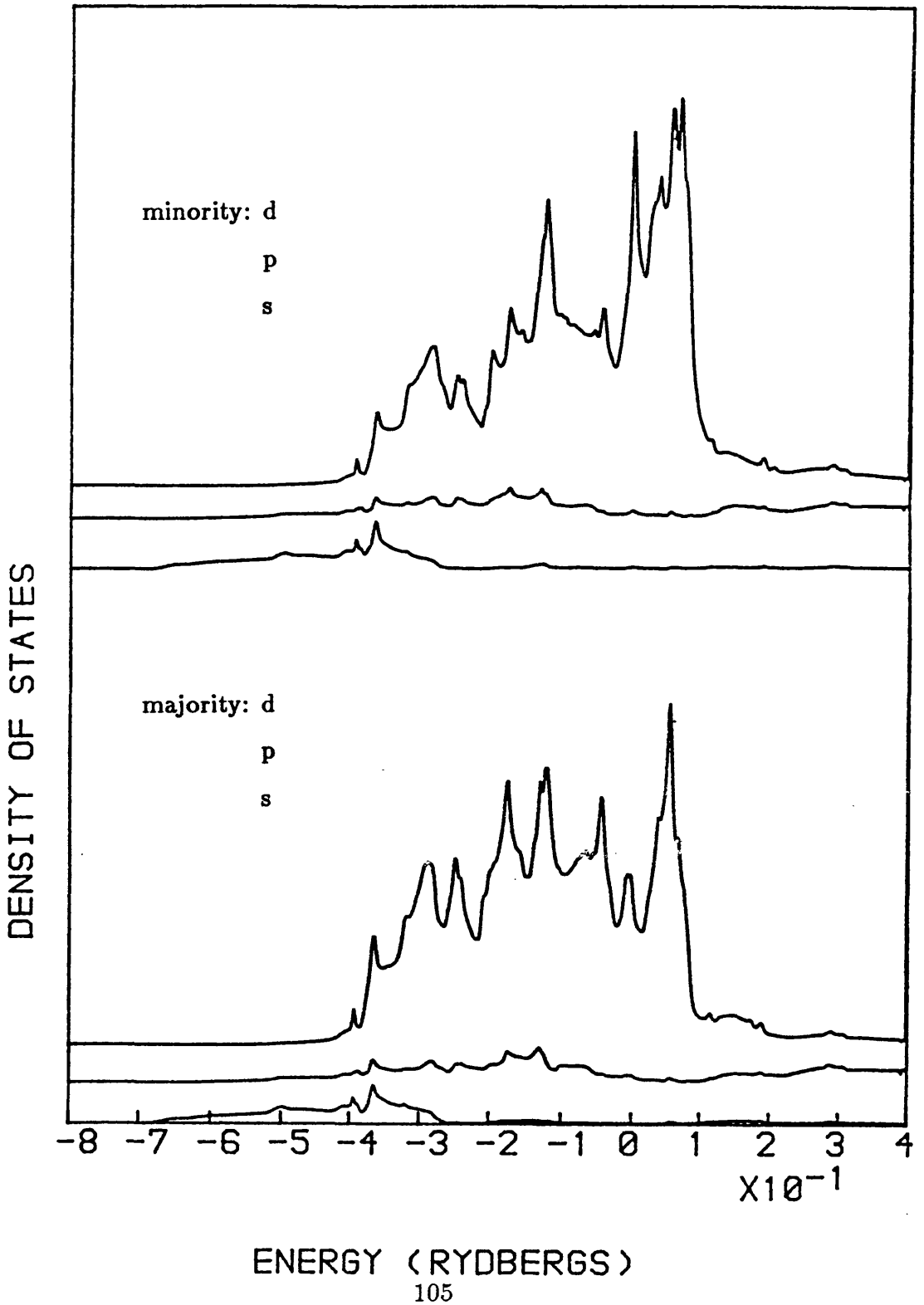

Figure 3.22: Projected DOS for the DSDW in Fe.
(scale = 0.40 states/Ryd./atom/cm)

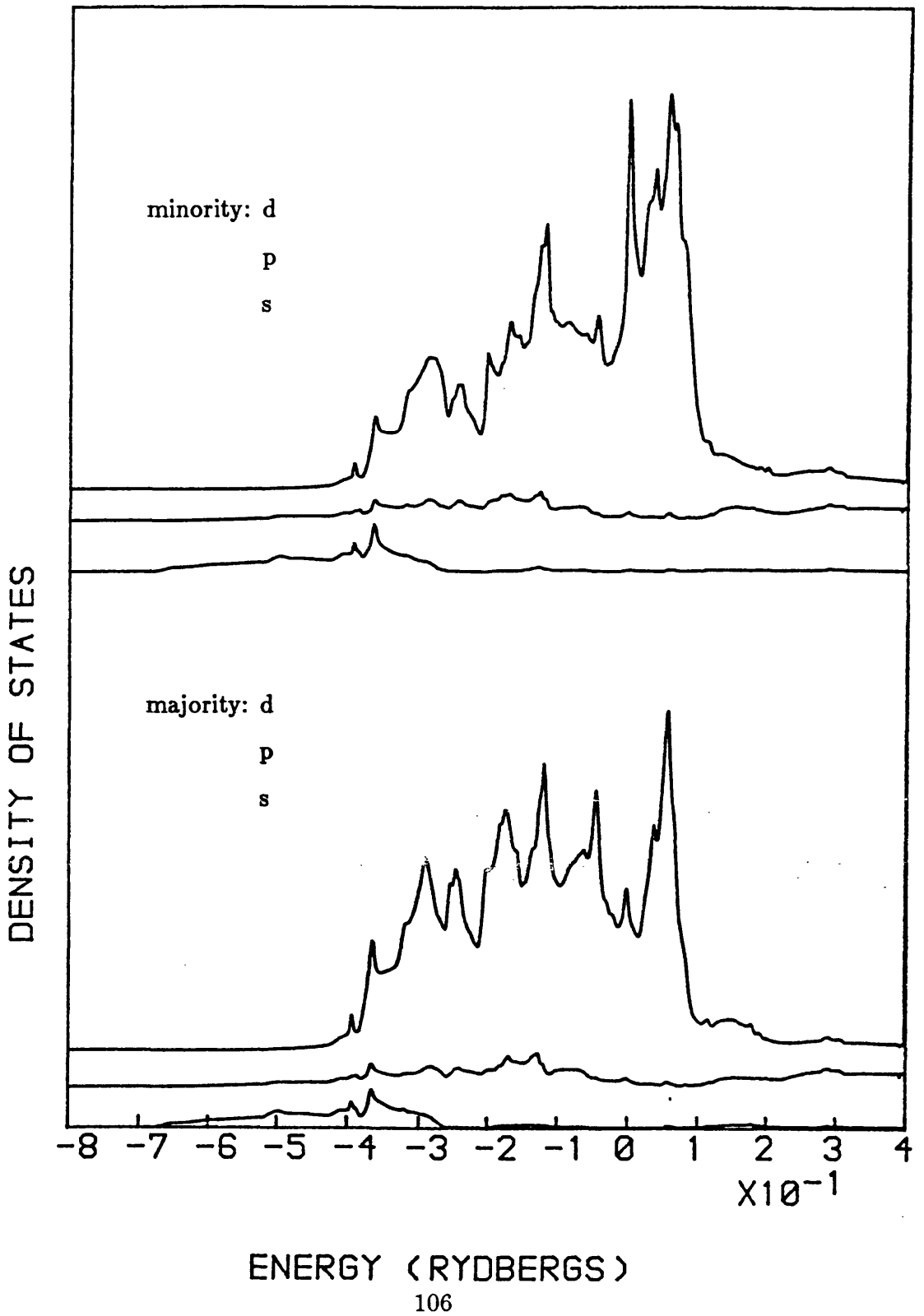

Figure 3.23: Projected DOS for the TSDW in Fe.
(scale = 0.40 states/Ryd./atom/cm)

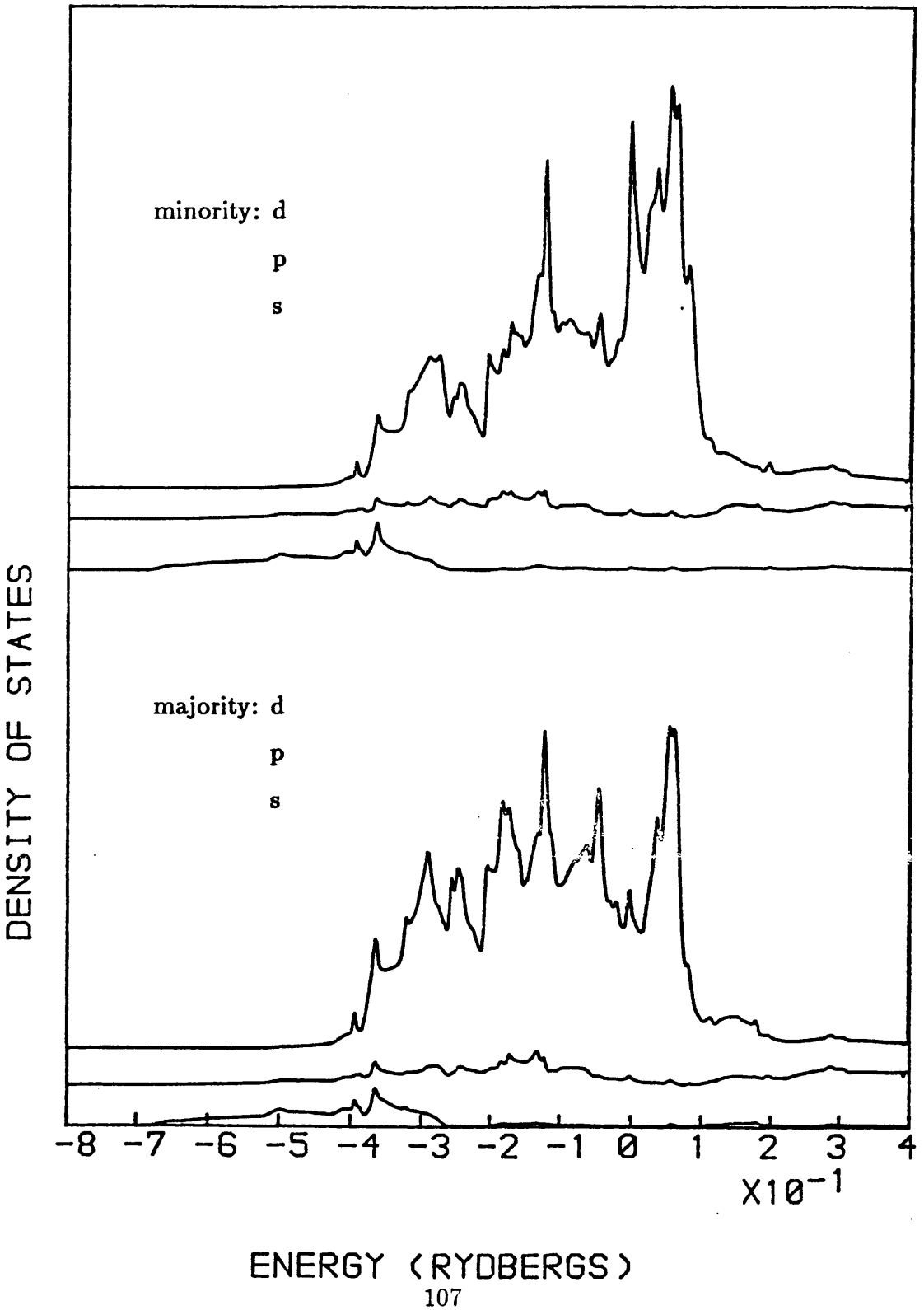

Figure 3.24: d magnetisation density in Mn.

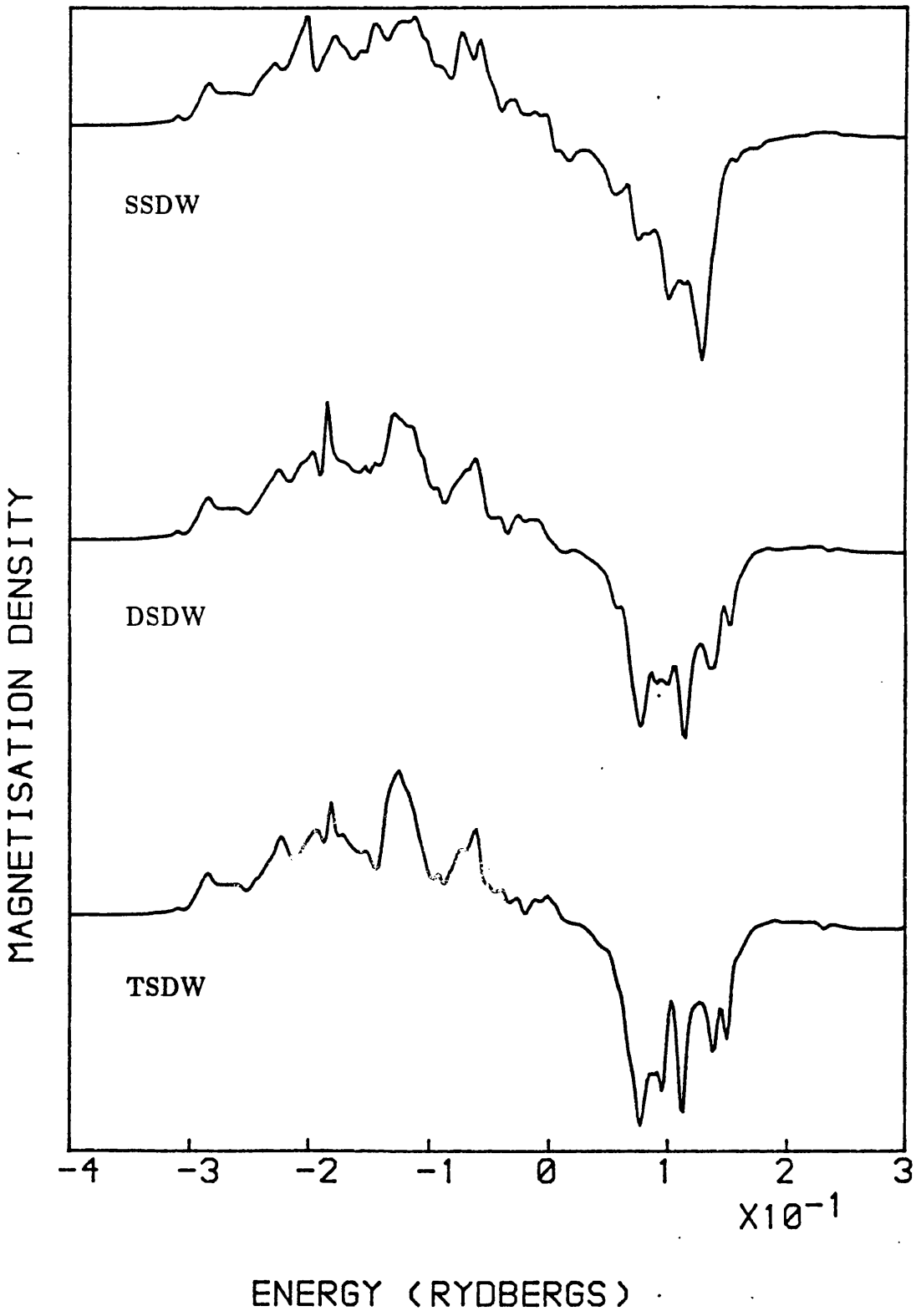

Figure 3.25: *d* magnetisation density in Fe.

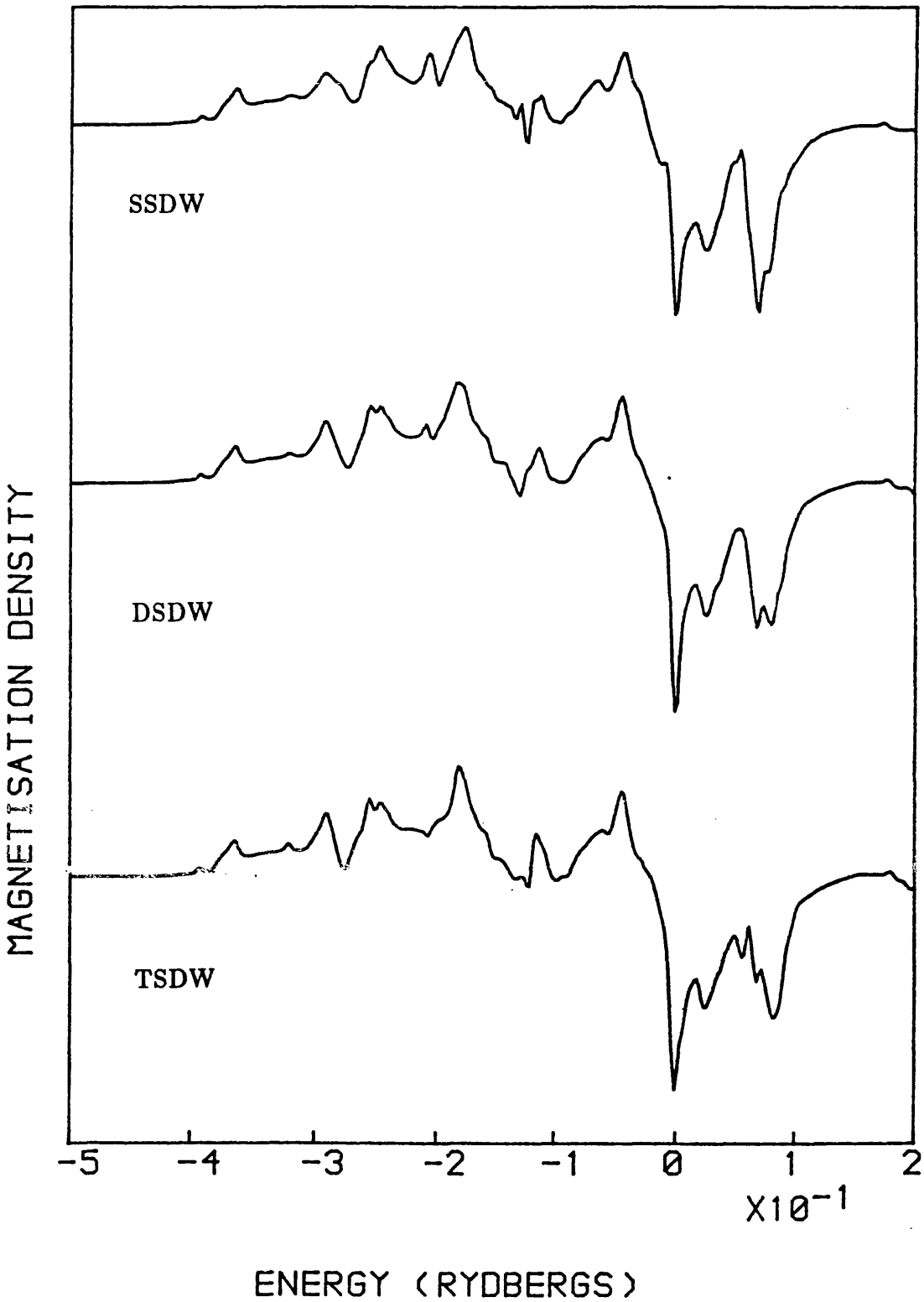

Figure 3.26: integrated d magnetisation density in Mn.
(scale = $0.31\mu_B$/atom/cm)

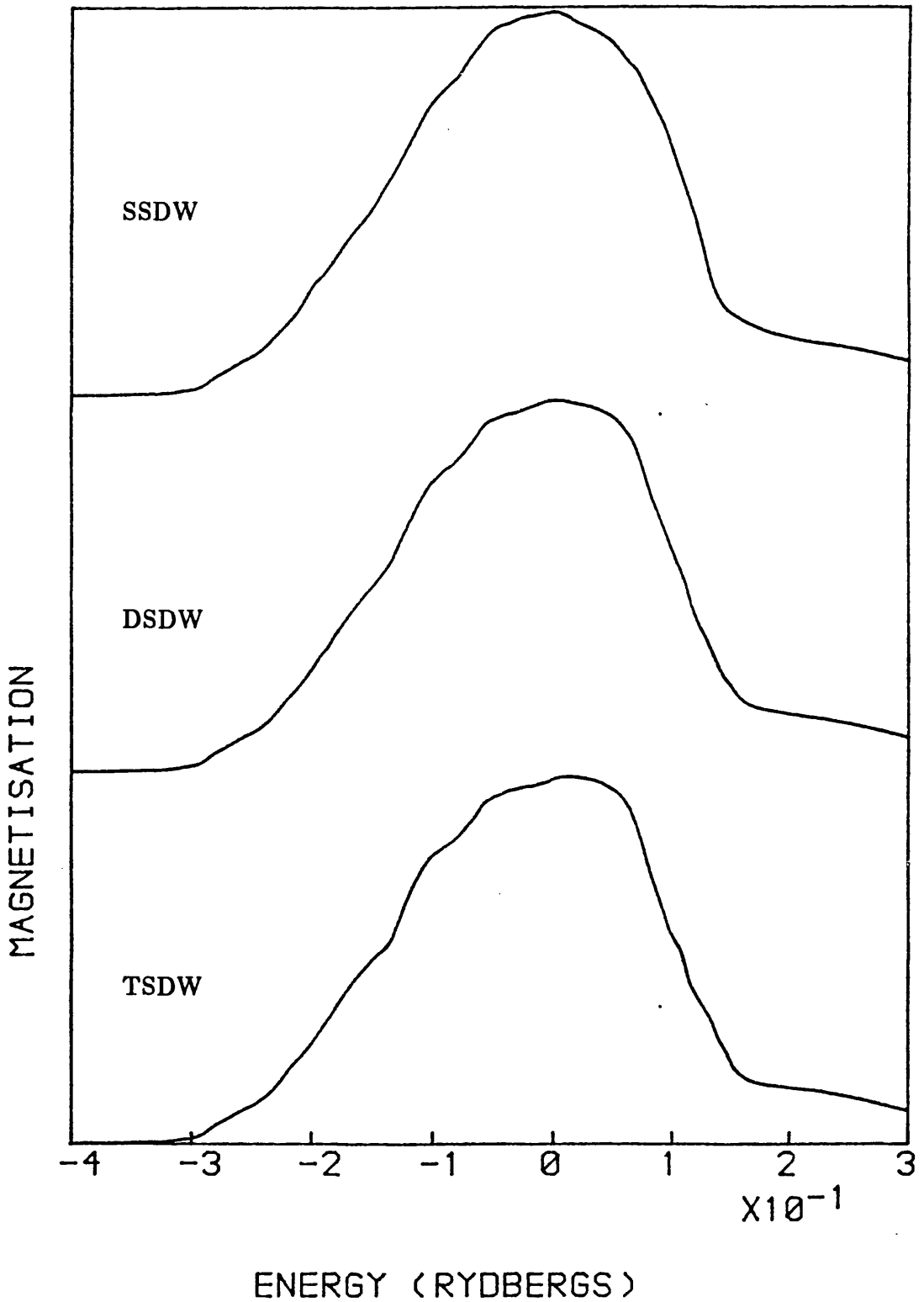

Figure 3.27: integrated d magnetisation density in Fe.
(scale = $0.13\mu_B$/atom/cm)

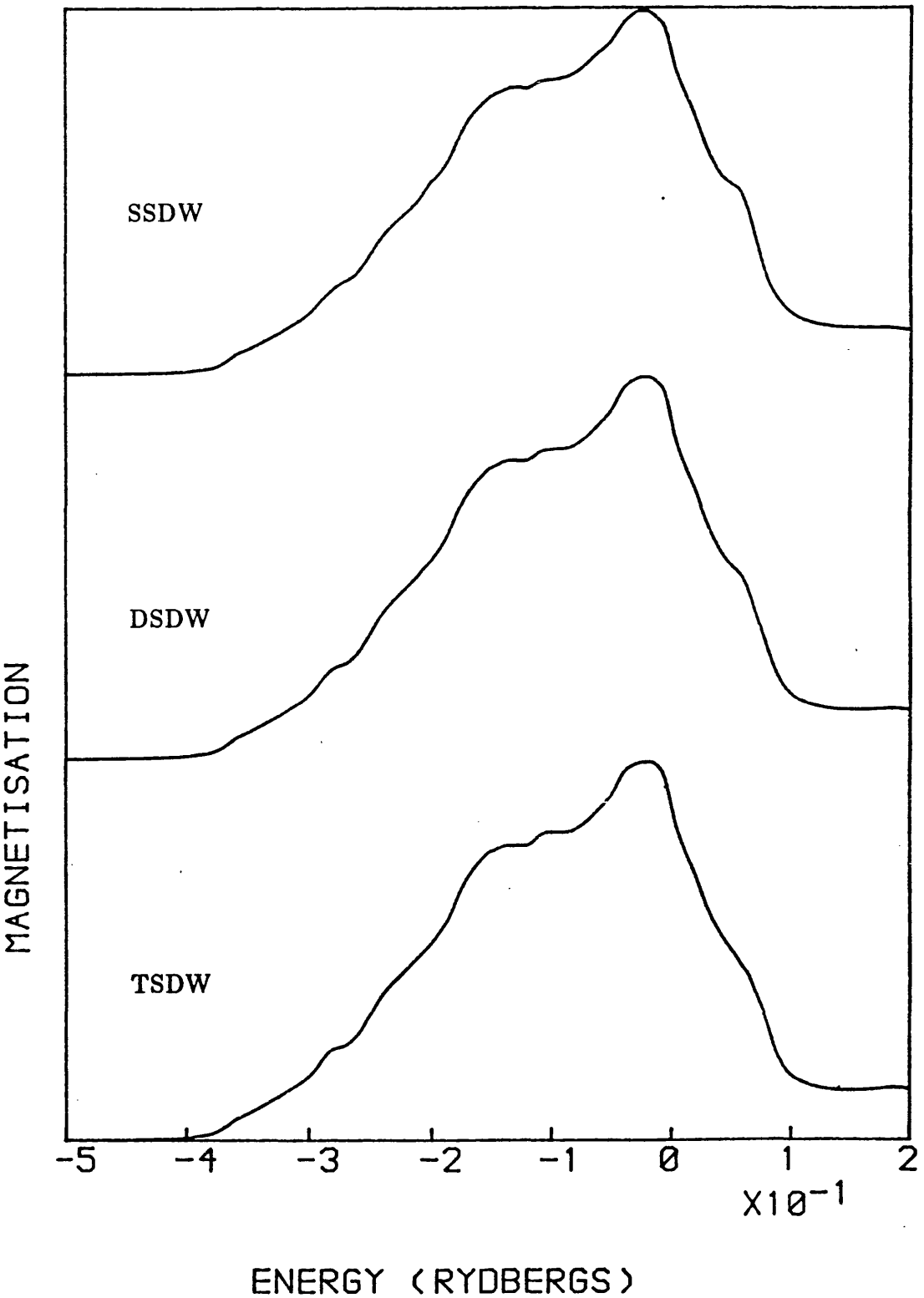

Figure 3.28: m-projected magnetisation density for SSDW in Mn.

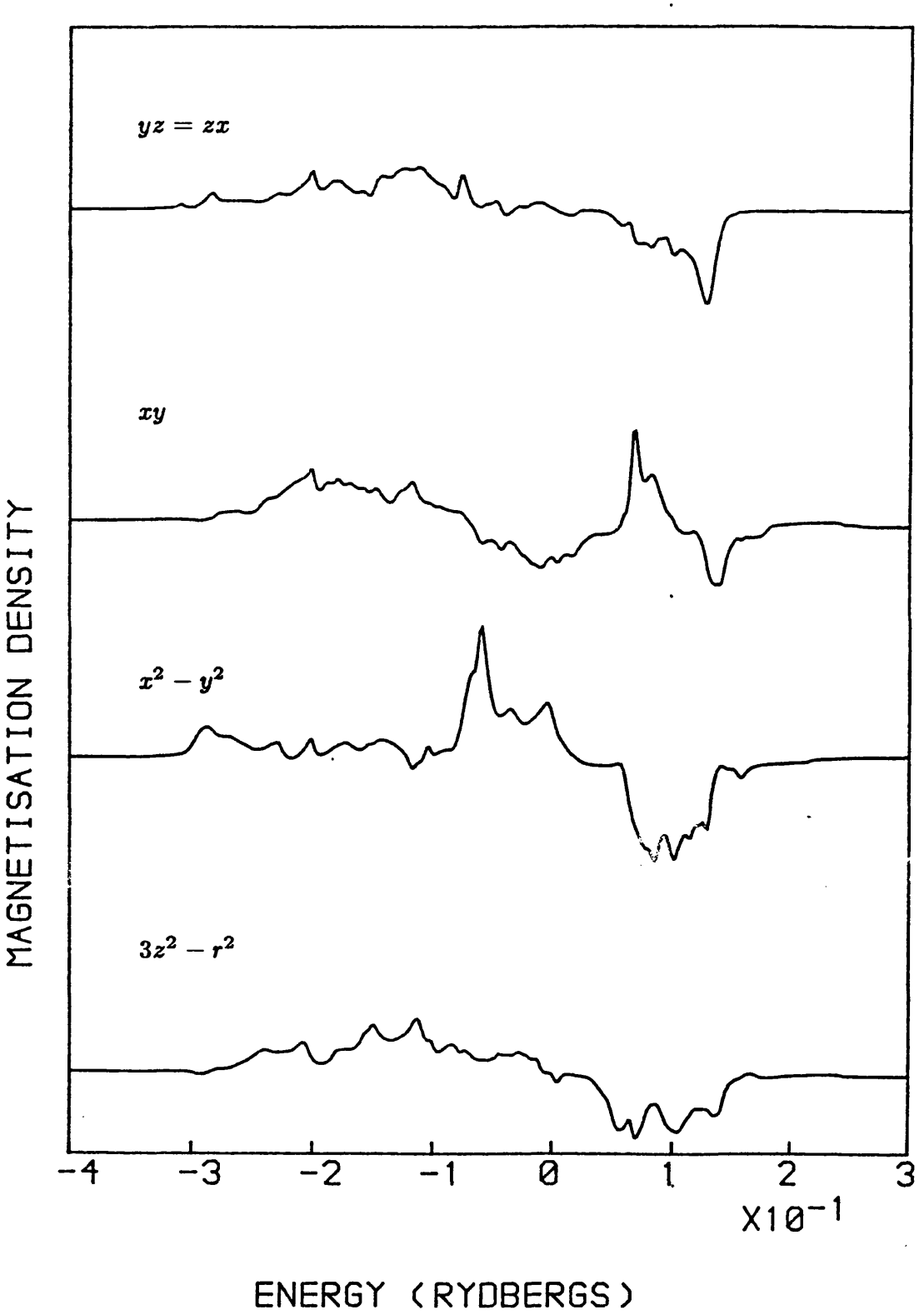

Figure 3.29: m-projected magnetisation density for DSDW in Mn.

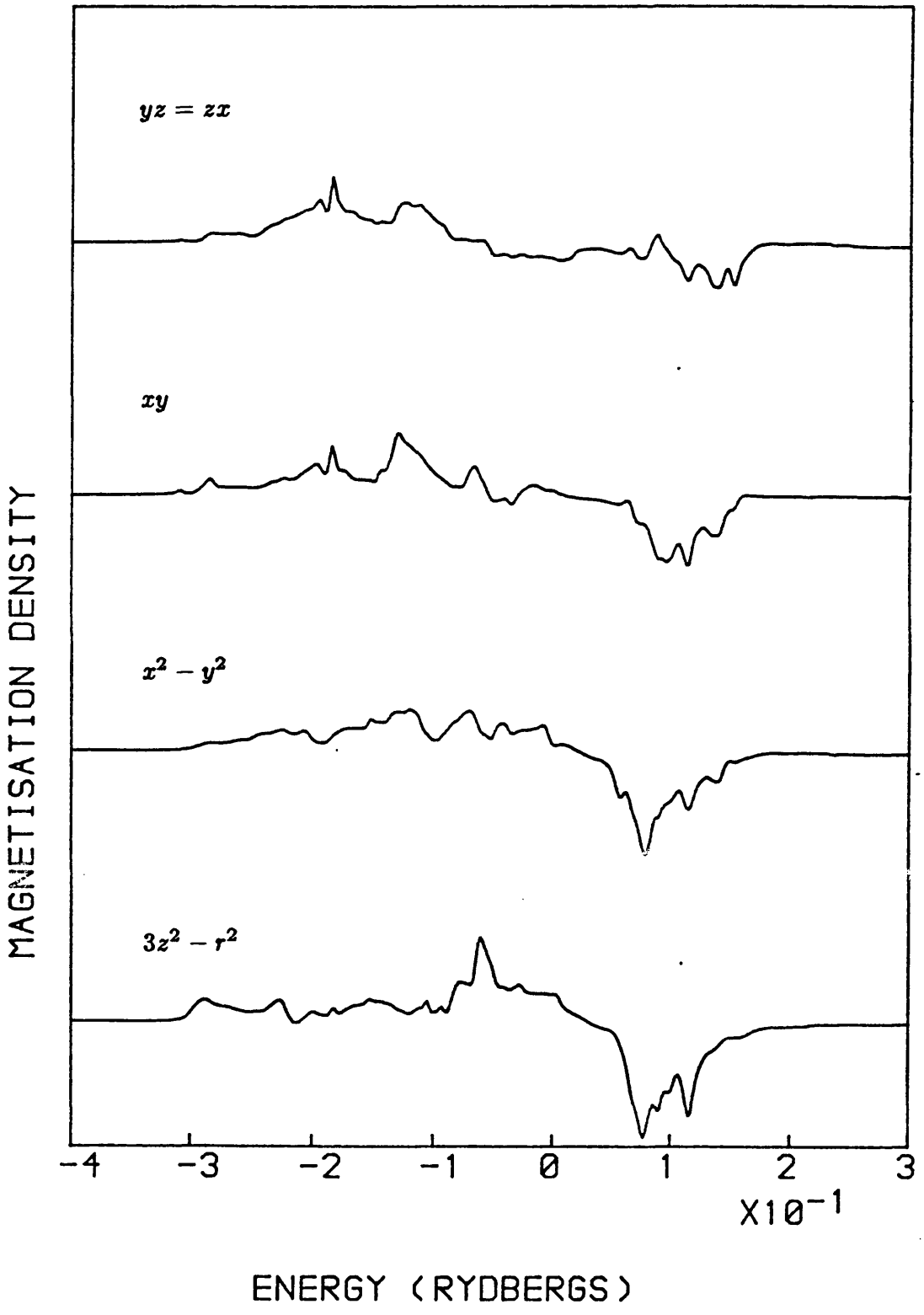

Figure 3.30: m-projected magnetisation density for TSDW in Mn.

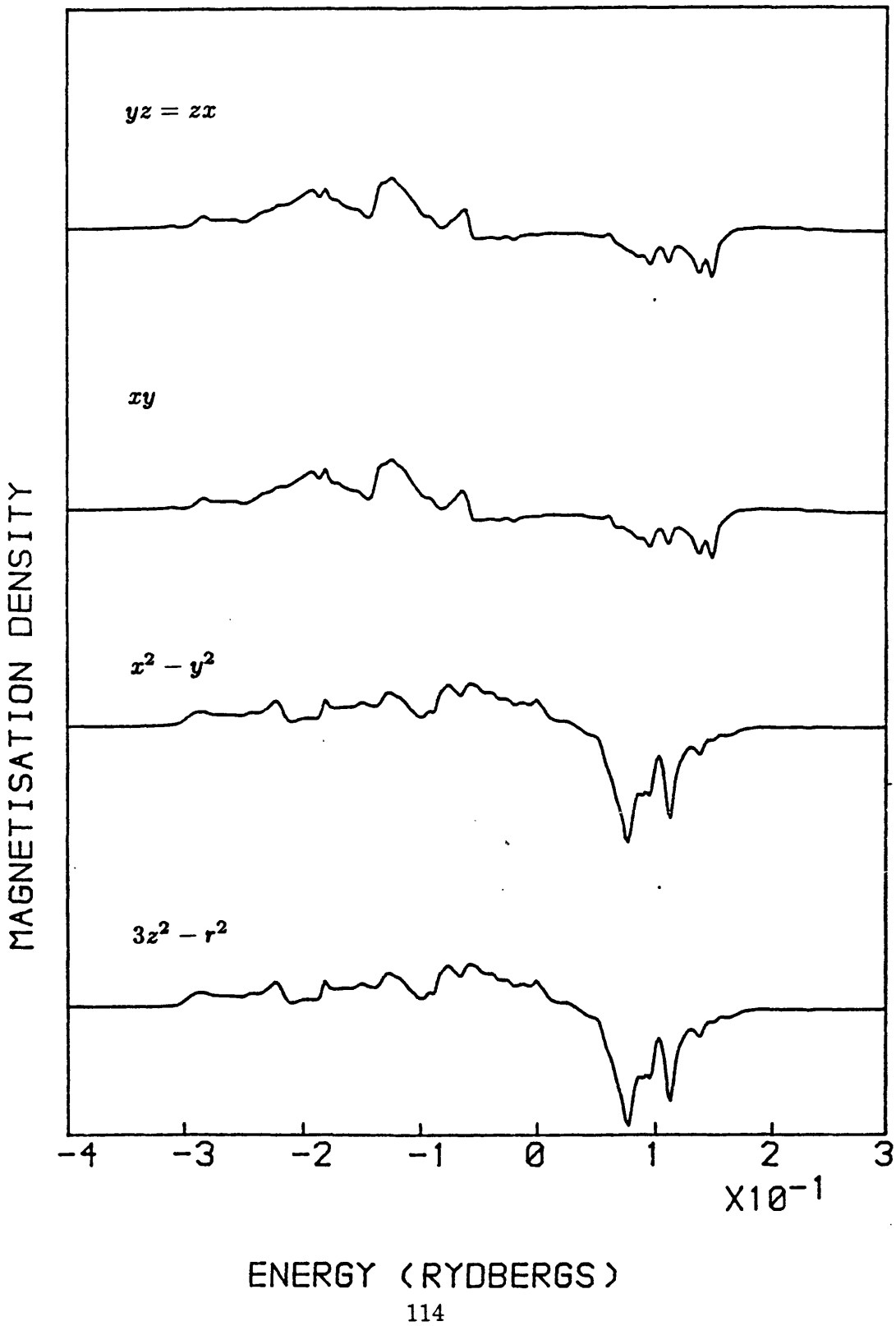

Figure 3.31: m-projected magnetisation density for SSDW in Fe.

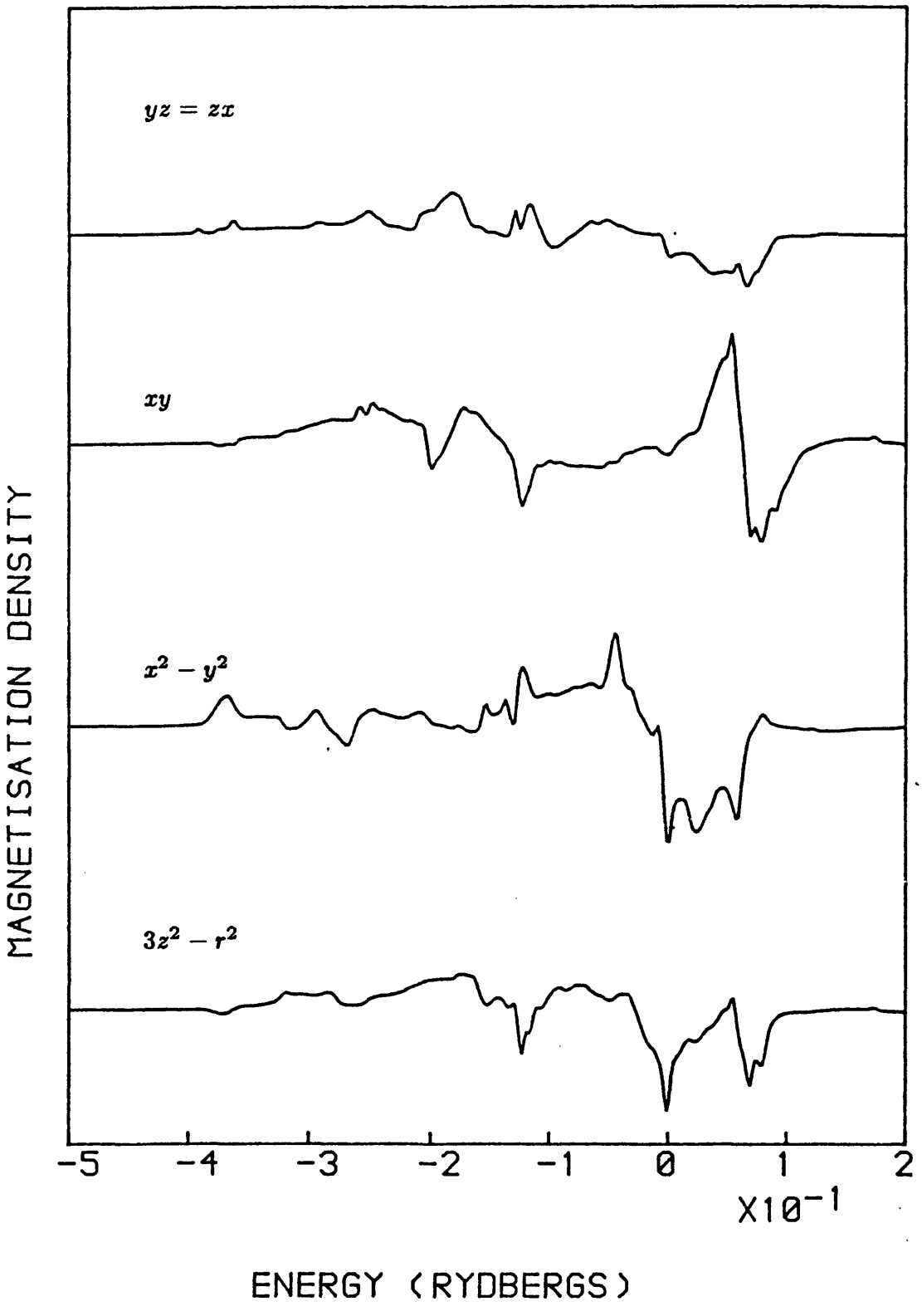

Figure 3.32: m-projected magnetisation density for DSDW in Fe.

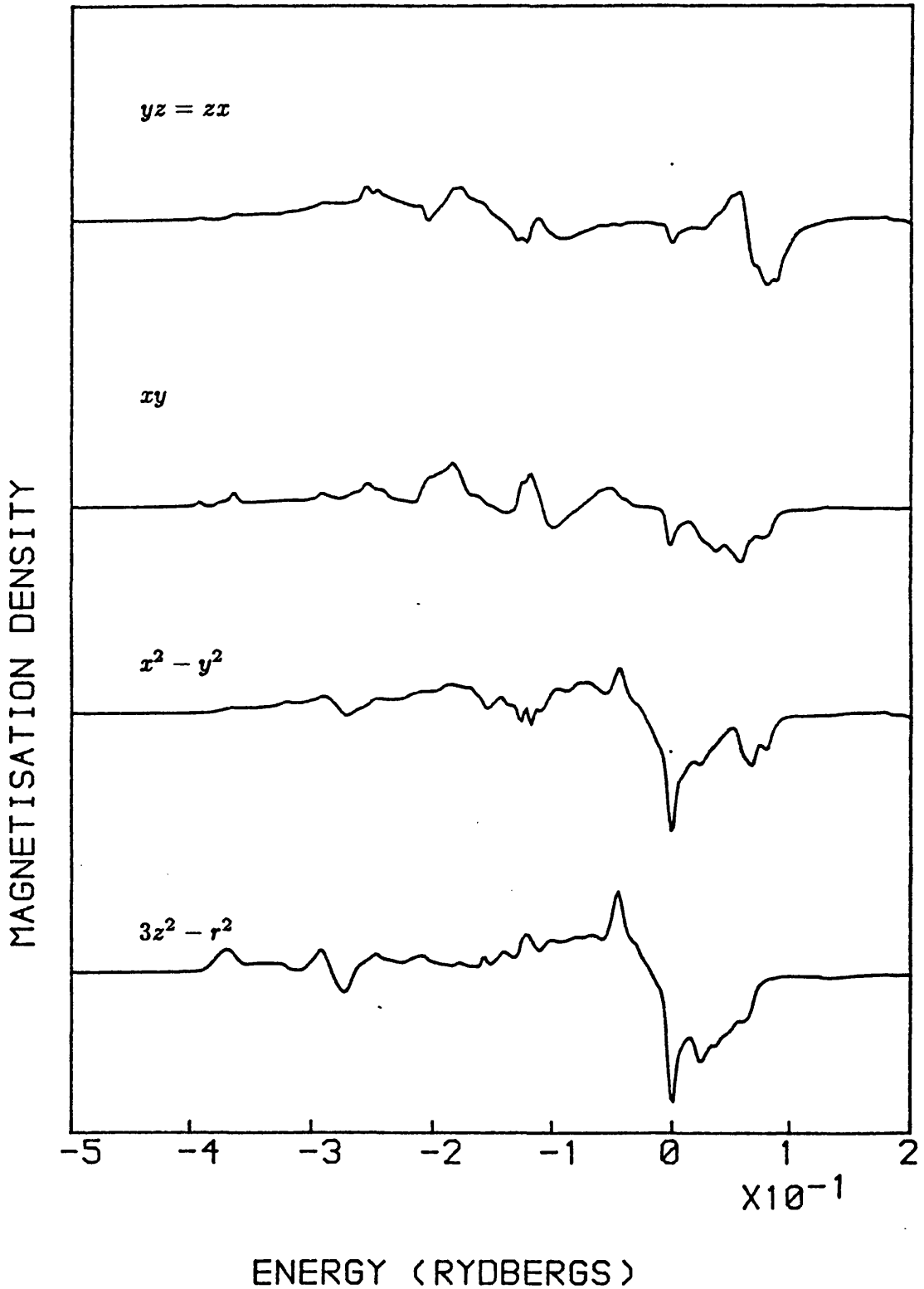

Figure 3.33: m-projected magnetisation density for TSDW in Fe.

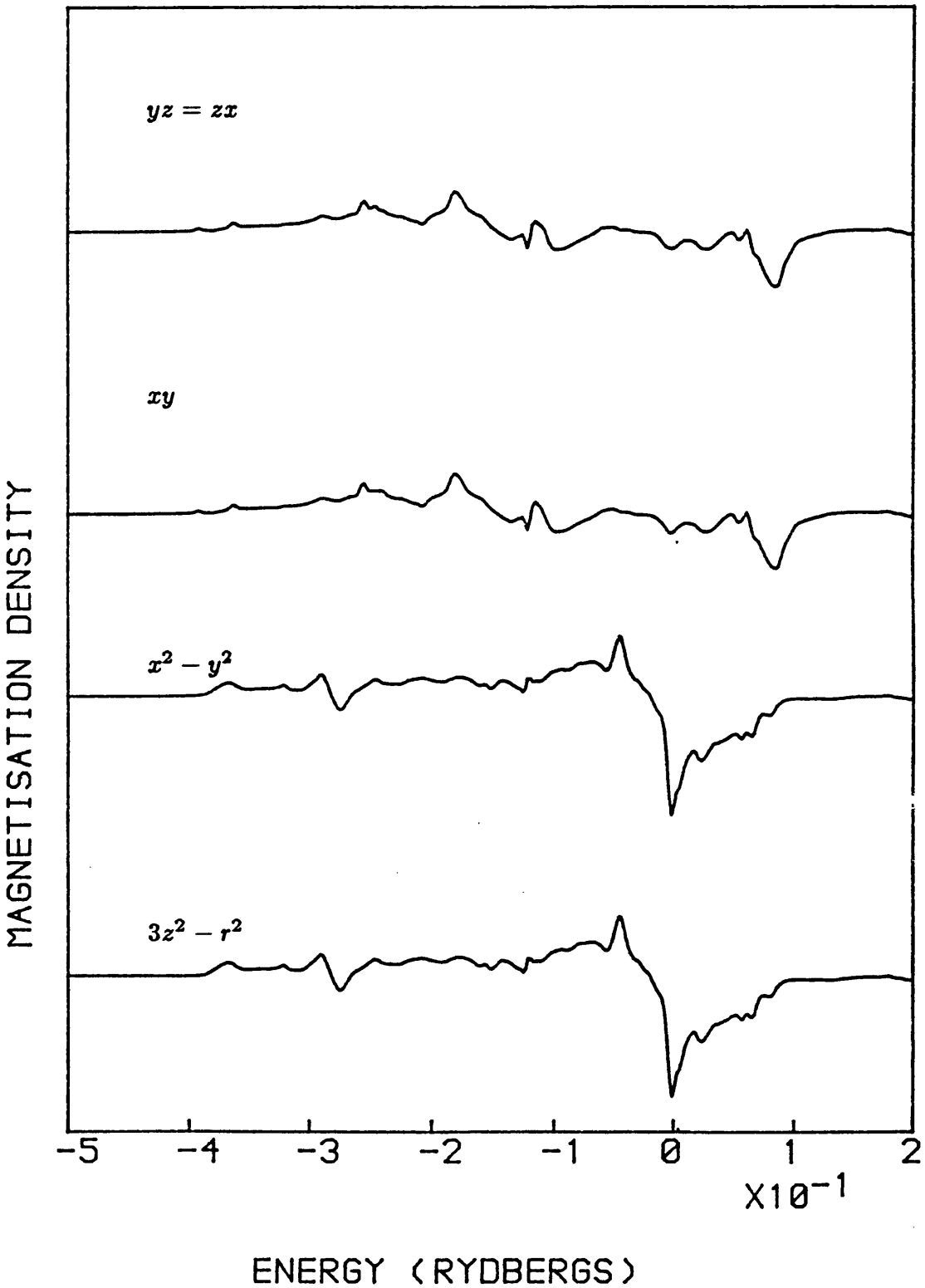

its projections onto azimuthal angular momentum m. The magnetisations carried by the various orbitals, in cubic harmonic form, are given in tables 3.3 and 3.4, and the magnetisation densities in figures 3.28–3.33. The densities of states for the SSDW in Mn were plotted and compared favourably with the work of Cade (1981b). The yz and zx orbitals are equivalent in all the structures owing to the symmetry under reflection in $x = y$. It can be seen from the tables that the two projections that carry most of the moment are the $3z^2 - r^2$ and $x^2 - y^2$. In addition, these projections exchange first and second position on going from the SSDW to the DSDW. A similar exchange occurs with the xy and the yz/zx projections. In the TSDWs the projections within the e_g ($3z^2 - r^2$ and $x^2 - y^2$) and t_{2g} (xy, yz, zx) groups respectively carry the same magnetic moment. Similar behaviour is shown in the graphs of the magnetisation density (figures 3.28–3.33): the $3z^2 - r^2$ and $x^2 - y^2$ graphs do to some extent swap over on going from the SSDW to the DSDW, and similarly the xy and yz/zx graphs. It should be noted that for the DSDW there is a general loss of distinction between graphs within a given group (e_g or t_{2g}). This is an intermediate step on the way to the TSDW, where the graphs within a group cannot be distinguished at all.

Table 3.3: Mn magnetisation/μ_B.

orbital	SSDW	DSDW	TSDW
$3z^2 - r^2$	0.4188	0.4565	0.4334
$x^2 - y^2$	0.4993	0.4300	0.4334
xy	0.2170	0.3476	0.3002
$yz = zx$	0.3536	0.2857	0.3002
total d	1.842	1.804	1.768

Table 3.4: Fe magnetistion/μ_B.

orbital	SSDW	DSDW	TSDW
$3z^2 - r^2$	0.1357	0.2167	0.1899
$x^2 - y^2$	0.2289	0.1681	0.1899
xy	0.0491	0.1414	0.1088
$yz = zx$	0.1364	0.0975	0.1088
total d	0.686	0.721	0.706

The easiest (but not necessarily the best) way to interpret these results is in terms of the localised limit (§3.2) for the d-electrons. It has to be emphasised that the output of an LDA calculation is likely to be nearer the delocalised limit (as electron correlations are not properly treated), and this should be borne in mind when considering the results. The advantage of the localised limit is that it provides a simple real-space picture, and atomic type magnetism can be be attributed to the orbitals. Thinking then in terms of atomic orbitals it can be seen (figure 3.34) that whereas the t_{2g} orbitals point directly at the nearest neighbours the e_g orbitals point at second nearest neighbours. It is therefore reasonable to expect the t_{2g} orbitals to have greater overlap than the e_g, and to be more delocalised. In fact, if the e_g electrons obey Hund's first rule this gives an explanation of the observed moment of manganese. In this case, the two localised e_g orbitals are both singly occupied and yield two Bohr magnetons of magnetic polarisation, and kinetic exchange (Mattis, 1981) gives rise to AF ordering. The remaining electrons go into the t_{2g} orbitals and form the conduction bands. For iron the moment cannot be explained in this way as we have an extra electron to deal with. Nevertheless, the picture does give an indication of why the e_g orbitals should carry the biggest moments. Moreover,

Figure 3.34: *d*-orbital directions in a cubic octant.

(a) e_g orbitals.

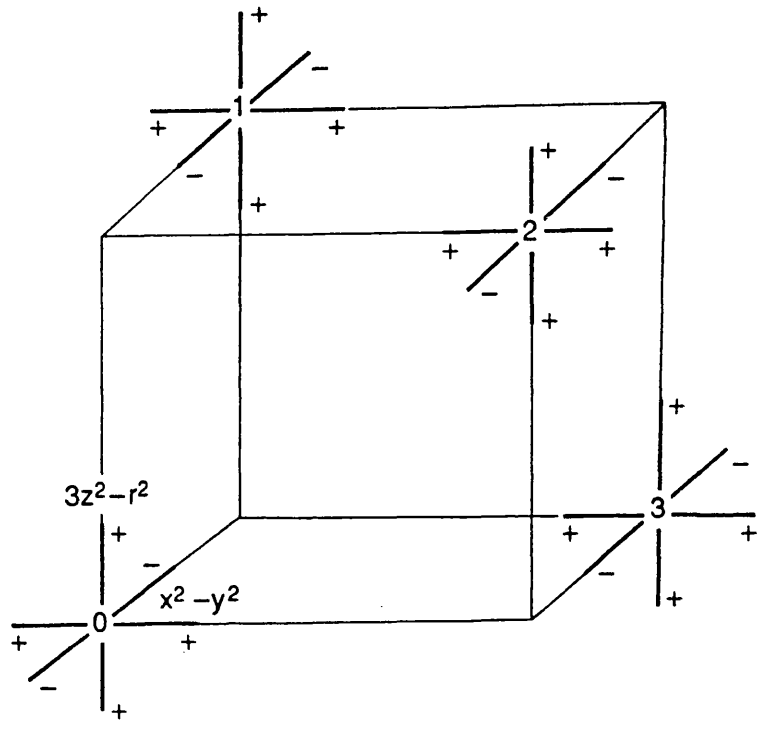

(b) t_{2g} orbitals.

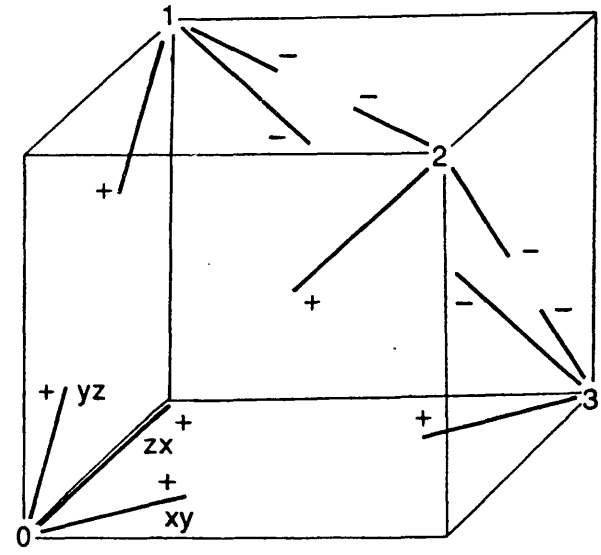

it is easy to see in this picure why the orbitals within a symmetry group (e_g or t_{2g}) are equivalent in the TSDW: all orbitals within a group make equal angles with the direction of the local moment (figure 3.34).

The degree of overlap between localised orbitals can be expressed more formally by means of the Slater-Koster integrals (Slater & Koster, 1954). According to this scheme any *dd* overlap can be written as a linear combination of three types of integral, corresponding to the so-called σ, π and δ bonds. Given that the relative magnitudes of these sorts of overlap are typically 6:4:1 (Bullett, private communication) we shall consider figure 3.34 including only the σ and π bonds. Looking at the non-zero σ and π contributions in the three atomic planes ($\{xy, yz, zx\} = \{03, 01, 02\}$) we obtain:

Table 3.5: modulus of $dd\sigma$ overlap integrals/$V_{dd\sigma}$.

orbitals	xy-plane	yx-plane	zx-plane
xy, xy	$\frac{3}{4}$	–	–
yz, yz	–	$\frac{3}{4}$	–
zx, zx	–	–	$\frac{3}{4}$
$xy, 3z^2 - r^2$	$\frac{\sqrt{3}}{4}$	–	–
$yz, 3z^2 - r^2$	–	$\frac{\sqrt{3}}{8}$	–
$yz, x^2 - y^2$	–	$\frac{3}{8}$	–
$zx, 3z^2 - r^2$	–	–	$\frac{\sqrt{3}}{8}$
$zx, x^2 - y^2$	–	–	$\frac{3}{8}$
$x^2 - y^2, x^2 - y^2$	–	$\frac{3}{16}$	$\frac{3}{16}$
$x^2 - y^2, 3z^2 - r^2$	–	$\frac{\sqrt{3}}{16}$	$\frac{\sqrt{3}}{16}$
$3z^2 - r^2, 3z^2 - r^2$	$\frac{1}{4}$	$\frac{1}{16}$	$\frac{1}{16}$

Table 3.6: modulus of $dd\pi$ overlap integrals/$V_{dd\pi}$.

orbitals	xy-plane	yx-plane	zx-plane
xy, xy	–	$\frac{1}{2}$	$\frac{1}{2}$
xy, yz	–	–	$\frac{1}{2}$
xy, zx	–	$\frac{1}{2}$	–
t_{2g}/e_g	–	–	–
x^2-y^2, x^2-y^2	1	$\frac{1}{4}$	$\frac{1}{4}$
$x^2-y^2, 3z^2-r^2$	–	$\frac{\sqrt{3}}{4}$	$\frac{\sqrt{3}}{4}$
$3z^2-r^2, 3z^2-r^2$	–	$\frac{3}{4}$	$\frac{3}{4}$

It can be seen that, for the σ bond at least, a t_{2g}/t_{2g} overlap is about twice as big as a t_{2g}/e_g, which is twice as big as an e_g/e_g. For the π bond the t_{2g}/t_{2g} and e_g/e_g overlaps look pretty similar on the whole and the t_{2g}/e_g overlaps are zero. Given the weighting towards the σ bond these numbers confirm the intuitive ideas of the last paragraph. In order to see how the change over of the e_g orbitals between SSDW and DSDW might occur consider the largest overlaps in and out of the xy plane.

Table 3.7: largest overlaps involving e_g orbitals.

	$3z^2-r^2$	x^2-y^2
in xy plane	$\frac{3}{8}\sigma$	π
out of xy plane	$\frac{3}{16}\sigma+\frac{3}{4}\pi$	$\frac{3}{8}\sigma+\frac{3}{8}\pi$

Putting $\sigma = 3$ and $\pi = 2$ these become,

Table 3.8: numerical values for largest e_g overlaps.

	$3z^2 - r^2$	$x^2 - y^2$
in xy plane	1.1	2.0
out of xy plane	2.1	1.9

which indicate that for the $3z^2 - r^2$ orbital the most important overlap occurs out of the xy plane whilst for the $x^2 - y^2$ orbital it occurs in plane. Bearing in mind that Pauli exclusion will reduce hopping involving orbitals of the same spin it can be seen from this that in the SSDW, where the xy plane has a common spin polarization, the hopping involving $x^2 - y^2$ orbitals will be reduced whereas in the DSDW, where nearest neighbours out of the plane have the same polarization, the hopping involving the $3z^2 - r^2$ orbitals will be reduced. Given that the polarization is atomic in character then a reduced hopping should produce a larger moment. Therefore the $x^2 - y^2$ orbitals should carry a greater moment in the SSDW and the $3z^2 - r^2$ in the DSDW, as observed from the LMTO calculations.

It should be pointed that the numbers given in table 3.8 do not make the above arguments clear cut and the localised picture should not be taken *too* seriously. Nevertheless, it does provide some indication of why the *d*-electrons behave as they do.

3.12) Axial distortion in SDW structures.

It was mentioned in §3.4 how, working within a localised electron picture, we might expect the SSDW and DSDW to distort tetragonally. In the SSDW a distortion to a structure with $\frac{c}{a} < 1$ would render the unfavourable parallel spins

of the xy-plane further apart and the favourable antiparallel spins of adjacent xy-planes closer together (figure 3.6). For the DSDW the situation is reversed (figure 3.7) and the expected distortion is to $\frac{c}{a} > 1$. In the TSDW there is no anisotropy due to the spin configuration (figure 3.8) and we therefore expect the structure to remain cubic.

In this section we present estimates for the tetragonal distortions of the SSDW, DSDW and TSDW, and compare them (where possible) to the experimental values. The predictions are based on a calculation of the axial pressure using the LMTO-ASA code (see next chapter). The axial pressure is a measure of the tendency of a structure to change its $\frac{c}{a}$ ratio with respect to some axis and its value may be fed into classical elasticity theory (§4.9) to provide the following results for the equilibrium deviation from ideal $\frac{c}{a}$ (=1 for an FCT lattice).

Table 3.9: estimated % deviations from $\frac{c}{a} = 1$.

	SSDW	DSDW	TSDW
Mn	−3.8	1.4	0.02
Fe	−0.02	−0.08	0.0003

It can be seen that the distortion for the TSDW in Mn, and all the structures in Fe, may be taken to be zero beside those of the SSDW and DSDW in Mn. The latter values are in good agreement with the respective experimental estimates of −6% (Cowlam, Bacom & Gillott, 1977; Smith & Vance, 1969) and 1% (Honda, Tanji & Nakagawa, 1976). In the case of Fe there appear to be no definite values for the distortion from ideal, but the work of Endoh & Ishikawa (1971) suggests that pure γ Fe may be cubic. The fact that the Mn results are in line with the expectations of the localised picture while the Fe distortions appear to be zero

suggests that the magnetism in γ-Fe may be more itinerant in character than that in γ-Mn.

The elasticity theory used above may also be used to estimate the energy savings associated with these distortions. The results for the SSDW and DSDW in Mn (where the distortion is sufficiently large to be significant) are -0.0011Ryd. and -0.00013Ryd. respectively, which when added to the total energies of table 3.1 yield equilibrium values of -126.1268Ryd. and -126.1259Ryd. The difference between these two values is still very small but it does at least suggest that the SSDW should be the more stable, which is in line with the experimental results (§3.4).

CHAPTER FOUR: THE AXIAL PRESSURE.

4.1) Introduction.

Given a self-consistent ground state we might expect to be able to calculate structural properties such as lattice constants, or for hexagonal and tetragonal systems, the $\frac{c}{a}$ ratio. The obvious way of determining these would be to plot the total energy as a function of the parameter, a or $\frac{c}{a}$, and to find the value of the parameter for which the energy is a minimum. This is not wholly satisfactory because the total energy obtained from a band structure calculation tends to be large compared to the sort of energy changes observed when varying structural parameters, and there are often doubts as to whether it can be relied upon to this degree of accuracy. Nevertheless, the method works reasonably well in the determination of lattice constants, as shown for copper (with experimental $S_{\mathbf{ws}} =$ 2.66AU) in figure 4.1. Where the method breaks down is in the determination of other structural parameters. About the simplest case we can consider is the $\frac{c}{a}$ ratio of a hexagonal or tetragonal system, and for this the method is disastrous. A typical curve for an ASA calculation at constant volume is that for zinc, which is given in figure 4.2, and whose turning point is a *maximum* rather than a minimum. The reason for the failure lies in the approximate treatment given to the electrostatic forces between the atoms: for non-uniform distortions a proper description of these forces is needed (Christensen, 1984).

Leaving out the question of the electrostatic forces for the moment, there is an alternative approach to the determination of structural parameters which involves the calculation of *pressures*. The bulk or isotropic pressure is derived from the derivative of the Kohn-Sham energy (2.13) with respect to the lattice

Figure 4.1: Total energy curve for FCC copper.

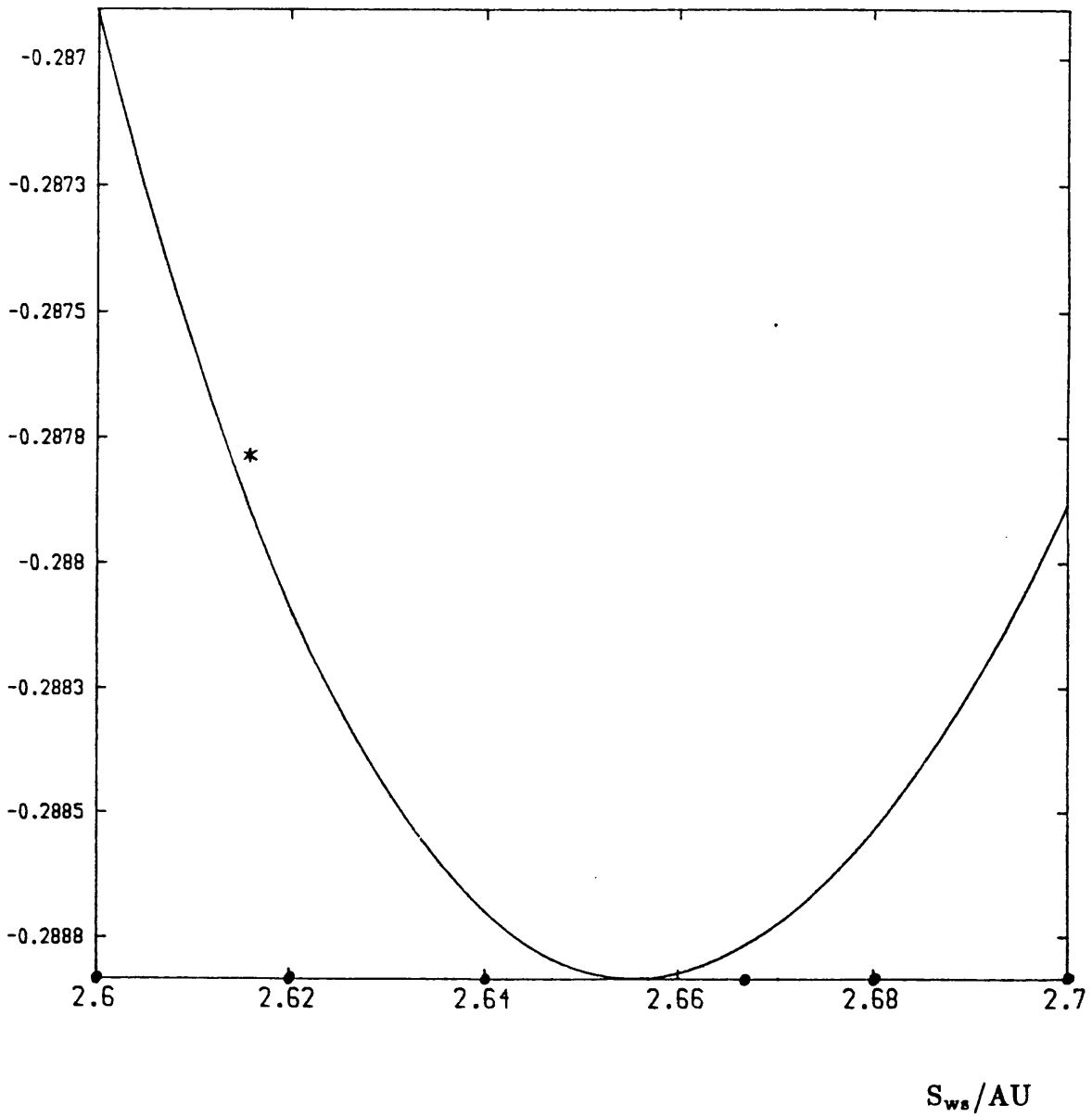

* total energy: cubic spline from marked points

Figure 4.2: Total energy curve for zinc.

(Energy+258.0)/Ryd.

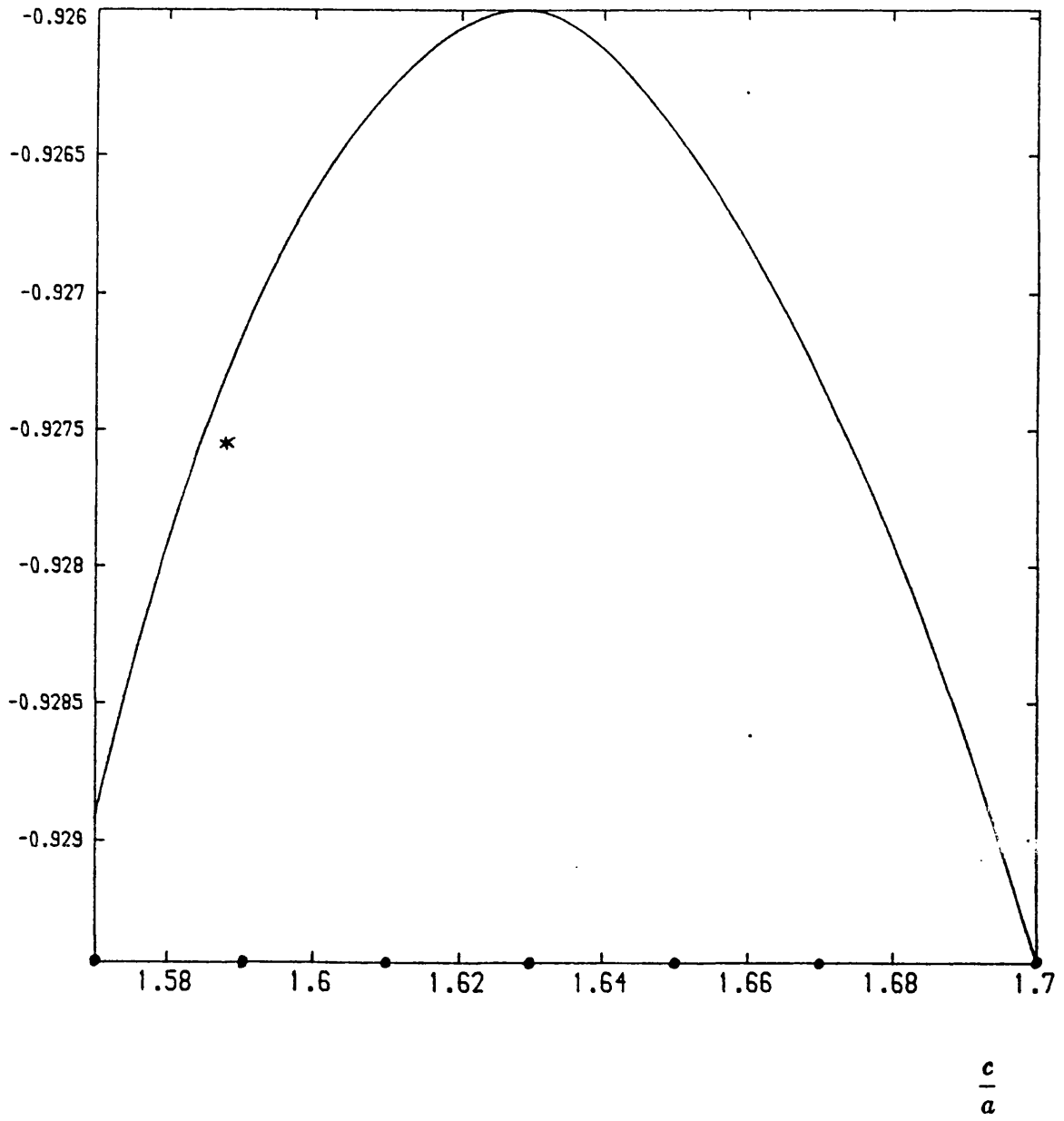

* total energy: cubic spline from marked points

constant and corresponds to the outward pressure exerted on the boundaries of the unit cell. We can define by analogy a hexagonal or tetragonal pressure by finding the derivative of the Kohn-Sham energy with respect to $\frac{c}{a}$. This corresponds to a pressure at the boundaries of the unit cell that acts so as to change the $\frac{c}{a}$ ratio. The hexagonal and tetragonal pressures are identical because in both systems a change in $\frac{c}{a}$ ratio is the only non-uniform distortion that preserves the symmetry. Henceforth we shall refer to both pressures as axial. In principle the lattice parameters can be found by looking at the value of a or $\frac{c}{a}$ for which the relevant pressure is zero. Again this works very well for the lattice constant, the values obtained for the transition metals being only a few per cent from the experimental values (Andersen, Jepsen & Glötzel, 1985), but we cannot expect it to work for the $\frac{c}{a}$ ratio. The reason is exactly the same as for the total energy method: the pressure is calculated within a scheme that does not adequately take into account the electrostatic effects. A clear advantage of the pressure method, however, is that it is analytic and does not involve looking at small differences between large numbers.

The obvious question that arises from what has been said so far is, "why is the ASA treatment of the electrostatic term good enough when it comes to the lattice constant but not for the $\frac{c}{a}$ ratio?" In §4.6 it is shown that the answer may lie in the neglect of the repulsion between charges from different spheres in the sphere overlaps. This is not significant for the case of a uniform expansion, but it is significant when we distort a structure non-uniformly. The exact calculation of the repulsive energy due to the overlaps is difficult. However, given the assumptions of a uniform charge density in the overlaps and a very short-

rangedelectrostatic interaction it can be shown (§4.6) that for an elemental HCP or FCT solid this energy is stationary at the ideal close packing $\frac{c}{a}$ ($= \sqrt{\frac{8}{3}}$ for HCP, unity for FCT). This means that, within the ASA, the electrostatic error in the gradient of the Kohn-Sham energy should be of second order, provided we calculate the gradient *at ideal* $\frac{c}{a}$. We might try to derive this quantity by numerically differentiating the total energy with respect to $\frac{c}{a}$ but it is preferable to work with the pressure, as this is an analytic expression and relates directly to the required derivative. Given a reliable value for this we can estimate the equilibrium $\frac{c}{a}$ ratio using classical elasticity theory (§4.8) together with experimental values for the elastic constants. In this analysis we assume that the sphere sizes can be chosen so as to give electrically neutral spheres, which is always possible for a close-packed element, so that the only interaction between spheres is through the overlaps.

At this stage it should be made clear that the pressure expression is derived (indirectly) from the Kohn-Sham energy (2.13) for the *non spherically averaged* charge density. The energy expression used in the LMTO code, however, is based on (2.13) with the spherical density (1.66) as input: the non-averaged density is never actually calculated. Hence we cannot demand that the pressure exactly correspond to the derivative of the total energy produced by the program. Nevertheless, for the case of the bulk pressure the two do correspond very well (see, for example, figure 4.12). The reason for this is that a pressure projects out the component of the charge density with the symmetry of the distortion, and for the bulk pressure this is spherical. We shall consider the agreement with the axial pressure in §4.7 and §4.9.

The pressures associated with non-isotropic distortions of a crystal are not nearly as well investigated as the bulk pressure. The only published calculation of which the author is aware was done by Cade (1981b), who deduced an expression for the axial pressure from the Liberman (1971) expression for the bulk pressure, but did not give the details of his derivation. This was applied to antiferromagnetic γ-manganese and a result was obtained which agreed in sign with the observed distortion in the $\frac{c}{a}$ ratio. What will be done here is essentially a continuation of Cade's work, looking at non-collinear magnets as well as collinear, but first of all applying the technique to "simpler" paramagnetic materials. Section 4.2 gives the background to the calculation of pressures and in §4.3 we derive a first-order expression for the change in Kohn-Sham energy associated with a completely general lattice distortion. In §4.4 we go on to consider exactly what is meant by a pressure and produce an expression for the pressure associated with an axial distortion by analogy with the bulk case. In §4.5 this result is evaluated within the ASA, and is found to differ from Cade's (1981b) expression in a number of respects. In §4.6 we show that in the HCP and FCT lattices the electrostatic contribution to the change in energy caused by a distortion should be of second order in the distortion at ideal $\frac{c}{a}$. From this it follows that the contribution to the pressure should also be of second order. In §4.7 the axial pressures of a number of HCP transition metals are presented and interpreted and in §4.8 these results are applied to the estimation of the $\frac{c}{a}$ ratios using classical elasticity theory. Finally, in §4.9 the work of §4.7 and §4.8 is repeated for the SDWs in γ manganese and iron. It should be noted that all energies in this section are in atomic Rydberg units (see §1.1).

4.2) Background to pressure calculations.

There are three different derivations of the pressure expression of which the author is aware but the most interesting employ respectively the "force theorem" of Andersen and the virial theorem (but note also Nieminen & Hodges, 1976).

The force theorem (Mackintosh & Andersen, 1980; Heine, 1980) gives the most straightforward derivation of the bulk or isotropic pressure associated with a uniform expansion of the lattice. To derive it we divide up the lattice into atomic cells and consider a displacement of the cells: for the bulk pressure the cells would be uniformly separated. The force theorem then states that the associated change in total energy is given to first order in the displacement by,

$$\delta U_{\rm tot} = \delta \sum_i E_i + \delta E_{\rm Coul}. \qquad (4.1)$$

Here the E_i are the one electron eigenvalues, which are summed over the occupied states, and $E_{\rm Coul}$ is the change in electrostatic energy between the cells. The exact meaning of the first term is important: what is done is to run a single bandstructure calculation using the self-consistent potential for the undistorted structure, shifted unchanged along with the cells. The force theorem says that the change in Kohn-Sham energy (2.13) associated with a distortion is related directly to the change in one-electron energies, without the complication of double counting terms.

There a number of questions that arise from the description of the force theorem given above. Firstly, in order to run a bandstructure calculation we have to know the potential in all space, and in the expanded structure there will be gaps between the atomic cells where the potential is not defined, so how can we do the calculation? Secondly, why do we not have to find the *self-consistent*

potential of the expanded structure? Thirdly, the Kohn-Sham energy, written in the form (2.14), has two parts: the one electron sum and the double counting term. So why does the latter not figure in (4.1)? It turns out that the answers to these questions are related. The exact form of the potential in the region between the old and new atomic cells is in fact arbitrary. The reason for this is that the self-consistent potentials of the expanded and unexpanded lattices can differ at most by terms of order δr, the distance that the cell boundary is displaced (Heine, 1980). This means that the corresponding wave functions can differ at most by terms of order δr. As the Kohn-Sham equations are derived from the variational principle (see §2.2) the corresponding difference in total energy must be of order $(\delta r)^2$. But we are interested in the first derivative of the one-electron energies with respect to r, so in the limit as $r \rightarrow 0$ this difference will not be significant. Given this arbitrariness, the potential can be chosen to make the integrals over the gaps come to nothing. The argument also provides the answer to the second question: the use of the self-consistent potential will make no difference to the one-electron eigenvalues, to the order of our calculations. As far as the disappearance of the double-counting term is concerned, it can be shown (Heine, 1980) that the change in the double-counting term due to the expansion of the lattice is exactly cancelled by the error caused by using the self-consistent potential of the undistorted structure, rather than that of the expanded one. Hence, the use of the potential for the undistorted structure in the bandstructure calculation makes no difference to the eigenvalues but is *essential* when it comes to the omission of double-counting terms from (4.1).

Assume now that we are justified in replacing the atomic cells by atomic spheres (the ASA). Then if the sphere radii can be chosen to make the spheres electrically neutral the second term in (4.1) disappears (Heine, 1980). The change in energy associated with an increase in the radius of the Wigner-Seitz sphere from s to $s + \delta s$ is given by,

$$\delta U_{\text{tot}} = -4\pi s^2 P \delta s, \tag{4.2}$$

where P is the bulk pressure. Hence,

$$P = -\frac{1}{4\pi s^2} \sum_i \frac{dE_i}{ds}. \tag{4.3}$$

It turns out that the derivatives here are readily expressible in terms of the logarithmic derivatives at the sphere boundary, and these are of course basic quantities in any ASA calculation. Thus in the ASA the bulk pressure is easily obtained. It should be noted that even if the atomic spheres cannot be made neutral without making the sphere overlaps large, the second term in (4.1) can still be handled within the ASA by replacing the charge at the sphere surface by an equivalent charge (in the sense of Gauss's Law) at the sphere centre and doing an Ewald summation. The force theorem of Andersen, although discussed here with the bulk pressure in mind, is equally valid for any distortion of the crystal. However, it not readily applicable to non-isotropic pressures as the derivative of E_i with respect to $\frac{c}{a}$ is not as natural a quantity in the ASA as the derivative with respect to s, and it is difficult to get past (4.3). Christensen (1984) did use the force theorem to calculate shear elastic constants but he used it to calculate the total energy difference δE rather than the pressure.

The virial approach to the bulk pressure is based on a paper by Liberman (1971). The starting point used by Liberman is the virial theorem for a solid

with fixed nuclei. This states that,

$$PV = \tfrac{2}{3}(T - \Upsilon), \tag{4.4}$$

$$\text{where} \quad \Upsilon = -\frac{1}{2}\int d^3\mathbf{r}\,|\Phi|^2\,(\sum_i \mathbf{r}_i.\nabla_i + \sum_\alpha \mathbf{r}_\alpha.\nabla_\alpha)\,\mathcal{V}. \tag{4.5}$$

Here the i-sum and α-sum are over the electron and nuclear coordinates respectively, $\mathcal{V}$ is the total potential energy and T is the kinetic energy. The function Φ is the wave function for both the electrons and the nuclei. It is claimed by Liberman (1971) that the nuclear part of the virial Υ must be zero for a crystal which is symmetric with respect to inversion. The author does not understand this argument. What is done here is to treat the nuclear part of the problem as classical electrostatics, and to assume that we can divide up space into regions that are electrically neutral. In practice, this means adopting the ASA and assuming that the sphere sizes can be chosen to yield neutrality. Given this assumption the virial becomes a function of the electron coordinates only and $|\Phi|^2$ becomes the total electron density. Adopting the Kohn-Sham formalism with single particle wave functions $\psi_i(\mathbf{r})$ and effective potential v_{eff} (§2.2) we obtain:

$$\Upsilon = -\frac{1}{2}\sum_i \int d^3\mathbf{r}\,|\psi_i(\mathbf{r})|^2[\mathbf{r}.\nabla v_{\text{eff}}(\mathbf{r})]. \tag{4.6}$$

Given (4.6) the right hand side of (4.4) can be converted into a surface integral (Liberman, 1971; Slater, 1933) so that,

$$PV = \frac{1}{6}\sum_i \int d^2\mathbf{S}.[(\nabla\psi_i^*)\mathbf{r}.\nabla\psi_i - \psi_i^*\nabla(\mathbf{r}.\nabla\psi_i) + c.c.] + \frac{1}{3}\int d^2\mathbf{S}.\mathbf{r}\,n^2(\mathbf{r})\frac{d\varepsilon_{\text{xc}}}{dn}, \tag{4.7}$$

where *c.c.* is the complex conjugate of the first term in the square brackets. It turns out that (4.7) can be expressed in terms of logarithmic derivatives at the

atomic sphere (Pettifor, 1976) and the expression for the pressure is (fortunately) in exact agreement with the result of the force theorem.

As mentioned in §4.1, the ASA bulk pressure has had considerable success with the materials for which the ASA works, the lattice constants being usually a little smaller than the experimental ones (Andersen, Jepsen & Glötzel, 1985). It has also been possible to interpret the observed trends among the transition metals in terms of the s, p and d pressure contributions (Pettifor, 1977), and so to get some physical insight into what would otherwise be just another number. In brief, what Pettifor did was to produce expressions for the contributions to the pressure in terms of the potential parameters. For the filled d band the pressure contribution was shown to be a balance between the Coulomb repulsion of the d states and an attractive force due to exchange-correlation, whereas for a partly-filled d band the contribution was attractive due to bonding. For the s and p bands Pettifor observed that the contribution depended strongly on the size of the core, owing to the repulsion of the neighbouring cores for the relatively extended sp states. Hence in the middle of the series, where the core size is large, the s and p contributions are repulsive but towards the ends there is a balance and the contribution may become attractive. More recently, Christensen and Heine (1985) have produced a detailed analysis of the pressure in noble metals.

4.3) The scaling procedure.

In order to calculate the pressure associated with a given distortion we have one main task to face: the calculation of the total energy change caused by a distortion of infinitesimal magnitude. When a crystal is distorted the change in total energy observed can be ascribed to two sources: a change due to the

movement of the nuclei and a change due to the distortion of the electron cloud. As the nucleus is so much more massive than the electrons we shall adopt the Born-Oppenheimer approximation (Bransden & Joachain, 1983) and treat the nuclear contribution as a problem in classical electrostatics. Assuming further that we can reasonably divide up space so that the forces between the nuclei are fully screened (in the electrostatic sense) then we can consider the problem to be a purely electronic one. The electronic problem can be approched using the idea of scaling (if you like German, see Fock, 1930). In the following we are considering a single Wigner-Seitz sphere, so in a lattice with a basis there would be a summation over basis labels preceding all that follows.

It has to be emphasised that we are only using part of the ASA at this stage: the potential and charge density inside the atomic spheres need not be spherical. In standard ASA calculations one forces the charge density to be spherically symmetric by taking a spherical average and this naturally gives rise to a spherically symmetric potential, through Poisson's equation. This is how an optimum spherical potential is obtained, using a self-consistency loop, but having obtained the optimum potential we cannot use this procedure to work out the axial pressure: a spherically symmetric charge density would give zero. What is done therefore is to perform a single band structure calculation from the ASA potential and feed the raw wavefunctions into the pressure calculation. This means that (at least in principle) it is the non-averaged charge density that is used. The theory given before §4.5 is therefore completely general: it is only in that section that we bring in the spherical potential of the ASA (because we are starting from the output of an ASA self-consistency loop) and the pressure

calculation does not use the spherical density at all.

To understand the scaling idea it is probably best to start with a uniform distortion of the crystal, e.g. an expansion. We want to know the change in electronic energy associated with an infinitesimal expansion of the electron density. This can be thought of in terms of stretching the wave functions into a larger sphere, so that when we take the energy expectation the argument of the Hamiltonian "extends farther" than in the undistorted structure (figure 4.3). However, in order to compare the energies we have to make sure that the normalisation of the wave functions is kept constant during the distortion. Thinking of a one-dimensional example the normalisation of the one-electron wave function ψ can be defined to be,

$$\int_0^1 |\psi(x)|^2 dx, \tag{4.8}$$

in which case the energy E is,

$$\int_0^1 \psi^*(x)\hat{H}(x)\psi(x)\,dx. \tag{4.9}$$

By construction, an expression for the energy E' of the expanded structure that satisfies both our requirements is,

$$\int_0^1 \psi^*(x)\hat{H}[x(1+\delta)]\psi(x)\,dx. \tag{4.10}$$

This expression is consistent with the normalisation given by (4.8) because if we set the Hamiltonian equal to unity then (4.8) and (4.10) are identical. Moreover at the boundary the Hamiltonian has become $\hat{H}(1+\delta)$ rather than $\hat{H}(1)$, so the energy integral is in a sense over a "larger volume" than in (4.9). In section (d) below we shall have to think precisely about what we are doing in terms of the

Figure 4.3: the scaling procedure for a uniform expansion.

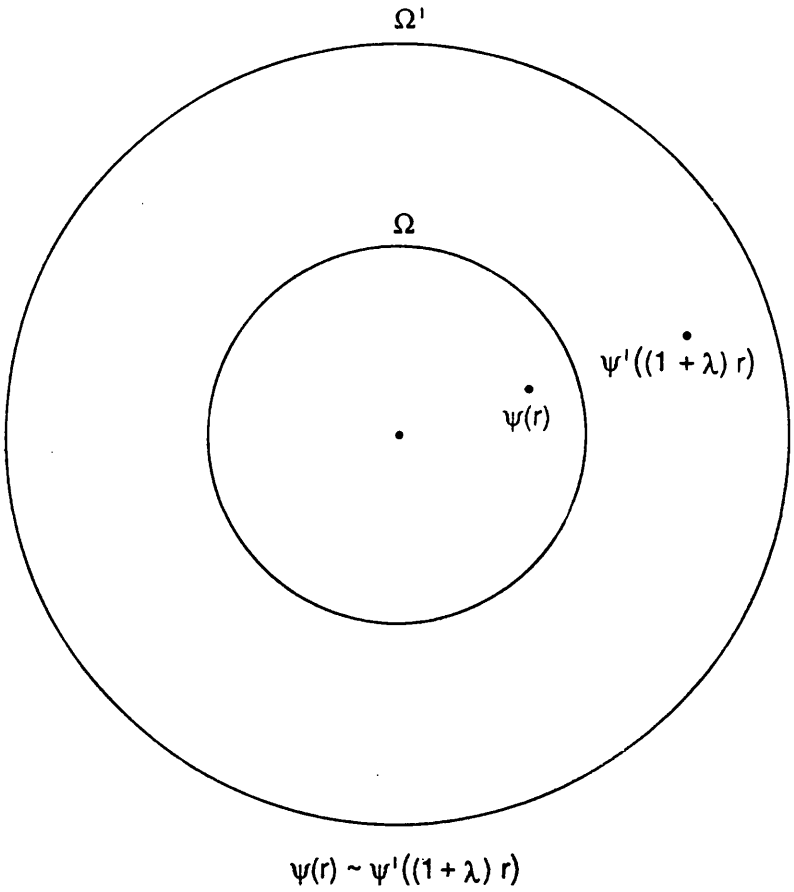

wave functions but for the moment let's see what can be done using the simple expression (4.10).

The above ideas should be equally valid in three dimensions and for non-uniform distortions of the electron cloud. In this case we replace $\mathbf{r}$ in the Hamiltonian by $(\underline{1} + \lambda\underline{\varepsilon})\mathbf{r}$, where $\underline{\varepsilon}$ is the strain tensor corresponding to the required distortion and λ is a small parameter, and get,

$$\int_{\Omega} \psi^*(\mathbf{r})\, \hat{H}[(\underline{1} + \lambda\underline{\varepsilon})\mathbf{r}]\, \psi(\mathbf{r})\, d^3\mathbf{r}\,. \tag{4.11}$$

Note that the integration is over the undistorted sphere Ω even though we are evaluating the energy of the distorted structure.

Given an expression for the single-electron energy associated with a distortion we can go about finding the corresponding energy difference for a many-electron system. Adopting the Kohn-Sham formalism (§2.2) the total energy of the undistorted system can be written as,

$$\begin{aligned} E = &-\sum_i \int \psi_i\, \nabla^2 \psi_i(\mathbf{r})\, d^3\mathbf{r} + \int n(\mathbf{r})\, U(\mathbf{r})\, d^3\mathbf{r} \\ &+ \frac{1}{2} \int n(\mathbf{r})\, d^3\mathbf{r} \int n(\mathbf{s})\, V(\mathbf{r}-\mathbf{s})\, d^3\mathbf{s} \\ &+ \int n(\mathbf{r})\, \epsilon_{xc}[n]\, d^3\mathbf{r}\,, \end{aligned} \tag{4.12}$$

where the i-summation is over the occupied states $\psi_i(\mathbf{r})$, U is the ion core potential and V is the Coulomb potential. Now the argument presented for the single-electron case did not depend for its validity on the operator being the Hamiltonian. Hence the transformation given by (4.11) can be applied to each part of (4.12) in turn (the exchange-correlation is a bit more complicated, as we shall see) in order to obtain the Kohn-Sham energy E' of the distortedelectron

gas. The energy change associated with the distortion is then given by $\delta E = E' - E$. We shall evaluate this piecewise.

(a) The kinetic energy term.

In order to find the kinetic energy of the distorted structure we have to find the operator ∇ which differentiates, not with respect to $\mathbf{r}$, but with respect to $\mathbf{r}' = (\underline{1} + \lambda\underline{\varepsilon})\mathbf{r}$. Now the transformation law for the differential must be,

$$d\mathbf{r}' = (\underline{1} + \lambda\underline{\varepsilon})d\mathbf{r}, \tag{4.13}$$

and we also know that the transformation law for the gradient is opposite to that of the differential (i.e. covariant rather than contravariant). Hence the transformed gradient must be given by,

$$\nabla' = (\underline{1} + \lambda\underline{\varepsilon})^{-1}\nabla. \tag{4.14}$$

Expanding the transformed Laplacian (with the aid of an arbitrary function f) we get,

$$\begin{aligned}(\nabla')^2 f &= [(\underline{1} - \lambda\underline{\varepsilon})\nabla \,.\, (\underline{1} - \lambda\underline{\varepsilon})\nabla]\, f \\ &= \nabla^2 f - 2\nabla.\lambda\underline{\varepsilon}.\nabla f + O(\lambda^2) \\ \Rightarrow (\nabla')^2 &= \nabla^2 - 2\nabla.\lambda\underline{\varepsilon}.\nabla + O(\lambda^2).\end{aligned} \tag{4.15}$$

The kinetic energy is given to first order by,

$$E' = \sum_i \int_\Omega d^3\mathbf{r}\, \left[\psi_i^*(\mathbf{r})\, \left(-\nabla^2 + 2\nabla.\lambda\underline{\varepsilon}.\nabla\right)\, \psi_i(\mathbf{r}) + c.c.\right], \tag{4.16}$$

and the change due to the distortion is,

$$\delta E = \lambda \sum_i \int_\Omega d^3\mathbf{r}\, \left[\psi_i^*(\mathbf{r})\, \nabla.\underline{\varepsilon}.\nabla\psi_i(\mathbf{r}) + c.c.\right]. \tag{4.17}$$

Here we have taken an average with the complex conjugate in order to ensure that we end up with a real quantity, as there is no guarantee that $\nabla.\underline{\varepsilon}.\nabla$ is Hermitian.

(b) The ion core term.

The evaluation of this term is more straightforward than the last because the "operator" is only the function $U(\mathbf{r})$. Expanding to first order,

$$\begin{aligned} E' &= \int_\Omega d^3\mathbf{r}\, n(\mathbf{r})\, U[(\underline{1} + \lambda\underline{\varepsilon})\mathbf{r}] \\ &= \int_\Omega d^3\mathbf{r}\, n(\mathbf{r})\, [U(\mathbf{r}) + \mathbf{r}.\,\lambda\underline{\varepsilon}\,.\nabla U(\mathbf{r})]. \end{aligned} \tag{4.18}$$

The energy change is thus given by,

$$\delta E = \lambda \int_\Omega d^3\mathbf{r}\, n(\mathbf{r})\, [\mathbf{r}.\,\underline{\varepsilon}\,.\nabla U(\mathbf{r})]. \tag{4.19}$$

(c) The Hartree term.

As in (b) we expand to first order in λ to get,

$$\begin{aligned} E' &= \frac{1}{2}\int_\Omega d^3\mathbf{r}\, n(\mathbf{r}) \int_\Omega d^3\mathbf{s}\, n(\mathbf{s})\, V[(\underline{1} + \lambda\underline{\varepsilon})(\mathbf{r}-\mathbf{s})] \\ &= \frac{1}{2}\int_\Omega d^3\mathbf{r}\, n(\mathbf{r}) \int_\Omega d^3\mathbf{s}\, n(\mathbf{s})\, [V(\mathbf{r}-\mathbf{s}) + (\mathbf{r}-\mathbf{s}).\,\lambda\underline{\varepsilon}\,.\nabla V(\mathbf{r}-\mathbf{s})]. \end{aligned} \tag{4.20}$$

Hence the energy change is,

$$\begin{aligned} \delta E &= \frac{\lambda}{2}\int_\Omega d^3\mathbf{r}\, n(\mathbf{r}) \int_\Omega d^3\mathbf{s}\, n(\mathbf{s})\, [(\mathbf{r}-\mathbf{s}).\,\underline{\varepsilon}\,.\nabla V(\mathbf{r}-\mathbf{s})] \\ &= \lambda \int_\Omega d^3\mathbf{r}\, n(\mathbf{r}) \int_\Omega d^3\mathbf{s}\, n(\mathbf{s})\, [\mathbf{r}.\,\underline{\varepsilon}\,.\nabla V(\mathbf{r}-\mathbf{s})], \end{aligned} \tag{4.21}$$

where the last line has been obtained by interchanging $\mathbf{r}$ and $\mathbf{s}$ and using the identity $\nabla V(-\mathbf{a}) = -\nabla V(\mathbf{a})$.

(d) The exchange-correlation term.

The expression (4.11) for the change in energy due to distortion is simple and intuitive but does not work for the exchange-correlation term. The reason for this is that the previous terms have involved the scaling of the wave function relative to a *static* potential (or ∇^2). The exchange-correlation however does not involve a static potential: ε_{xc} is a function of $\mathbf{r}$ only through its dependence on $n(\mathbf{r})$ and we cannot treat it like the $U(\mathbf{r})$ in (b). We shall therefore have to formalise the scaling procedure a little better.

Recalling the beginning of this section consider what the energy is if the electrons are expanded into a larger sphere Ω' while the potential is kept fixed. We have to be specific about how we expand the electrons so let's define a "stretched" wave function $\psi'(\mathbf{r})$ to be proportional to the wave function at the corresponding point in the original sphere Ω. Thinking in terms of the uniform distortion (i.e. the expansion) but writing the expression for a general distortion we define,

$$\psi'(\mathbf{r}) = k\psi[(\underline{1} + \lambda\underline{\varepsilon})^{-1}\mathbf{r}]. \tag{4.22}$$

According to (4.22) if $\lambda > 0$ the wave function ψ' achieves the proportional value to ψ only by going farther from the origin. For example, taking the boundary of the original sphere to be at $r = s$, to achieve the value proportional to $\psi(s)$ the argument of ψ' must be $(1 + \lambda)s$, which is greater than s. Hence, $\lambda > 0$ must correspond to an expansion of the wave function. In order to determine the constant k we bring in the requirement that the normalisation of $\psi'(\mathbf{r})$ over the expanded sphere Ω' must be the same as that of $\psi(\mathbf{r})$ over the original sphere

Ω, so that,

$$\int_{\Omega'} |\psi'(\mathbf{r})|^2 \, d^3\mathbf{r} = \int_{\Omega'} k^2 |\psi[(\underline{1} + \lambda\underline{\varepsilon})^{-1}\mathbf{r}]|^2 \, d^3\mathbf{r}. \tag{4.23}$$

Making the substitution $\mathbf{r}' = (\underline{1} + \lambda\underline{\varepsilon})^{-1}\mathbf{r}$, (4.23) becomes,

$$k^2 \int_{\Omega} |\psi(\mathbf{r}')|^2 (1 + \lambda \operatorname{tr}\underline{\varepsilon}) . \, d^3\mathbf{r}' \tag{4.24}$$

Here we have used the fact that to first order $\det(\underline{1} + \lambda\underline{\varepsilon}) = 1 + \lambda \operatorname{tr}\underline{\varepsilon}$. This factor is the Jacobian of the transformation $\mathbf{r} \rightarrow \mathbf{r}'$ (to first order) and $\lambda \operatorname{tr}\underline{\varepsilon}$ gives the volume change, so for a volume-conserving transformation $\lambda \operatorname{tr}\underline{\varepsilon}$ is zero. The normalisation requirement now gives,

$$\begin{aligned} k^2 \int_{\Omega} |\psi(\mathbf{r}')|^2 (1 + \lambda \operatorname{tr}\underline{\varepsilon}) \, d^3\mathbf{r}' &= \int_{\Omega} |\psi(\mathbf{r})|^2 \, d^3\mathbf{r} \\ \Rightarrow k^2 &= 1 - \lambda \operatorname{tr}\underline{\varepsilon}. \end{aligned} \tag{4.25}$$

Hence according to the new view of the scaling procedure the recipe for the energy of the distorted system is simply to replace the $\psi(\mathbf{r})$ in the integral by the $\psi'(\mathbf{r})$ given by (4.22) and (4.25), and integrate over Ω' instead of Ω. Applied to a one dimensional system where Ω runs from zero to one and $\lambda = \delta$ it is easy to see that we end up with (4.10), just as we should. With the new perspective it can be seen that all this is very much in the spirit of the variational procedure: we are finding the energy of the trial wavefunction given by (4.22) with the value of k constrained to be such that the normalisation over the sphere is conserved.

We are now in a position to write down an expression for the E' due to exchange-correlation,

$$\begin{aligned} E' &= \int_{\Omega'} d^3\mathbf{r} \, n'(\mathbf{r}) \varepsilon_{xc}[n'(\mathbf{r})] \\ &= \int_{\Omega'} (1 - \lambda \operatorname{tr}\underline{\varepsilon}) \, d^3\mathbf{r} \, n[(\underline{1} + \lambda\underline{\varepsilon})^{-1}\mathbf{r}] \, \varepsilon_{xc}\big[(1 - \lambda \operatorname{tr}\underline{\varepsilon}) \, n[(\underline{1} + \lambda\underline{\varepsilon})^{-1}\mathbf{r}]\big], \end{aligned}$$

Here the terms $1 - \lambda \,\mathrm{tr}\,\underline{\varepsilon}$ come from the substitution of k^2. Making the substitution $\mathbf{r}' = (\underline{1} + \lambda\underline{\varepsilon})^{-1}\mathbf{r}$ this becomes,

$$\begin{aligned} E' &= \int_\Omega d^3\mathbf{r}' n(\mathbf{r}')\, \varepsilon_{xc}[(1 - \lambda\,\mathrm{tr}\,\underline{\varepsilon})\, n(\mathbf{r}')] \\ &= \int_\Omega d^3\mathbf{r}'\, n(\mathbf{r}') \left\{ \varepsilon_{xc}[n(\mathbf{r}')] - \lambda\,\mathrm{tr}\,\underline{\varepsilon}\, n(\mathbf{r}') \frac{d\varepsilon_{xc}}{dn} \right\}. \end{aligned} \tag{4.26}$$

Hence the energy change is given by,

$$\delta E = -\lambda\,\mathrm{tr}\,\underline{\varepsilon} \int_\Omega d^3\mathbf{r}\; n^2(\mathbf{r})\, \frac{d\varepsilon_{xc}}{dn}. \tag{4.27}$$

Finally, we can put all the bits together to obtain a change in Kohn-Sham energy given by,

$$\begin{aligned} \delta E = \lambda \Bigg[& \sum_i \int_\Omega d^3\mathbf{r}\, [\psi_i^*(\mathbf{r})\, \nabla . \underline{\varepsilon} . \nabla \psi_i(\mathbf{r}) \; + c.c.] \\ & + \int_\Omega d^3\mathbf{r}\, n(\mathbf{r})\, [\mathbf{r} . \underline{\varepsilon} . \nabla U(\mathbf{r})] \\ & + \int_\Omega d^3\mathbf{r}\, n(\mathbf{r}) \int_\Omega d^3\mathbf{s}\, n(\mathbf{s})\, [\mathbf{r} . \underline{\varepsilon} . \nabla V(\mathbf{r} - \mathbf{s})] \\ & - \mathrm{tr}\,\underline{\varepsilon} \int_\Omega d^3\mathbf{r}\; n^2(\mathbf{r})\, \frac{d\varepsilon_{xc}}{dn} \Bigg]. \end{aligned} \tag{4.28}$$

It is this expression that will form the basis of the subsequent work on the pressure.

4.4) The axial pressure.

In this section we shall start by considering the meaning of the bulk pressure and move on to define a pressure associated with a volume conserving axial distortion, working by analogy.

Consider a cube of material of macroscopic dimension l and place it in the corner of a box so that three faces are flush with the the walls of the box and three are exposed. Suppose that cube is under a uniform stress that tends to

expand it, so that we have to apply an external pressure to prevent this. As the stress is uniform it must act equally on each face and must have symmetry,

$$\begin{pmatrix} 1 & 0 & 0 \\ 0 & 1 & 0 \\ 0 & 0 & 1 \end{pmatrix}. \tag{4.29}$$

If we now allow the cube to do work in a reversible fashion against the external pressure, with each free face moving out a distance δl, then the strain parameter λ is given by $\lambda = \frac{\delta l}{l}$ and the work that is done by the cube is to first order $3PV\lambda$ (figure 4.4). Given that this can be determined quantum mechanically (as in the last section) we obtain the following equation for the outward pressure of the cube,

$$P = -\frac{1}{3V}\frac{dE}{d\lambda}. \tag{4.30}$$

The minus sign in (4.30) arises because we want the outward pressure to be positive but for the case described δE must be negative.

To obtain an axial pressure, consider the same cube under a stress that acts in an axial manner and take the edges of the box as the usual Cartesian axes. We require a measure of the cube's tendency to distort axially, independent of any volume effects, so we must look at a distortion which is volume conserving. Given that we are in the Hooke's Law regime, the cube must distort with the symmetry of the stress, i.e. strain proportional to stress. Hence, assuming the internal stress is trying to elongate the z-axis at the expense of the x and y-axes the strain (and the stress) tensor must be proportional to,

$$\begin{pmatrix} -1 & 0 & 0 \\ 0 & -1 & 0 \\ 0 & 0 & 2 \end{pmatrix}. \tag{4.31}$$

This is so because the volume of the distorted cube is given by the determinant of the transformation matrix $(\underline{1} + \lambda\underline{\varepsilon})$, where $\underline{\varepsilon}$ is the strain, and for a diagonal

Figure 4.4: work done by a uniform pressure.

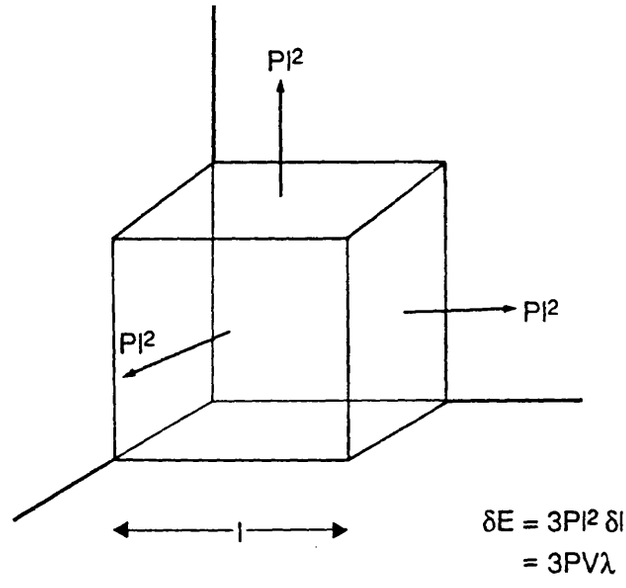

Figure 4.5: work done by an axial pressure.

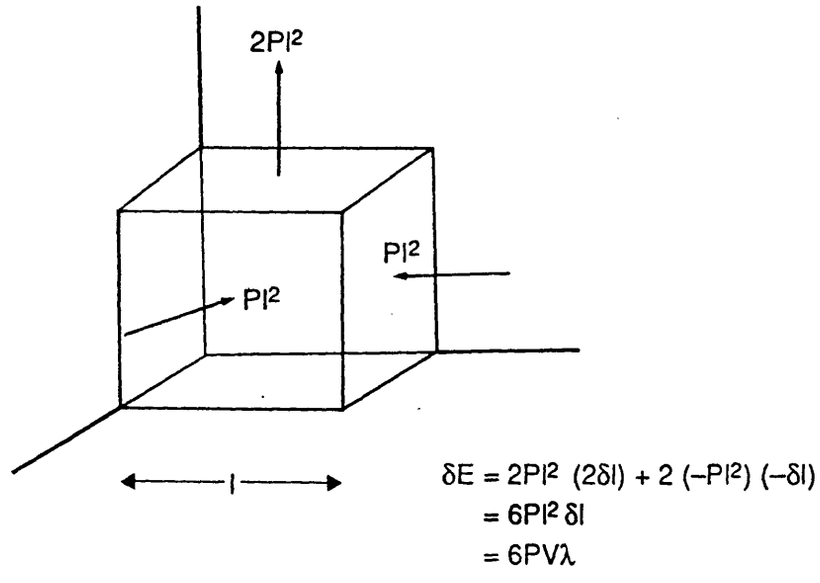

strain this is equal to $1 + \lambda \, \mathrm{tr}\, \underline{\varepsilon}$. The strain tensor must therefore have zero trace and (4.31) is the only axial strain tensor that satisfies this requirement. We shall take the strain tensor $\underline{\varepsilon}$ to be exactly (4.31). Given a strain parameter λ we can now deduce that the work done by the cube when it is allowed to distort is $6PV\lambda$ (figure 4.5). This must equal the quantum mechanical value δE given by (4.28), so the axial pressure P can be defined by (Cade, 1981b),

$$P = -\frac{1}{6V}\frac{dE}{d\lambda}. \tag{4.32}$$

Again, the minus sign arises because we want a pressure that tends to elongate the z-axis to be positive, and the energy change in a crystal where this is energetically favourable will be negative.

4.5) Evaluation in the ASA.

Equations (4.28) and (4.32) give the axial pressure in terms of volume integrals. However, it is possible to convert this result into a surface integral, and computationally this is much easier to evaluate, especially in the ASA. The argument which leads to the surface integral was referred to by Liberman (1971) in the derivation of his bulk pressure expression and is essentially that used by Slater (1933) in his proof of the virial theorem. To prove the virial theorem Slater showed that $T - \Upsilon$ could be equated to a surface term, where T is the kinetic energy and Υ is the virial. In Slater's system the boundary was at infinity so the surface term had to be zero, hence proving the theorem. What Liberman did was to note that in his system the boundary was not at infinity (so the wave function didn't vanish there) and that $PV = \frac{2}{3}(T - \Upsilon)$, where P is the bulk pressure and V the volume. The extension of this argument to thecase

of a non-uniform distortion is presented in Appendix A. The main result (A.16) of Appendix A is,

$$P = \frac{1}{16\pi s^3}\sum_i \int d^2\mathbf{S}.\left[(\nabla\psi_i^*)\,\mathbf{r}.\underline{\varepsilon}.\nabla\psi_i - \psi_i^*\nabla(\,\mathbf{r}.\underline{\varepsilon}.\nabla\psi_i) + c.c.\right] + \frac{1}{8\pi s^3}\int d^2\mathbf{S}.\underline{\varepsilon}.\mathbf{r}\; n^2(\mathbf{r})\frac{d\varepsilon_{\rm xc}}{dn}, \tag{4.33}$$

(c.f. 4.7). Here the i-summation is over the occupied valence bands (for clarity the summations over spin and site are not shown). In this section we shall evaluate the two terms of (4.33) separately. The final result will then be compared to Cade's (1981b) expression and to the bulk pressure (Pettifor, 1976).

Up till now we have used the ASA only to get rid of the difficult electrostatic term. To evaluate the first integral in (4.33) we make use also of the spherical symmetry of the sphere potential. Given this spherical symmetry the function $\psi_i = \psi_{n\mathbf{k}}(E,\mathbf{r})$ can be expanded quite simply in terms of the partial waves $\phi_{nL}(E,\mathbf{r})$, where n is the principal quantum number and $L = l,m$. We have (c.f. (1.37)),

$$\psi_{n\mathbf{k}}(E,\mathbf{r}) = \sum_L u_{n\mathbf{k}L}\,\phi_{nl}(E,\mathbf{r}), \tag{4.34}$$

with,

$$\phi_{nL}(E,\mathbf{r}) = i^l\phi_{nl}(E,r)\,Y_L(\theta,\phi). \tag{4.35}$$

Since the core wave functions are not needed to represent valence states we can assume that for each value of l there is only one relevant value of n and forget about the n index in what follows. The natural coordinate system for ψ_i is now spherical polar so we have to transform $\mathbf{r}.\underline{\varepsilon}$ from Cartesian (x,y,z) coordinates to spherical (r,θ,ϕ) coordinates. For the volume conserving axial strain of (4.31)

we obtain (Cade, 1981b),

$$r\,(-\sin\theta\cos\phi \quad -\sin\theta\sin\phi \quad 2\cos\theta)\begin{pmatrix}\sin\theta\cos\phi & \cos\theta\cos\phi & -\sin\phi\\ \sin\theta\sin\phi & \cos\theta\sin\phi & \cos\phi\\ \cos\theta & -\sin\theta & 0\end{pmatrix}$$

$$= r\,(3\cos^2\theta - 1 \quad -3\sin\theta\cos\theta \quad 0)\,. \tag{4.36}$$

Substituting in (4.33) and using Schrödinger's equation to eliminate the second derivatives we end up with (after much uninteresting algebra),

$$\frac{1}{16\pi s^3}\sum_{\mathbf{k}LL'} s[i^{l'-l}u^*_{\mathbf{k}L}u_{\mathbf{k}L'}\phi_l(E_\mathbf{k},s)\phi_{l'}(E_\mathbf{k},s)I_{\mathbf{k}LL'} + c.c.] \tag{4.37}$$

where,

$$I_{\mathbf{k}LL'} = s\left[D_lD_{l'} + D_l - l(l+1) + s^2(E_\mathbf{k} - v_{\text{eff}}(s))\right]\int d^2S\; Y_L^*Y_{L'}(3\cos^2\theta - 1)$$
$$+ 3(D_l - D_{l'})\int d^2S\,\frac{\partial Y_L^*}{\partial\theta}Y_{L'}\sin\theta\,\cos\theta, \tag{4.38}$$

and $D_l(E_\mathbf{k})$ is the logarithmic derivative of $\phi_l(E_\mathbf{k})$ at the sphere. There are two sorts of non-trivial integrals here: an integral of a product of three spherical harmonics ($3\cos^2\theta - 1 = (\frac{16\pi}{5})^{\frac{1}{2}}Y_{20}$) and an integral involving a derivative of a spherical harmonic. The former can be solved in terms of Clebsch-Gordon coefficients while the latter turns out to be zero for all but one of the relevant LL' combinations (the gory details are given in Appendix B). When these integrals are done we obtain,

$$\frac{1}{4\pi s^3}\sum_{\mathbf{k}} s\Big\{\,A_{pp}\phi_1^2\left(D_1^2 + D_1 - 2 + s^2(E_\mathbf{k} - v_{\text{eff}})\right)$$
$$+ A_{dd}\phi_2^2\left(D_2^2 + D_2 - 6 + s^2(E_\mathbf{k} - v_{\text{eff}})\right)$$
$$+ A_{sd}\phi_0\phi_2\left(-D_0D_2 + D_2 - 2D_0 + 3 - s^2(E_\mathbf{k} - v_{\text{eff}})\right)\Big\}, \tag{4.39}$$

where (c.f. (1.63)),

$$A_{pp} = \frac{1}{5}\left[2|u_{\mathbf{k}10}|^2 - |u_{\mathbf{k}11}|^2 - |u_{\mathbf{k}1-1}|^2\right] \tag{4.40}$$

$$A_{dd} = \frac{1}{7}\left[2|u_{\mathbf{k}20}|^2 + |u_{\mathbf{k}21}|^2 + |u_{\mathbf{k}2-1}|^2 - 2|u_{\mathbf{k}22}|^2 - 2|u_{\mathbf{k}2-2}|^2\right] \tag{4.41}$$

$$A_{sd} = \frac{1}{\sqrt{5}}[u^*_{\mathbf{k}00}u_{\mathbf{k}20} + u^*_{\mathbf{k}20}u_{\mathbf{k}00}], \tag{4.42}$$

$\phi_l = \phi_l(E_{\mathbf{k}}, s)$ and v_{eff} is evaluated at s. These quantities correspond to the "axial weights" given by Cade (1981b) and would be zero for a spherically symmetric charge density. The $\mathbf{k}$-summations of (4.39) can be made more tractable by defining the modified densities of states,

$$n_{\alpha\beta}(E) = \frac{1}{4\pi}\sum_n \int_{\text{B.Z.}} d\mathbf{k}\, A_{\alpha\beta}\, \delta(E - E_{n\mathbf{k}}), \tag{4.43}$$

where the square bracket is one of (4.40)–(4.42) and the integration is over the Brillouin zone. This is twice the usual definition of a density of states: what we are doing is assuming spin degeneracy. The extension to a non spin-degenerate system is straightforward: we just add spin labels to everything and sum over them, and define (4.43) with factor $\frac{1}{8\pi}$. Expression (4.39) now becomes,

$$\begin{aligned}\frac{1}{4\pi s^3}\int_{-\infty}^{E_f} s\,dE \Big\{ & n_{pp}\phi_1^2\left(D_1^2 + D_1 - 2 + s^2(E - v_{\text{eff}})\right) \\ & + n_{dd}\phi_2^2\left(D_2^2 + D_2 - 6 + s^2(E - v_{\text{eff}})\right) \\ & + n_{sd}\phi_0\phi_2\left(-D_0D_2 + D_2 - 2D_0 + 3 - s^2(E - v_{\text{eff}})\right)\Big\},\end{aligned} \tag{4.44}$$

This agrees with Cade's (1981b) expression in everything except the coefficent of n_{sd}. In the Cade expression this is $\phi_0\phi_2(D_0 - D_2)$. It seems likely that the first integral in (4.38) was believed to be zero in the *sd* term. In this case the only *sd* contribution would come from the second integral (Appendix B) and this would then yield the form given by Cade.

We come next to the second integral in (4.33), which is a bit more interesting than the first. This term was originally missed out by Liberman (1970) because he started from an expression involving the many-body wave function, which of course did not make reference to the exchange-correlation function of density functional theory. With $d^2\mathbf{S} = d^2S\,\hat{\mathbf{r}}$ and (4.36) this term can be converted into,

$$\frac{1}{8\pi s^3}\int s\,d^2S\,(3\cos^2\theta - 1)n^2\frac{d\varepsilon_{\mathbf{xc}}}{dn}. \tag{4.45}$$

We are now faced with a problem: how do we handle n? As the first integral in (4.33) makes use directly of the wave function it knows (implicitly) about the non-spherical charge density. For consistency therefore we ought to write $n(\mathbf{r})$ as,

$$n(\mathbf{r}) = \sum_i |\psi_i(\mathbf{r})|^2, \tag{4.46}$$

and then substitute in (4.45) and proceed as before, evaluating the integral using Clebsch-Gordan coefficients. But $\varepsilon_{\mathbf{xc}}$ is a non-linear functions of $n(\mathbf{r})$, so the best we can do is use a Taylor expansion.

Adopting the standard ASA assumption that the non-spherical component δn of n is small we can write,

$$n = n^{ASA} + \delta n + O(\delta n)^2. \tag{4.47}$$

Differentiating $n^2\,\frac{d\varepsilon_{\mathbf{xc}}}{dn}$ with respect to n we obtain,

$$v_{\mathbf{xc}} - \varepsilon_{\mathbf{xc}} + n\left(\frac{dv_{\mathbf{xc}}}{dn} - \frac{d\varepsilon_{\mathbf{xc}}}{dn}\right) = n\frac{dv_{\mathbf{xc}}}{dn}, \tag{4.48}$$

where we have used the result,

$$n\frac{d\varepsilon_{\mathbf{xc}}}{dn} = v_{\mathbf{xc}} - \varepsilon_{\mathbf{xc}}. \tag{4.49}$$

This follows directly from the definition (2.8) of v_{xc}. To first order in δn (4.45) must therefore become,

$$\frac{1}{8\pi s^3}\int s\,d^2S\,(3\cos^2\theta-1)\,n\,n^{ASA}\,\frac{dv_{xc}}{dn}\bigg|_{n^{ASA}}, \tag{4.50}$$

where δn has been replaced by n, as the difference n^{ASA} must integrate to zero. Making use of (4.46), (4.34) and (4.35) to write n in terms of partial waves we obtain,

$$\frac{1}{8\pi s^3}\sum_{\mathbf{k}LL'} s\,i^{l'-l}A^*_{\mathbf{k}L}A_{\mathbf{k}L'}\phi_l\phi_{l'}\,n^{ASA}\,\frac{dv_{xc}}{dn}\bigg|_{n^{ASA}} \int d^2S\;Y^*_LY_{L'}(3\cos^2\theta-1), \tag{4.51}$$

and observe that the spherical integral is identical to that of the first term of (4.38). So by analogy (4.51) becomes,

$$\frac{1}{4\pi s^3}n^{ASA}\,\frac{dv_{xc}}{dn}\bigg|_{n^{ASA}(s)}\int_{-\infty}^{E_f} s\,dE\,\{n_{pp}\phi_1^2+n_{dd}\phi_2^2-n_{sd}\phi_0\phi_2\}. \tag{4.52}$$

Finally, the two parts of (4.33) can be collected together to give:

$$\begin{aligned}P=\frac{1}{4\pi s^3}\int_{-\infty}^{E_f} s\,dE\,\{&n_{pp}\phi_1^2(D_1^2+D_1-2+\Delta)\\&+n_{dd}\phi_2^2(D_2^2+D_2-6+\Delta)\\&+n_{sd}\phi_0\phi_2(-D_0D_2+D_2-2D_0+3-\Delta)\},\end{aligned} \tag{4.53}$$

where Δ is given by,

$$\Delta=s^2\left(E-v_{\rm eff}(s)+n^{ASA}(s)\,\frac{dv_{xc}}{dn}\bigg|_{n^{ASA}(s)}\right), \tag{4.54}$$

It is interesting to compare (4.53) with the standard result for the bulk pressure (Pettifor, 1976),

$$\begin{aligned}P=\frac{1}{4\pi s^3}\int_{-\infty}^{E_f} s\,dE\,\{&n_{ss}\phi_0^2(D_0^2+D_0+\Delta)\\&+n_{pp}\phi_1^2(D_1^2+D_1-2+\Delta)\\&+n_{dd}\phi_2^2(D_2^2+D_2-6+\Delta)\},\end{aligned} \tag{4.55}$$

where Δ is given by,

$$s^2 \left(E - v_{\rm eff}(s) + n^{ASA}(s) \left. \frac{d\varepsilon_{\rm xc}}{dn} \right|_{n^{ASA}(s)} \right), \tag{4.56}$$

and the n_{ll} are the *conventional* projected densities of states (1.62). Apart from the fact that the axial expression includes a mixed sd term instead of an ss term, (4.55) is very similar in form to (4.53). What is interesting is the term Δ, which indicates that n has simply been replaced by its spherical average in the exchange-correlation term (see (4.45) and (4.49)) but not elsewhere. Given that for the bulk pressure (Pettifor, 1976) the term corresponding to (4.45) is proportional to,

$$\int s\, d^2S\, n \frac{d\varepsilon_{\rm xc}}{dn},$$

and that, by definition,

$$\int s\, d^2S\, \delta n = 0,$$

it can be seen that the first non-zero term in the integrated expansion involves $(\delta n)^2$. So the standard bulk pressure is also correct to first order in δn. It should be noted that (4.56) is exactly the term used by Cade (1981b) in his axial pressure expression. Given that the first order term does not integrate to zero for the axial case (see 4.50) it follows that Cade's expression is only correct to zeroth order in δn.

In this section we have evaluated (4.33) in the ASA and so arrived at an expression (4.53) which is easily evaluated within an LMTO-ASA program. This expression is similar to Cade's result, but differs in that is involves a different sd contribution and is correct to a higher order in the non-spherical component of the charge density. In §4.7 we shall apply (4.53) to a number of HCP transition

metals and in §4.8 these results shall be used to estimate the equilibrium $\frac{c}{a}$ ratios. In §4.9 this work will be repeated for the SDWs in FCC manganese and iron.

4.6) Why ideal $\frac{c}{a}$ is special in HCP and FCT structures.

In this section an argument is put forward as to why the neglect of electrostatic energy inherent in the ASA does not seem to affect the bulk pressure. This leads to the assumption that, for non-uniform distortions, there is some correspondence between the electrostatic energy and the overlap of the Wigner-Seitz spheres. Given this assumption it is then shown that, on purely geometrical grounds, the electrostatic error should be of second order importance for HCP and FCT structures at ideal $\frac{c}{a}$.

Recall first the force theorem (§4.2) and reconsider the case of an expansion: the atomic cells are moved uniformly apart and the gaps that are left are filled in with a constant potential as prescribed by the Andersen scheme (Heine, 1980). This leads to a change in total energy due to two parts: a sum of one-electron energies and an electrostatic term. It should be noted that the gaps that develop here do so in a spherically symmetric fashion. In the ASA, therefore, it would be reasonable to suppose that an expansion can be expressed solely by a change of scale of the spheres: the change in sphere overlap associated with this should not be significant.

For a non-uniform distortion the situation is quite different. Consider the very relevant example of a volume conserving, axial distortion, with the expansion taking place in the direction of the z-axis, say. In the force theorem picture there will be gaps between atomic cells in the z-direction and overlaps will de-

velop between adjacent cells in the xy-plane. The important point here is that the gaps and overlaps do not appear in a spherically symmetric fashion, and they ought to be taken into account when we go over to the ASA. The simplest way to do this is to work out the repulsive energy between the electrons from different spheres in the overlaps, and then to see how this changes as the structure is distorted. Even this is not an easy task if done exactly. We therefore assume that the change in electrostatic energy of the overlaps is proportional to the change in volume. This approximation is hard to justify but for a good ASA material (where the density is uniform near the sphere boundary) and for a highly screened (and hence short-ranged) Coulomb interaction it may not be too bad. The question of the electrostatic energy then becomes one of geometry.

It is not difficult to show that for two spheres of radius s whose centres are separated by a distance d the volume of overlap v is given by,

$$v = \frac{\pi}{12}(16s^3 + d^3 - 12s^2 d), \tag{4.57}$$

where $d \leq 2s$. Consider first an HCP element whose $\frac{c}{a}$ ratio is not too far from ideal. There are then only two sorts of sphere overlap possible: an overlap α between spheres in the same hexagonal layer and an overlap β between spheres in different layers (figure 4.6). For type α the distance between sphere centres is a while for type β it is $(\frac{1}{3}a^2 + \frac{1}{4}c^2)^{\frac{1}{2}}$, which can be rewritten as $a\left(\frac{1}{3} + \frac{1}{4}(\frac{c}{a})^2\right)^{\frac{1}{2}}$. As Wigner-Seitz spheres are space-filling and we want our distortion to be volume conserving we can obtain a relation between a, s and $\frac{c}{a}$. Using the fact that the volume of an HCP unit cell is $a^2 c\frac{\sqrt{3}}{2}$ we get,

$$\begin{aligned} a^2 c\frac{\sqrt{3}}{2} &= 2\,\frac{4}{3}\pi s^3 \\ \Rightarrow \qquad a^3 &= s^3 \frac{16\pi}{3\sqrt{3}}\left(\frac{c}{a}\right)^{-1}. \end{aligned} \tag{4.58}$$

Figure 4.6: nearest neighbour positions in a HCP structure.

3 atoms in plane above

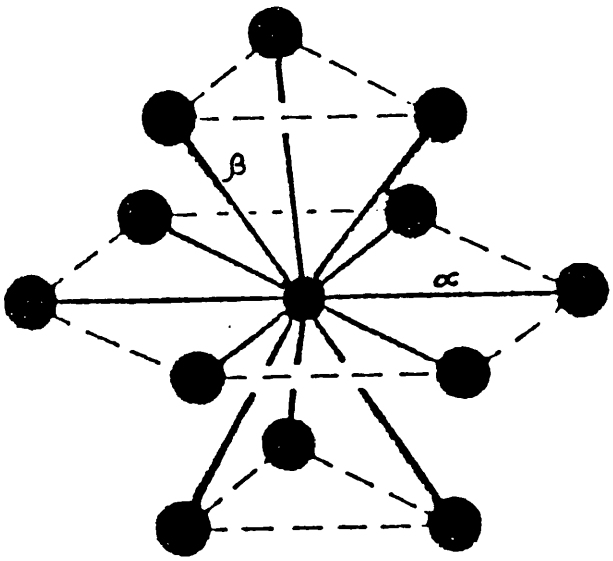

6 atoms in plane

3 atoms in plane below

Substituting for the a in the distance expressions and using (4.57) we obtain expressions for the volumes of the two sorts of overlap in terms of s and $\frac{c}{a}$, and these can be differentiated with respect to $\frac{c}{a}$. The results are,

$$\frac{dv_\alpha}{d\left(\frac{c}{a}\right)} = -\frac{16\pi}{3\sqrt{3}}\left(\frac{c}{a}\right)^{-2} + \frac{8}{\sqrt{3}}(2\pi)^{\frac{1}{3}}\left(\frac{c}{a}\right)^{-\frac{4}{3}} \tag{4.59}$$

and

$$\begin{aligned}\frac{dv_\beta}{d\left(\frac{c}{a}\right)} = \frac{16\pi}{27}&\left[\frac{9}{4} - \left(1+\frac{3}{4}\left(\frac{c}{a}\right)^2\right)\left(\frac{c}{a}\right)^{-2}\right]\left(1+\frac{3}{4}\left(\frac{c}{a}\right)^2\right)^{\frac{1}{2}} \\ &- 8(2\pi)^{\frac{1}{3}}\left[\frac{3}{4}\left(\frac{c}{a}\right)^{\frac{2}{3}} - \frac{1}{3}\left(1+\frac{3}{4}\left(\frac{c}{a}\right)^2\right)\left(\frac{c}{a}\right)^{-\frac{4}{3}}\right]\left(1+\frac{3}{4}\left(\frac{c}{a}\right)^2\right)^{-\frac{1}{2}}\end{aligned} \tag{4.60}$$

ignoring a common factor of $\frac{\pi s^3}{12}$. However, putting $\frac{c}{a} = \sqrt{\frac{8}{3}}$ we find,

$$\frac{dv_\alpha}{d\left(\frac{c}{a}\right)} = -\frac{dv_\beta}{d\left(\frac{c}{a}\right)} = -\frac{2\pi}{\sqrt{3}} + 2(2\pi)^{\frac{1}{3}}3^{\frac{1}{6}}. \tag{4.61}$$

Moreover, of the twelve neighbours of an atom in an HCP structure it can be seen that there are six in the same layer and six in other layers (figure 4.6b). Hence, the total overlap volume of any atom in an HCP structure is stationary at ideal $\frac{c}{a}$. The above argument is easily adapted for a FCT structure. In this case the derivative of the overlap between atoms in the xy plane at $\frac{c}{a} = 1$ is,

$$\frac{\pi s^3}{3}\left[-\frac{\sqrt{2}}{3}\pi + \sqrt{2}\left(\frac{2\pi}{3}\right)^{\frac{1}{3}}\right],$$

and that of an overlap out of the plane is minus half this value. There are twice as many of the latter overlaps as of the former, for any particular atom, so the total derivative is zero.

From the above geometrical arguments and given our initial assumptions it follows that the change in electrostatic energy at ideal $\frac{c}{a}$ is of second order in the distortion parameter. From (4.28) and (4.32) it can be seen that the

axialpressure requires only first order accuracy in the the distortion parameter. It might therefore be hoped that, evaluated for ideal $\frac{c}{a}$, the axial pressure will yield reasonable results even in the ASA. Similarly, when dealing with the curve of total energy against $\frac{c}{a}$ (e.g. figure 4.2) one might expect that the *slope* of the curve at ideal $\frac{c}{a}$ should be correct, even though the rest of the curve is wrong.

4.7) Axial pressures for some HCP metals.

Consider the standard method of evaluating an expression like (4.53) in the LMTO method. What we have is essentially,

$$\int_{-\infty}^{E_f} dE\, n_{ll'}(E)\, f[\phi_l, \phi_{l'}, \dot{\phi}_l, \dot{\phi}_{l'}], \tag{4.62}$$

where $n_{ll'}(E)$ is a modified density of states (4.43) and $f = f_{ll'}(E,s)$ is determined by (4.53). From (4.40)-(4.43) it can be seen that $n_{ll'}(E)$ gives the availability of an electron transfer to a state that points in the z-direction from one that doesn't, where both states concerned have energy E. The function $f_{ll'}(E)$ is like a matrix element: it governs the contribution of an electron transfer to the axial pressure. Expression (4.62) is of the same form as the expressions for the spherically averaged charge density and bulk pressure (except that for these $l \equiv l'$) and what we do is expand (see Skriver, 1984) $f_{ll'}(E)$ as a Taylor series about $E = E_\nu$ to obtain,

$$\begin{aligned} g_0 \int_{-\infty}^{E_f} dE\, n_{ll'}(E) + g_1 \int_{-\infty}^{E_f} dE\, n_{ll'}(E)(E - E_\nu) \\ + \frac{1}{2} g_2 \int_{-\infty}^{E_f} dE\, n_{ll'}(E)(E - E_\nu)^2 + \ldots \end{aligned} \tag{4.63}$$

This procedure is analogous to that described for the charge density in §1.9. The coefficient g_n is the nth derivative of f with respect to E and is a function of ϕ_l, $\phi_{l'}$ and their energy derivatives, evaluated at (E_ν, s). The integrals are called the moments of $n_{ll'}$ about E_ν and the first three are analogous to the mass, moment and moment of inertia in classical mechanics. Given that $n_{ll'}(E)$ is the probability of an electron transfer at energy E it it clear that the zeroth moment represents the total transfer of electrons into orbitals that point in the z-direction (for a given l, l'). The first moment then takes into account whether

the "hump" in $n_{ll'}(E)$ is above or below E_ν, the second how far the hump is from E_ν, and so on. In practice this sort of expansion is generally well converged when taken as far as the third order.

The program used in chapter 3 was adapted to calculate axial pressures by means of (4.63). This involved the replacement of the code to calculate spherical moments (Skriver, 1984) by code designed to calculate (4.40)-(4.42) and the insertion of the code to evaluate (4.63) after the charge density part of the program (as the charge density is needed to calculate the exchange-correlation functions). To produce this code the coefficients g had to be expressed in terms of the potential parameters, which are the quantities available in the LMTO program (Skriver, 1984). A number of calculations were done on HCP materials, using 48 k-points in the irreducible wedge of the Brillouin zone. The results obtained are given in table 4.1. Included here are all the non-magnetic HCP metals of the first two transition series. The third and fourth columns refer to the pressure expression with Δ given by (4.56) and (4.54) respectively, the second has all exchange-correlation set to zero in Δ, and the fifth uses the Cade (1981b) expression. A positive sign indicates a pressure that tends to extend the c-axis. Following the ideas of §4.6 all calculations were done at ideal $\frac{c}{a}$ $(= \sqrt{\frac{8}{3}})$. It is interesting to note that these values are at least an order of magnitude smaller a "typical" bulk pressure.

Table 4.1: axial pressures/kbar. (for ideal $\frac{c}{a}$)

Element	$v_{xc} = \varepsilon_{xc} = 0$	0th order	1st order	Cade
Sc	1.24	−1.10	−0.89	−1.76
Y	0.72	−0.59	−0.48	−0.96
Ti	9.93	4.71	5.20	3.45
Zr	8.66	3.45	3.92	2.48
Tc	−4.79	−0.86	−1.25	−0.66
Ru	−5.74	−3.66	−3.86	−4.04
Cu (HCP)	0.58	−0.19	−0.12	1.53
Ag (HCP)	0.27	0.27	0.27	−0.44
Zn	−1.46	−1.60	−1.59	1.36
Cd	4.17	−0.54	−0.14	2.46

The discussion of table 4.1 will be divided into a number of parts. First of all, we will compare the effects of the various expressions for the axial pressure, including that of leaving out the second integral of (4.33) altogether (by putting $\varepsilon_{xc} = v_{xc} = 0$). The reasoning behind including the FCC materials copper and silver, treating them as if they were HCP, is then explained. Next we consider zinc and cadmium, and why the method does not work for them. Finally, by breaking down the pressure into *sd*, *pp* and *dd* components, and looking at the contributions from the first two moment terms, some attempt is made to explain these results in terms of electronic behaviour.

Comparing the $\varepsilon_{xc} = v_{xc} = 0$ column of table 4.1 with the others it can be seen that the second integral in (4.33) is just as important as the first, and in some cases (e.g. Sc, Y) it is the dominant one. This second term has been inter-

preted (Christensen & Heine, 1985) as the correction necessary to convert the pressure of a gas of non-interacting electrons into that due to the gas of quasi-particles consisting of each electron and its exchange-correlation hole. Certainly, the result is in keeping with that of Liberman (1970), who found that on missing out this term the density of lithium was predicted to be only 50% of its experimental value. The results also suggest that the difference between the zero and first-order (in δn) expressions is generally rather small. This implies that at the densities commonly found at the atomic sphere,

$$\varepsilon_{\rm xc}[n^{ASA}] \approx \frac{1}{4\pi s^2} \int d^2S\, \varepsilon_{\rm xc}[n(\mathbf{r})], \tag{4.64}$$

which suggests that $\varepsilon_{\rm xc}[n]$ is approximately linear at these densities. Finally, from the last two columns of table 4.1 it is evident that the omission implicit in the Cade (1981b) axial pressure does not in general produce large errors, although copper is a fair way out. From this point the pressure will always refer to expression (4.54).

The inclusion of copper and silver in a table of HCP metals might well arouse some curiosity. These materials were run as HCP structures in order to provide an additional test for the method. The FCC structure that they naturally assume differs from the HCP only in the manner of stacking of triangular layers, it is ideally close-packed (with respect to FCT structures), and has a similar density of states to the HCP (Pettifor, 1977). Hence we might well expect copper and silver to take up the ideal close-packed structure when forced in our calculations to be HCP, and this would mean that the axial pressure at ideal $\frac{c}{a}$ should be zero. It can be seen from table 4.1 that, while not exactly zero, the pressures for Cu and Ag are certainly much smaller than the others, so the

method appears to pass this test.

Consider now the results for zinc and cadmium. From the sign of the axial pressure we would expect equilibrium $\frac{c}{a}$ ratios that are less than ideal, but experimentally (Ashcroft & Mermin, 1976) the ratios are found to be much bigger than ideal (1.856 for Zn, 1.886 for Cd, ideal =1.633). The reason for this failure lies in the moment expansion evaluation (4.62) of the axial pressure expression (4.53). To see why consider the breakdown of the pressure for zinc and also for a material that works, scandium say.

Table 4.2: axial pressure contributions for zinc/kbar.

n	*sd*	*pp*	*dd*
0	−0.0054	0.7194	0.0001
1	0.2756	−1.3914	0.5626
2	0.0173	−0.0174	−0.5434
3	−0.2743	−0.0007	−0.9343

Table 4.3: axial pressure contributions for scandium/kbar.

n	*sd*	*pp*	*dd*
0	−0.2134	−0.4474	−0.8254
1	0.9378	−0.5106	0.0947
2	0.0705	−0.0040	0.0016
3	0.0087	0.0001	0.0000

It is immediately seen that while the convergence of the moment expansion is very good in Sc, for Zn it is poor, and in particular for the *dd* component of the pressure. Concentrating on the *dd*, we can break this down further to see whether the trouble arises due to the coefficients or the moments:

Table 4.4: *dd* coefficients and axial moments for zinc.

n	g_n	moment/10^{-4}
0	0.0053	0.53
1	5.761	2.03
2	−10.688	1.06
3	−28.766	0.68

Table 4.5: *dd* coefficients and axial moments for scandium.

n	g_n	moment/10^{-4}
0	−0.5044	56.37
1	2.960	1.10
2	0.6447	0.09
3	−0.0523	0.01

Comparing these tables it appears that, while the moments are not particularly well converged in zinc, most of the convergence problem comes from the coefficients. What this tells us about the zinc *d*-electrons is that although most of the electron transfer takes place not too far from $E_{\nu d}$, that which has the most weighting in the axial pressure takes place a long way above $E_{\nu d}$. This is so because it is at the Fermi level that an electron may transfer between states and alter the total energy of the system, and this brings us to the physical origin of the problem: unlike the other examples considered zinc has a full *d*-shell and as a result the *d*-bands have sunk considerably in energy and become narrower. This can be seen clearly by comparing the potential parameters of zinc with those of neighbouring copper:

Table 4.6: potential parameters and Fermi energy for Cu and Zn.

	Cu	Zn
E_f/Ryd.	−0.1270	−0.1087
$E_{\nu d}/Ryd.$	−0.3346	−0.7048
$10s\Phi_d(-)^2/Ryd.$	0.1776	0.0756

As shown in Skriver (1984), E_ν is the centre of mass of the occupied part of a band while $10s\Phi(-)^2$ is approximately equal to the width. It seems reasonable to assume that the trouble with the sd-component of the pressure arises in a similar way due to its d-dependence. The well-behaved nature of the p-component in zinc is then explained because we have $E_{\nu p} = -0.3911$ Ryd. and $10s\Phi_p(-)^2 = 0.2361$ Ryd.

There are two questions that might arise from this. The first is "how can a band whose centre is as given in table 4.6 possibly affect what's happenning at E_f?" The answer is hybridization: the d-band may still contribute to states near E_f, and while $10s\Phi(-)^2$ is good for comparisons of band widths but does not set absolute limits on the band width. The second question is "why isn't this a problem with the bulk pressure?" In fact, it is a problem with the bulk pressure as well, as the coefficients and moments for the d-band show:

Table 4.7: bulk coefficients and moments for the d band in zinc.

n	$g_n(E_\nu)$	moment/10^{-4}	product
0	0.0088	99300	874
1	5.554	−0.11	0.611
2	−7.803	236	1840
3	−26.240	60.6	1590

This presumably accounts for the fact that the tables of equilibrium sphere radii obtained from the ASA bulk pressure (e.g. Skriver, 1984; Andersen, Jepsen & Glötzel, 1985) always seem to stop before the zinc column, although this problem is not specifically mentioned.

Turning to the other materials it is found experimentally (see e.g. Ashcroft & Mermin, 1976) that all the HCP transition metals, apart from zinc and cadmium, show a $\frac{c}{a}$ ratio that is slightly less than ideal. Hence titanium and zirconium stand out as going strongly the wrong way. Making the assumption that the first two terms in the moment expansion are the most important (i.e. the expansion is well converged) we shall look at these results first of all in comparison with the zeroth moments (for the three ll' components), and then with the first moments. The ll' components of the total pressure, along with the zeroth moments, are given in table 4.8.

Table 4.8: zeroth moments and total pressure components.

	zeroth moment			pressure components/kbar		
	sd	*pp*	*dd*	*sd*	*pp*	*dd*
Sc	0.001	−0.007	0.006	0.804	−0.962	−0.729
Y	0.005	−0.007	0.007	1.104	−1.002	−0.575
Ti	0.010	−0.001	−0.028	3.209	−0.294	2.291
Zr	0.015	−0.004	−0.026	3.631	−1.002	1.287
Tc	−0.005	0.003	0.000	−2.377	2.002	−0.873
Ru	−0.007	0.001	−0.005	−2.175	0.764	−2.448
Cu	0.002	0.000	0.000	−0.157	−0.141	0.176
Ag	−0.001	0.000	0.000	−0.008	−0.031	0.313

Probably the most noticeable feature of table 4.8 is that the *dd* components for titanium and zirconium are much larger than those of the other materials. However, they are no larger than those of magnetic Mn (§4.9), for which the resultant pressure is very reasonable. Given that zinc and cadmium are pathological, that the calculation fails for titanium and zirconium, and that copper and silver give pressures that are close to zero, there seems little point in trying to do the sort of analysis that Pettifor (1977) did for the bulk pressure components (where there was a complete period to look at, apart from cadmium). However, looking at the *pp* columns of table 4.6 we can see immediately that for materials in the same group of the periodic table the *p*-pressure is pretty much proportional to the zeroth moment. The *sd* columns are similar to the *pp* in that the sign of the pressure contribution correlates with that of the zeroth moment (except for Cu and Ag, where the numbers are much smaller anyway) although we have lost the proportionality. This loss must be due to the position of the bands (and hence the first moment) being more important, presumably due to the *d*-dependence. When we turn to the *dd* columns we lose the correlation with the zeroth moment altogether. Given that the *d*-bands are narrower and further away from E_f than the *s* or *p* we would expect a stronger dependence on the position of the *d*-bands, and hence a significant contribution from the first moment. That this is so is evidenced by the play-off between the zeroth and first moment contributions to the pressure:

Table 4.9: *dd* contributions to total pressure/kbar.

	from 0th moment	from 1st moment	sum
Sc	−0.825	0.095	−0.730
Y	−0.748	0.172	−0.576
Ti	5.191	−2.855	2.336
Zr	3.807	−2.477	1.330
Tc	0.009	−0.833	−0.824
Ru	0.494	−2.853	−2.359
Cu	−0.001	0.154	0.153
Ag	−0.001	0.294	0.293

It is interesting to note the very small zero moment components in Tc, and in Cu and Ag. This can be explained if (neglecting hybridization) the *d*-shell in technetium is half-filled, as then the zeroth moment component of the pressure cannot be other than small. In a similar way if the *d*-shells in copper and silver are completely filled then we have a very small zero moment pressure. Looking at the first moment column we see that when the *d*-shell is more than one electron away from being full or empty the contribution is negative. This is presumably connected with the way the shape of *d*-bands alter with filling but the author could find no obvious connection.

As mentioned in §4.1, it will be interesting to compare the results of the axial pressure calculations with the total energy produced by the program (Andersen, Jepsen & Glötzel, 1985), which is calculated from the spherical density (1.66). We know that the axial pressure depends on the derivative of the Kohn-Sham energy with respect to $\frac{c}{a}$, so probably the best way to achieve a comparison is to

integrate the pressure and plot the curves side by side. The axial pressure was therefore calculated for a number of different $\frac{c}{a}$ values, for each material, with the volume held constant at the experimental value. It should be emphasised here that for the sake of the comparison we are now abandoning the ideas of §4.6, which claimed that the axial pressure is valid only at ideal $\frac{c}{a}$.

To be specific about the relation between the pressure and the energy derivative we start with equation (4.32) which says that,

$$P = -\frac{1}{6V}\frac{dE}{d\lambda},$$

where λ is the distortion parameter. Now with a distortion defined by (4.31) we have,

$$\begin{aligned} c' &= c(1+2\lambda), \\ \text{and} \quad a' &= a(1-\lambda). \end{aligned} \tag{4.65}$$

Hence,

$$\begin{aligned} \left(\frac{c}{a}\right)' = \left(\frac{c}{a}\right)\frac{1+2\lambda}{1-\lambda} &= \left(\frac{c}{a}\right)(1+3\lambda) + O(\lambda^2) \\ \Rightarrow \quad \Delta\left(\frac{c}{a}\right) &= 3\left(\frac{c}{a}\right)\lambda \\ \Rightarrow \quad \frac{d\lambda}{d(\frac{c}{a})} &= \frac{1}{3(\frac{c}{a})}. \end{aligned} \tag{4.66}$$

So substituting in (4.32) gives,

$$\frac{dE}{d(\frac{c}{a})} = -\frac{2VP}{(\frac{c}{a})}. \tag{4.67}$$

Given a P measured in kbar and a V in AU^3 we should also have to multiply (4.67) by the factor 6.798×10^{-6} to get a derivative in Rydbergs.

The curves for scandium, titanium, technetium, ruthenium and copper (representing each of the relevant transition metal groups) are presented in figures

4.7–4.11, where the pressure derived curve has in each case been shifted to make its maximum coincide in energy with that of the total energy curve. Figure 4.12 gives the corresponding curves for the *bulk pressure* in copper. These curves are produced in an analogous manner and serve as a yardstick for comparing the agreement of the axial curves. In each case the curve has been produced by fitting a cubic spline through the points marked on the horizontal axis. The first thing that comes across from the axial figures is that (with the exception of figure 4.8, for titanium) the turning point of the pressure derived curve is very close (as a proportion of $\frac{c}{a}$) to that of the total energy curve. The figure for titanium shows a pressure derived curve with a turning point which is a long way off that of the total energy curve. This is only to be expected, given that the pressure at ideal $\frac{c}{a}$ looks completely wrong. As stated in §4.1, the axial curves have turning points that are maxima rather than minima, owing to the improper treatment of the electrostatic term. In the axial cases the pressure derived curves have much smaller curvatures than the total energy curves. It was mentioned in §4.1 how the curves need not agree in detail, owing to the fact that the total energy is calculated from a spherical density. However, for the bulk case the agreement is very good, both in terms of the position of the turning point and the curvature. The author has no definite explanation for these discrepancies in curvature (but see conclusions). Given that the curvatures in the axial cases are so different, and hence also the implied pressures at ideal $\frac{c}{a}$, it will be interesting to see how the pressure and total energy fare in the estimation of the $\frac{c}{a}$ ratios. This will be the subject of the next section.

Figure 4.7: Total energy curves for scandium.

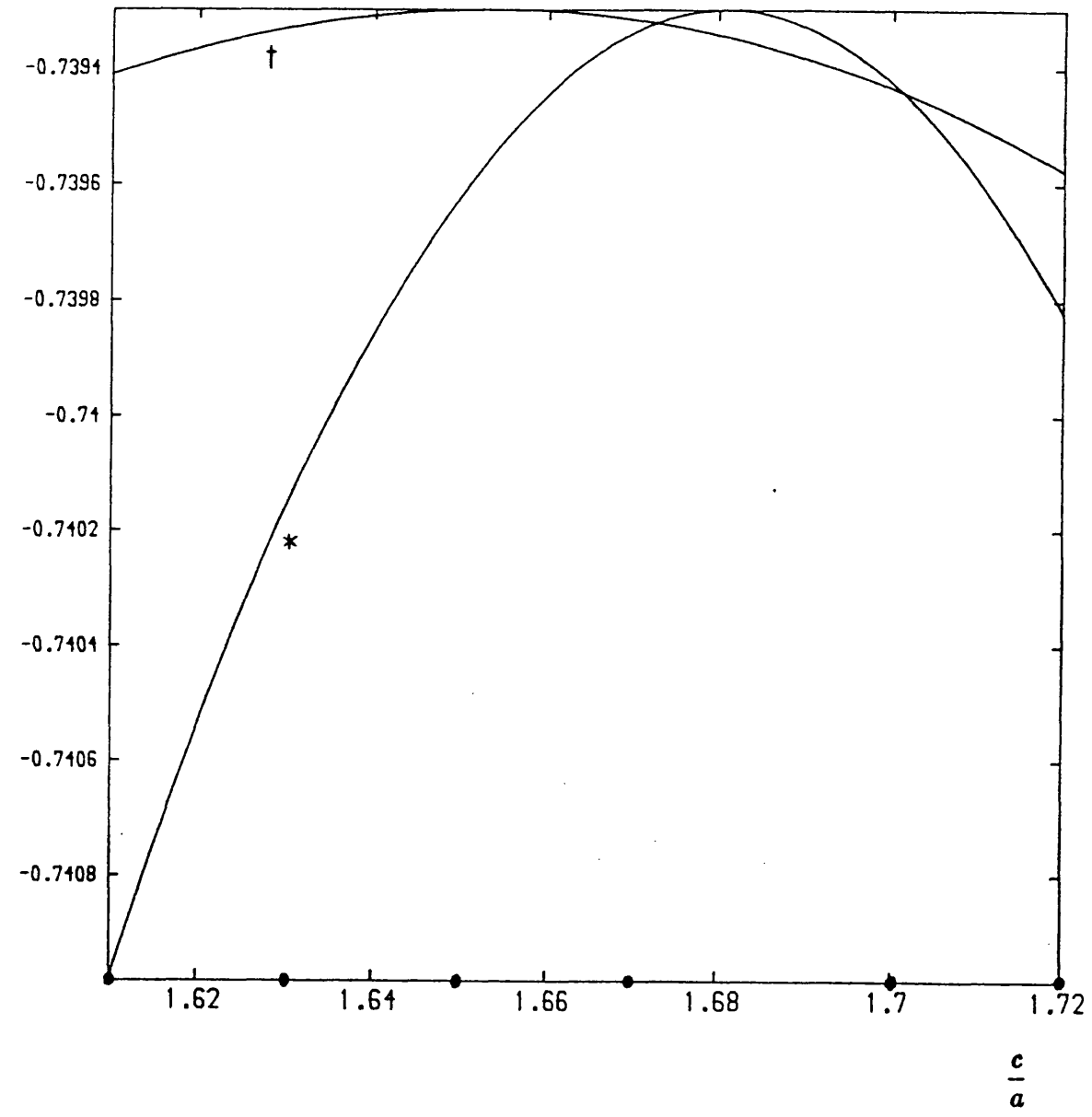

* program total energy: cubic spline from marked points

† pressure derived curve: from points as above

Figure 4.8: Total energy curves for titanium.

(Energy+15.0)/Ryd.

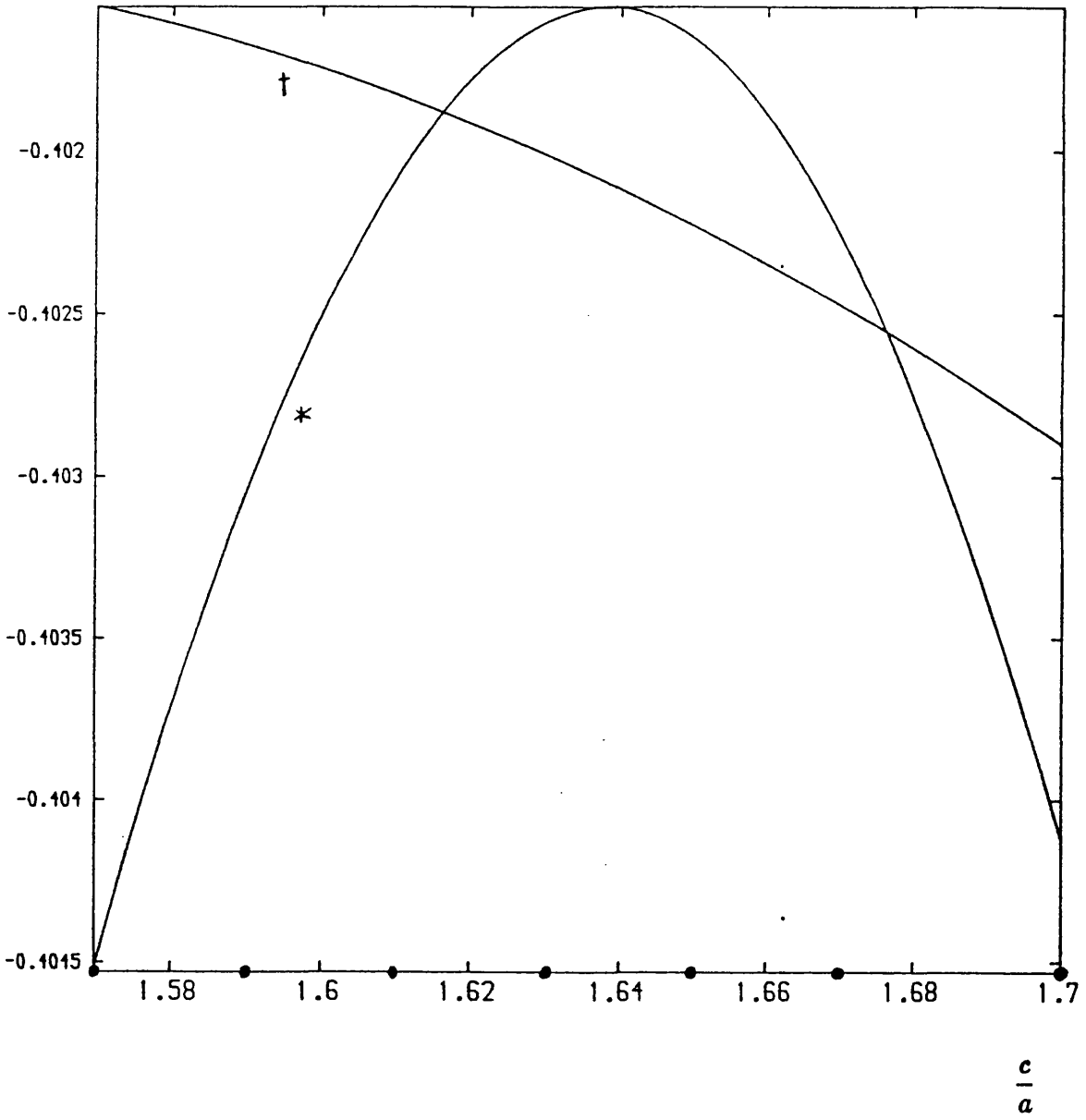

* program total energy: cubic spline from marked points

† pressure derived curve: from points as above

Figure 4.9: Total energy curves for technetium.

(Energy+49.0)/Ryd.

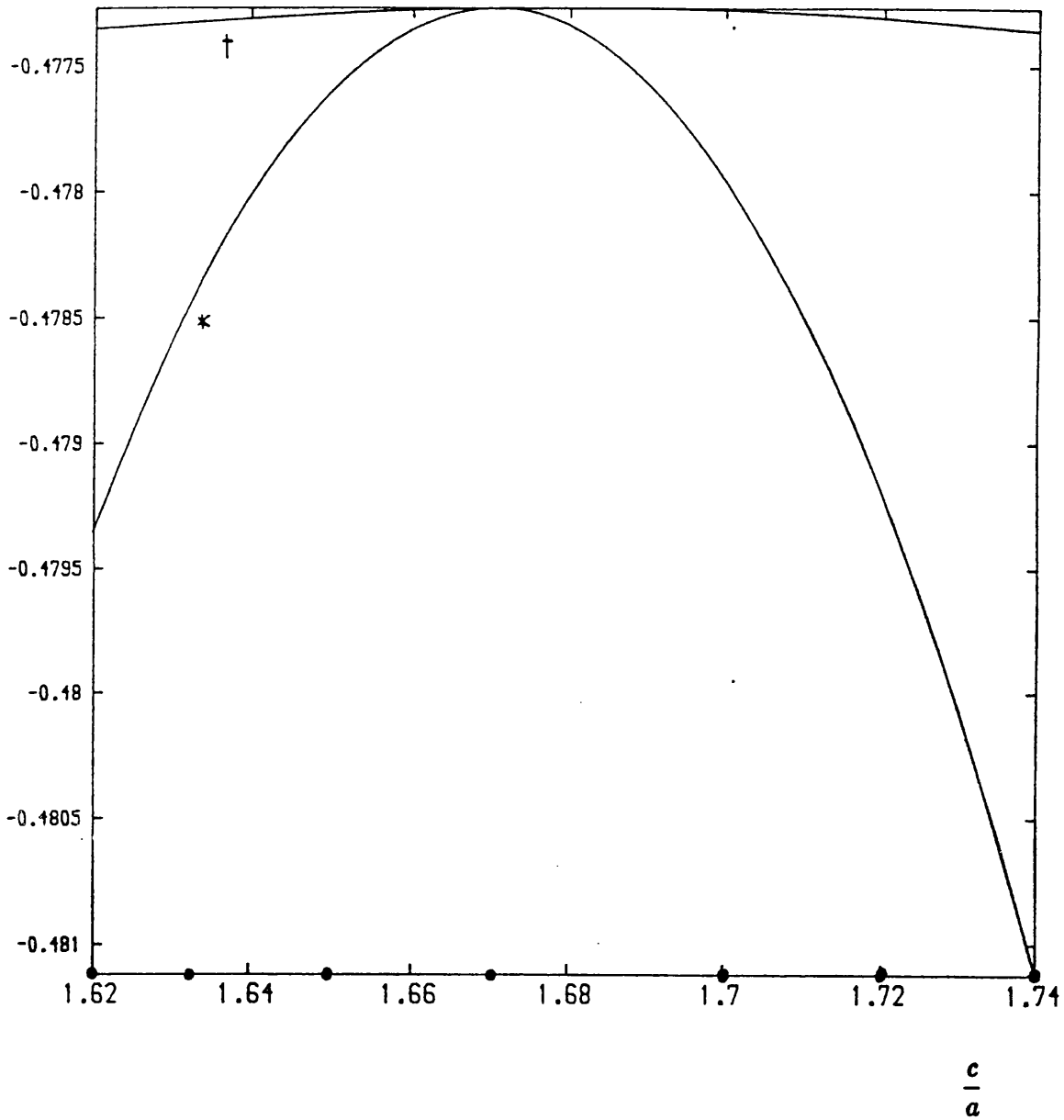

* program total energy: cubic spline from marked points

† pressure derived curve: from points as above

Figure 4.10: Total energy curves for ruthenium.

(Energy+69.0)/Ryd.

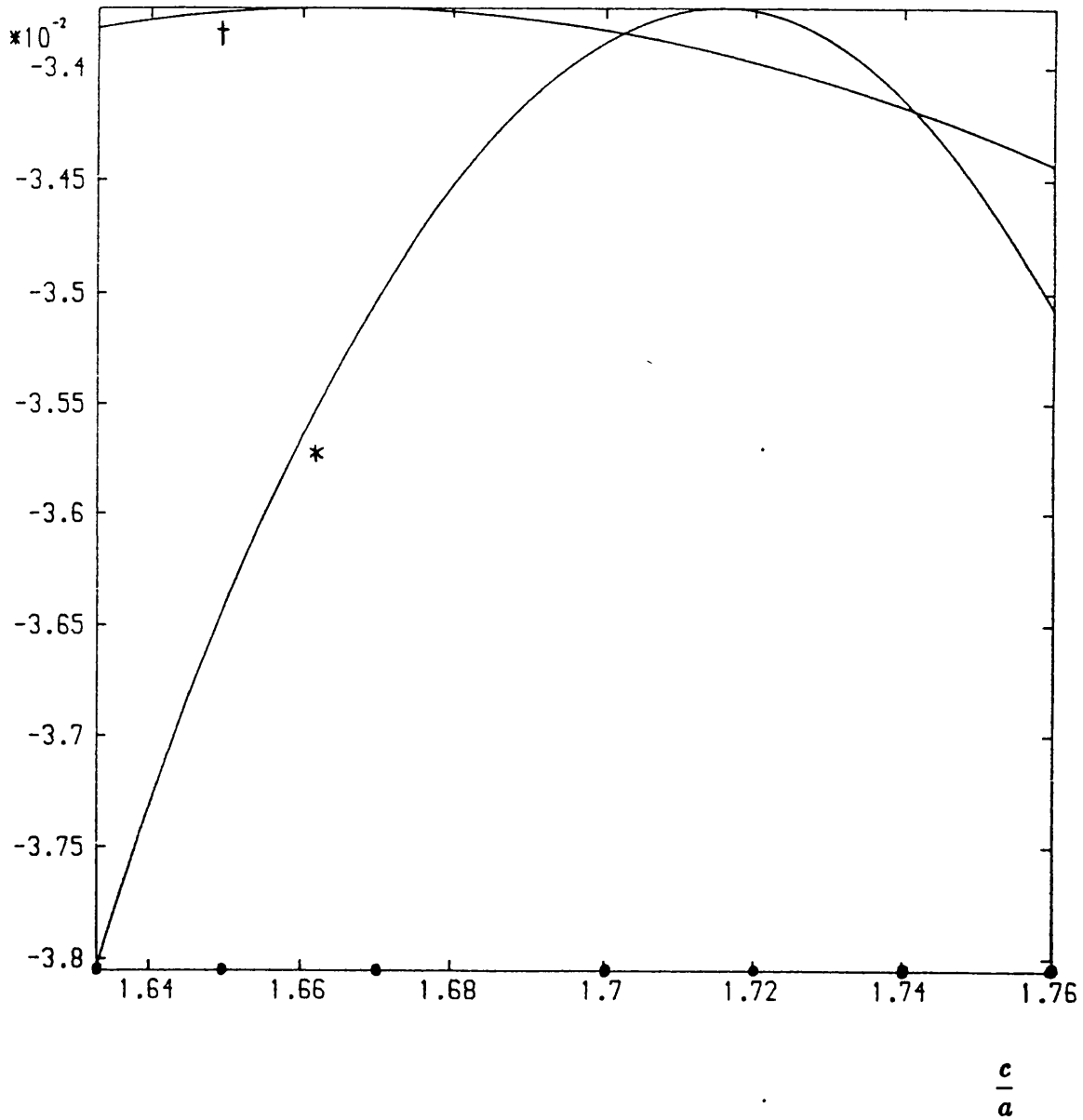

* program total energy: cubic spline from marked points

† pressure derived curve: from points as above

Figure 4.11: Total energy curves for copper (HCP).

(Energy+206.0)/Ryd.

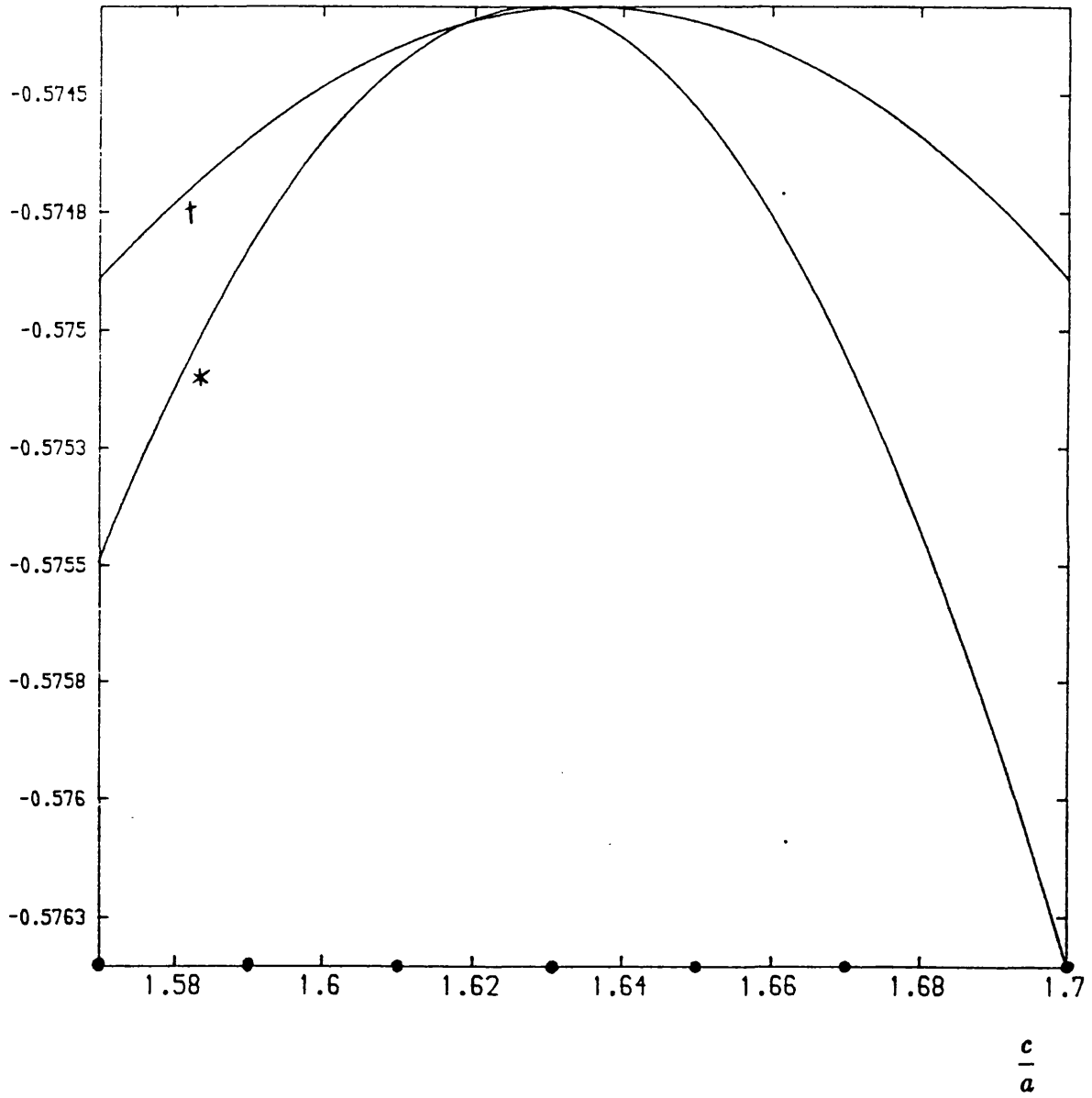

* program total energy: cubic spline from marked points

† pressure derived curve: from points as above

Figure 4.12: Total energy curves for copper (FCC).

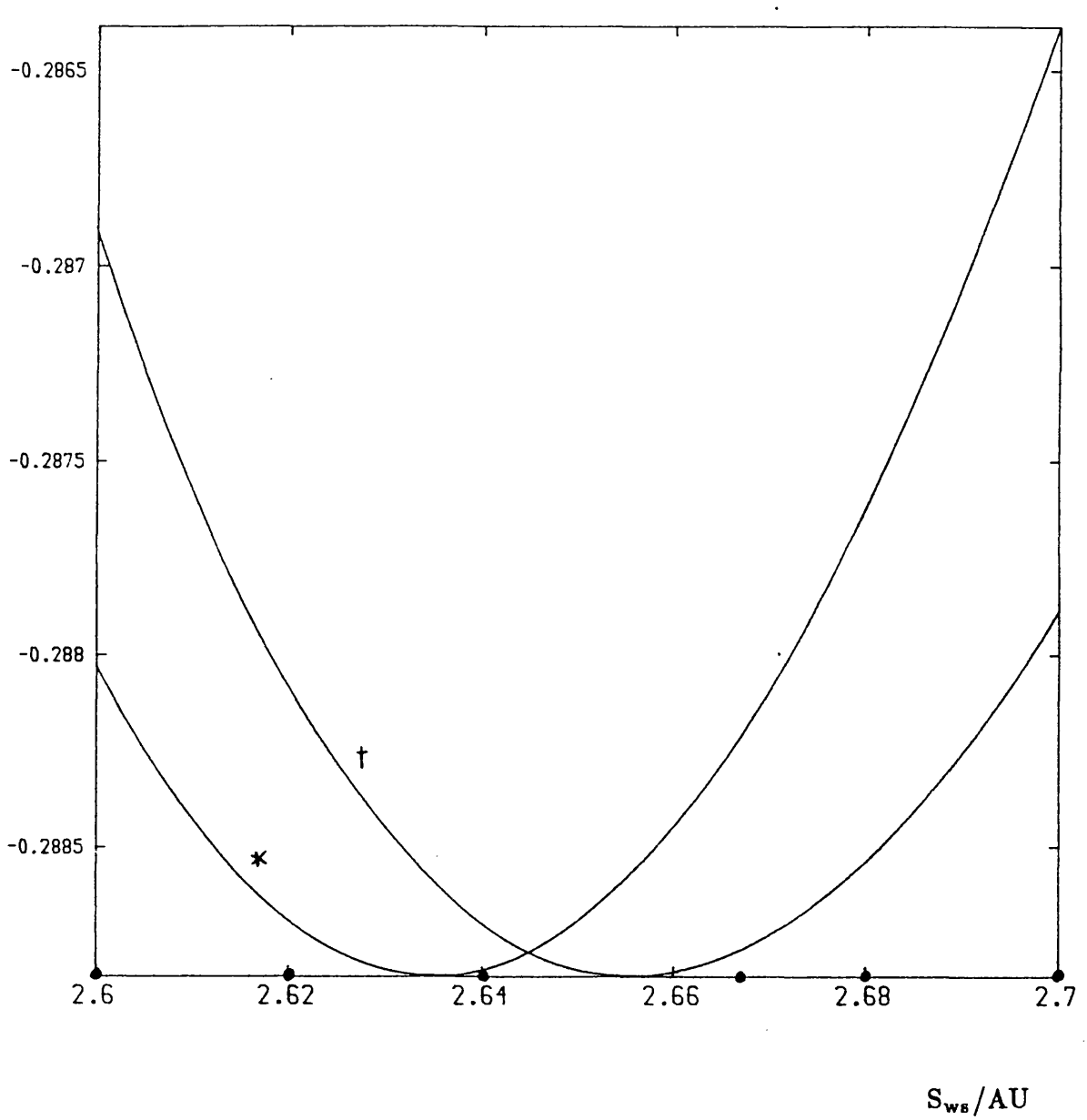

* program total energy: cubic spline from marked points

† pressure derived curve: from points as above

4.8) The equilibrium $\frac{c}{a}$ ratio.

In this section we shall use classical elasticity theory to make estimates of the equilibrium $\frac{c}{a}$ ratio for a number of HCP transition metals (the SDWs, which are FCC, will be dealt with in the next section). The method is simply that of finding the turning point of a quadratic function given its gradient at a particular point. This gradient will be calculated both from the axial pressure and from the total energy curves, and the estimates obtained will be compared.

Consider the second order expansion of the classical elastic energy about equilibrium (Kittel, 1968),

$$\frac{E}{V} = \frac{1}{2}\sum_{i=1}^{6}\sum_{j=1}^{6} C_{ij}e_i e_j, \tag{4.68}$$

Here the C_{ij}s are the elastic constants and the e_is are the strain components. For a hexagonal material the only non-zero constants are $C_{11} = C_{22}$, C_{12}, $C_{13} = C_{23}$, C_{33} and C_{44}. Moreover, for a volume-conserving axial strain we have $e_1 = e_2 = -\lambda$, $e_3 = 2\lambda$ and $e_4 = 0$, so that (4.68) becomes,

$$\begin{aligned} \frac{E}{V} &= 6\lambda^2 C', \\ \text{where} \quad C' &= \frac{1}{6}(C_{11} + C_{12} + 2C_{33} - 4C_{13}). \end{aligned} \tag{4.69}$$

Differentiating with respect to λ then gives,

$$\frac{1}{V}\frac{dE}{d\lambda} = 12\lambda C', \tag{4.70}$$

and substituting from (4.32) we have,

$$\begin{aligned} -6P &= 12\lambda C' \\ \Rightarrow \quad \lambda &= -\frac{1}{2}\frac{P}{C'}, \end{aligned} \tag{4.71}$$

This relates the distortion λ from equilibrium to the axial pressure P. All we have done here is to use the curvature C' of the (assumed) parabolic energy dependence (4.68), together with the relation (4.32) between P and $\frac{dE}{d\lambda}$, to obtain an expression for P in terms of λ.

The above relation clearly provides a means of estimating the distortion from ideal $\frac{c}{a}$ at equilibrium, given the axial pressure for a given value of λ. It will be more convenient to re-express (4.71) in terms of $\frac{c}{a}$ ratios and we can do this by rearranging the first line of (4.66),

$$\lambda = \frac{1}{3}\frac{(\frac{c}{a})' - (\frac{c}{a})}{(\frac{c}{a})} + O(\lambda^2),$$

and then substituting in (4.71),

$$\left(\frac{c}{a}\right)' = \left(\frac{c}{a}\right)\left[1 - \frac{3}{2}\frac{P}{C'}\right]. \tag{4.72}$$

Here $(\frac{c}{a})$ is the value (equilibrium, $P = 0$) about which we are expanding and $(\frac{c}{a})'$ is the value (ideal) at which we know P, i.e.

$$\begin{aligned} \left(\frac{c}{a}\right)_{\text{ideal}} &= \left(\frac{c}{a}\right)_{\text{eqm.}}\left[1 - \frac{3P_{\text{ideal}}}{2C'}\right] \\ \Rightarrow \quad \left(\frac{c}{a}\right)_{\text{eqm.}} &= \left(\frac{c}{a}\right)_{\text{ideal}}\left[1 + \frac{3P_{\text{ideal}}}{2C'}\right], \quad \frac{3|P_{\text{ideal}}|}{2C'} = 3|\lambda| \ll 1. \end{aligned} \tag{4.73}$$

Applied to the materials of table 4.1 that gave non-zero results of the right sign we obtain,

Table 4.10: % deviation from ideal $\frac{c}{a}$ (from axial pressure).

element	Sc	Y	Tc	Ru
pressure/kbar	−0.888	−0.473	−1.245	−3.86
*C'/kbar	392	301	†2385	2212
estimated $\Delta\frac{c}{a}$	−0.37	−0.24	−0.12	−0.31
expt. $\Delta\frac{c}{a}$	−2.38	−3.80	−1.78	−3.00

* (Smithell, 1983)

†for rhenium, owing to radioactivity of technetium

This indicates that the $\frac{c}{a}$ estimate from the axial pressure is generally an order of magnitude too small. We can compare these with the estimates made from the LMTO-ASA total energy curves using (4.67):

Table 4.11: % deviation from ideal $\frac{c}{a}$ (from total energy gradient).

element	Sc	Y	Ti	Zr
P/kbar	−11.42	−7.64	−3.49	1.75
C'/kbar	392	301	580	470
estimated $\Delta\frac{c}{a}$	−4.16	−3.67	−0.92	0.55
expt. $\Delta\frac{c}{a}$	−2.38	−3.80	−2.75	−2.45

element	Tc	Ru	Zn	Cd
P/kbar	−37.1	−69.4	5.89	9.14
C'/kbar	2385	2212	199.5	159.7
estimated $\Delta\frac{c}{a}$	−2.26	−4.47	4.65	8.57
expt. $\Delta\frac{c}{a}$	−1.78	−3.00	13.65	15.49

It can be seen that these results are much more in line with experiment, although the titanium and zirconium results, as in the axial pressure case, are considerably

out. Hence it seems that the total energy gradient at ideal $\frac{c}{a}$ is far more reliable than the axial pressure.

4.9) Results for SDW materials.

The axial pressures for the SSDW, DSDW and TSDW in Mn and Fe were calculated from the self-consistent potentials obtained as described in the last chapter. To do this the SDW program was modified to calculate the axial weights (4.40)-(4.42) rather than the conventional angular momentum weights (1.63), and the code to evaluate (4.63) was inserted after the charge density routine. It should be noted that the calculation of the axial weights does not interfere with the SDW representation of §3.9: the former involves manipulation of the eigenvectors using lm labels only while the latter involves the spin/sublattice labels. As in §3.11, the k-space integration was performed over the orthorhombic wedge of the Brillouin zone with a mesh of 64 points. The results for the axial pressure expressions described in §4.5 and §4.7 evaluated at $\frac{c}{a} = 1$ are given below:

Table 4.12: axial pressures for SDW materials.

material	$v_{xc} = \varepsilon_{xc} = 0$	0th order	1st order	Cade
Mn-SSDW	−6.588	−10.734	−11.596	−3.743
Mn-DSDW	2.869	4.008	4.488	0.863
Mn-TSDW	0.120	0.039	0.049	0.039
Fe-SSDW	−0.945	0.092	−0.078	0.886
Fe-DSDW	0.209	−0.343	−0.248	−0.781
Fe-TSDW	−0.092	0.022	0.001	0.022

The first order results come from the most accurate expression (4.64) for the axial pressure and it to this we shall refer in future. As in §4.7, it can be seen

that the zeroth order expression is very close to the first order while the others differ from it by $\sim 50\%$ or more. It is also evident that the values for Mn are in accord with the predictions of the localised electron picture: the SSDW is trying to shrink along the c axis, the DSDW to expand, and the TSDW remains cubic. In fact, given the form of the axial weights (4.40)-(4.42) and the fact that the TSDW is cubic to start with it is evident that the axial pressure for the TSDW has got to be zero, and this gives us a yardstick. By this criterion the pressures for the SSDW and DSDW in Fe should probably be taken to be zero also. The difference in magnitudes between Mn and Fe could suggest that the magnetism in Mn is better represented by a localised picture than that in Fe. By the same argument used for the TSDW the pressures for paramagnetic calculations on Mn and Fe must be zero, suggesting that the significant axial pressures obtained for the SDWs in Mn derive from the magnetic ordering.

As mentioned in §4.7, the axial pressure is made up from contributions due to three types of electron transfer: from the s orbital to the $3z^2 - r^2$, from the p_x/p_y to the p_z, and from the other d orbitals into the $3z^2 - r^2$. In practice it is evaluated using a Taylor expansion (4.63). For the SDWs in Mn and Fe the convergence of the expansion is very good, as exemplified by the SSDWs.

Table 4.13: axial pressure contributions in Mn (SSDW).

	majority spin			minority spin		
order	*sd*	*pp*	*dd*	*sd*	*pp*	*dd*
0th	0.81	−0.66	0.45	3.14	−0.08	6.34
1st	1.75	1.04	−3.14	−12.62	−0.85	−7.05
2nd	0.083	0.002	−0.0086	−0.86	−0.002	−0.009
3rd	0.006	−0.0001	−0.006	0.096	0.0002	0.050

Table 4.14: axial pressure contributions in Fe (SSDW).

	majority spin			minority spin		
order	*sd*	*pp*	*dd*	*sd*	*pp*	*dd*
0th	0.40	0.16	0.22	−0.03	0.08	−0.01
1st	0.60	1.08	−1.05	−1.83	−0.63	0.99
2nd	0.0007	0.0070	−0.038	−0.052	−0.004	0.058
3rd	0.0002	−0.0002	−0.026	0.008	0.00003	−0.002

These numbers indicate that the Taylor expansion is dominated by its first two terms. The size of the first order contribution indicates that the pressure is very sensitive to the energies of the states between which electrons transfer when the material is distorted, as well as the number of electrons transferred. This suggests that the electrons responsible for the pressure should be relatively localised. In addition, the contributions from majority and minority spins are generally very different, suggesting again that the pressures are primarily a consequence of the spin polarisation. A similar breakdown to the above can be made for the MSDWs, although in this case, due to the lack of a common spin axis, the terms majority and minority are no longer really appropriate. The TSDW contributions are all close to zero but for the DSDWs we get,

Table 4.15: axial pressure contributions in Mn (DSDW).

order	*sd*	*pp*	*dd*
0th	−1.79	0.28	−2.40
1st	4.97	−0.14	3.24
2nd	0.350	−0.001	0.032
3rd	−0.045	−0.000	−0.005

Table 4.16: axial pressure contributions in Fe (DSDW).

order	*sd*	*pp*	*dd*
0th	−0.195	−0.134	−0.008
1st	0.602	−0.223	−0.327
2nd	0.025	−0.002	−0.016
3rd	−0.003	0.000	0.018

It difficult to make very much of these results: the contributions involving the *d* electrons appear more important in the Mn materials and it is certainly true that, comparing the same spin structure in Mn and Fe, the breakdowns look very different.

We can also compare the axial pressures of table 4.12 with results derived from the curve of total energy against $\frac{c}{a}$ using (4.74). This was done for the SSDW and DSDW in Mn: the total energy was computed for four different $\frac{c}{a}$ ratios and the points were fitted with a cubic spline. The bare results are,

Table 4.17: total energy curves for Mn.

$\frac{c}{a}$	0.990	0.995	1.000	1.005
SSDW	−126.126930	.126381	.125781	.125263
DSDW	−126.125317	.125557	.125830	.126168

and they yield gradients of 0.11623Ryd. and −0.06003Ryd. respectively at $\frac{c}{a} = 1$. Using (4.74), with $S_{ws} = 2.73$ A.U. and 1kbar=6.798×10^{-6} Ryd./AU^3, we get predicted axial pressures of −25.08kbar and 12.95kbar, which are a factor of about two bigger than the calculated pressures. This is much better

than for the HCP materials of §4.7, where the difference was generally an order of magnitude.

The axial pressures can also be used in a classical elasticity model to estimate the equilibrium $\frac{c}{a}$ ratio and the energy saving associated with the distortion from $\frac{c}{a} = 1$ (§4.8). For this we require experimental values for the elastic constants of FCC Mn and Fe, but as these have not been measured (the γ phases are not sufficiently stable) we will make do with those of nickel, which are given by,

Table 4.18: elastic constants for nickel /kbar (Smithell, 1983) .

C_{11}	C_{12}	C_{44}
2470	1530	1220

Noting that for a cubic crystal $C_{12} = C_{13}$ and $C_{11} = C_{33}$ we obtain from (4.69) that $C' = \frac{1}{2}(C_{11} - C_{12}) = 470$kbar. Hence from (4.73) with $\left(\frac{c}{a}\right)_{\text{ideal}} = 1$ the equilibrium deviations are given by,

Table 4.19: estimated % deviation from $\frac{c}{a} = 1$.

	SSDW	DSDW	TSDW
Mn	−3.8	1.4	0.02
Fe	−0.02	−0.08	0.0003

The values for the SSDW and DSDW in Mn are in good agreement with the respective experimental estimates of −6% (Cowlam, Bacon & Gillott, 1977; Smith & Vance, 1969) and 1% (Honda, Tanji & Nakagawa, 1976) while for Fe a distortion from the cubic structure does not appear to have been reported. The values in the other cases are all close to zero, as expected given the small

axial pressures involved. Using the equation preceding (4.72) to convert the $\frac{c}{a}$ change into a value of λ, (4.69) can then be employed to estimate the associated change in energy. Applied to the SSDW and DSDW in Mn the energy changes are -0.0011Ryd. and -0.00013Ryd. respectively. These values give rise to the correct relative stabilities when added to the ASA total energies for ideal $\frac{c}{a}$ (§3.12).

CONCLUSIONS.

In this thesis the LMTO-ASA technique has been applied to the calculation of some electronic properties of transition metals. The work is new in two respects: firstly in the consideration of non-collinear magnetism in γ manganese and iron, and secondly in the attempt to say something about *non-spherical* properties.

In chapter 3 the band structures and associated quantities were calculated for the SSDW, DSDW and TSDW structures in FCC Mn and Fe (§3.11). The results were consistent with experimental work and, in addition, they seemed to indicate that the magnetism in Mn is of different origin to that in Fe: Mn could be made to fit reasonably well into a localised electron model (§3.11 & §3.12) whereas Fe could not.

In chapter 4 the tendency of a material to distort so as to change its $\frac{c}{a}$ ratio was investigated by calculation of the axial pressure (Cade, 1981b). When applied to the SDW materials of chapter 3 it yielded results that could be described by a localised spin model in Mn and which were inconclusive (probably zero) for Fe (§4.9). In both cases the results were consistent with experimental work (where available). When applied to the non-magnetic HCP metals of the first two transition series reasonable values were obtained only for Sc, Y, Tc and Ru (§4.7). The failure in Zn and Cd was shown to be inherent in the method of calculation but the failure in Ti and Zr could not be explained. Moreover, when used to estimate the equilibrium $\frac{c}{a}$ ratio within a classical elasticity model it was found that the results were an order of magnitude too small (§4.8), in contrast to the SDWs where very reasonable results were obtained (§4.9). The

same estimation technique was applied to data obtained from curves of the ASA total energy and was found to give values in surprisingly good agreement with experiment (§4.8 & §4.9).

The success of the total energy curve data in the estimation of the $\frac{c}{a}$ ratios and the failure of the axial pressure data (for the non-magnetic materials) is contrary to what was expected when this work was began. The axial pressure is based on the Kohn-Sham energy for the non spherically averaged charge density that can be produced at the end of an ASA calculation. This has been shown to be quite close to that produced by the LAPW method, which uses the full, non-spherical potential, and it was suggested that it ought to be good enough for calculations involving symmetry lowering distortions (Andersen, Pawlowska & Jepsen, 1986). Given that the author's treatment of the electrostatic energy really does seem to work (considering the calculations based on total energy curve data) the results suggest that the non-spherical ASA density is generally not good enough for this sort of calculation. However, it is still necessary to explain why the total energy curves yielded good results, and why the axial pressure seems to work for the SDW materials. In the author's opinion, what the results are trying to tell us is that the output of an ASA calculation should generally be used in a manner consistent with the ASA philosophy: it is better to find the total energies of a set of spheres containing spherical ASA densities for two slightly different configurations than to find the axial pressure of the non-spherical density, simply because the former is more consistent with the ASA. This principle evidently outweighs the inaccuracies caused by finding a very small number as the difference of two large numbers.

In the light of the work of Christensen (1984) it is perhaps not surprising that, once the electrostatic term is taken care of, the total energy curve should give good results. Christensen successfully applied the force theorem to the calculation of elastic constants, despite the fact that this should require second order accuracy in the distortion parameter and the force theorem only gives first order accuracy (§4.2). To do this he did calculate the electrostatic term non-spherically, but using a multipole expansion up to $l = 12$, which involves some very intensive computing (the work does not appear to have been followed up). It was shown by Brovman, Kagan & Kholas (1970) that the non-sphericity of the charge is important in the electrostatic contribution to elastic constants. However, for the bandstructure contribution Christensen essentially took the difference in bandstructure energies, working from *spherical* charge densities. This procedure is much more in line with finding the difference between ASA total energies. It was shown (§4.6) that at ideal $\frac{c}{a}$ the electrostatic term is of second order, and we require only first order accuracy for the energy difference.

Going back to the SDW materials the essential difference with the HCP case is that the significant axial pressures obtained are a *direct consequence* of the magnetic order (for paramagnetic calculations the results must be zero). Unlike the HCP materials the pressure is not a consequence of small, non-spherical charge transfer effects, which might tend to be "washed out" in an ASA calculation. Magnetism is an attribute of spin space and as such should be less severely affected by a spherical average in real space than is the charge transfer.

There a number of things that could be done to continue this work. As far as the SDWs are concerned it would be interesting to repeat the band struc-

ture calculations for imaginary materials with the number of valence electrons varying between 7 and 8, as this might give some indication of how the Mn/Fe alloy behaves with solute concentration (see Asano & Yamashita, 1971). This would probably involve considerable modification to the atomic part of a LMTO program. On the axial pressure side, it would be interesting to calculate the Kohn-Sham energy directly from a non spherical density, so as to test the author's conclusions on the usefulness of the ASA density. In addition, there is room for investigation of the anomolous behaviour of titanium and zirconium, which seem to give trouble even when total energy curve data is used.

APPENDIX A.

Conversion of the generalised pressure to a surface integral.

We shall start by writing down the Liberman expression (4.7) for the bulk pressure due to a single Wigner-Seitz sphere,

$$PV = \frac{1}{6}\sum_i \int d^2\mathbf{S}.[(\nabla\psi_i^*)\mathbf{r}.\nabla\psi_i - \psi_i^*\nabla(\mathbf{r}.\nabla\psi_i) + c.c.] + \frac{1}{3}\int d^2\mathbf{S}.\mathbf{r}\, n^2(\mathbf{r})\frac{d\varepsilon_{xc}}{dn}. \qquad (A.1)$$

What we want to do is show that the pressure associated with the general strain tensor $\underline{\varepsilon}$ can also be expressed expressed as a surface integral. To do this it will be necessary to consider the first integral of $(A.1)$ with the virial $\mathbf{r}.\nabla$ replaced by a new operator $\mathbf{r}.\underline{\varepsilon}.\nabla$. It will be shown that this gives the δE expression of (4.28), with the exchange-correlation term replaced by an unwanted term. Looking at the second integral of $(A.1)$ it will then be found that, with the same subtitution of $\mathbf{r}.\nabla$ by $\mathbf{r}.\underline{\varepsilon}.\nabla$, we get exactly the exchange-correlation term of (4.28) minus the unwanted term from above. The sum of the two parts will therefore yield the full result (4.28). For convenience of comparison with the expressions of §4.3 we shall work with the energy change δE rather than the pressure, which for the axial case are related by (4.32).

Looking at the first integral of $(A.1)$ and considering the integrand without its complex conjugate and for a single state ψ we write,

$$\delta E \propto -\lambda[\nabla\psi^*(\mathbf{r}.\underline{\varepsilon}.\nabla\psi) - \psi^*\nabla(\mathbf{r}.\underline{\varepsilon}.\nabla\psi)], \qquad (A.2)$$

where the $-\lambda$ has come from (4.32). The surface integral of $(A.2)$ can be expressed as a volume integral through Gauss' theorem with integrand,

$$-\lambda\nabla.[\nabla\psi^*(\mathbf{r}.\underline{\varepsilon}.\nabla\psi) - \psi^*\nabla(\mathbf{r}.\underline{\varepsilon}.\nabla\psi)]$$

$$= \lambda[\psi^* \nabla^2(\mathbf{r}.\underline{\varepsilon}.\nabla\psi) - \nabla^2\psi^*(\mathbf{r}.\underline{\varepsilon}.\nabla\psi)]$$

$$= \lambda[2\psi^* (\nabla.\underline{\varepsilon}.\nabla\psi) + \psi^* \mathbf{r}.\underline{\varepsilon}.\nabla(\nabla^2\psi) - \nabla^2\psi^*(\mathbf{r}.\underline{\varepsilon}.\nabla\psi)]. \qquad (A.3)$$

Here the second line follows from the identity,

$$\nabla.(a\mathbf{b}) = \nabla a.\mathbf{b} + a\,\nabla.\mathbf{b}, \qquad (A.4)$$

while the last line follows from,

$$\nabla^2(\mathbf{r}.\underline{\varepsilon}.\nabla\psi) = 2(\nabla.\underline{\varepsilon}.\nabla\psi) + \mathbf{r}.\underline{\varepsilon}.\nabla(\nabla^2\psi), \qquad (A.5)$$

which can be proved using index notation. We can substitute for the Laplacian terms in $(A.3)$ using Schrödinger's equation in the form,

$$\nabla^2\psi = (v_{\text{eff}} - E)\psi, \qquad (A.6)$$

to get,

$$\lambda\{2\psi^* (\nabla.\underline{\varepsilon}.\nabla\psi) + \psi^* \mathbf{r}.\underline{\varepsilon}.\nabla[(v_{\text{eff}} - E)\psi] - (v_{\text{eff}} - E)\psi^* (\mathbf{r}.\underline{\varepsilon}.\nabla\psi)\}$$

$$= \lambda\{2\psi^* (\nabla.\underline{\varepsilon}.\nabla\psi) + \psi^* [(\mathbf{r}.\underline{\varepsilon}.\nabla v_{\text{eff}})\psi + (v_{\text{eff}} - E)(\mathbf{r}.\underline{\varepsilon}.\nabla\psi)]$$

$$- (v_{\text{eff}} - E)\psi^* (\mathbf{r}.\underline{\varepsilon}.\nabla\psi)\}$$

$$= 2\lambda\psi^* (\nabla.\underline{\varepsilon}.\nabla\psi) + \lambda\psi^* (\mathbf{r}.\underline{\varepsilon}.\nabla v_{\text{eff}})\psi. \qquad (A.7)$$

Summing over the occupied states this becomes,

$$2\lambda \sum_i \psi_i^* (\nabla.\underline{\varepsilon}.\nabla\psi_i) \; + \lambda(\mathbf{r}.\underline{\varepsilon}.\nabla v_{\text{eff}})n(\mathbf{r}), \qquad (A.8)$$

where $n(\mathbf{r})$ is the density at $\mathbf{r}$. As in (4.17) we have to take the average of (A.8) and its complex conjugate to get,

$$\lambda \sum_i [\psi_i^* \nabla.\underline{\varepsilon}.\nabla\psi_i \; + c.c.] \; + \lambda(\mathbf{r}.\underline{\varepsilon}.\nabla v_{\text{eff}})n(\mathbf{r}). \qquad (A.9)$$

The first term here is precisely the kinetic energy term from (4.28). Moreover expanding v_{eff} yields,

$$\lambda n(\mathbf{r})\left\{\mathbf{r}.\underline{\varepsilon}.\nabla U(\mathbf{r})+\int_{\Omega} d^3\mathbf{s}\, n(\mathbf{s})\left[\mathbf{r}.\underline{\varepsilon}.\nabla V(\mathbf{r}-\mathbf{s})\right]+\mathbf{r}.\underline{\varepsilon}.\nabla v_{\text{xc}}\right\}, \qquad (A.10)$$

indicating that (A.9) also contains the ion-core and Hartree terms of (4.28). Hence what we have so far can be summarised by,

$$\frac{\lambda}{2}\sum_i \int d^2\mathbf{S}.[\psi_i^*\nabla(\mathbf{r}.\underline{\varepsilon}.\nabla\psi_i)-(\nabla\psi_i^*)\mathbf{r}.\underline{\varepsilon}.\nabla\psi_i+c.c.]-\lambda\int d^3\mathbf{r}\,(\mathbf{r}.\underline{\varepsilon}.\nabla v_{\text{xc}})\,n(\mathbf{r})$$
$$=\delta E+\lambda \text{tr}\,\underline{\varepsilon}\int d^3\mathbf{r}\, n^2(\mathbf{r})\frac{d\varepsilon_{\text{xc}}}{dn}. \qquad (A.11)$$

We shall next consider the second integral in $(A.1)$ for the general strain, ignoring the factor of $\frac{1}{3}$. By Gauss' theorem this is equivalent to the volume integral of,

$$\nabla.\left[\underline{\varepsilon}.\mathbf{r}\,n^2\frac{d\varepsilon_{\text{xc}}}{dn}\right]=\mathbf{r}.\underline{\varepsilon}.\nabla\left(n^2\frac{d\varepsilon_{\text{xc}}}{dn}\right)+\nabla.\underline{\varepsilon}.\mathbf{r}\,n^2\frac{d\varepsilon_{\text{xc}}}{dn}$$
$$=\mathbf{r}.\underline{\varepsilon}.\nabla\left(n^2\frac{d\varepsilon_{\text{xc}}}{dn}\right)+\text{tr}\,\underline{\varepsilon}\,n^2\frac{d\varepsilon_{\text{xc}}}{dn}, \qquad (A.12)$$

where we have again used $(A.4)$. We can rewrite the first term on the right of $(A.12)$ using the the chain rule for differentiation and the definition of v_{xc},

$$\mathbf{r}.\underline{\varepsilon}.\nabla\left(n^2\frac{d\varepsilon_{\text{xc}}}{dn}\right)=(\mathbf{r}.\underline{\varepsilon}.\nabla n)\left[\frac{d^2}{dn^2}(n\varepsilon_{\text{xc}})\right]n(\mathbf{r})$$
$$=\mathbf{r}.\underline{\varepsilon}.\nabla\left[\frac{d}{dn}(n\varepsilon_{\text{xc}})\right]n(\mathbf{r})$$
$$=(\mathbf{r}.\underline{\varepsilon}.\nabla v_{\text{xc}})\,n(\mathbf{r}). \qquad (A.13)$$

Hence, substituting for the first term in $(A.12)$ and expressing the left hand side as a surface integral we get,

$$-\int d^3\mathbf{r}\,(\mathbf{r}.\underline{\varepsilon}.\nabla v_{\text{xc}})\,n(\mathbf{r})=\text{tr}\,\underline{\varepsilon}\int d^3\mathbf{r}\,n^2\frac{d\varepsilon_{\text{xc}}}{dn}-\int d^2\mathbf{S}.\underline{\varepsilon}.\mathbf{r}\,n^2\frac{d\varepsilon_{\text{xc}}}{dn}. \qquad (A.14)$$

Substituting in $(A.11)$ then gives,

$$\delta E = \frac{\lambda}{2}\sum_i \int d^2\mathbf{S}.[\psi_i^* \nabla(\mathbf{r}.\underline{\varepsilon}.\nabla\psi_i) - (\nabla\psi_i^*)\mathbf{r}.\underline{\varepsilon}.\nabla\psi_i + c.c.]$$
$$- \lambda \int d^2\mathbf{S}.\underline{\varepsilon}.\mathbf{r}\, n^2(\mathbf{r})\frac{d\varepsilon_{\mathbf{xc}}}{dn}. \qquad (A.15)$$

So using $(A.15)$ in (4.32) we end up with,

$$P = \frac{1}{16\pi s^3}\sum_i \int d^2\mathbf{S}.\,[(\nabla\psi_i^*)\,\mathbf{r}.\underline{\varepsilon}.\nabla\psi_i - \psi_i^*\nabla(\mathbf{r}.\underline{\varepsilon}.\nabla\psi_i) + c.c.]$$
$$+ \frac{1}{8\pi s^3}\int d^2\mathbf{S}.\underline{\varepsilon}.\mathbf{r}\; n^2(\mathbf{r})\frac{d\varepsilon_{\mathbf{xc}}}{dn}. \qquad (A.16)$$

APPENDIX B.

Evaluation of the integrals of (4.38).

The first non-trivial integral of (4.38) is,

$$\int d^2\Omega\, Y^*_{lm} Y_{l'm'}(3\cos^2\theta - 1), \qquad (B.1)$$

where $d^2\Omega$ is an element of solid angle. We can use the definition,

$$Y_{20} = \left(\frac{5}{16\pi}\right)^{\frac{1}{2}} (3\cos^2\theta - 1) \qquad (B.2)$$

(Bransden & Joachain, 1983, Table 2.1) to rewrite this in terms of three spherical harmonics and we get,

$$\int d^2\Omega\, Y^*_{lm} Y_{l'm'}(3\cos^2\theta - 1) = 2\left(\frac{2l'+1}{2l+1}\right)^{\frac{1}{2}} C(l'\,2\,l, 0\,0\,0)\, C(l'\,2\,l, m'\,0\,m),$$

$$\text{if } |l'-2| \le l \le |l'+2| \text{ and } l'+2+l \text{ is even,}$$

$$= 0, \quad \text{otherwise,} \qquad (B.3)$$

This has been obtained using a standard result for the spherical integral of three spherical harmonics in terms of Clebsch-Gordon coefficients (Elliott & Dawber, 1979, A.4.6). From the conditions in $(B.3)$ and the fact that we include only s, p and d orbitals it can be seen that we only have to consider the ll' combinations given by (0,2), (1,1), (2,0) and (2, 2). Further, as an m label refers to $\mathcal{R}^2$ (which is additive) we must have $m' = m$. So using the formulae for the Clebsch-Gordon coefficients (Condon & Shortley, 1963, Table 4^3) we obtain the following table for the non-zero values of $(B.1)$:

l	l'	m	m'	$C(l'\,2\,l, m'\,0\,m)$	$(B.1)$
0	2	0	0	$\frac{1}{\sqrt{5}}$	$\frac{2}{\sqrt{5}}$
1	1	0	0	$-\frac{2}{\sqrt{10}}$	$\frac{4}{5}$
1	1	±1	±1	$\frac{1}{\sqrt{10}}$	$-\frac{2}{5}$
2	0	0	0	1	$\frac{2}{\sqrt{5}}$
2	2	0	0	$-\frac{\sqrt{2}}{\sqrt{7}}$	$\frac{4}{7}$
2	2	±1	±1	$-\frac{1}{\sqrt{14}}$	$\frac{2}{7}$
2	2	±2	±2	$\frac{2}{\sqrt{14}}$	$-\frac{4}{7}$

$(B.4)$

Looking at the second integral in (4.38) and substituting for $d^2\Omega$ we get,

$$\int_0^{\pi} d\theta \int_0^{2\pi} d\phi \frac{\partial Y^*_{lm}}{\partial \theta} Y_{l'm'} \sin\theta \cos\theta, \qquad (B.5)$$

Now we know that,

$$\int_0^{2\pi} d\phi\, e^{i\phi(m'-m)} = 0, \quad \text{unless } m' = m. \qquad (B.6)$$

Further, as $(B.5)$ is preceded by factor $(D_l - D_{l'})$ in (4.38) we need only consider cases for which $l \neq l'$, and as Y_{00} is a constant the case $l = 0$ can also be ruled out. Using the definitions given in Bransden & Joachain (1983, Table 2.1) for the spherical harmonics we hence end up with the following as the relevant set of integrands for $(B.5)$:

l	l'	m	m'	$(B.5)$
1	0	0	0	$-\frac{\sqrt{3}}{4\pi}\sin^3\theta\cos\theta$
1	2	0	0	$-\frac{\sqrt{15}}{8\pi}(3\cos^2\theta - 1)\sin^3\theta\cos\theta$
1	2	±1	±1	$\frac{3\sqrt{5}}{8\pi}\sin^3\theta\cos^3\theta$
2	0	0	0	$-\frac{3\sqrt{5}}{4\pi}\sin^3\theta\cos^2\theta$
2	1	0	0	$-\frac{3\sqrt{15}}{4\pi}\sin^3\theta\cos^3\theta$
2	1	±1	±1	$\frac{3\sqrt{5}}{8\pi}(\cos^2\theta - \sin^2\theta)\sin^3\theta\cos\theta$

$(B.7)$

We have,

$$\int_0^{\pi} d\phi \, \cos^n \theta \, \sin\theta = -\frac{1}{n+1} \left[\cos^{n+1} \theta\right]_0^{\pi} = 0, \quad \text{odd } n. \qquad (B.8)$$

So expanding $\sin^2 \theta$ in terms of $\cos^2 \theta$ we see that there is only one entry in $(B.7)$ that gives a non-zero integral, and this corresponds to $l\,l'\,m\,m' = 2000$. This integral is easily evaluated and yields $-\frac{2}{\sqrt{5}}$.

REFERENCES.

Abrahams S C, Guttman L & Kasper J S,
Phys. Rev., vol. 127, number 6, pp2052-55 (1962).

Andersen O K,
Phys. Rev. B, vol. 12, number 8, pp3060-83 (1975).

Andersen O K & Jepsen O,
Phys. Rev. Letters, vol. 53, number 27, pp2571-4 (1984).

Andersen O K, Jepsen O & Glötzel D, in "Highlights of
Condensed Matter Theory" (ed. F. Bassani et. al.), pp59-176,
North-Holland (1985).

Andersen O K, Jepsen O & Sob M, in "Electronic Band Structure &
its Applications" (ed. M Yussouff), Springer Lecture Notes (1987).

Andersen O K, Pawlowska Z & Jepsen O,
Phys. Rev. B, vol. 34, number 8, pp5253-69 (1986).

Anderson P W,
Phys. Rev., vol. 115, number 1, pp2-13 (1959).

Arrott A, in "Magnetism" (ed. Rado & Suhl), vol. 2B,
Academic Press (1966).

Asano S & Yamashita J,
J. Phys. Soc. Japan, vol. 31, number 4, pp1000-15 (1971).

Ashcroft N W & Mermin N D,
Solid State Physics, Holt-Saunders (1976).

Bacon G E, Dunmur I W, Smith J H & Street R,
Proc. Roy. Soc., A241, pp223-38 (1957).

Bradley C J & Cracknell A P,
"Mathematical Theory of Symmetry in Solids",
Clarendon Press (1972)

Bransden B H & Joachain C J,
"Physics of Atoms & Molecules", Longman (1983).

Brovman E G, Kagan Yu & Kholas A,
Sov. Phys. JETP, vol. 30, number 5, pp883-8 (1970).

Cade N A,
J. Phys. F, vol. 10, L187-91 (1980).

Cade N A, in "Physics of Transition Metals", IOP Conference
Series 55, pp351-4 (1981a).

Cade N A,
J. Phys. F, vol.11, pp2399-408 (1981b).

Cade N A & Young W,
J. Phys. F, vol. 10, pp2035-40 (1980).

Callaway J, "Quantum Theory of the Solid State",
Academic Press (1974).

Chambers S A, Wagener T J & Weaver J H,
Phys. Rev. B, vol. 36, pp8992-9002 (1987).

Christensen N E,
Solid State Comms., vol. 49, number 7, pp701-5 (1984).

Christensen N E & Heine V,
Phys. Rev. B, vol. 32, number 10, pp6145-56 (1985).

Condon E U & Shortley G H,
"The Theory of Atomic Spectra", CUP (1963).

Cowlam N, Bacon G E & Gillott L,
J. Phys. F, vol. 7, L315-9 (1977).

Edmonds A R, "Angular Momentum in Quantum Mechanics"
(2nd ed.), Princeton (1960).

Elliott R J, in "Magnetic Properties of Rare Earth Metals"
(ed. R. J. Elliott), Plenum (1972).

Elliott J P & Dawber P G,
"Symmetry in Physics", vol. 2, Macmillan (1979).

Fernando G W & Cooper B R,
Phys. Rev. B, vol. 38, p3016 (1988).

Endoh Y & Ishikawa Y,
J. Phys. Soc. Japan, vol. 30, number 6, pp1614-27 (1971).

Fu C L & Freeman A J,
Phys. Rev. B, vol. 35, pp925-32 (1987).

Fock V,
Zeit. Physik, vol. 63, numbers 11-12, pp855-8 (1930).

Giannozzi P & Erdos P,
J. Magn. Magn. Mater., vol. 67, number 1, pp75-87 (1987).

Glötzel D, Segall B & Andersen O K,
Solid State Comms., vol. 36, pp403-6 (1980).

Gunnarsson O, Harris J & Jones R O,
Phys. Rev. B, vol. 15, number 6, p3027-38, (1977).

Gunnarsson O & Lundqvist B I,
Phys. Rev. B, vol. 13, number 10, pp4274-98 (1976).

Ham F S & Segall B,
Phys. Rev., vol. 124, number 6, pp1786-96 (1961).

Harrison W A,
"Solid State Theory", McGraw-Hill (1970).

Hedin L & Lundqvist B I,
J. Phys. C, vol. 4, pp2064-83 (1971).

Heine V, in "Solid State Physics" (ed. H. Ehrenreich,
F. Seitz & D. Turnbull), Academic Press (1980).

Heine V & Samson J H,
J. Phys. F, vol. 13, pp2155-68 (1983).

Hohenberg P & Kohn W,
Phys. Rev., vol. 136, number 3B, pp864-71 (1964).

Honda N, Tanji Y & Nakagawa Y,
J. Phys. Soc. Japan, vol. 41, number 6, pp1931-7 (1976).

Jepsen O & Andersen O K,
Solid State Comms., vol. 9, pp1763-7 (1971).

Jo T,
J. Phys. F, vol. 13, L211-6 (1983).

Jones W & March N H,
"Theoretical Solid State Physics", vol. 1, Wiley (1973).

Kittel C,
"Introduction to Solid State Physics" (3rd ed.), Wiley (1968).

Kohn W & Sham L J,
Phys. Rev., vol. 140, number 4A, pp1133-8 (1965).

Kohn W & Vashishta P, in "Theory of the Inhomogeneous
Electron Gas" (ed. N. H. March & B. I. Lundquist),
Plenum (1983).

Kouvel J S & Kasper J S,
J. Phys. Chem. Solids, vol. 24, pp529-36 (1962).

Kübler J,
Phys. Letters, vol. 81A, number 1, pp81-3 (1981).

Kübler J, Höck K H, Sticht J & Williams A R,
J. Phys. F, vol. 18, pp469-83 (1988).

Lehmann G & Taut M,
Phys. Stat. Sol. (b), vol. 54, pp469-77 (1972).

Levy M,
Phys. Rev. A, vol. 26, number 3, pp1200-8 (1982).

Liberman D A, in "Computational Methods in Band Theory:
Proceedings of the Conference, New York, 1970", Plenum (1970).

Liberman D A,
Phys. Rev. B, vol. 3, number 6, pp2081-2 (1971).

Lomer W M,
Proc. Roy. Soc., vol. 80, pp489-96 (1962).

Long M W,
J. Phys. C/F, vol. 1, pp2857-74 (1989).

Long M W, Lowde R D & Sakata M,
Rutherford Appleton Lab. Report, RAL-88-022 (1987).

Long M W & Yeung W,
J. Phys. F, vol. 16, pp769-90 (1986).

Löwdin P O,
Adv. Phys., vol. 5, pp1-172 (1956).

Macedo W A A & Keune W,
Phys. Rev. Letters, vol. 61, pp475-8 (1988).

Mackintosh A R & Andersen O K, in "Electrons at the Fermi Surface" (ed. M. Springford), CUP (1980).

Mattheis L F,
Phys. Rev., vol. 133, number 5A, pp184-8 (1964).

Mattis D C,
"The Theory of Magnetism I", Springer-Verlag (1981).

Meneghetti D & Sidhu S S,
Phys. Rev., vol. 105, number 1, pp130-5 (1957).

Methfessel M,
Phys. Rev. B, vol. 38, number 2, pp1537-40 (1988).

Nieminen R M & Hodges C H,
J. Phys. F, vol. 6, number 4, pp573-85 (1976).

Pearson W B, "Handbook of Lattice Spacings and Structures of Metals and Alloys", American Society for Metals (1958).

Pettifor D G,
Communications in Physics, vol. 1, pp141-6 (1976).

Pettifor D G,
CALPHAD, vol. 1, number 4, pp305-324, Pergamon Press (1977).

Poulsen U K, Kollar J & Andersen O K,
J. Phys. F, vol. 6, number 9, L241-7 (1976).

Schiff L I, "Quantum Mechanics" (3rd ed.),
McGraw-Hill (1968).

Skriver H L,
"The LMTO Method", Springer-Verlag (1984).

Slater J C,
J. Chem. Phys., vol. 1, pp687-91 (1933).

Slater J C & Koster G F,
Phys. Rev., vol. 94, pp1498-524 (1954).

Smith J H & Vance E R,
J. Phys. C, series 2, vol. 2, pp761-3 (1969).

Smithell C J,
"Smithell's Metals Ref. Book", Butterworths (1983).

Uchishiba H,
J. Phys. Soc. Japan, vol. 31, number 2, pp436-40 (1971).

von Barth U & Hedin L,
J. Phys. C, vol. 5, pp1629-42 (1972).

Weyrich K H,
Phys. Rev. B, vol. 37, number 17, pp10269-82 (1988).

Weyrich K H, Brey L & Christensen N E,
Phys. Rev. B, vol. 38, number 2, pp1392-6 (1988).

White R M,
"Quantum Theory of Magnetism", Springer-Verlag (1983).

Williams A R, Kübler J & Gelatt C D,
Phys. Rev. B, vol. 19, pp6094-118 (1979).

Yamaoka T,
J. Phys. Soc. Japan, vol. 36, number 2, pp445-50 (1974).

Young W,
J. Phys. F, vol. 5, pp2343-61 (1975).

Ziman J M,
"Principles of the Theory of Solids" (2nd ed.), CUP (1972).